Agnieszka Sorensen

Searching for the QCD Critical Point with Heavy-Ion Collisions

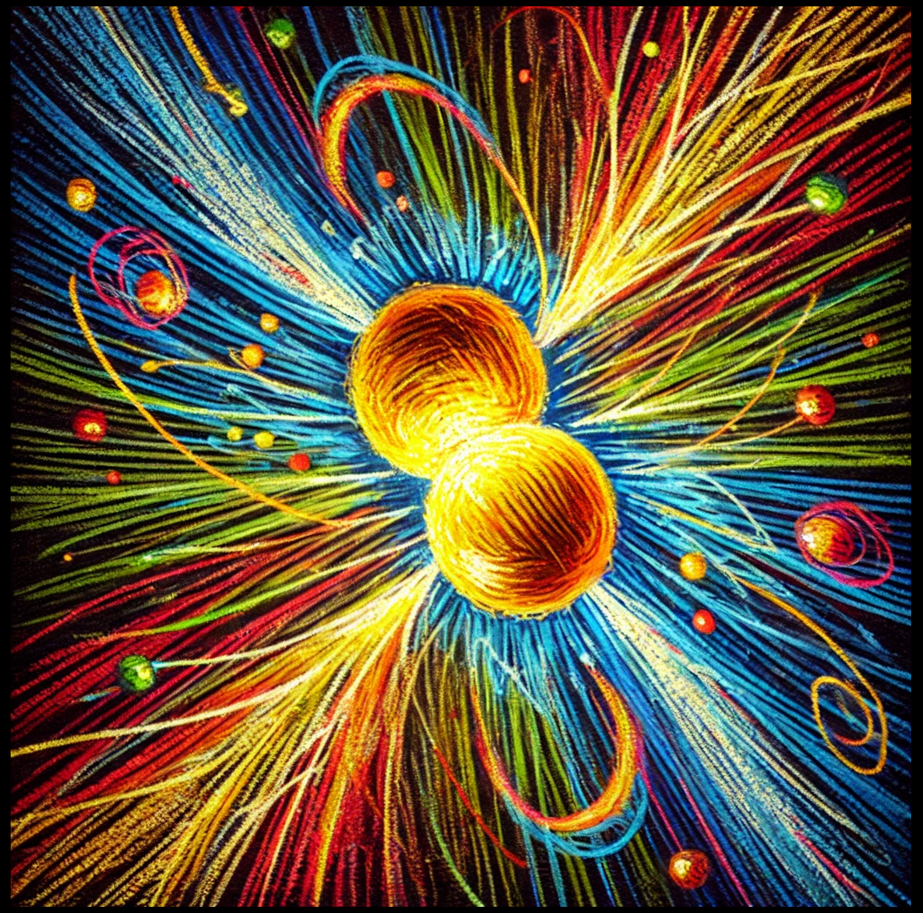

DALL-E

Facility for Rare Isotope Beams
Michigan State University

July 17, 2025
Nuclear Physics Colloquium

The QCD phase diagram: what do we know?

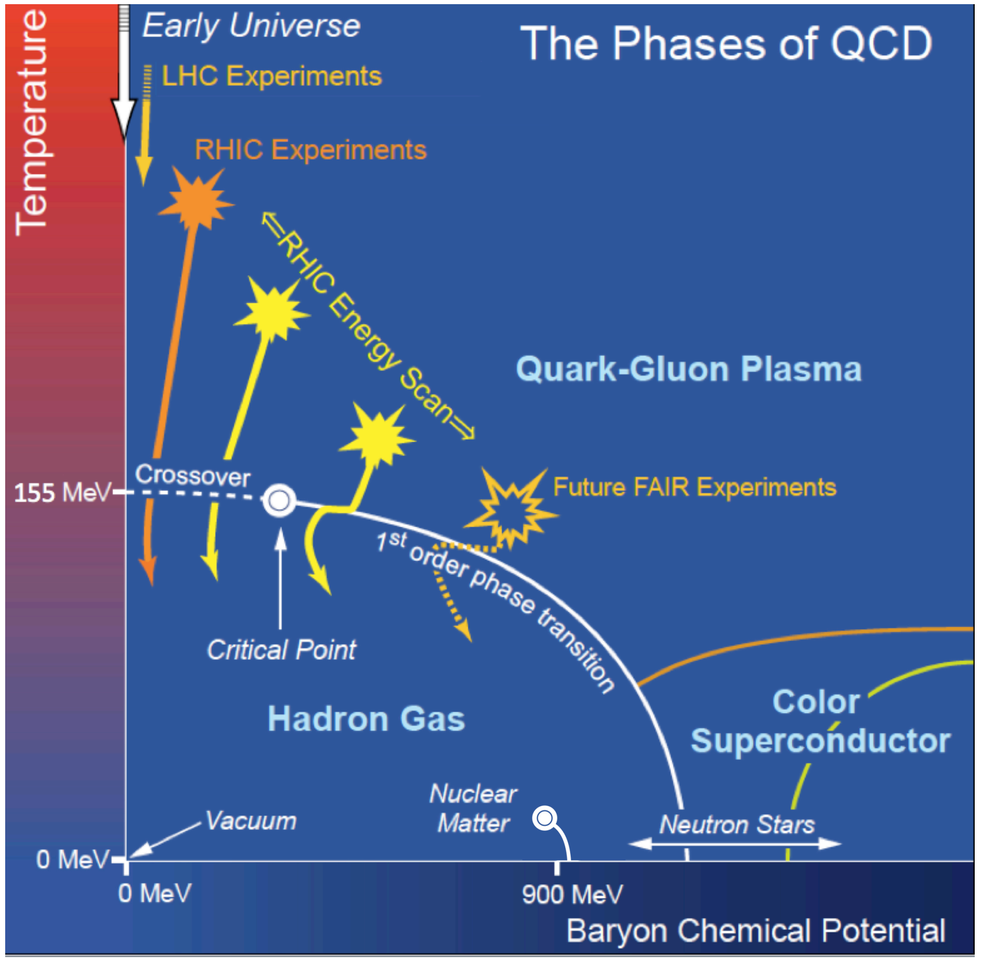

LRP 2007

The QCD phase diagram: what do we know?

LQCD EOS: $T_{pc}(\mu_B = 0) \approx 155$ MeV

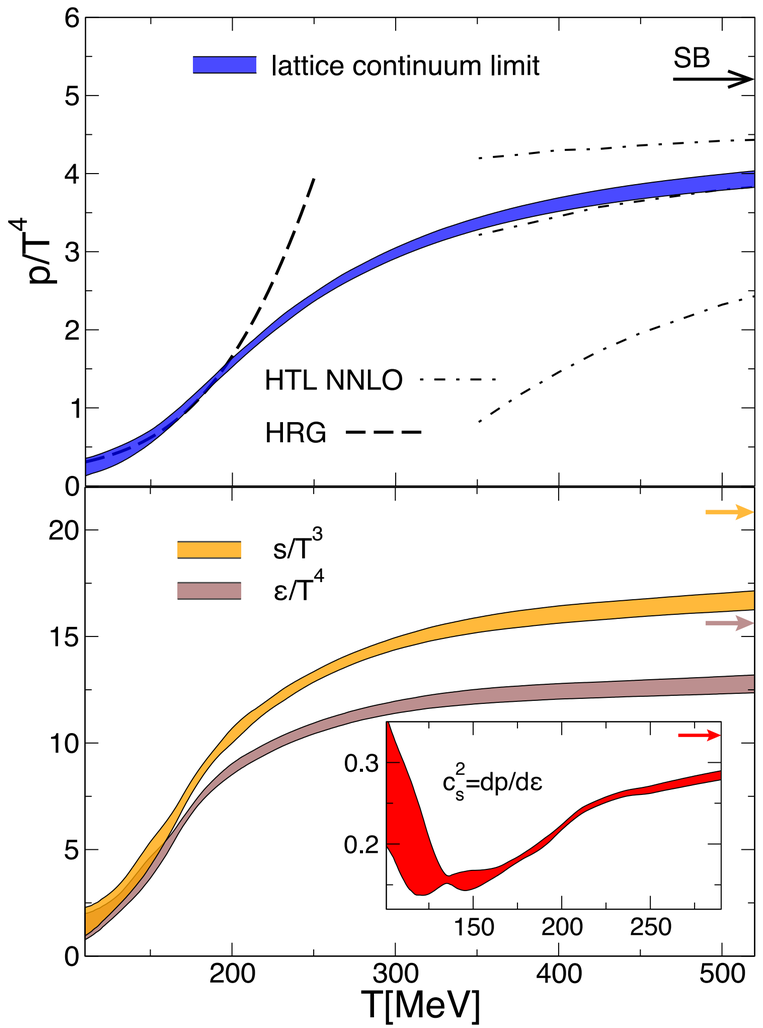

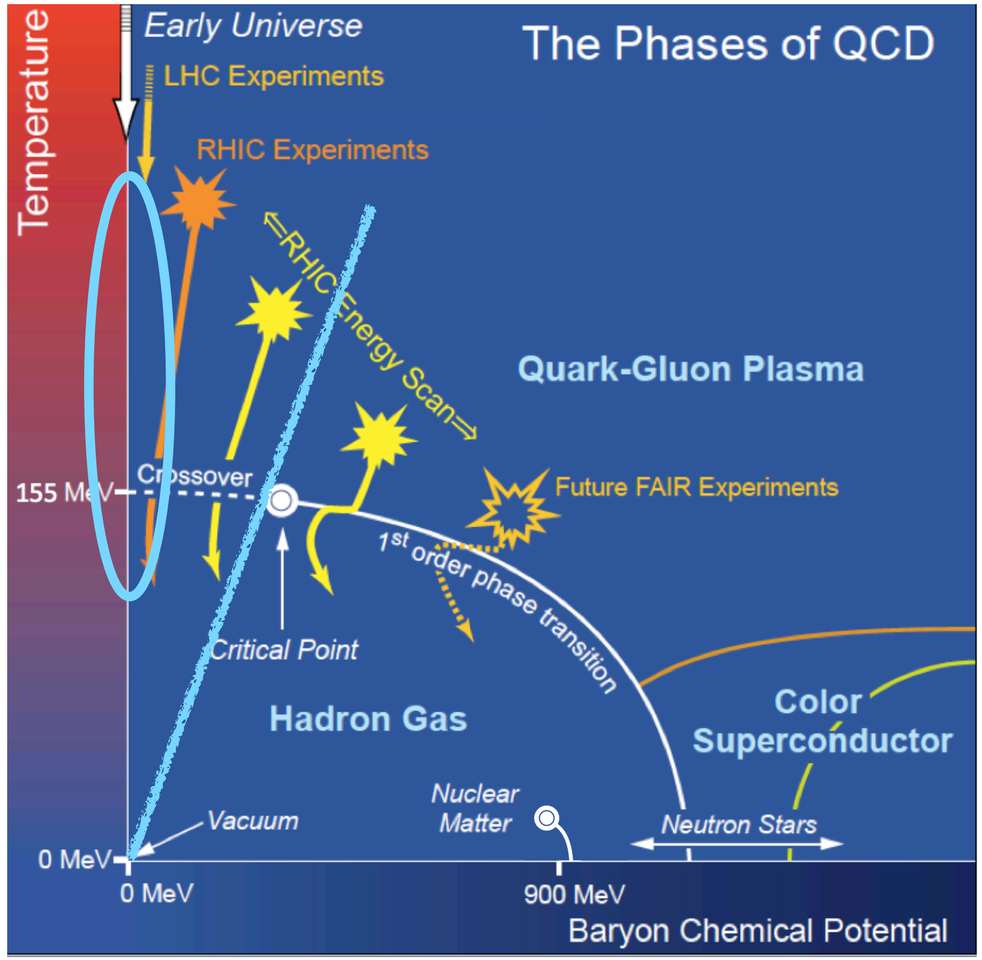

LRP 2007

S. Borsányi *et al.*, Phys. Lett. B **730** 99–104 (2014) arXiv:1309.5258

The QCD phase diagram: what do we know?

LQCD EOS: $T_{pc}(\mu_B = 0) \approx 155$ MeV

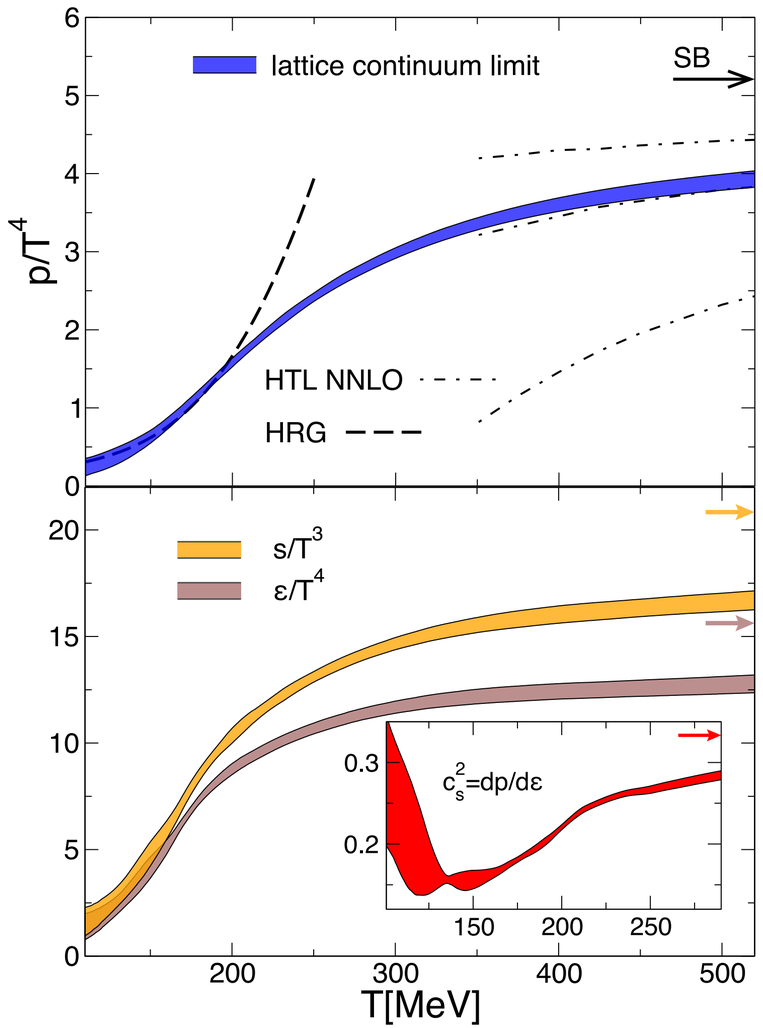

S. Borsányi *et al.*, Phys. Lett. B **730** 99–104 (2014) arXiv:1309.5258

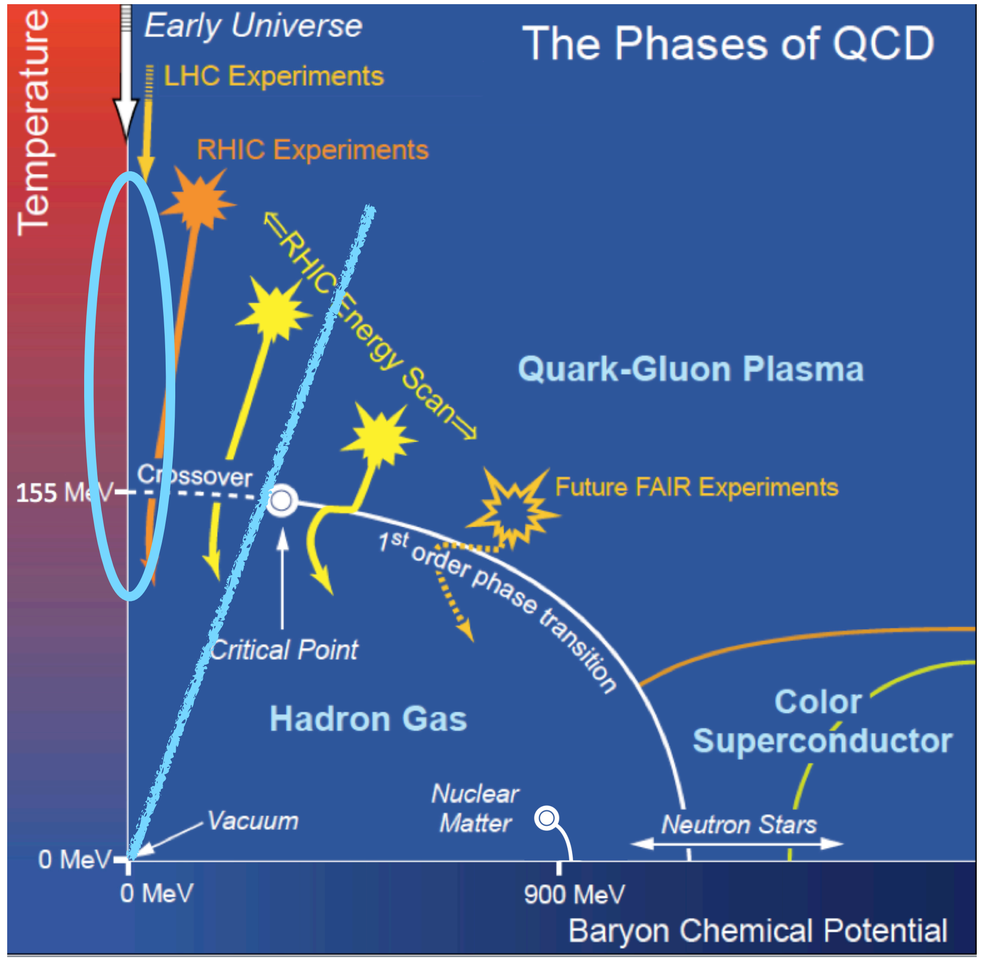

LRP 2007

Models predict a 1st order phase transition at large μ_B ~ large n_B

The QCD phase diagram: what do we know?

LQCD EOS: $T_{pc}(\mu_B = 0) \approx 155$ MeV

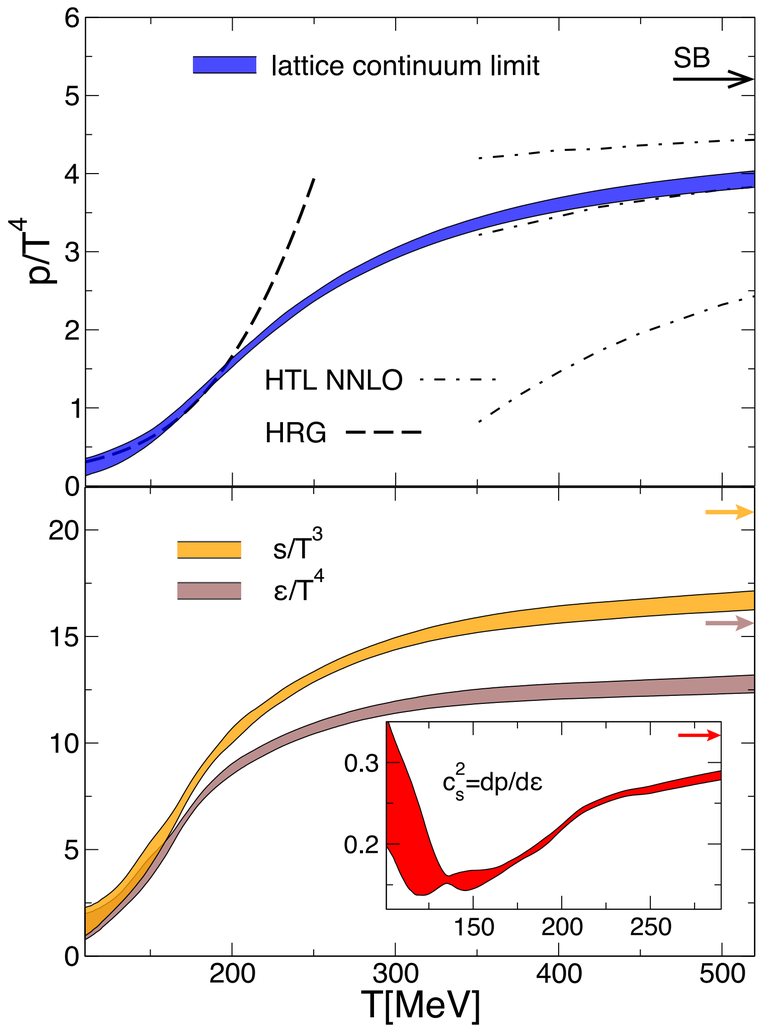

S. Borsányi *et al.*, Phys. Lett. B **730** 99–104 (2014) arXiv:1309.5258

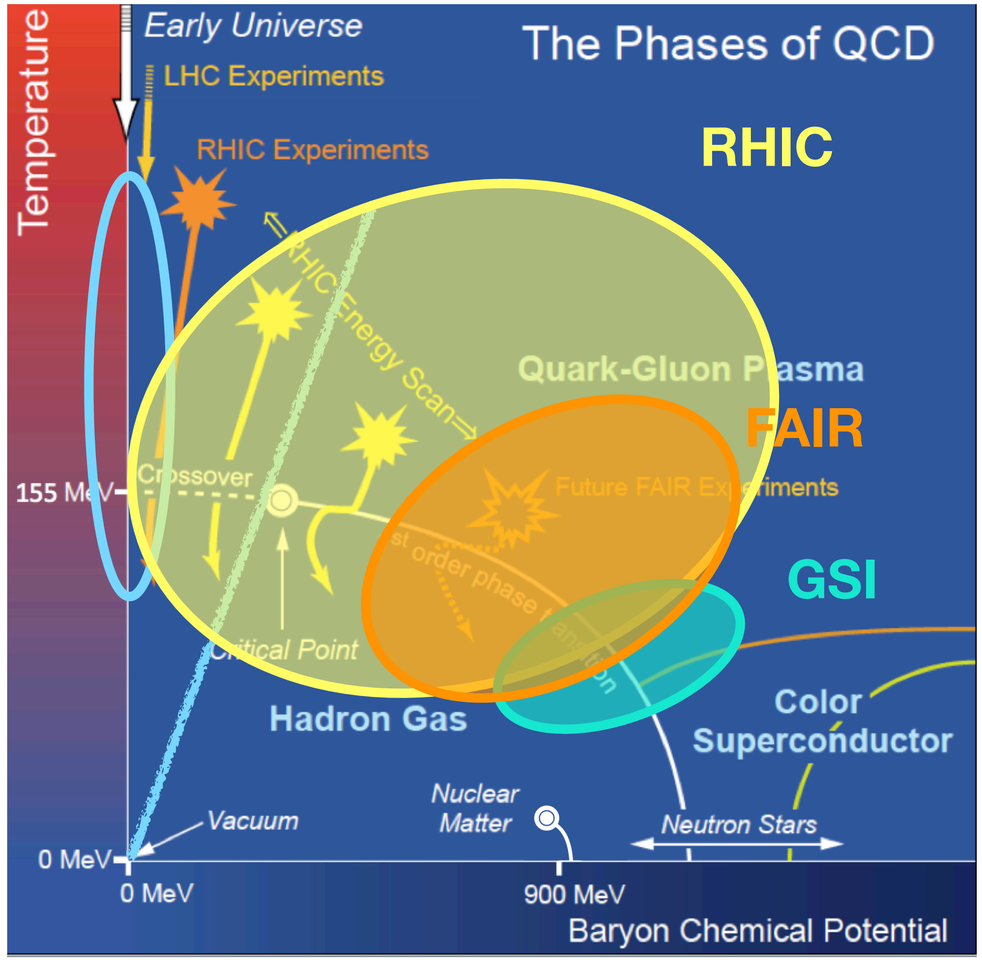

LRP 2007

Models predict a 1st order phase transition at large μ_B ~ large n_B

The QCD phase diagram: what do we know?

LQCD EOS: $T_{pc}(\mu_B = 0) \approx 155$ MeV

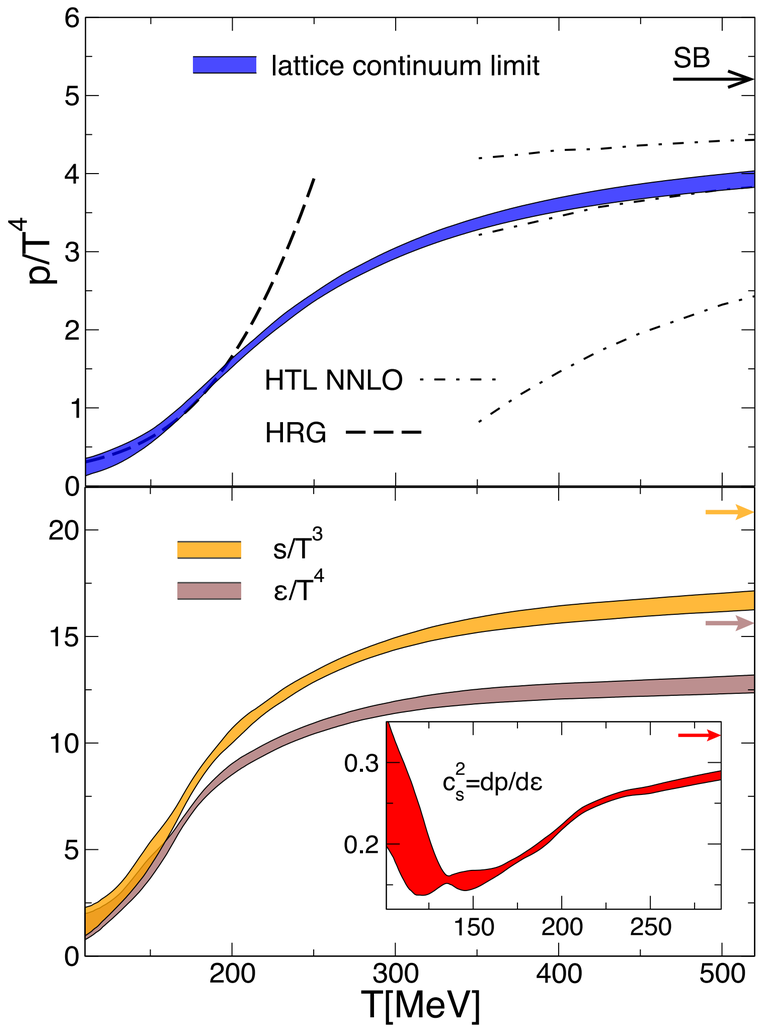

S. Borsányi *et al.*, Phys. Lett. B **730** 99–104 (2014) arXiv:1309.5258

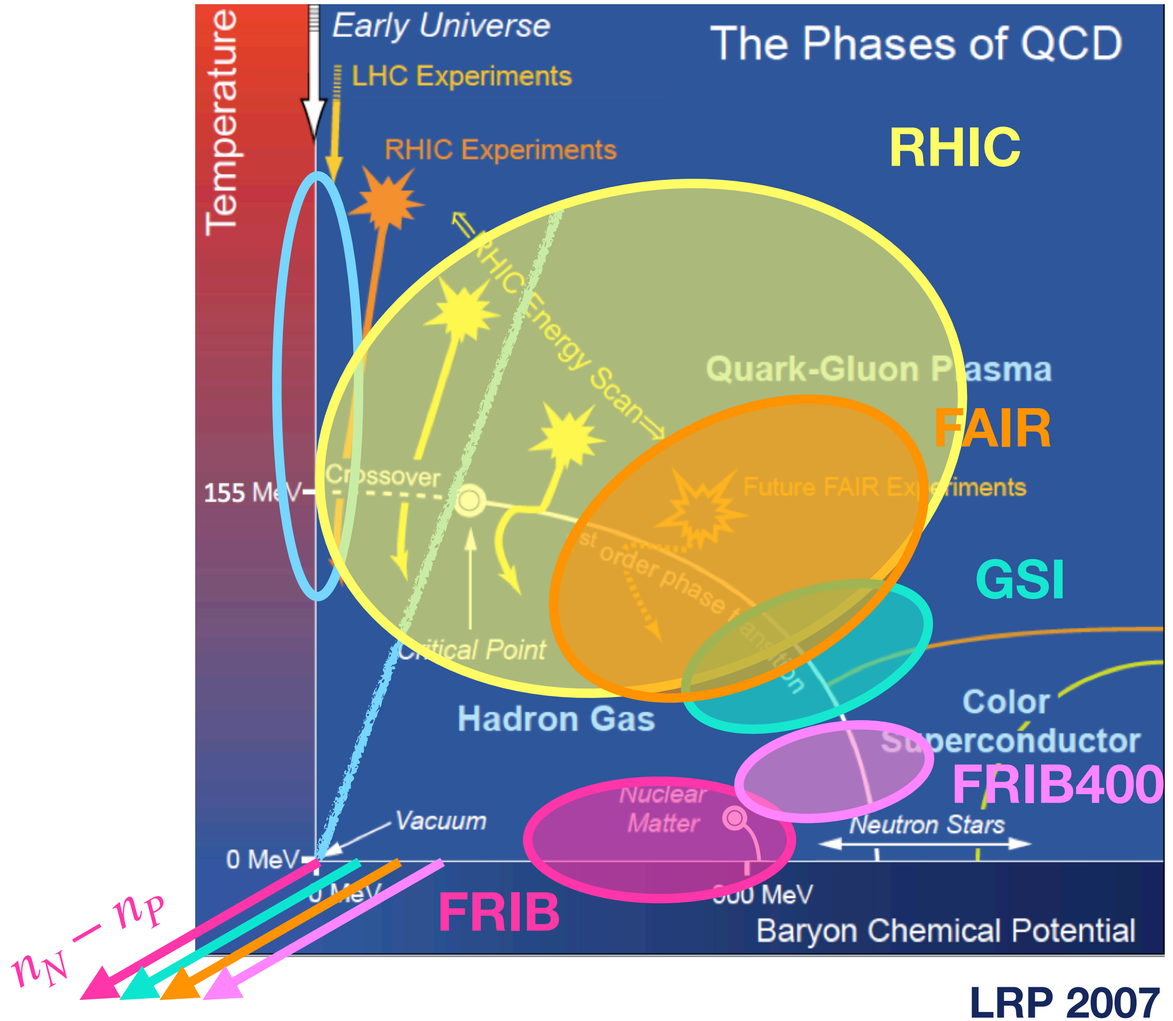

LRP 2007

Models predict a 1st order phase transition at large μ_B ~ large n_B

Recent EOS constraint using SMASH with flexible potentials

directed flow $v_1(y)$, slope $\mathrm{d}v_1/dy(y \approx 0)$

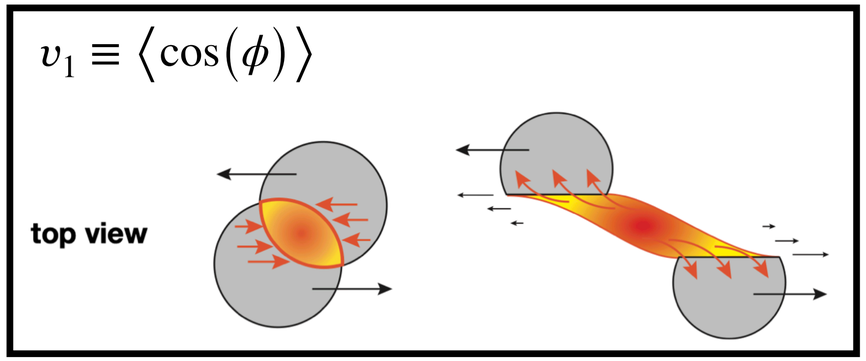

elliptic flow $v_2(y)$, at midrapidity $v_2(y \approx 0)$

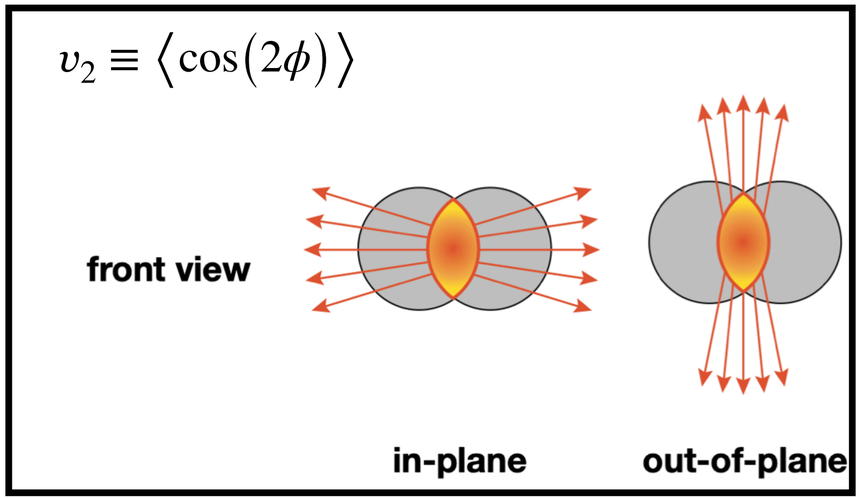

illustrations from a presentation by B. Kardan (HADES)

Recent EOS constraint using SMASH with flexible potentials

directed flow $v_1(y)$, slope $\mathrm{d}v_1/dy(y \approx 0)$

$$v_1 \equiv \langle \cos(\phi) \rangle$$

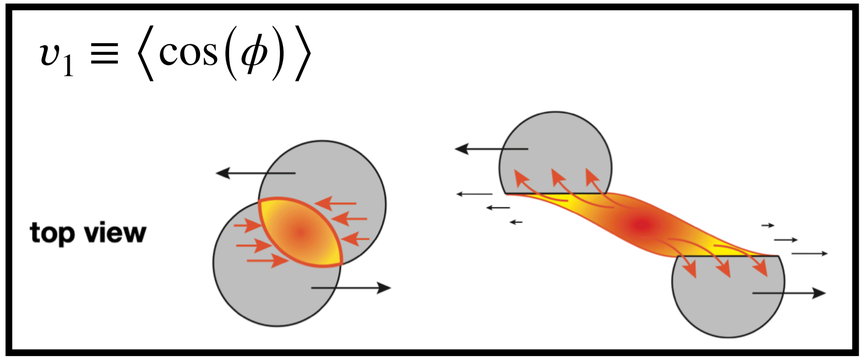

elliptic flow $v_2(y)$, at midrapidity $v_2(y \approx 0)$

$$v_2 \equiv \langle \cos(2\phi) \rangle$$

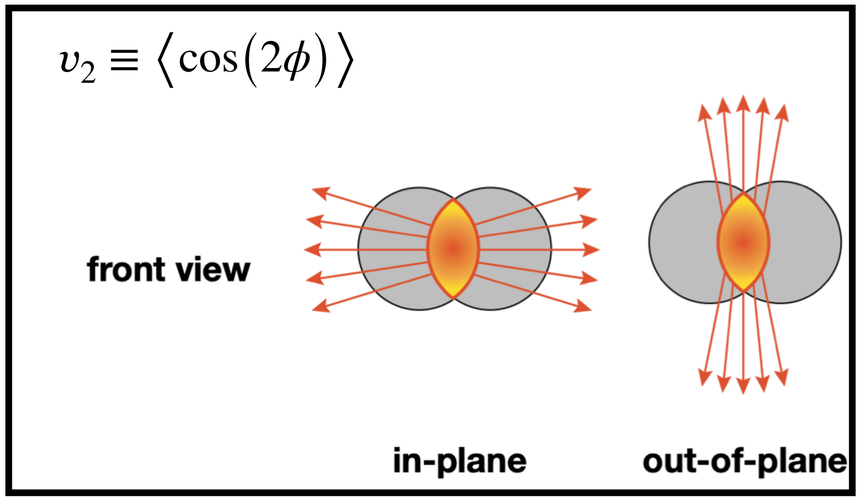

illustrations from a presentation by B. Kardan (HADES)

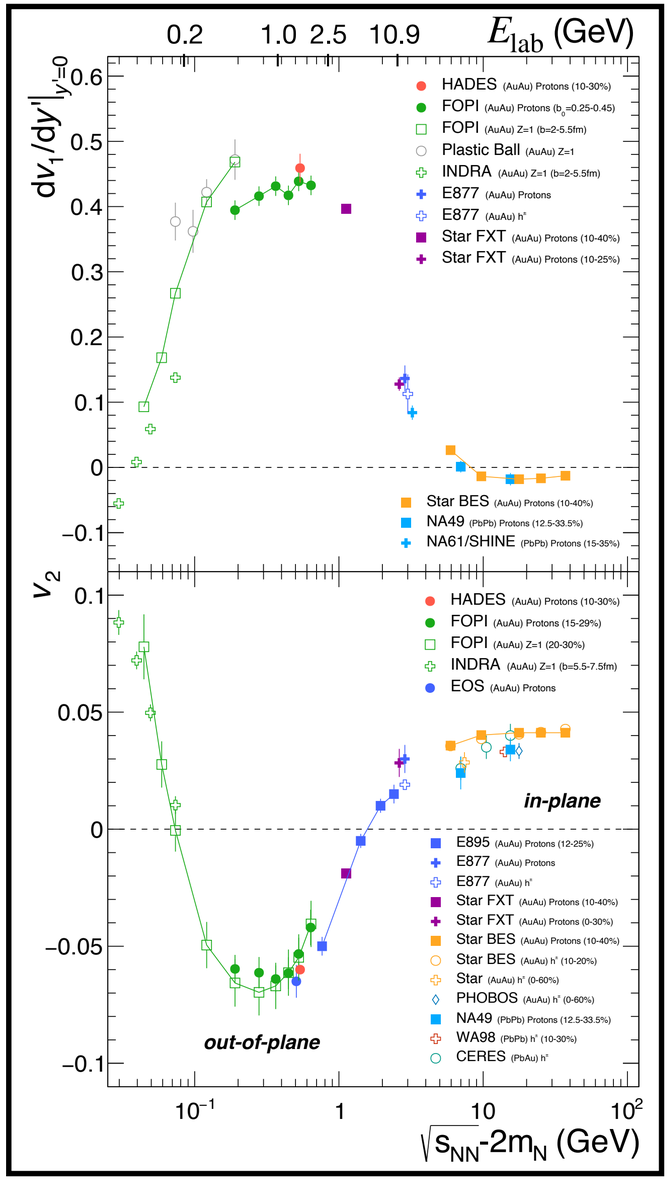

Recent EOS constraint using SMASH with flexible potentials

directed flow $v_1(y)$, slope $\mathrm{d}v_1/dy(y \approx 0)$

$v_1 \equiv \langle \cos(\phi) \rangle$

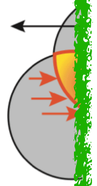

Experiments:
BES FXT,
FRIB & FRIB400,
HADES, CBM, ...

elliptic flow $v_2(y)$, at midrapidity $v_2(y \approx 0)$

$v_2 \equiv \langle \cos(2\phi) \rangle$

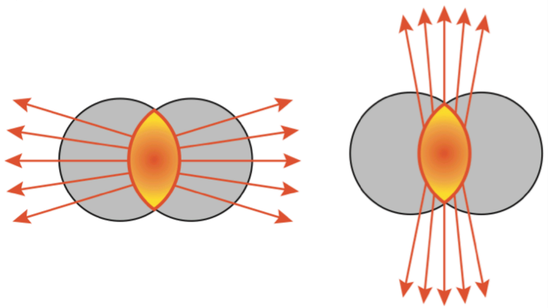

illustrations from a presentation by B. Kardan (HADES)

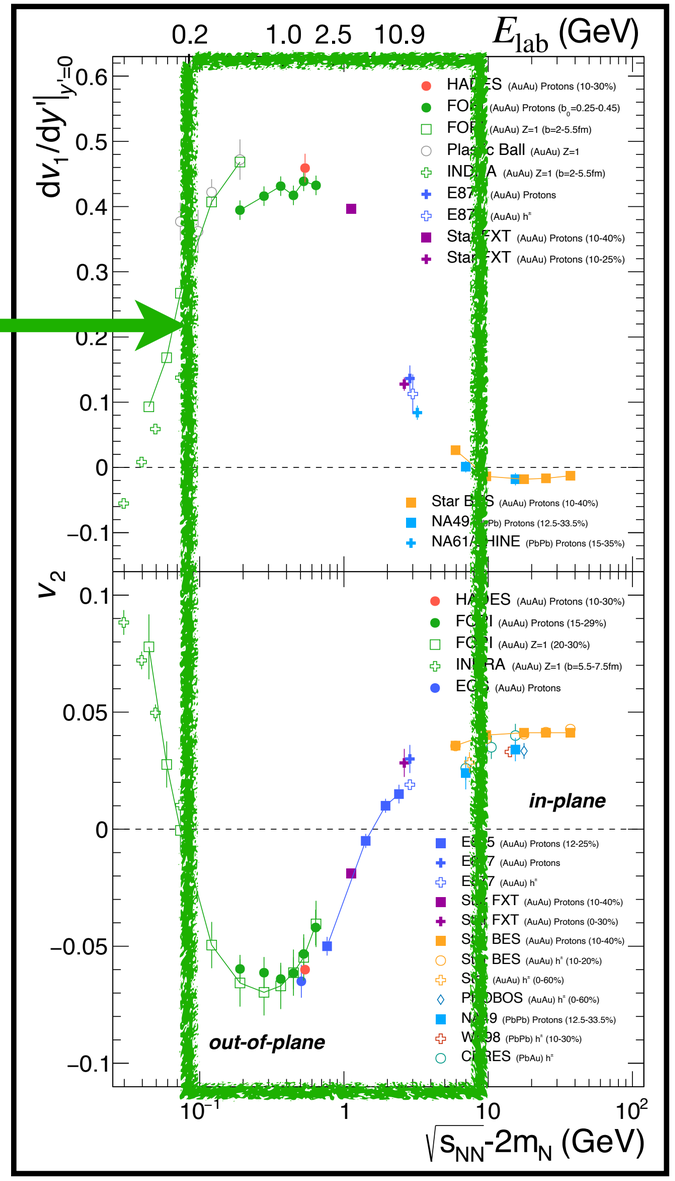

Recent EOS constraint using SMASH with flexible potentials

directed flow $v_1(y)$, slope $dv_1/dy(y \approx 0)$

$v_1 \equiv \langle \cos(\phi) \rangle$

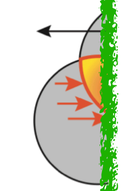

Experiments:
BES FXT,
FRIB & FRIB400,
HADES, CBM, ...

elliptic flow $v_2(y)$, at midrapidity $v_2(y \approx 0)$

$v_2 \equiv \langle \cos(2\phi) \rangle$

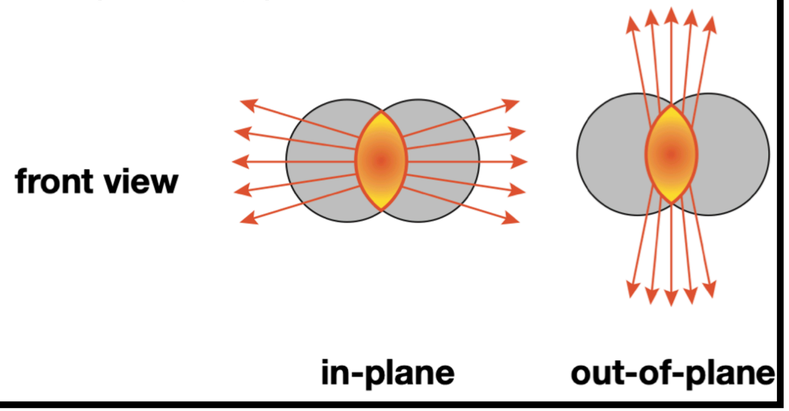

illustrations from a presentation by B. Kardan (HADES)

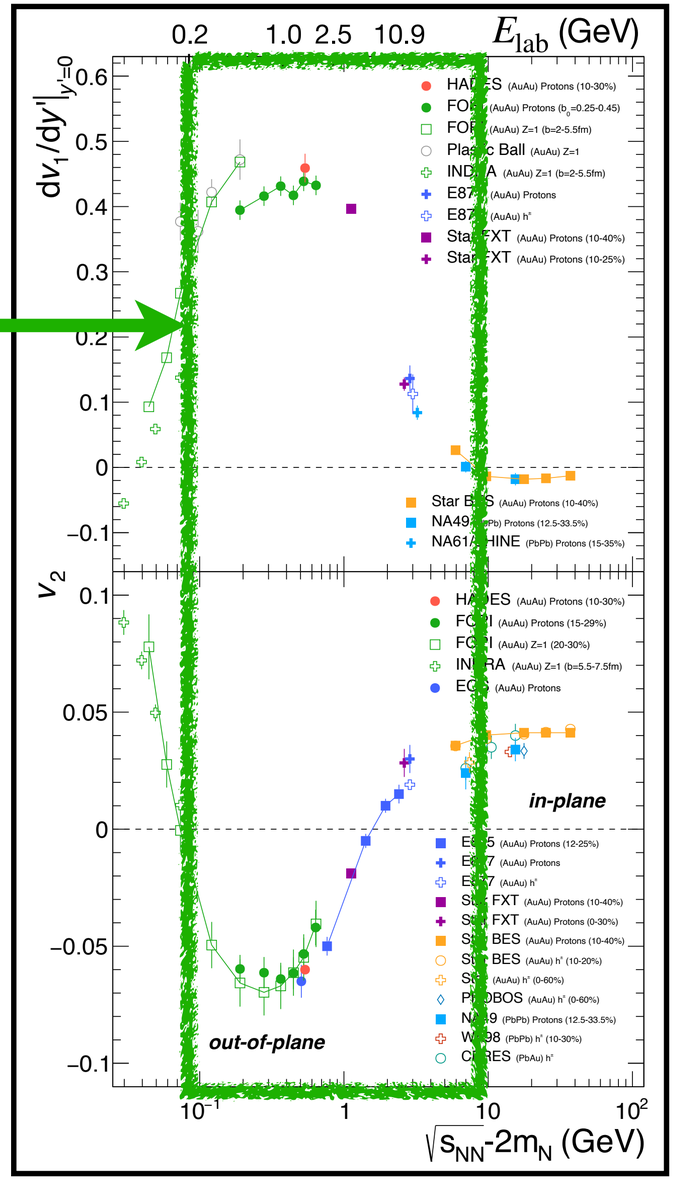

D. Oliinychenko, **A. Sorensen**, V. Koch, L. McLerran, Phys. Rev. C **108**, 3, 034908 (2023), arXiv:2208.11996

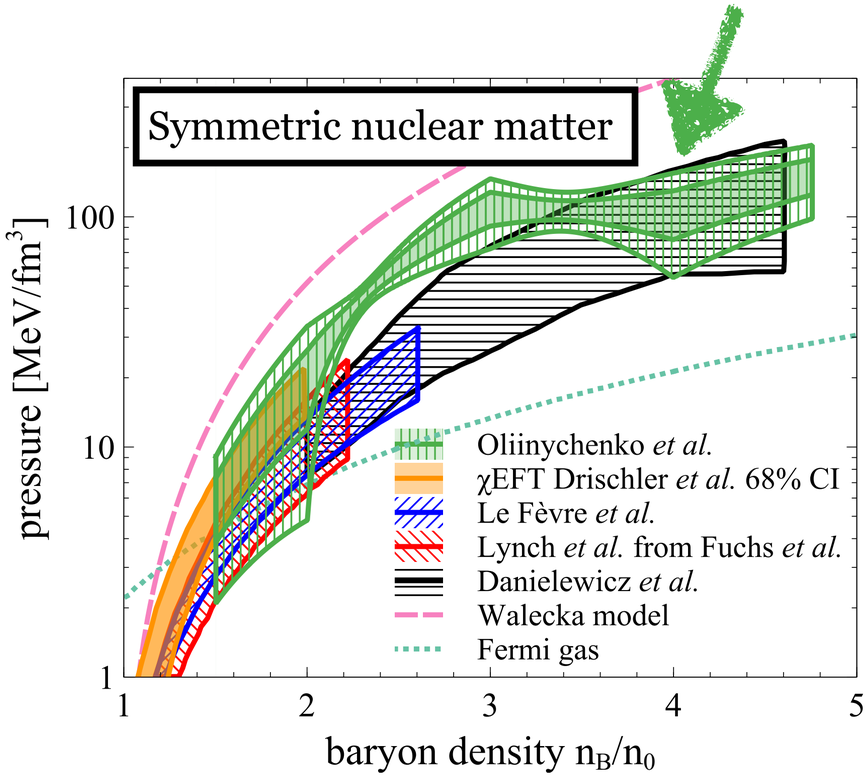

Possible first-order phase transition for
$n_B \in (3.0, 4.0)n_0 \quad \leftrightarrow \quad \sqrt{s_{NN}} \approx 4.5$ GeV

The QCD critical point: recent theoretical developments

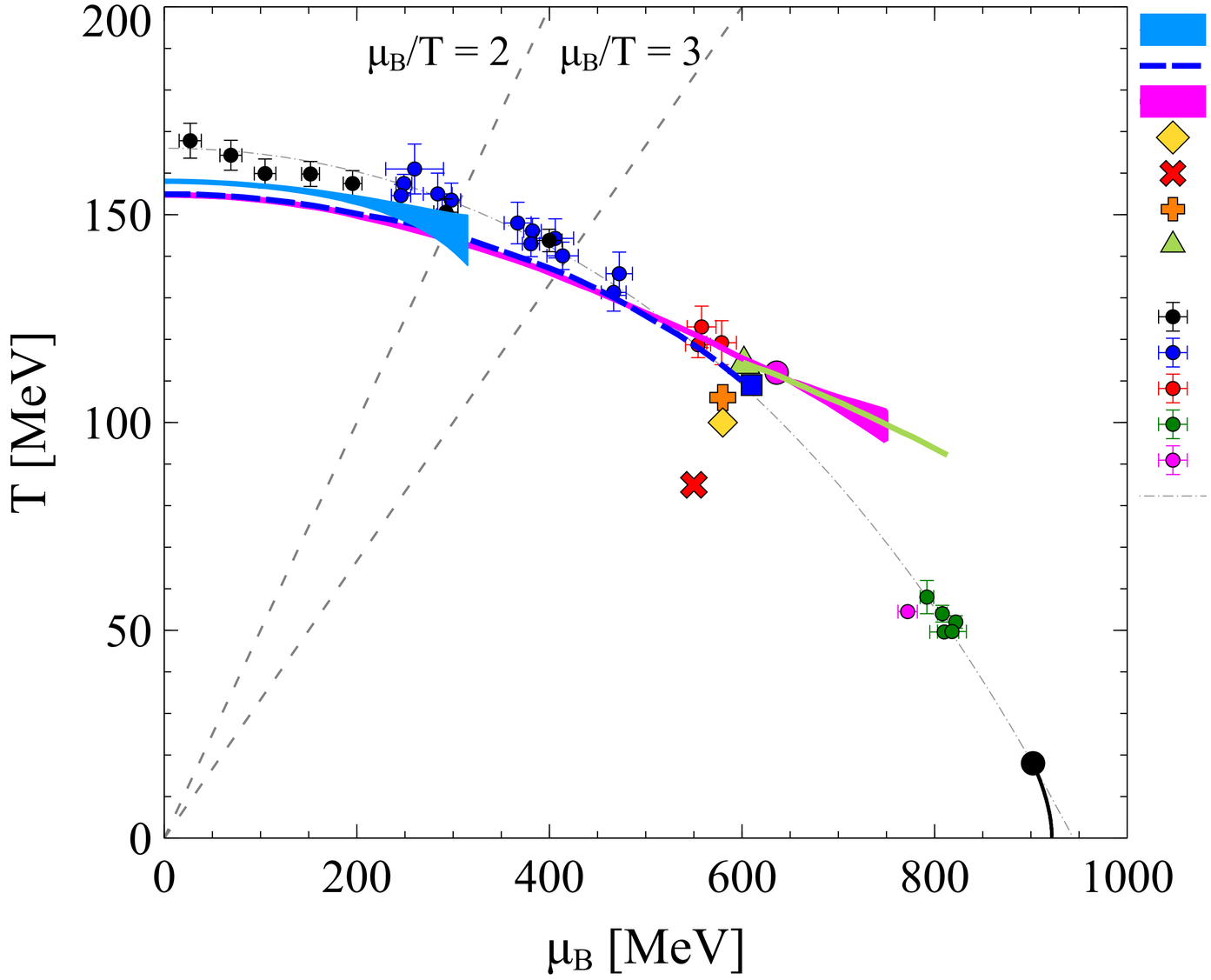

LQCD [Borsanyi et al., 2010.13705]
self-consistent fRG-DSE [Gao, Pawlowski 2010.13705]
truncated DSE [Gunkel, Fischer 2106.08356]
LYE Pade+conformal [Basar 2312.06952]
LYE Pade [Clarke et al., 2401.08820]
AdS/CFT [Hippert et al., 2309.00579]
s=const contours [Shah et al., 2410.16206]
freeze-outs:
RHIC BES-I [1701.07065]
SPS [hep-ph/0511092, nucl-th/0206014]
AGS [hep-ph/0511092, nucl-th/0206014]
SIS [nucl-th/9809027, hep-ph/0002267, nucl-ex/0012007]
HADES [2202.12750]
parametrization [Cleymans et al., hep-ph/0511094]

The QCD critical point: recent theoretical developments

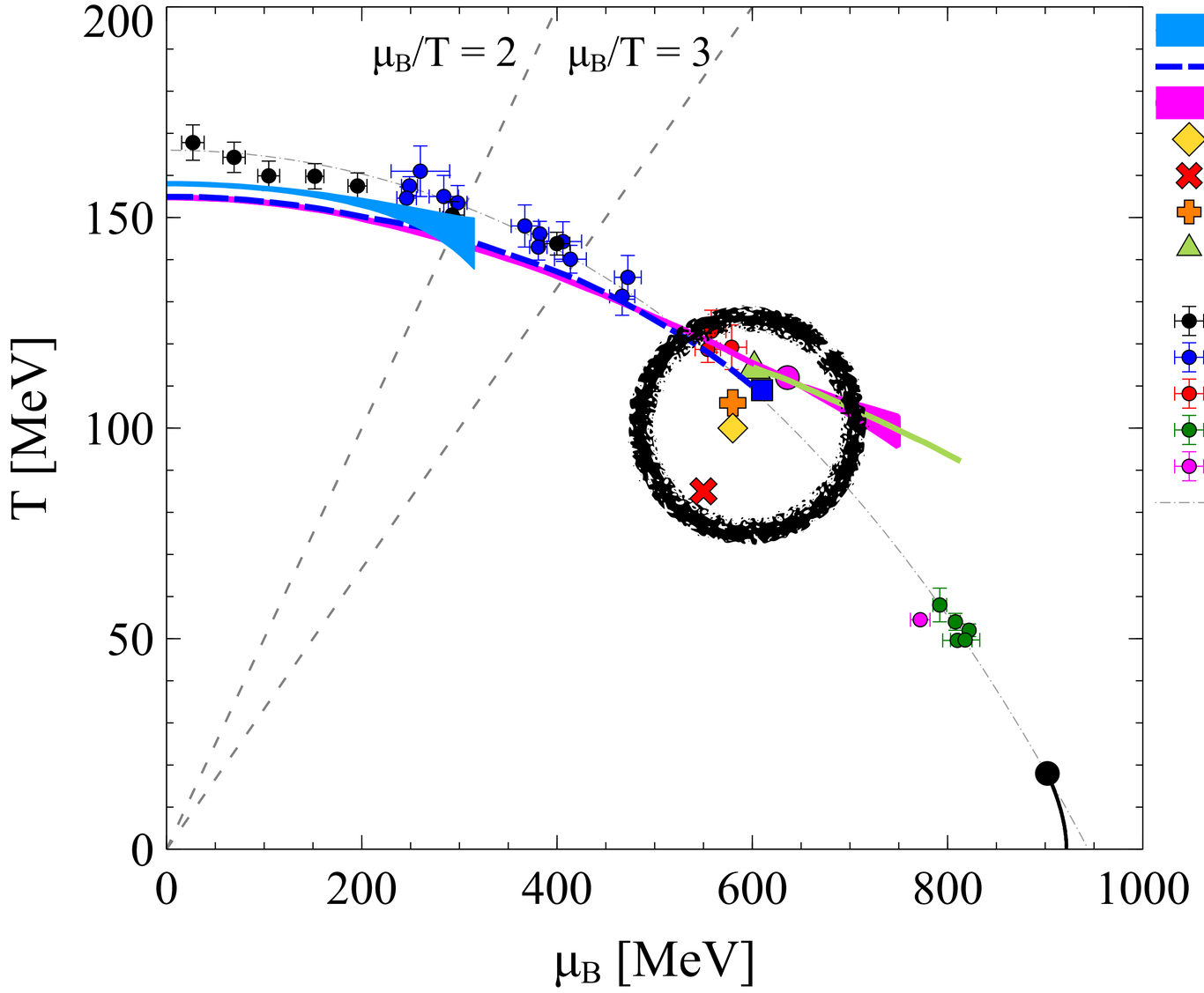

LQCD [Borsanyi et al., 2010.13705]
self-consistent fRG-DSE [Gao, Pawlowski 2010.13705]
truncated DSE [Gunkel, Fischer 2106.08356]
LYE Pade+conformal [Basar 2312.06952]
LYE Pade [Clarke et al., 2401.08820]
AdS/CFT [Hippert et al., 2309.00579]
s=const contours [Shah et al., 2410.16206]
freeze-outs:
RHIC BES-I [1701.07065]
SPS [hep-ph/0511092, nucl-th/0206014]
AGS [hep-ph/0511092, nucl-th/0206014]
SIS [nucl-th/9809027, hep-ph/0002267, nucl-ex/0012007]
HADES [2202.12750]
parametrization [Cleymans et al., hep-ph/0511094]

Dramatic change for the field:
the search for the CP is now
informed by theory.
This changes the path to discovery.
Previously: a “fishing expedition”.
Now: confirming/refuting predictions.

STAR experiment's search for the QCD CP

What observables are sensitive to the CP?

Baryon number susceptibilities:

$$\chi_B^{(k)} \equiv \left(\frac{\partial^k P}{\partial \mu_B^k} \right)_T$$

Related to cumulants of N_B:

$C_k = VT^{k-1}\chi_B^{(k)}$

Cumulants scale with the correlation length:

$C_2 \sim \xi^2 \ , \quad C_3 \sim \xi^{9/2} \ , \quad C_4 \sim \xi^7$

M.A. Stephanov, *Phys.Rev.Lett.* 102 (2009) 032301, arXiv:0809.3450

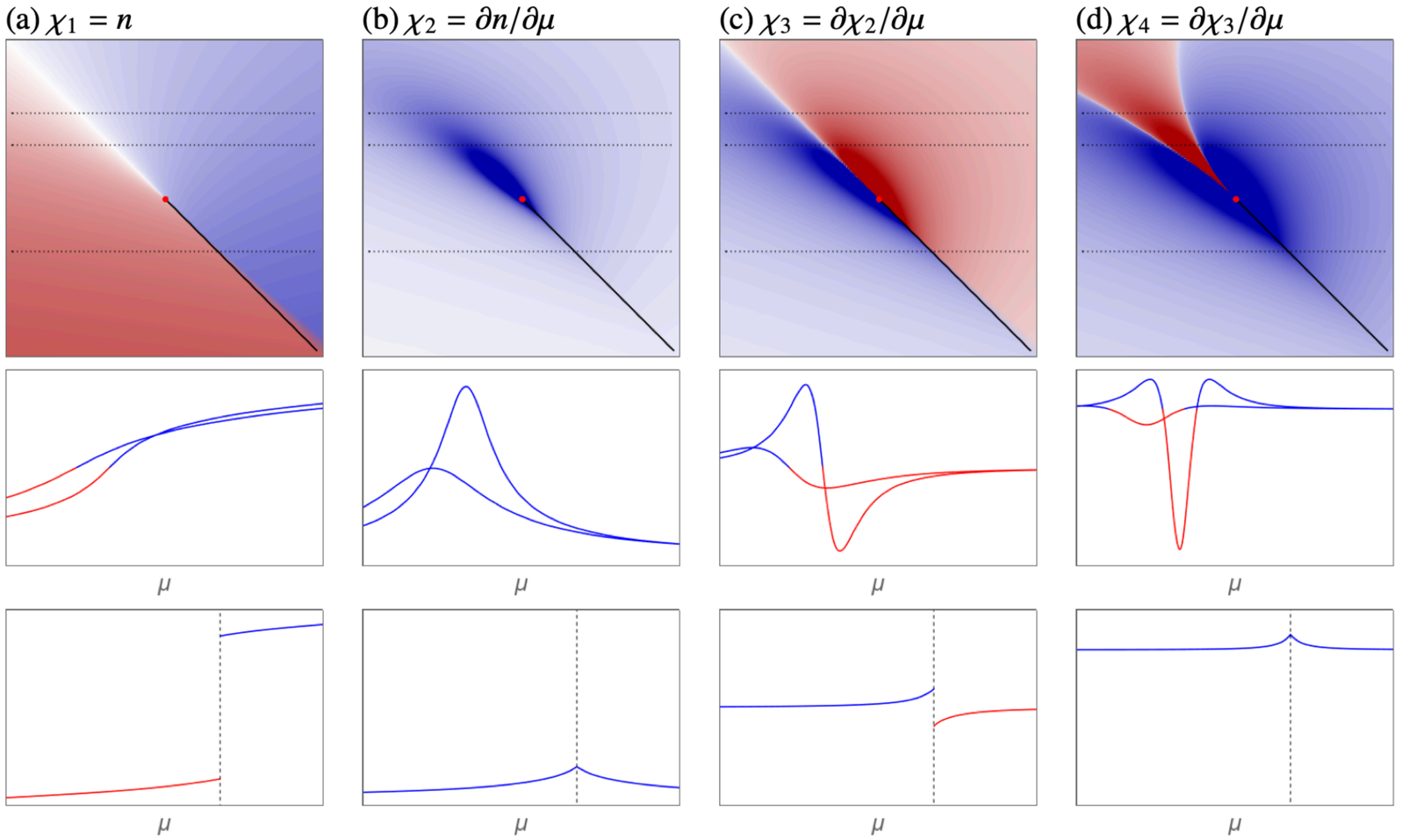

A. Bzdak, S. Esumi, V. Koch, J. Liao, M. Stephanov, N. Xu, *Phys.Rept.* 853 (2020) 1-87, arXiv:1906.00936

What observables are sensitive to the CP?

Baryon number susceptibilities:

$$\chi_B^{(k)} \equiv \left(\frac{\partial^k P}{\partial \mu_B^k} \right)_T$$

Related to cumulants of N_B:

$$C_k = VT^{k-1}\chi_B^{(k)}$$

Cumulants scale with the correlation length:

$$C_2 \sim \xi^2 \ , \quad C_3 \sim \xi^{9/2} \ , \quad C_4 \sim \xi^7$$

M.A. Stephanov, *Phys.Rev.Lett.* 102 (2009) 032301, arXiv:0809.3450

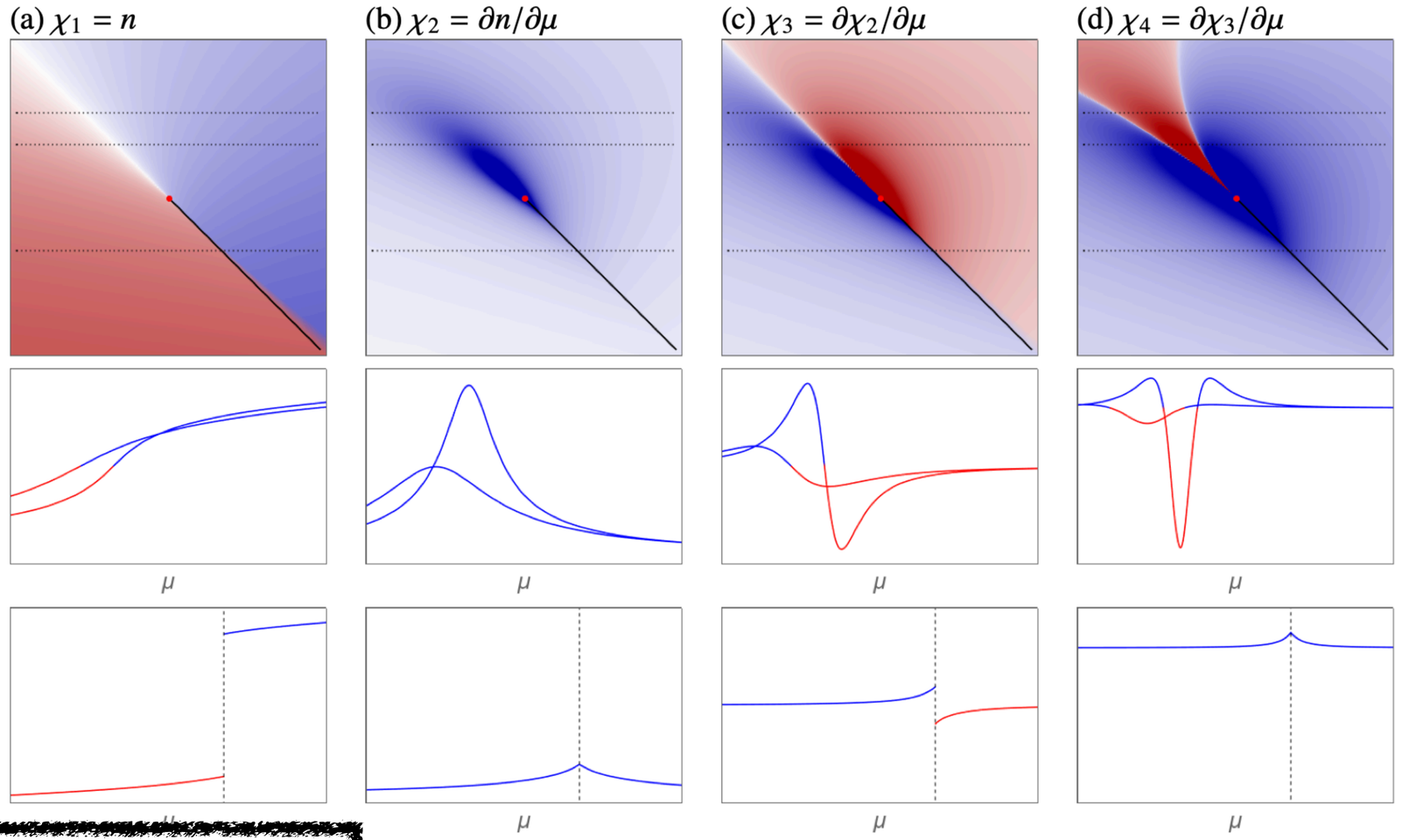

A. Bzdak, S. Esumi, V. Koch, J. Liao, M. Stephanov, N. Xu, *Phys.Rept.* 853 (2020) 1-87, arXiv:1906.00936

$$C_1 = \langle N \rangle$$
$$C_2 = \langle \left(N - \langle N \rangle\right)^2 \rangle = \sigma^2$$
$$C_3 = \langle \left(N - \langle N \rangle\right)^3 \rangle$$

measured in experiment!

High-order cumulants are a difficult and non-trivial measurement

- higher-order cumulants, by definition, measure the tails of the distribution: extremely difficult measurement, susceptible to detector, binning effects etc.
- critical slowing down: higher-order cumulants equilibrate at a *slower rate*
- still not enough statistics in C_4
- while C_2 has excellent statistics, there is no sign of a peak...
- how to compare cumulants measured with specific momentum cuts to infinite-matter expectations from theory???

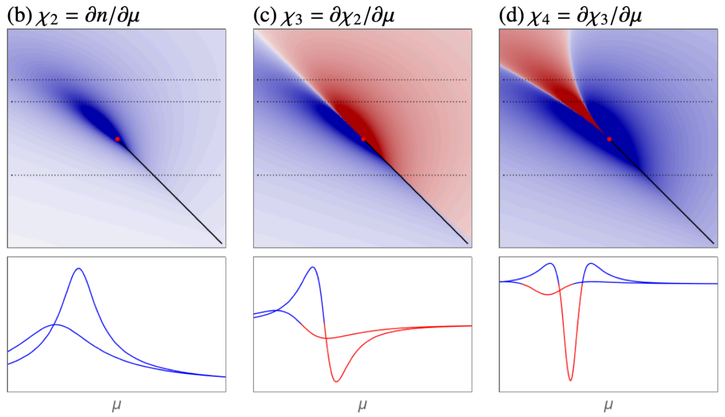

μ_B

$\sqrt{s}$

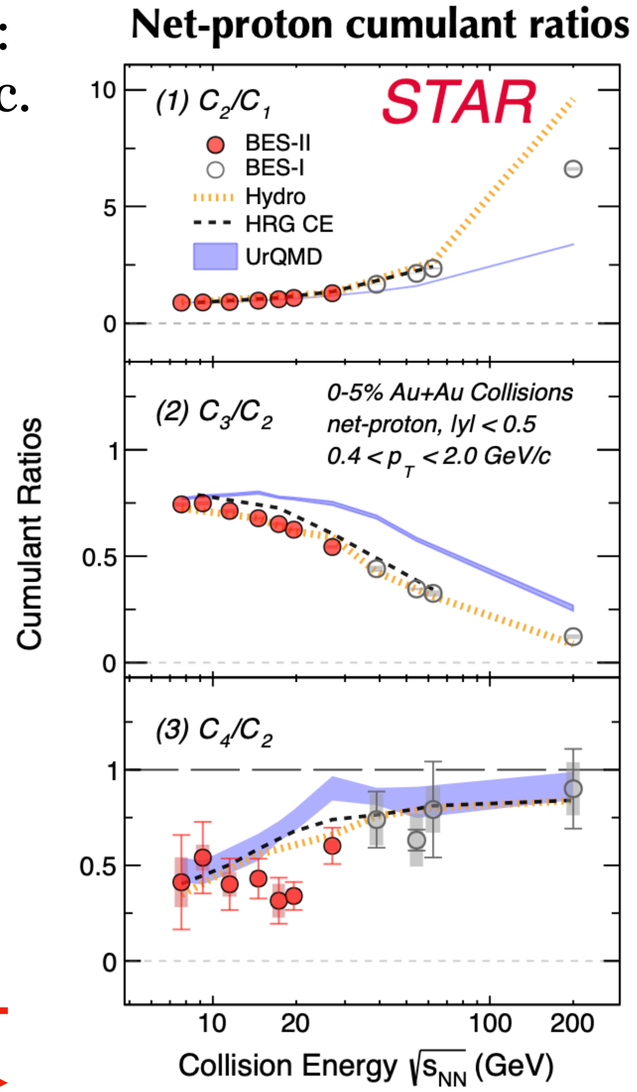

STAR, arXiv:2504.00817

High-order cumulants are a difficult and non-trivial measurement

- higher-order cumulants, by definition, measure the tails of the distribution: extremely difficult measurement, susceptible to detector, binning effects etc.
- critical slowing down: higher-order cumulants equilibrate at a *slower rate*
- still not enough statistics in C_4
- while C_2 has excellent statistics, there is no sign of a peak…
- how to compare cumulants measured with specific momentum cuts to infinite-matter expectations from theory???

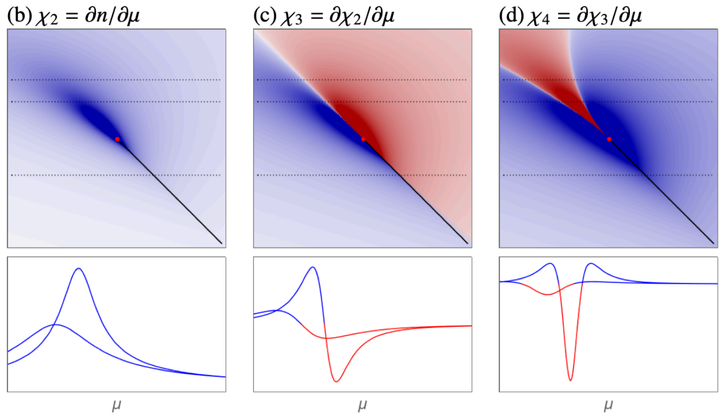

Possible approach: finite-size scaling?

- doesn't require measuring a peak
- leverages the universal scaling behavior
- explicitly uses the finite rapidity acceptance

μ_B

$\sqrt{s}$

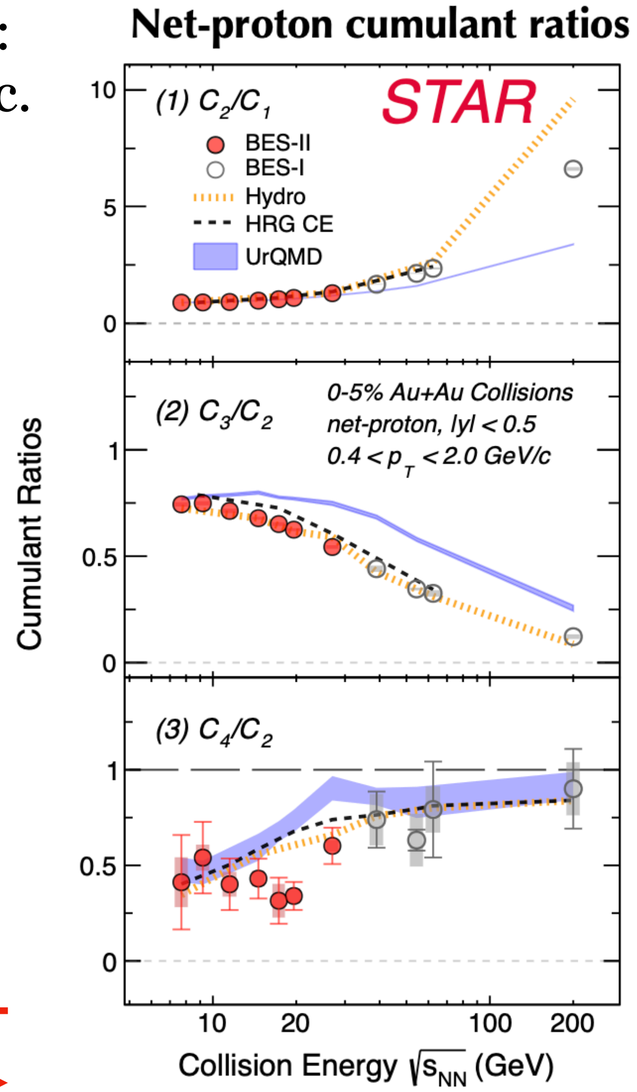

STAR, arXiv:2504.00817

Finite-size scaling

A. Sorensen, P. Sorensen, arXiv:2405.10278

Universal scaling behavior

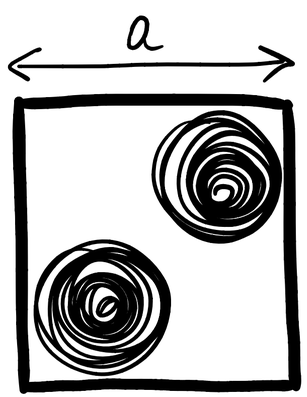

$L = a,\ \xi = \frac{a}{2} \ \Rightarrow\ x = \frac{1}{2}$

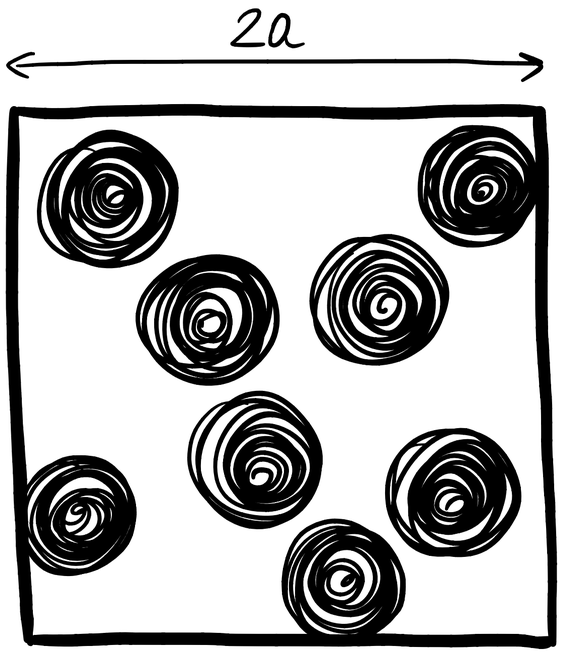

$L = 2a,\ \xi = \frac{a}{2} \ \Rightarrow\ x = \frac{1}{4}$

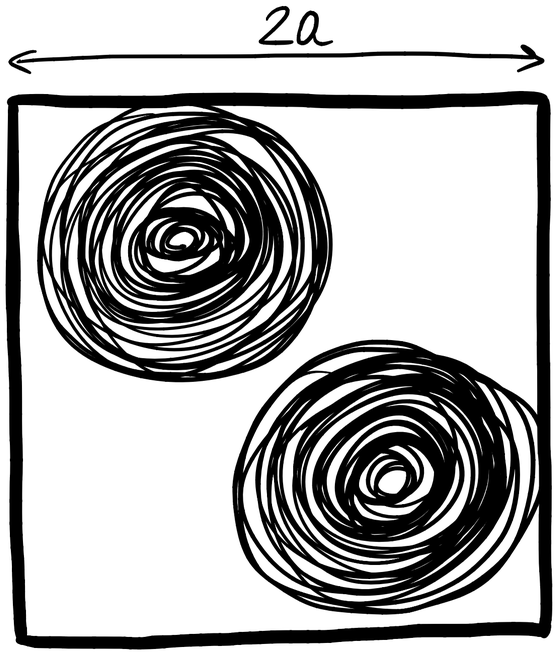

$L = 2a,\ \xi = a \ \Rightarrow\ x = \frac{1}{2}$

What the system "looks like" doesn't depend on the individual scales ξ, L,

but on their ratio $x = \frac{\xi}{L}$

Universal scaling behavior

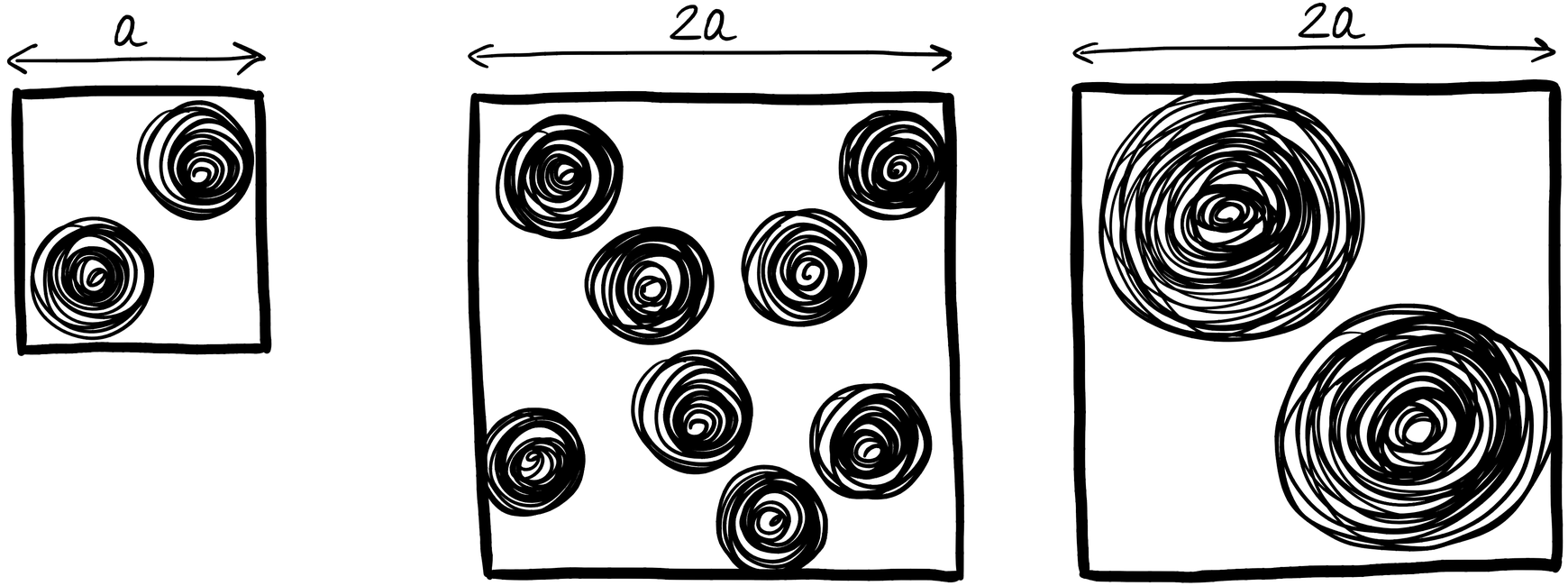

What the system "looks like" doesn't depend on the individual scales ξ, L, but on their ratio $x = \dfrac{\xi}{L}$

$L = a,\ \xi = \dfrac{a}{2} \ \Rightarrow\ x = \dfrac{1}{2}$ $\qquad$ $L = 2a,\ \xi = \dfrac{a}{2} \ \Rightarrow\ x = \dfrac{1}{4}$ $\qquad$ $L = 2a,\ \xi = a \ \Rightarrow\ x = \dfrac{1}{2}$

Usually: ξ constrained by finite range of the interaction, not thermodynamic conditions.
Near the CP: changing T or μ_B leads to appreciable changes in ξ (diverging when $T \approx T_c$ and $\mu_B \approx \mu_{B,c}$)

i.e., if at T_1 we have $\xi(T_1) = L/2$, there exists T_2 such that for $L_2 = \alpha L_1$ one again has $\xi(T_2) = \dfrac{L_2}{2} = \dfrac{(\alpha L_1)}{2} = \alpha \dfrac{L_1}{2} = \alpha \xi(T_1)$

Universal scaling behavior

$$\xi \sim \left| \frac{T - T_c}{T_c} \right|^{-\nu} = |t|^{-\nu}$$

scale which controls the system's behavior: $x = \dfrac{|t|^{-\nu}}{L}$

convenient to use *the scaling variable* $u = x^{-1/\nu} = |t| L^{1/\nu}$

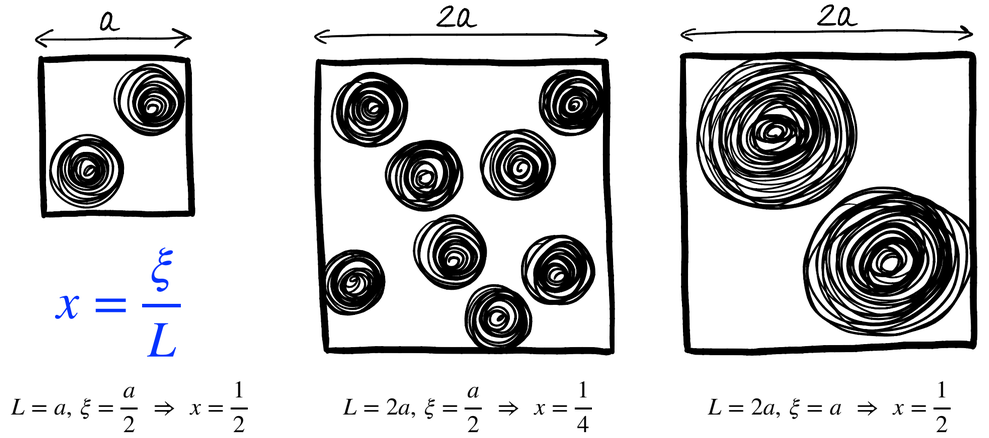

$x = \dfrac{\xi}{L}$

$L = a,\ \xi = \frac{a}{2} \Rightarrow x = \frac{1}{2}$ $L = 2a,\ \xi = \frac{a}{2} \Rightarrow x = \frac{1}{4}$ $L = 2a,\ \xi = a \Rightarrow x = \frac{1}{2}$

plotting observables at different T and L against u:
systems which "look the same" will have the same position on the u-axis

Universal scaling behavior

$$\xi \sim \left| \frac{T - T_c}{T_c} \right|^{-\nu} = |t|^{-\nu}$$

scale which controls the system's behavior: $x = \dfrac{|t|^{-\nu}}{L}$

convenient to use *the scaling variable* $u = x^{-1/\nu} = |t| L^{1/\nu}$

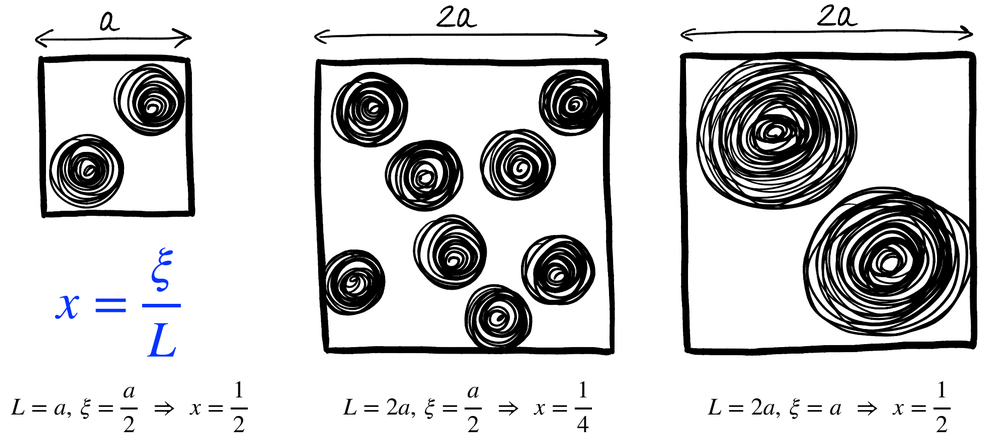

$x = \dfrac{\xi}{L}$

$L = a,\ \xi = \frac{a}{2} \Rightarrow x = \frac{1}{2}$ $L = 2a,\ \xi = \frac{a}{2} \Rightarrow x = \frac{1}{4}$ $L = 2a,\ \xi = a \Rightarrow x = \frac{1}{2}$

plotting observables at different T and L against u:
systems which "look the same" will have the same position on the u-axis

Can we also align observables measured at different T and L? Yes!

susceptibility: $\chi \sim |t|^{-\gamma} \sim \xi^{\gamma/\nu} = (xL)^{\gamma/\nu} = u^{-\gamma} L^{\gamma/\nu}$

plotting $\tilde{\chi} = \chi L^{-\gamma/\nu}$ at different T and L against u:
systems which "look the same" will have the same position on the u-axis *and* the same value on the $\tilde{\chi}$-axis

Universal scaling behavior

$$\xi \sim \left| \frac{T - T_c}{T_c} \right|^{-\nu} = |t|^{-\nu}$$

scale which controls the system's behavior: $x = \dfrac{|t|^{-\nu}}{L}$

convenient to use *the scaling variable* $u = x^{-1/\nu} = |t| L^{1/\nu}$

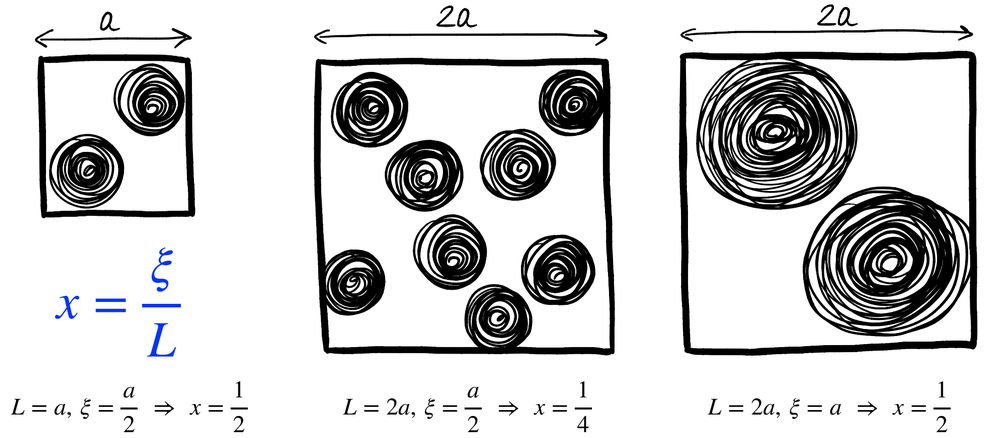

$x = \dfrac{\xi}{L}$

$L = a,\ \xi = \frac{a}{2} \Rightarrow x = \frac{1}{2}$ $L = 2a,\ \xi = \frac{a}{2} \Rightarrow x = \frac{1}{4}$ $L = 2a,\ \xi = a \Rightarrow x = \frac{1}{2}$

plotting observables at different T and L against u:
systems which "look the same" will have the same position on the u-axis

Can we also align observables measured at different T and L? Yes!

provided that we use the correct value of u = we know T_c

susceptibility: $\chi \sim |t|^{-\gamma} \sim \xi^{\gamma/\nu} = (xL)^{\gamma/\nu} = u^{-\gamma} L^{\gamma/\nu}$

plotting $\tilde{\chi} = \chi L^{-\gamma/\nu}$ at different T and L against u:
systems which "look the same" will have the same position on the u-axis *and* the same value on the $\tilde{\chi}$-axis

Universal scaling behavior

$$\xi \sim \left| \frac{T - T_c}{T_c} \right|^{-\nu} = |t|^{-\nu}$$

scale which controls the system's behavior: $x = \dfrac{|t|^{-\nu}}{L}$

convenient to use *the scaling variable* $u = x^{-1/\nu} = |t| L^{1/\nu}$

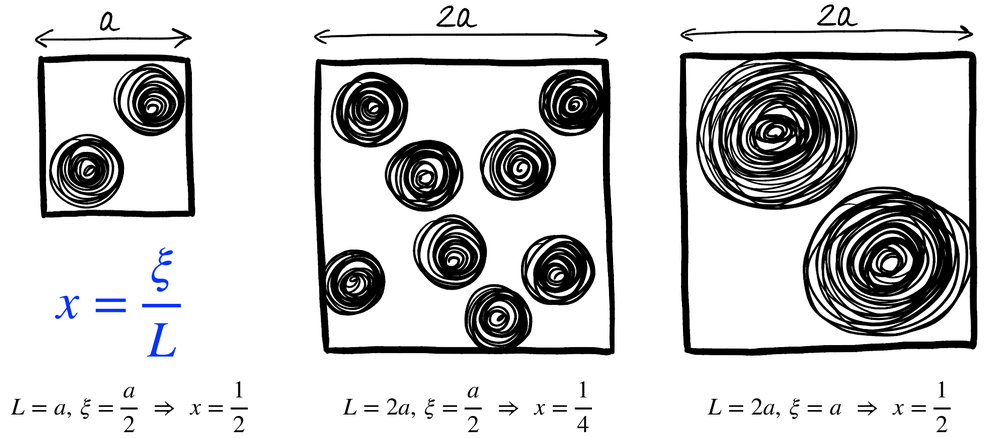

$x = \dfrac{\xi}{L}$

$L = a,\ \xi = \frac{a}{2} \Rightarrow x = \frac{1}{2}$ $L = 2a,\ \xi = \frac{a}{2} \Rightarrow x = \frac{1}{4}$ $L = 2a,\ \xi = a \Rightarrow x = \frac{1}{2}$

plotting observables at different T and L against u:
systems which "look the same" will have the same position on the u-axis

Can we also align observables measured at different T and L? Yes!

provided that we use the correct value of u = we know T_c

susceptibility: $\chi \sim |t|^{-\gamma} \sim \xi^{\gamma/\nu} = (xL)^{\gamma/\nu} = u^{-\gamma} L^{\gamma/\nu}$

one can find T_c *by plotting:* test different T_c until things align!

plotting $\tilde{\chi} = \chi L^{-\gamma/\nu}$ at different T and L against u:
systems which "look the same" will have the same position on the u-axis *and* the same value on the $\tilde{\chi}$-axis

Universal scaling behavior

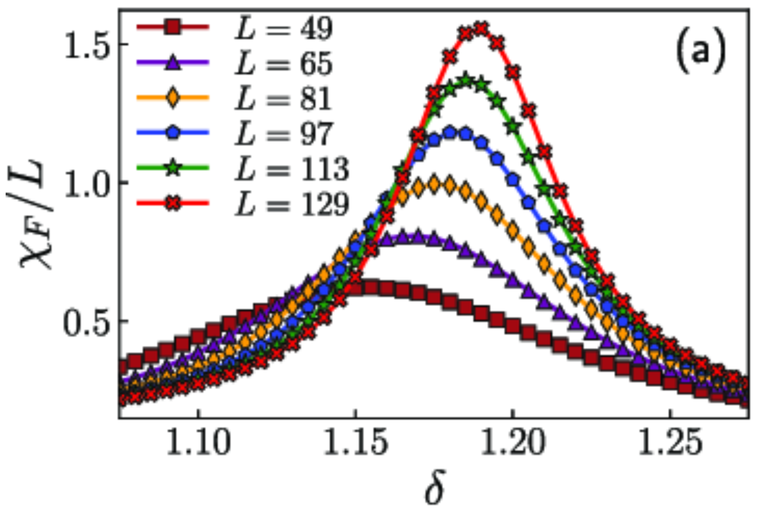

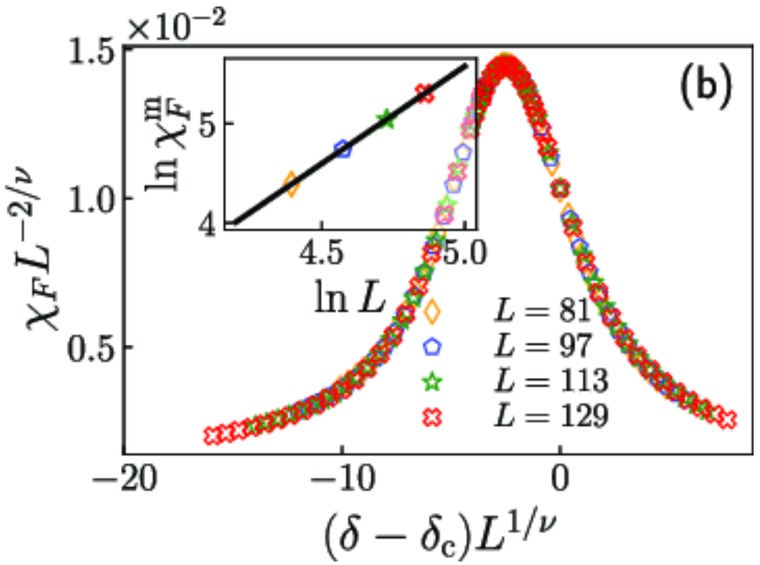

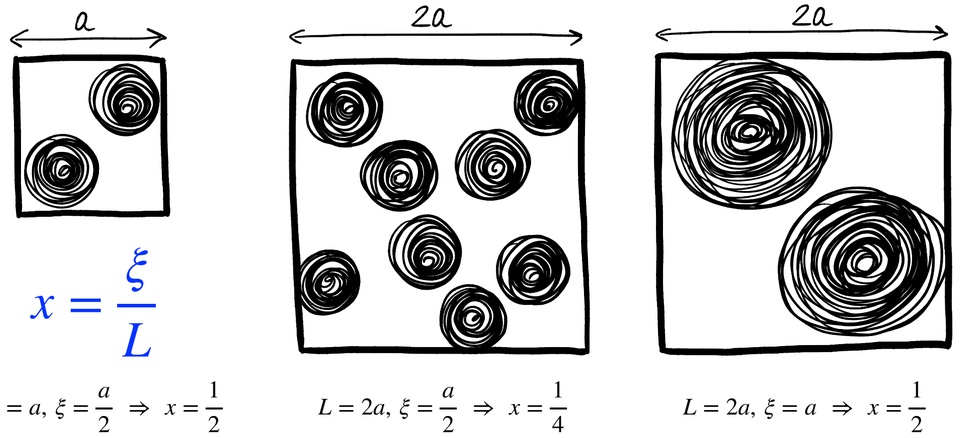

X.-J. Yu, S. Yang, J. Xu, J.-B. Xu, L. Xu, *Fidelity susceptibility as a diagnostic of the commensurate-incommensurate transition: A revisit of the programmable Rydberg chain*, *Phys. Rev. B* **106**, 165124 (2022), arXiv:2207.08337

provided that we use the correct value of u = we know T_c

susceptibility: $\chi \sim |t|^{-\gamma} \sim \xi^{\gamma/\nu} = (xL)^{\gamma/\nu} = u^{-\gamma} L^{\gamma/\nu}$

one can find T_c by plotting: test different T_c until things align!

plotting $\tilde{\chi} = \chi L^{-\gamma/\nu}$ at different T and L against u:
systems which "look the same" will have the same position on the u-axis *and* the same value on the $\tilde{\chi}$-axis

Finite size vs. window size

$$\chi L^{-\frac{\sigma}{\nu}} = \phi(tL^{\frac{1}{\nu}})$$

Finite-size scaling: change the size of the system, calculate $\chi(T, L)$, repeat

However, changing SIZE is not always possible or doesn't probe the same system:
bird flocks, heavy-ion collisions, ...

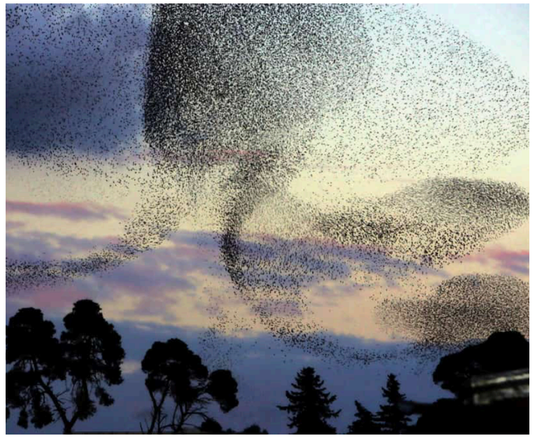

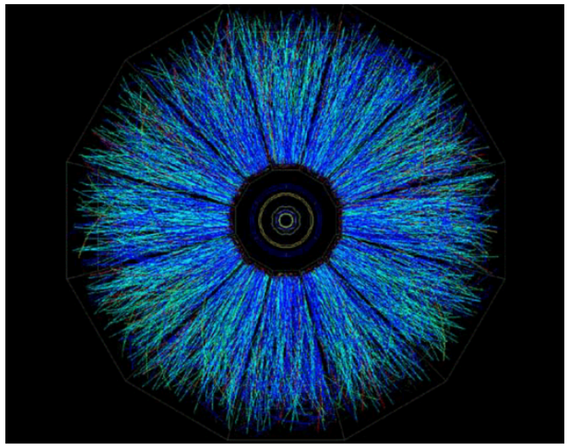

Finite size vs. window size

$$\chi L^{-\frac{\sigma}{\nu}} = \phi(tL^{\frac{1}{\nu}})$$

Finite-size scaling: change the size of the system, calculate $\chi(T, L)$, repeat

However, changing SIZE is not always possible or doesn't probe the same system:
bird flocks, heavy-ion collisions, ...

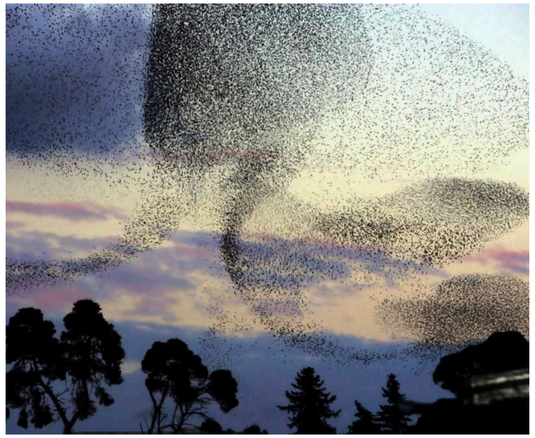

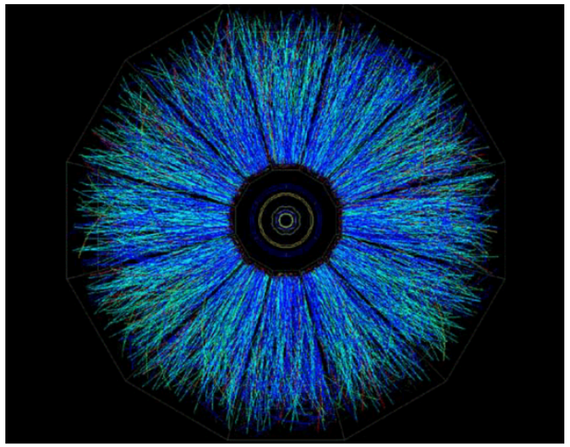

Solution: study the dependence of observables on the size of the *subsystem* that is considered

D. Martin, T. Ribeiro, S. Cannas, *et al.*, Box scaling as a proxy of finite size correlations, Sci Rep 11, 15937 (2021)

Finite size vs. window size

$$\chi L^{-\frac{\sigma}{\nu}} = \phi(tL^{\frac{1}{\nu}})$$

Finite-size scaling: change the size of the system, calculate $\chi(T, L)$, repeat

However, changing SIZE is not always possible or doesn't probe the same system:
bird flocks, heavy-ion collisions, ...

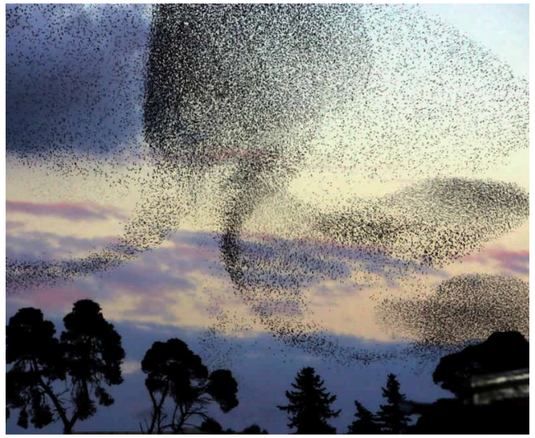

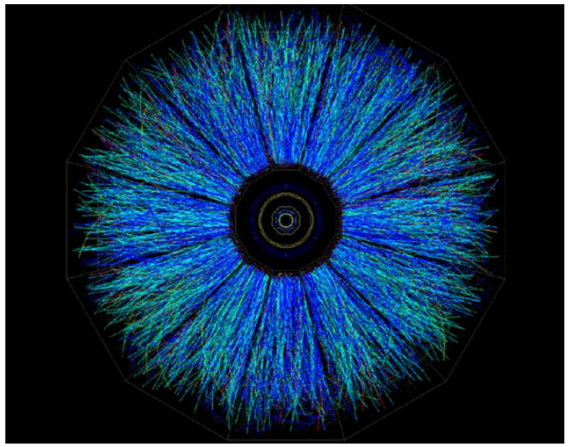

Solution: study the dependence of observables on the size of the *subsystem* that is considered

D. Martin, T. Ribeiro, S. Cannas, *et al.*, Box scaling as a proxy of finite size correlations, Sci Rep 11, 15937 (2021)

THIS WORK: the size of the *subsystem* = rapidity bin width W

A. Sorensen, P. Sorensen, arXiv:2405.10278

Finite size vs. window size

$$\chi L^{-\frac{\sigma}{\nu}} = \phi(tL^{\frac{1}{\nu}})$$

Finite-size scaling: change the size of the system, calculate $\chi(T, L)$, repeat

However, changing SIZE is not always possible or doesn't probe the same system:
bird flocks, heavy-ion collisions, …

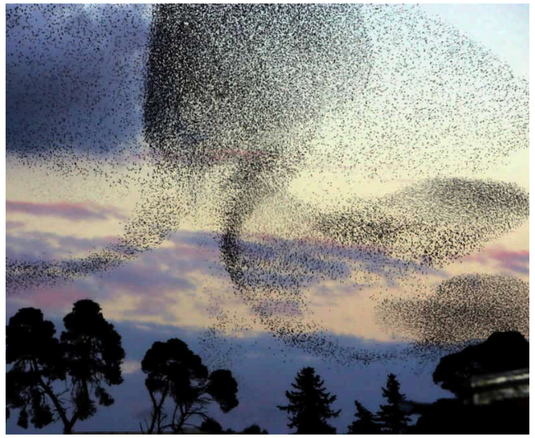

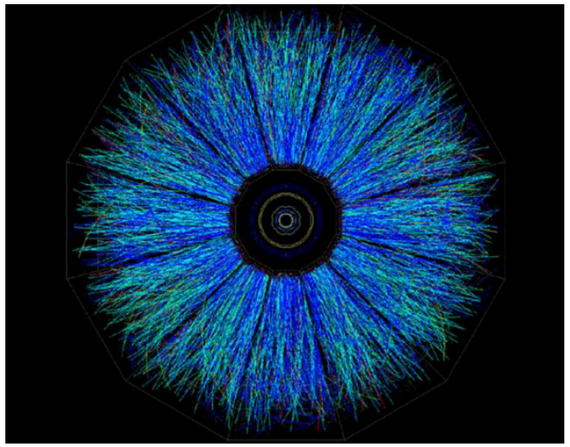

What are the scales relevant to the problem?

system size = rapidity window W, temperature, chemical potential

Tests in simulations

Finite-size scaling analysis of cumulants in a periodic box

- framework: hadronic transport with a *known* EOS (calculate κ_2/κ_1 “on paper”)
- simulation: box with periodic boundary conditions at chosen (n_B, T)
- uniform initialization at $t = 0$, development of fluctuations in response to the EOS

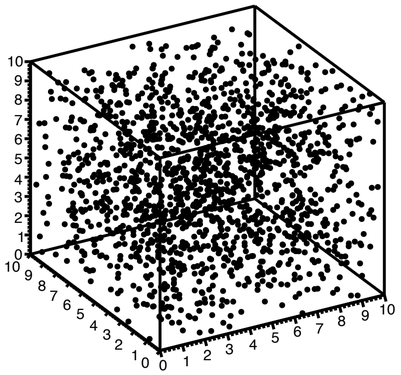

Finite-size scaling analysis of cumulants in a periodic box

- framework: hadronic transport with a *known* EOS (calculate κ_2/κ_1 "on paper")
- simulation: box with periodic boundary conditions at chosen (n_B, T)
- uniform initialization at $t = 0$, development of fluctuations in response to the EOS

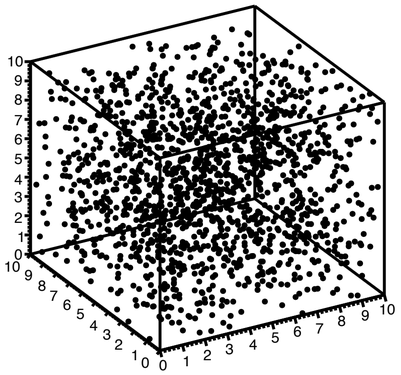

EOS: relativistic polynomial w/ 2 phase transitions

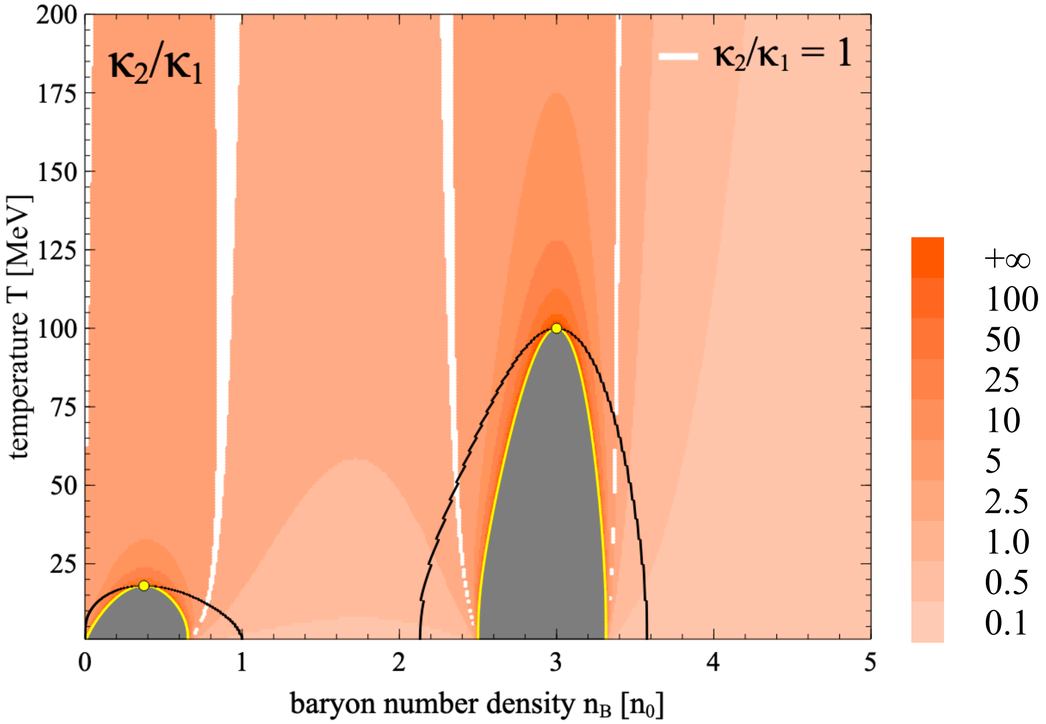

AS and V. Koch, Phys. Rev. C **104**, 3, 034904 (2021), arXiv:2011.06635

Finite-size scaling analysis of cumulants in a periodic box

- framework: hadronic transport with a *known* EOS (calculate κ_2/κ_1 "on paper")
- simulation: box with periodic boundary conditions at chosen (n_B, T)
- uniform initialization at $t = 0$, development of fluctuations in response to the EOS

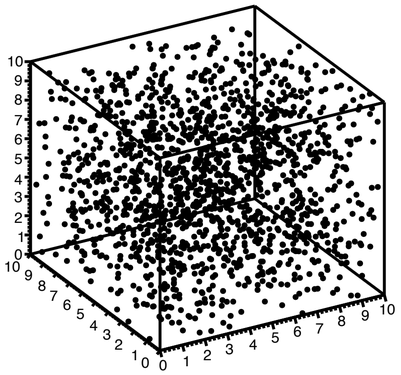

EOS: relativistic polynomial w/ 2 phase transitions

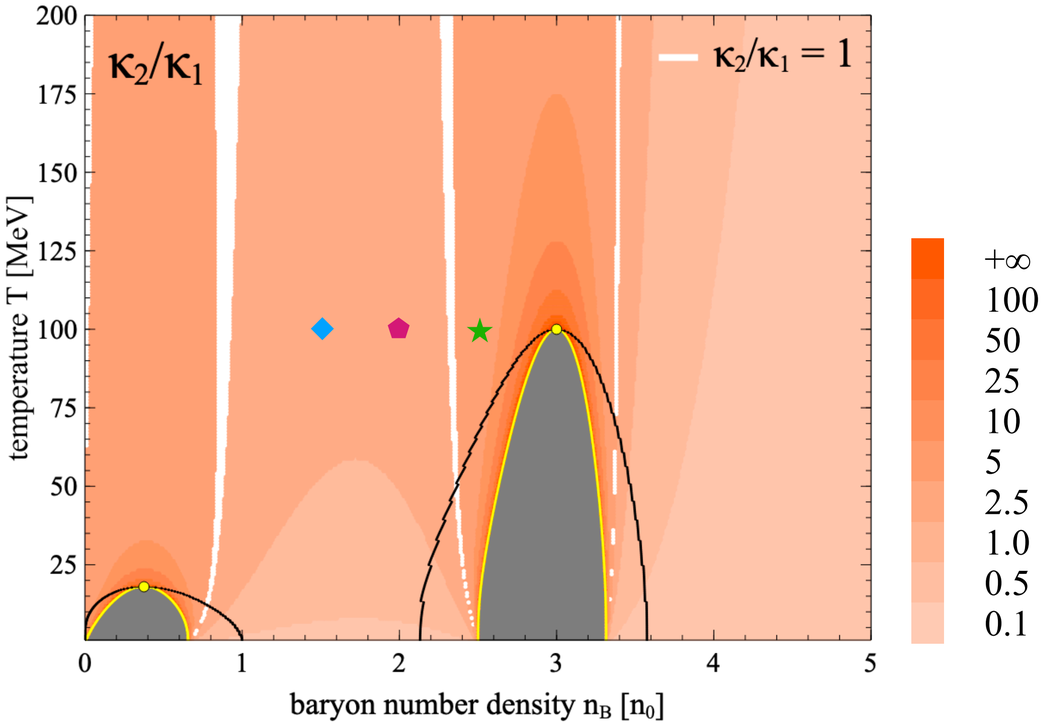

	◆	⬟	★
T [MeV]	100	100	100
nB [n0]	1.5	2.0	2.5
(k2/k1)inf	0.67	0.70	1.46

AS and V. Koch, Phys. Rev. C **104**, 3, 034904 (2021), arXiv:2011.06635

Finite-size scaling analysis of cumulants in a periodic box

- framework: hadronic transport with a *known* EOS (calculate κ_2/κ_1 "on paper")
- simulation: box with periodic boundary conditions at chosen (n_B, T)
- uniform initialization at $t = 0$, development of fluctuations in response to the EOS

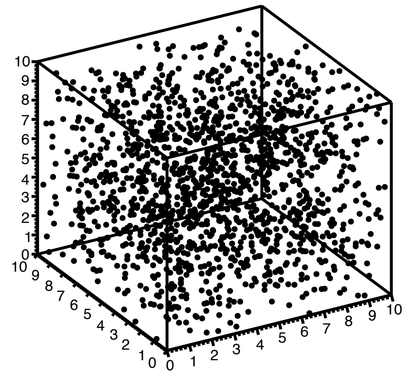

EOS: relativistic polynomial w/ 2 phase transitions

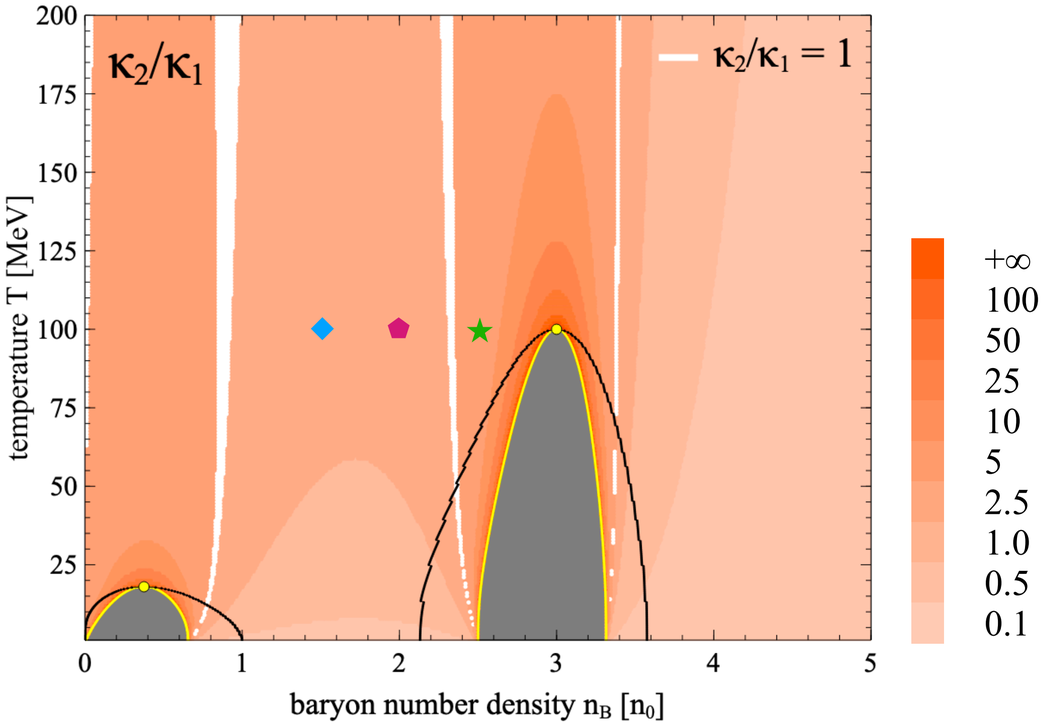

	◆	⬟	★
T [MeV]	100	100	100
nB [n0]	1.5	2.0	2.5
(k2/k1)inf	0.67	0.70	1.46

consider κ_2/κ_1
at different subvolumes

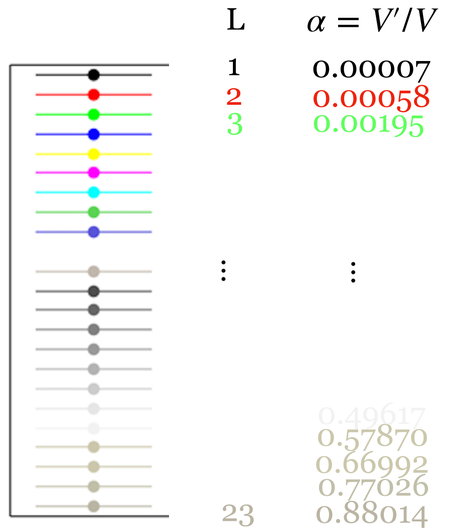

AS and V. Koch, Phys. Rev. C **104**, 3, 034904 (2021), arXiv:2011.06635

Finite-size scaling analysis of cumulants in a periodic box

- framework: hadronic transport with a *known* EOS (calculate κ_2/κ_1 "on paper")
- simulation: box with periodic boundary conditions at chosen (n_B, T)
- uniform initialization at $t = 0$, development of fluctuations in response to the EOS

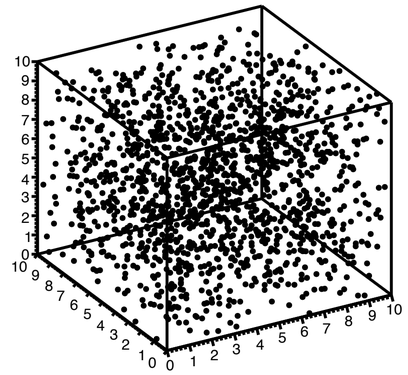

EOS: relativistic polynomial w/ 2 phase transitions

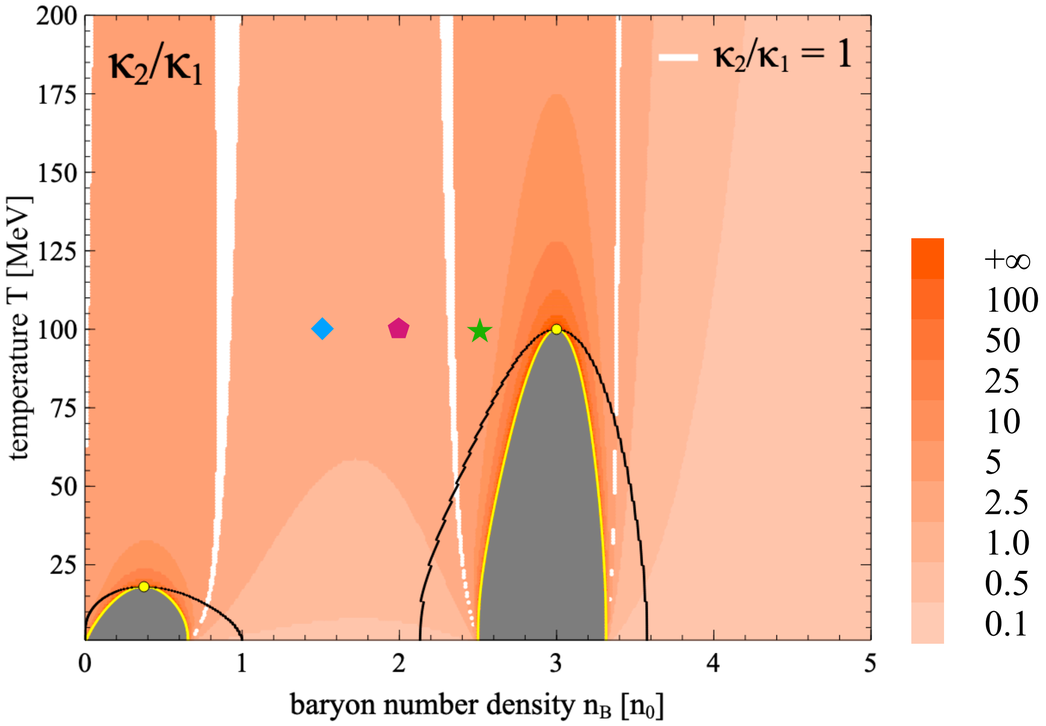

	◆	⬟	★
T [MeV]	100	100	100
nB [n0]	1.5	2.0	2.5
(k2/k1)inf	0.67	0.70	1.46

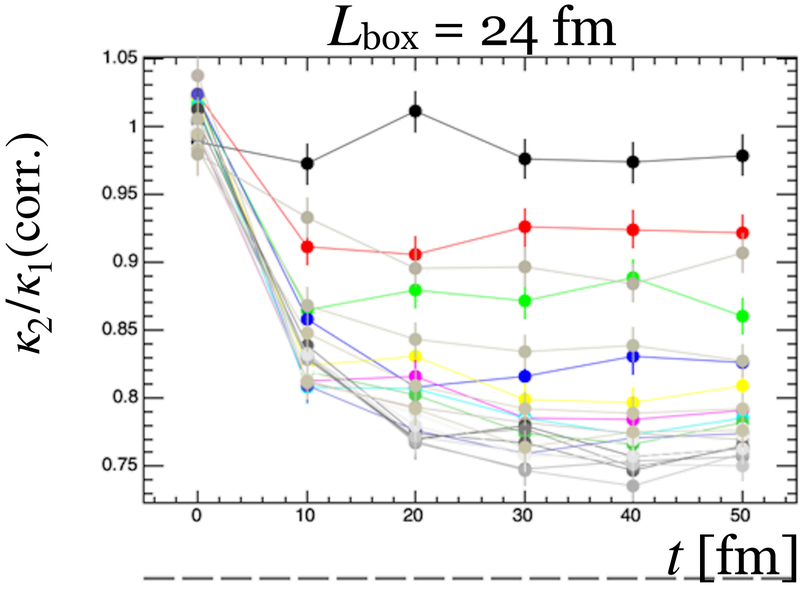

consider κ_2/κ_1
at different subvolumes

L	$\alpha = V'/V$
1	0.00007
2	0.00058
3	0.00195
⋮	⋮
23	0.88014

AS and V. Koch, Phys. Rev. C **104**, 3, 034904 (2021), arXiv:2011.06635

Finite-size scaling analysis of cumulants in a periodic box

- framework: hadronic transport with a *known* EOS (calculate κ_2/κ_1 "on paper")
- simulation: box with periodic boundary conditions at chosen (n_B, T)
- uniform initialization at $t = 0$, development of fluctuations in response to the EOS

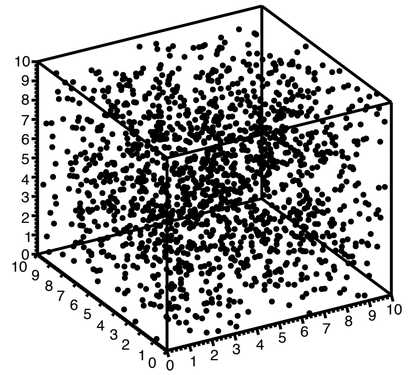

EOS: relativistic polynomial w/ 2 phase transitions

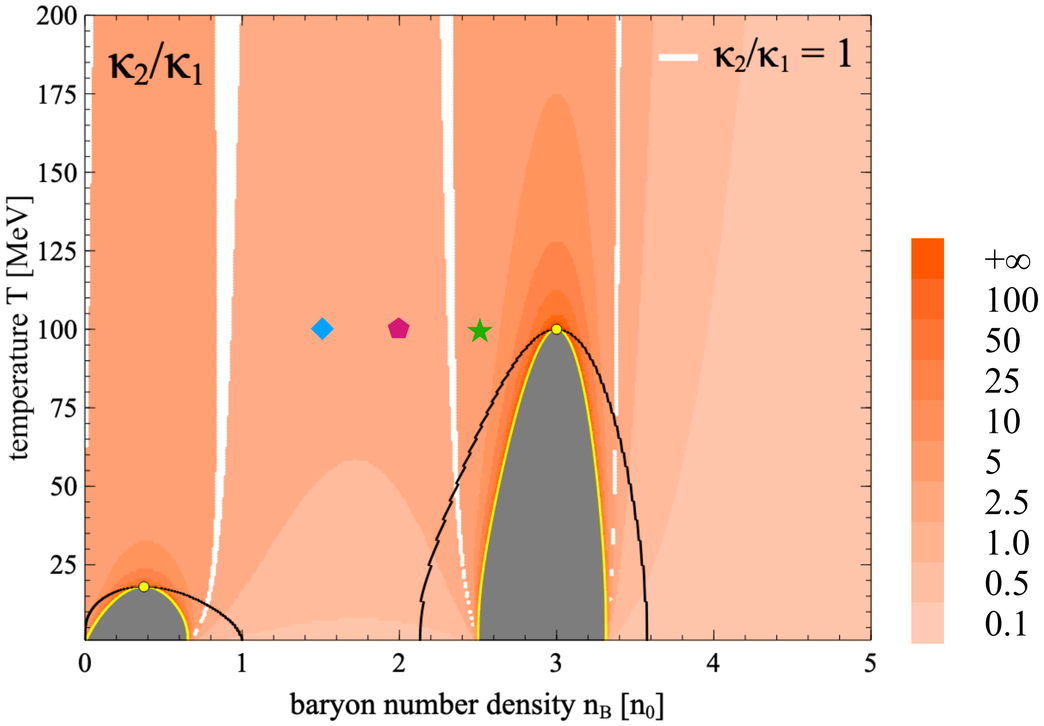

	◆	⬟	★
T [MeV]	100	100	100
nB [n0]	1.5	2.0	2.5
(k2/k1)inf	0.67	0.70	1.46

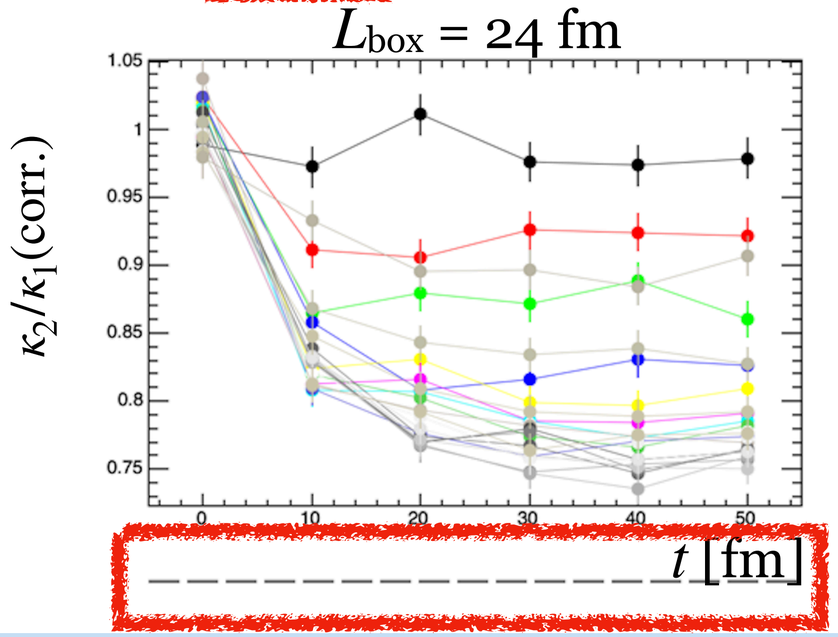

consider κ_2/κ_1
at different subvolumes

L	$\alpha = V'/V$
1	0.00007
2	0.00058
3	0.00195
⋮	⋮
23	0.88014

AS and V. Koch, Phys. Rev. C **104**, 3, 034904 (2021), arXiv:2011.06635

Finite-size scaling analysis of cumulants in a periodic box

$L_{\mathrm{box}} = 24\ \mathrm{fm}, t_{\mathrm{end}} = 50\ \mathrm{fm}/c$

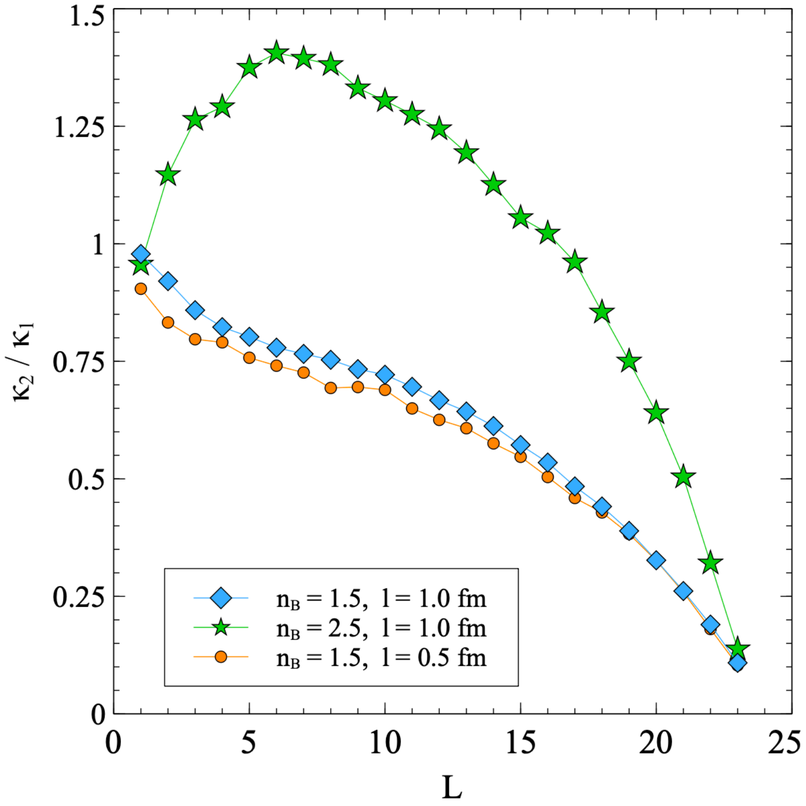

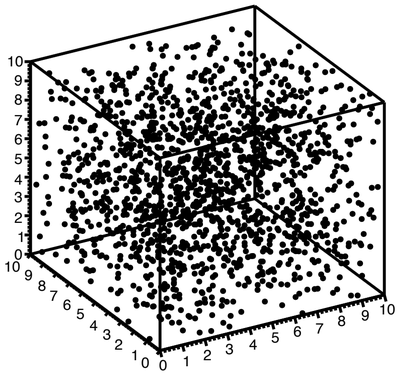

	◆	⬟	★
T [MeV]	100	100	100
nB [n0]	1.5	2.0	2.5
k2/k1	0.67	0.70	1.46

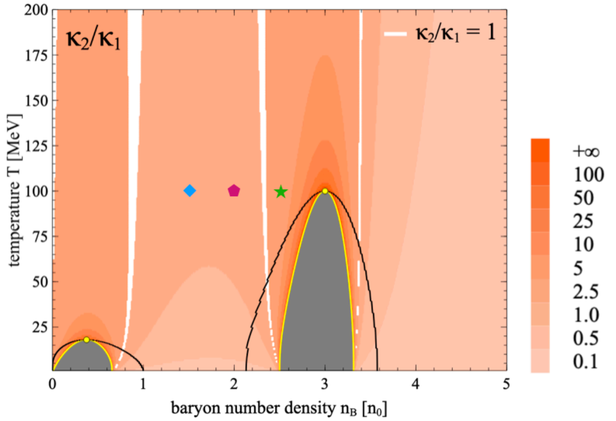

Finite-size scaling analysis of cumulants in a periodic box

$L_{\mathrm{box}} = 24$ fm, $t_{\mathrm{end}} = 50$ fm/c

correcting for effects of baryon number conservation:

V.A. Kuznietsov, O. Savchuk, M.I. Gorenstein, V. Koch, V. Vovchenko, Phys. Rev. C **105** no.4, 044903 (2022), arXiv:2201.08486

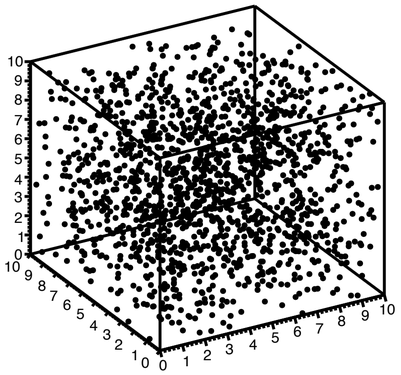

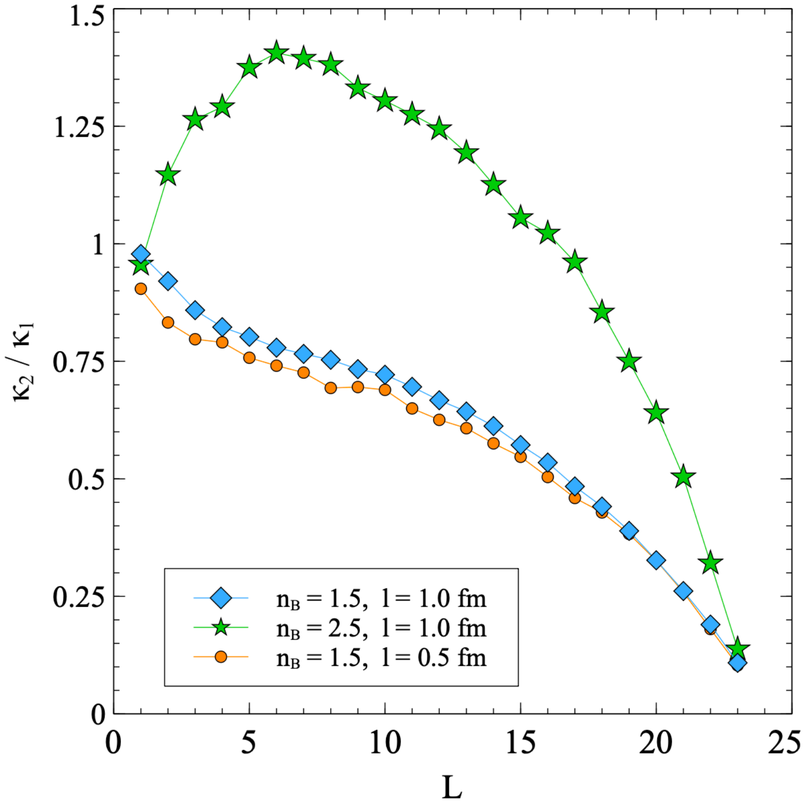

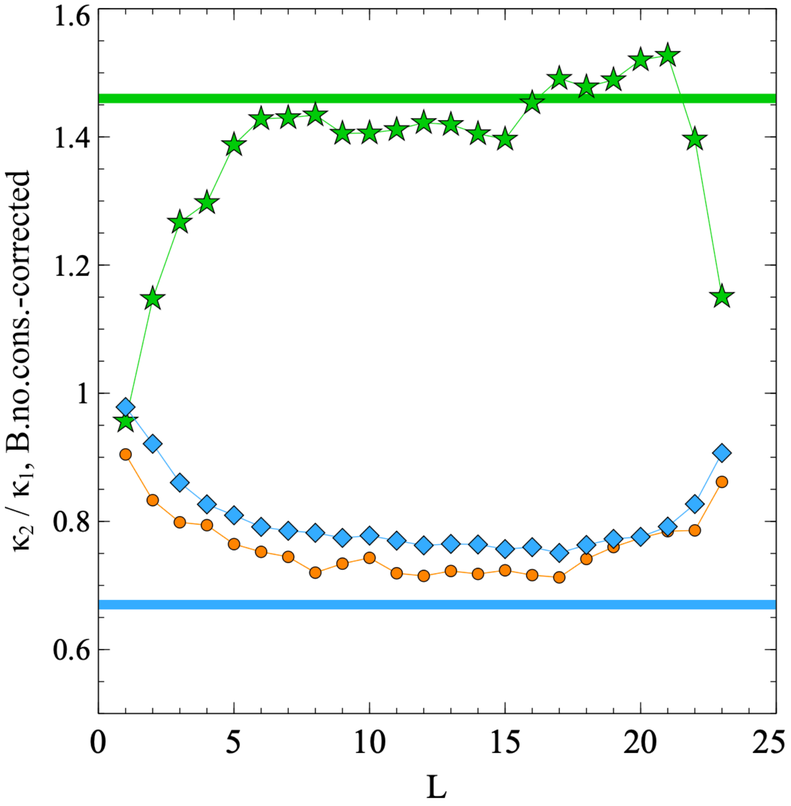

	◆	⬟	★
T [MeV]	100	100	100
nB [n0]	1.5	2.0	2.5
k2/k1	0.67	0.70	1.46

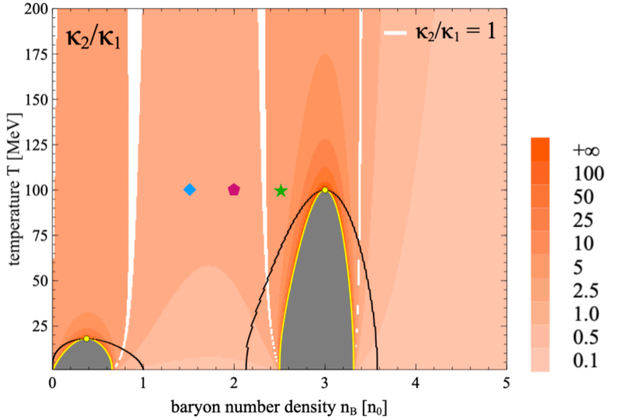

Finite-size scaling analysis of cumulants in a periodic box

$L_{\mathrm{box}} = 24$ fm, $t_{\mathrm{end}} = 50$ fm/c

correcting for effects of baryon number conservation:

V.A. Kuznietsov, O. Savchuk, M.I. Gorenstein, V. Koch, V. Vovchenko, Phys. Rev. C **105** no.4, 044903 (2022), arXiv:2201.08486

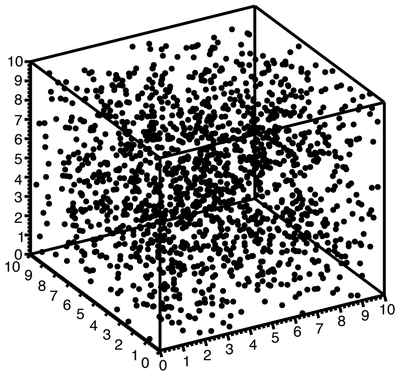

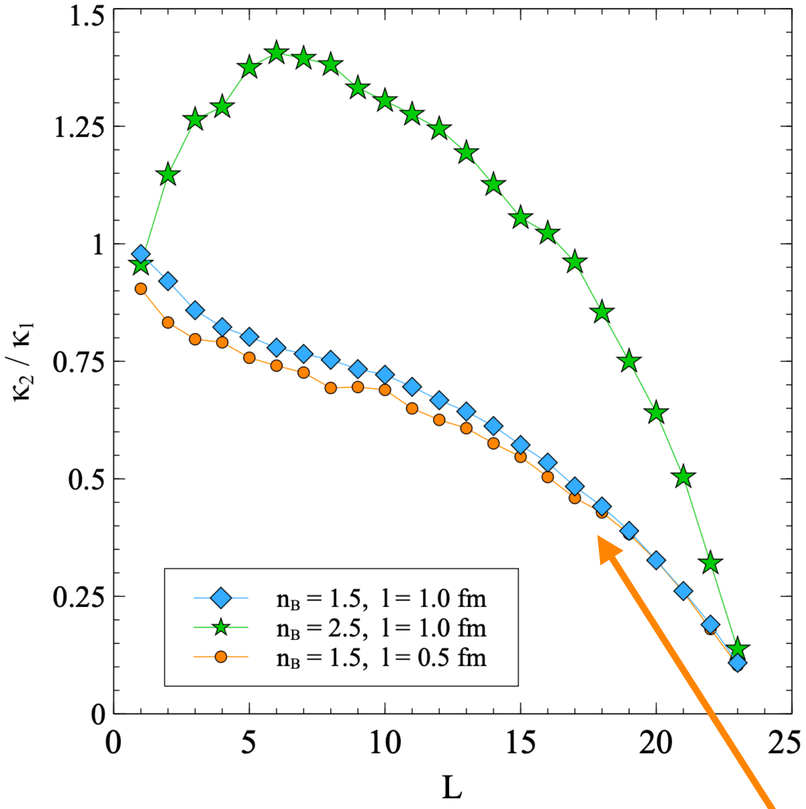

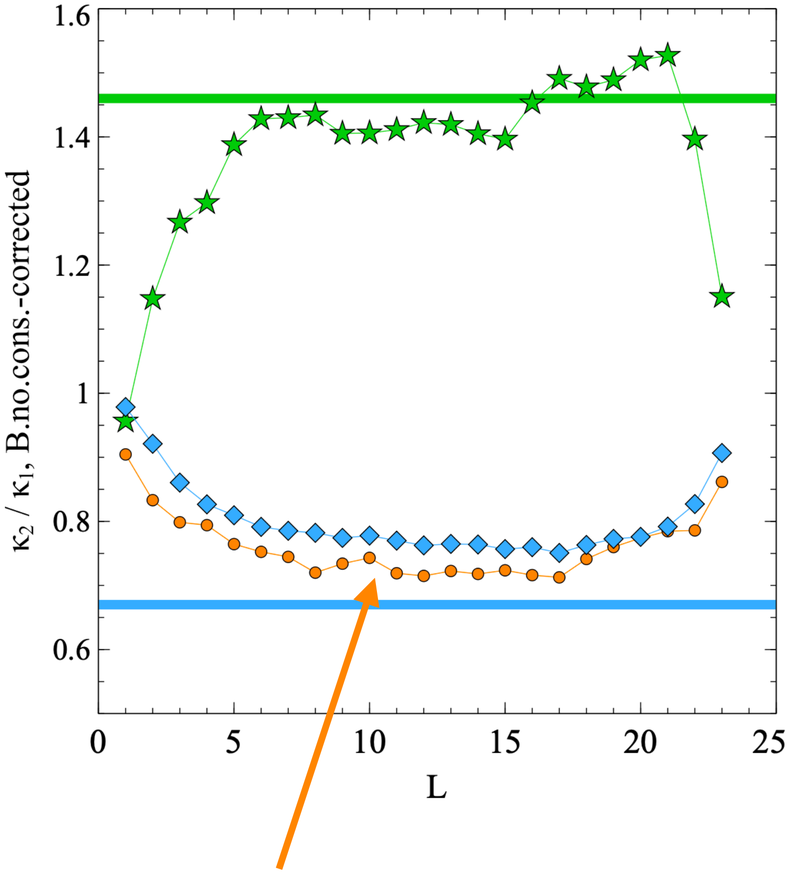

	◆	⬟	★
T [MeV]	100	100	100
nB [n0]	1.5	2.0	2.5
k2/k1	0.67	0.70	1.46

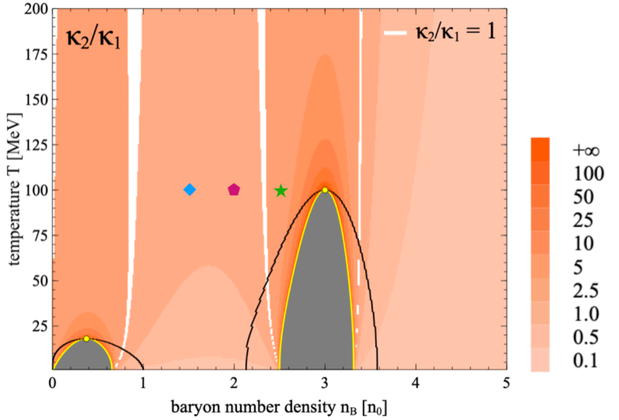

small dependence on the microscopic scale

Finite-size scaling analysis of cumulants in a periodic box

$L_{\text{box}} = 24$ fm

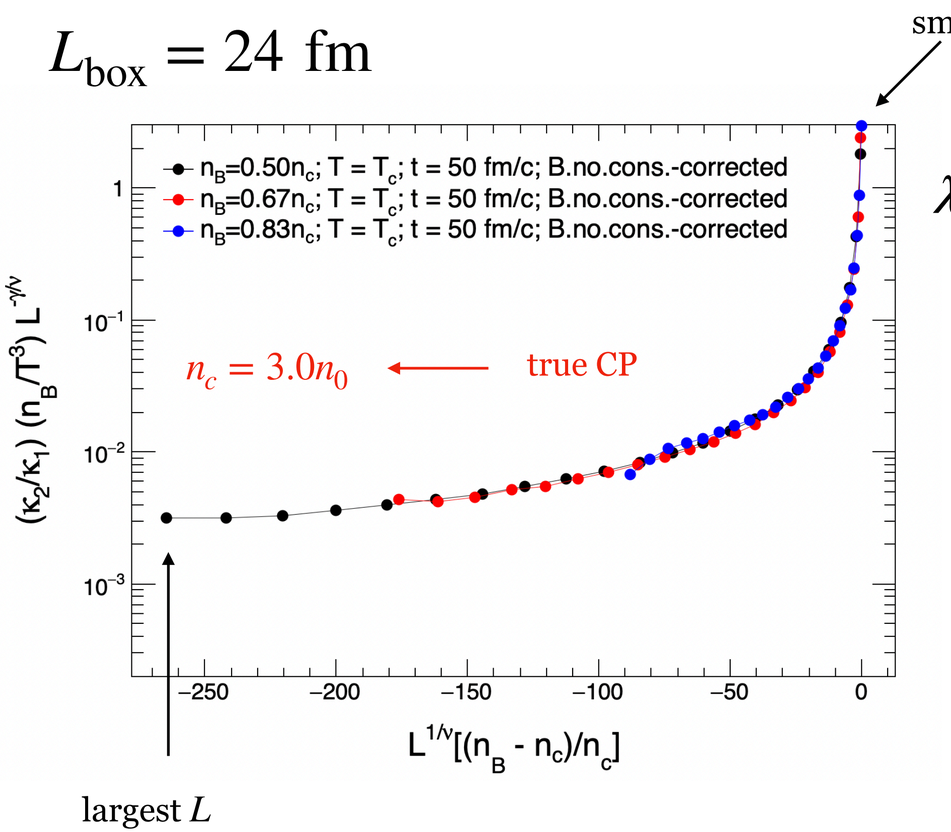

$$\chi_2 = \frac{C_2}{C_1}\frac{n_B}{T^3}$$

	◆	⬟	★
T [MeV]	100	100	100
nB [n0]	1.5	2.0	2.5
k2/k1	0.67	0.70	1.46

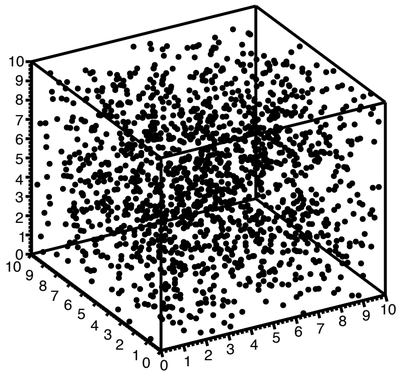

Finite-size scaling analysis of cumulants in a periodic box

$L_{\text{box}} = 24$ fm

smallest L

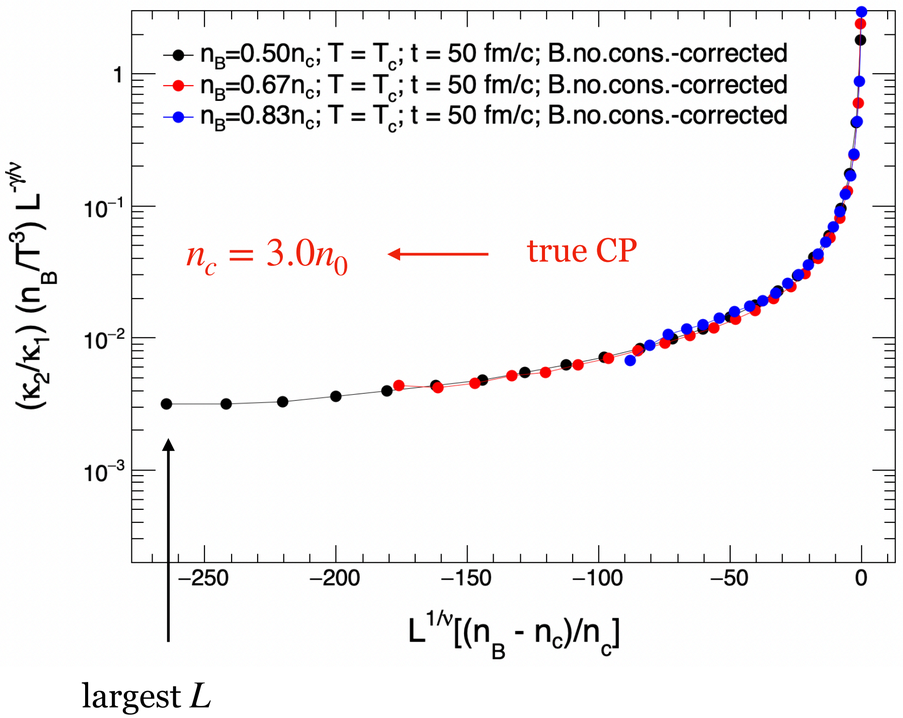

largest L

$$\chi_2 = \frac{C_2}{C_1}\frac{n_B}{T^3}$$

	◆	⬟	★
T [MeV]	100	100	100
nB [n0]	1.5	2.0	2.5
k2/k1	0.67	0.70	1.46

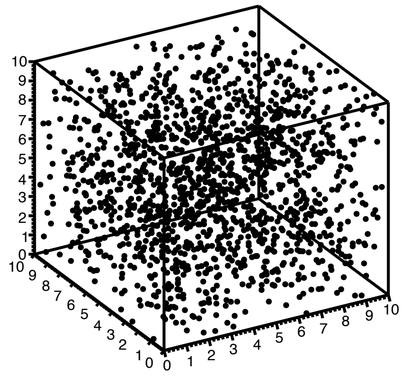

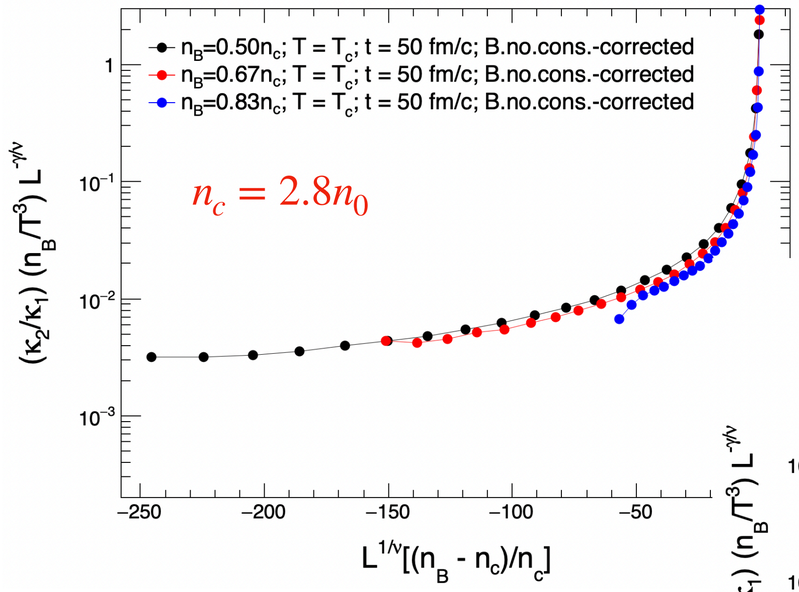

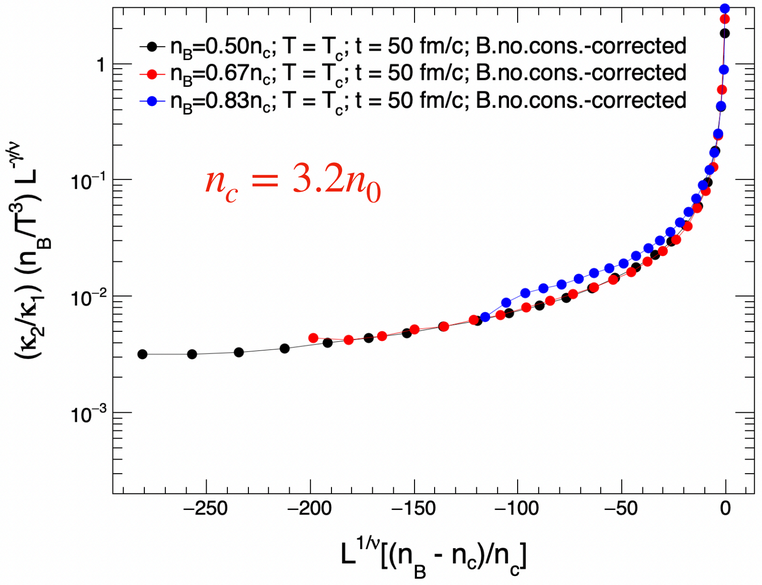

Finite-size scaling analysis of cumulants in a periodic box

$L_{\text{box}} = 24$ fm

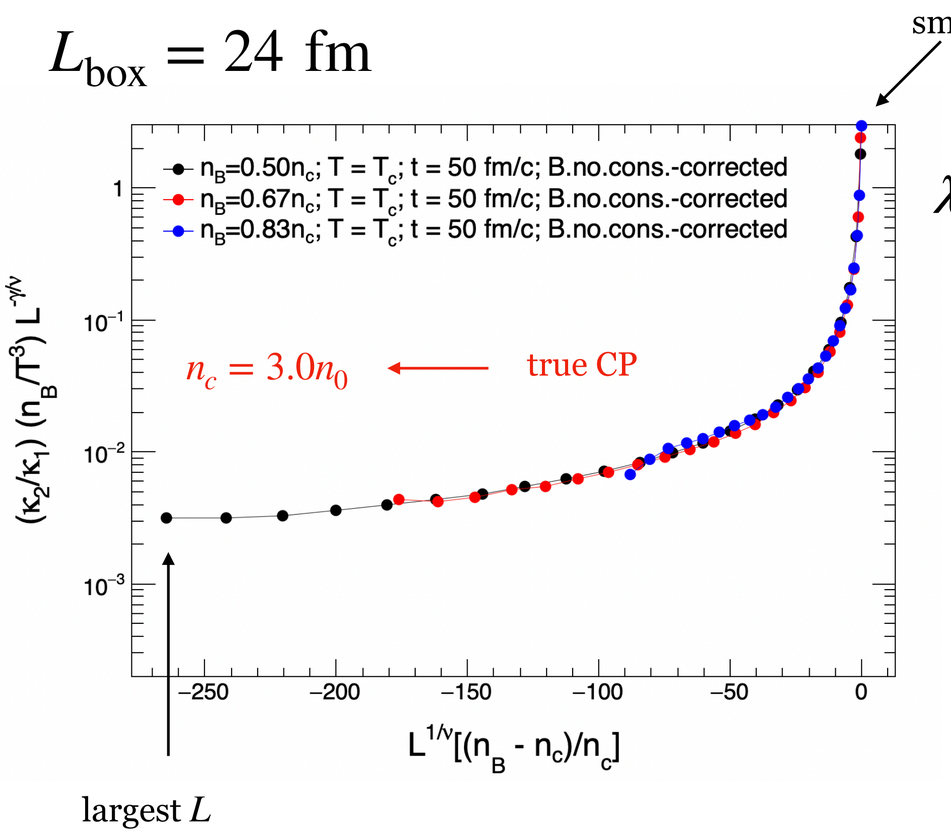

$$\chi_2 = \frac{C_2}{C_1}\frac{n_B}{T^3}$$

	◆	⬟	★
T [MeV]	100	100	100
nB [n0]	1.5	2.0	2.5
k2/k1	0.67	0.70	1.46

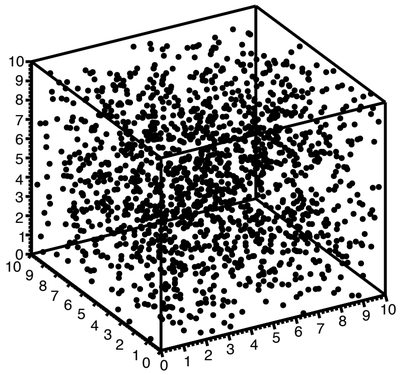

Finite-size scaling analysis of cumulants in a periodic box

$L_{\text{box}} = 24$ fm

smallest L

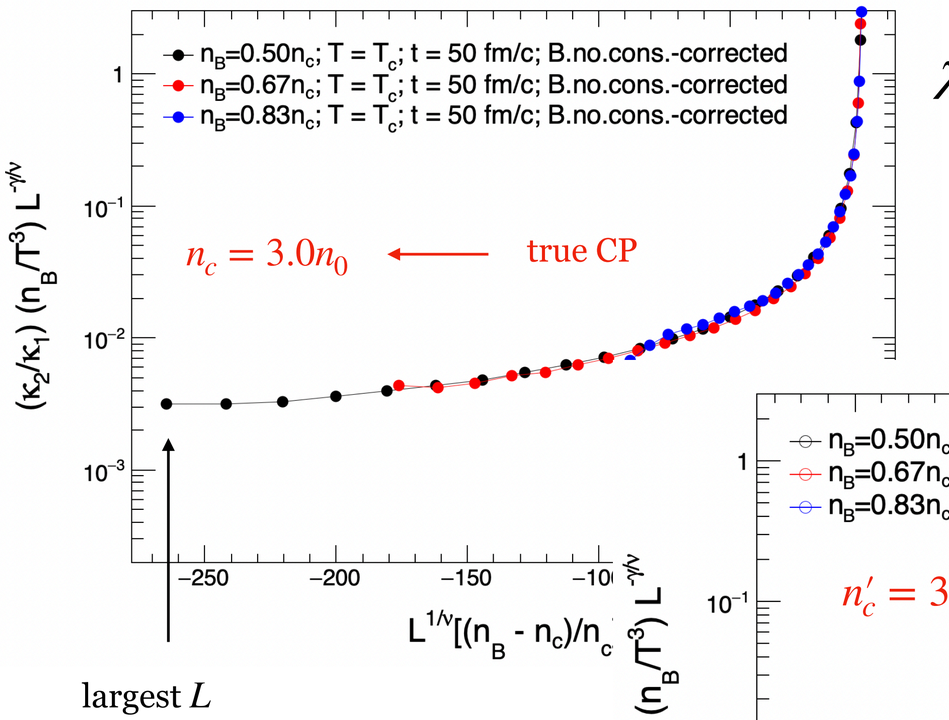

largest L

$$\chi_2 = \frac{C_2}{C_1}\frac{n_B}{T^3}$$

	◆	⬟	★
T [MeV]	100	100	100
nB [n0]	1.5	2.0	2.5
k2/k1	0.67	0.70	1.46

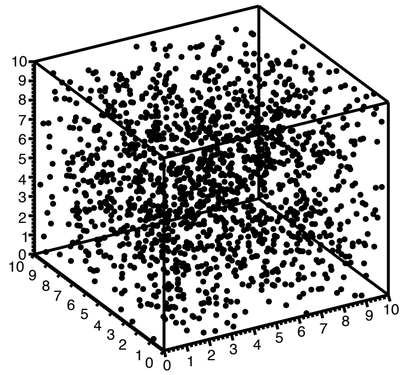

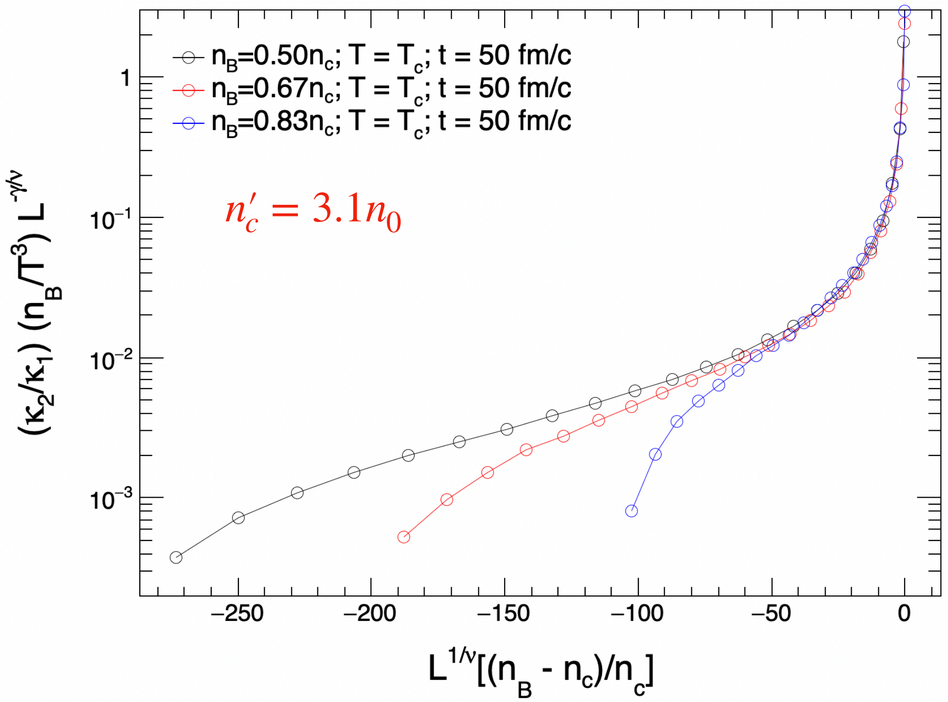

Finite-size scaling analysis of cumulants in a periodic box

$L_{\mathrm{box}} = 24$ fm

smallest L

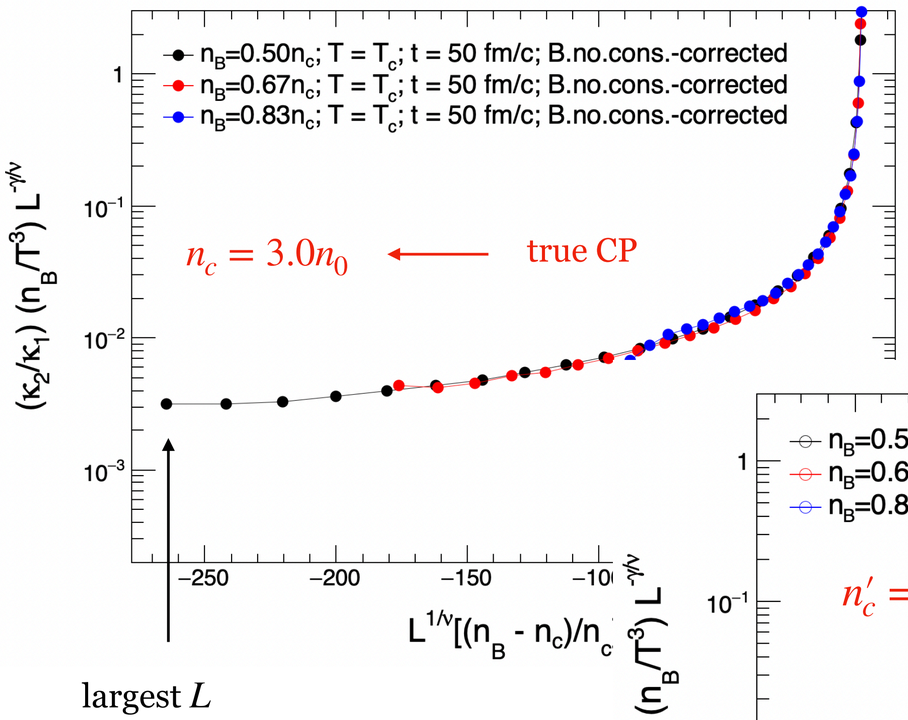

largest L

$$\chi_2 = \frac{C_2}{C_1}\frac{n_B}{T^3}$$

	◆	⬟	★
T [MeV]	100	100	100
nB [n0]	1.5	2.0	2.5
k2/k1	0.67	0.70	1.46

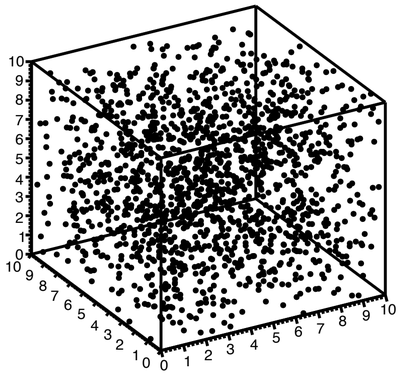

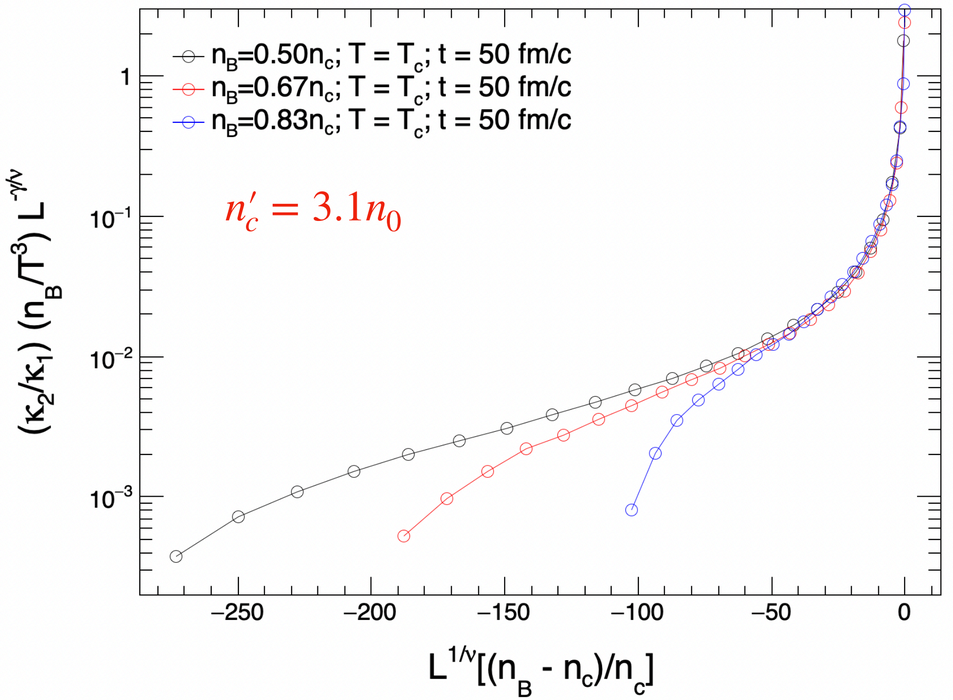

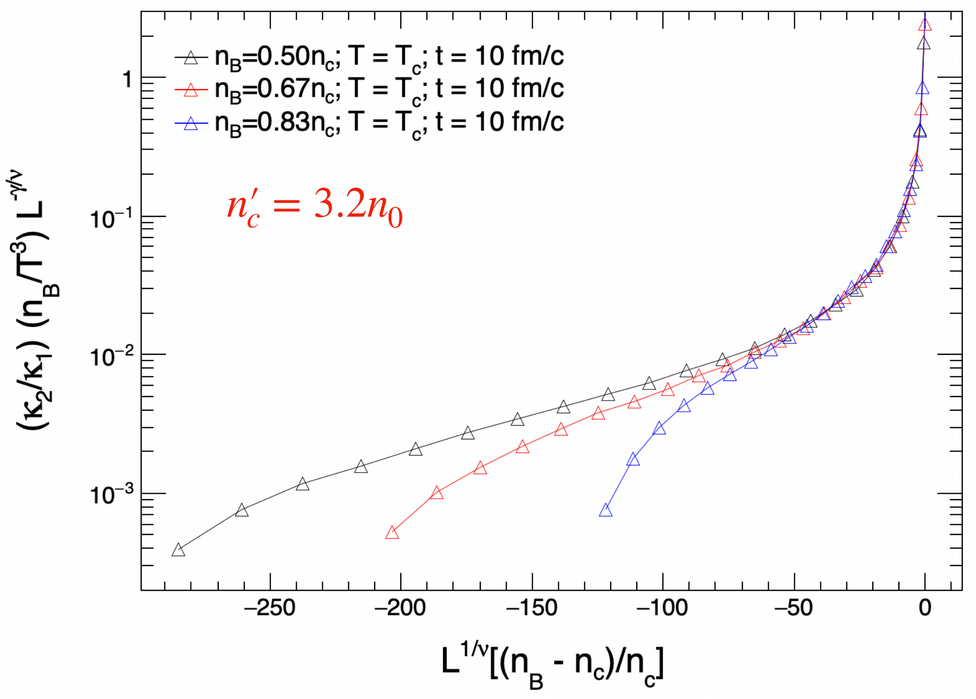

Finite-size scaling analysis of cumulants in a periodic box

$L_{\mathrm{box}} = 24$ fm

smallest L

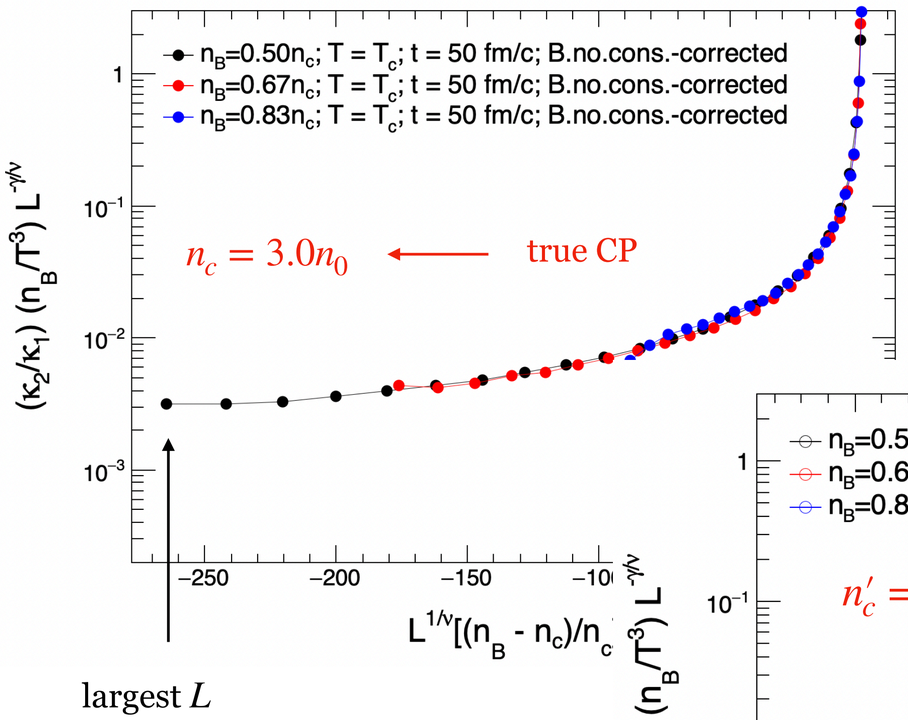

largest L

$$\chi_2 = \frac{C_2}{C_1}\frac{n_B}{T^3}$$

	◆	⬟	★
T [MeV]	100	100	100
nB [n0]	1.5	2.0	2.5
k2/k1	0.67	0.70	1.46

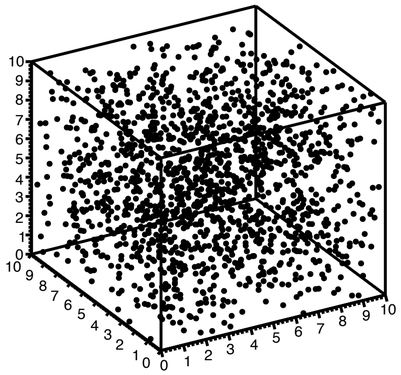

Baryon number conservation & finite time effects suppressed at $V'/V < 1/4$

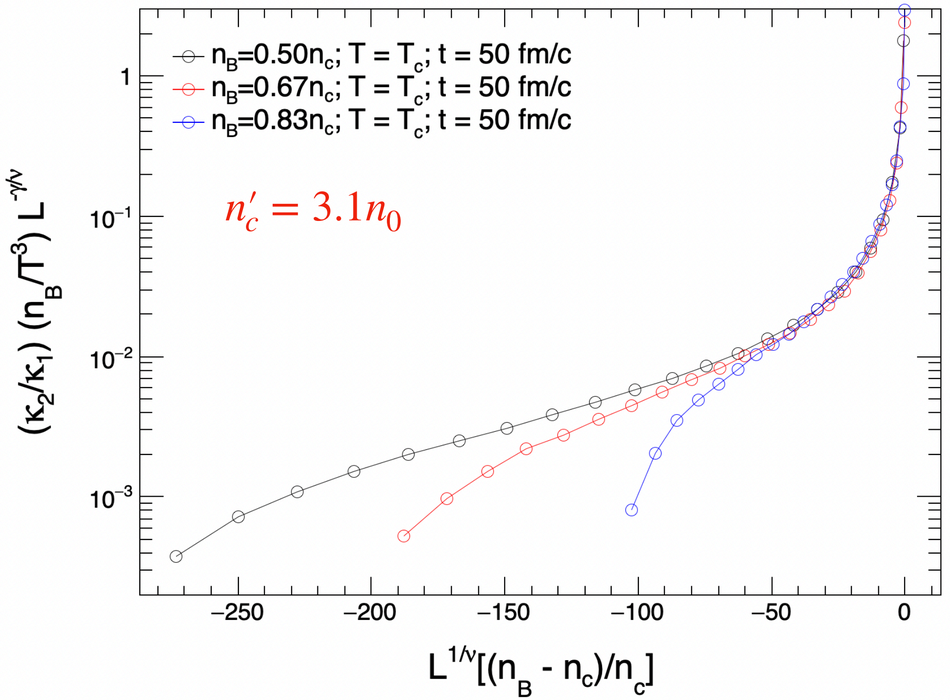

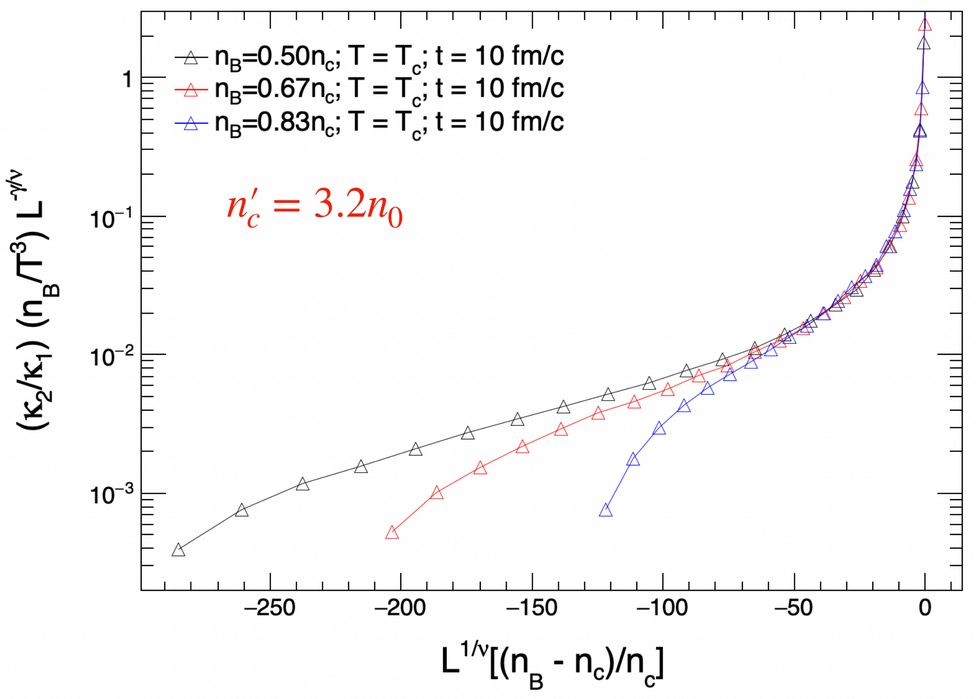

Scaling of experimental data

Scaling experimental data requires the thermal model

Observable: second-order susceptibility χ_2 : $\chi_\infty(t,0) \sim |t|^{-\gamma}$

Cumulants:

$$C_n = VT^{n-1}\left(\frac{\partial^n P}{\partial \mu_B^n}\right)_T$$

Susceptibilities:

$$\chi_B^{(n)} \equiv \frac{\partial^n (P/T^4)}{\partial (\mu_B/T)^n} \quad \Rightarrow \quad C_n = VT^3\chi_B^{(n)}$$

A. Sorensen, P. Sorensen, arXiv:2405.10278

Scaling experimental data requires the thermal model

Observable: second-order susceptibility χ_2 : $\chi_\infty(t,0) \sim |t|^{-\gamma}$

Cumulants:

$$C_n = VT^{n-1}\left(\frac{\partial^n P}{\partial \mu_B^n}\right)_T$$

Susceptibilities:

$$\chi_B^{(n)} \equiv \frac{\partial^n (P/T^4)}{\partial(\mu_B/T)^n} \quad \Rightarrow \quad C_n = VT^3\chi_B^{(n)}$$

$$\chi_2 = \frac{C_2}{T^3 V} \quad \Rightarrow \quad \chi_2(W,\mu_{\rm fo}) = \frac{C_2(W,\mu_{B,\rm fo})}{T_{\rm fo}^3 W dV_{\rm fo}/dy}$$

- We use rapidity bin width W as the subsystem size

A. Sorensen, P. Sorensen, arXiv:2405.10278

Scaling experimental data requires the thermal model

Observable: second-order susceptibility χ_2 : $\chi_\infty(t,0) \sim |t|^{-\gamma}$

Cumulants: $C_n = VT^{n-1}\left(\frac{\partial^n P}{\partial \mu_B^n}\right)_T$

Susceptibilities: $\chi_B^{(n)} \equiv \frac{\partial^n (P/T^4)}{\partial(\mu_B/T)^n}$ $\Rightarrow$ $C_n = VT^3\chi_B^{(n)}$

$$\chi_2 = \frac{C_2}{T^3 V} \quad \Rightarrow \quad \chi_2(W, \mu_{\rm fo}) = \frac{C_2(W, \mu_{B,\rm fo})}{T_{\rm fo}^3 W dV_{\rm fo}/dy}$$

- We use rapidity bin width W as the subsystem size
- We use published thermal model fits for $T_{\rm fo}$ and $\mu_{B,\rm fo}$

$\sqrt{s_{\rm NN}}$ (GeV)	$y_{\rm beam}$	$\mu_{\rm fo}$ (GeV)	$T_{\rm fo}$ (GeV)	$dV_{\rm fo}/dy$ (fm^3)
2.4	0.73	0.776	0.050	17157
3.0	1.05	0.720	0.080	4850
7.7	2.09	0.398	0.144	1044
11.5	2.50	0.287	0.149	1047
14.5	2.73	0.264	0.152	1080
19.6	3.04	0.188	0.154	1137
27	3.36	0.144	0.155	1218
39	3.73	0.103	0.156	1341
54.4	4.06	0.083	0.160	1487

J. Adamczewski-Musch et al. (HADES), Phys. Rev. C 102, 024914 (2020)
M. Abdallah *et al.* (STAR), Phys. Rev. C 104, 024902 (2021)
M. Abdallah *et al.* (STAR), Phys. Rev. C 107, 024908 (2023)
A. Andronic *et al.*, Acta Phys. Polon. B 40, 1005-1012 (2009)
A. Motornenko *et al.*, Phys. Lett. B 822, 136703 (2021)
S. Chatterjee *et al.*, Adv. High Energy Phys. 2015, 349013 (2015)

A. Sorensen, P. Sorensen, arXiv:2405.10278

Scaling experimental data requires the thermal model

Observable: second-order susceptibility χ_2 : $\chi_\infty(t,0) \sim |t|^{-\gamma}$

Cumulants: $C_n = VT^{n-1}\left(\frac{\partial^n P}{\partial \mu_B^n}\right)_T$

Susceptibilities: $\chi_B^{(n)} \equiv \frac{\partial^n (P/T^4)}{\partial(\mu_B/T)^n}$ $\Rightarrow$ $C_n = VT^3\chi_B^{(n)}$

$$\chi_2 = \frac{C_2}{T^3 V} \quad \Rightarrow \quad \chi_2(W, \mu_{\rm fo}) = \frac{C_2(W, \mu_{B,\rm fo})}{T_{\rm fo}^3 W dV_{\rm fo}/dy}$$

- We use rapidity bin width W as the subsystem size
- We use published thermal model fits for $T_{\rm fo}$ and $\mu_{B,\rm fo}$
- We parametrize $dV_{\rm fo}/dy$ from several publications. For 2.4 GeV, $T_{\rm fo}^3 V$ is highly uncertain, ranging from about 65 to 650

$\sqrt{s_{\rm NN}}$ (GeV)	$y_{\rm beam}$	$\mu_{\rm fo}$ (GeV)	$T_{\rm fo}$ (GeV)	$dV_{\rm fo}/dy$ (fm^3)
2.4	0.73	0.776	0.050	17157
3.0	1.05	0.720	0.080	4850
7.7	2.09	0.398	0.144	1044
11.5	2.50	0.287	0.149	1047
14.5	2.73	0.264	0.152	1080
19.6	3.04	0.188	0.154	1137
27	3.36	0.144	0.155	1218
39	3.73	0.103	0.156	1341
54.4	4.06	0.083	0.160	1487

J. Adamczewski-Musch et al. (HADES), Phys. Rev. C 102, 024914 (2020)
M. Abdallah *et al.* (STAR), Phys. Rev. C 104, 024902 (2021)
M. Abdallah *et al.* (STAR), Phys. Rev. C 107, 024908 (2023)
A. Andronic *et al.*, Acta Phys. Polon. B 40, 1005-1012 (2009)
A. Motornenko *et al.*, Phys. Lett. B 822, 136703 (2021)
S. Chatterjee *et al.*, Adv. High Energy Phys. 2015, 349013 (2015)

A. Sorensen, P. Sorensen, arXiv:2405.10278

Scaling experimental data requires the thermal model

Observable: second-order susceptibility χ_2 : $\chi_\infty(t,0) \sim |t|^{-\gamma}$

Cumulants: $C_n = VT^{n-1}\left(\frac{\partial^n P}{\partial \mu_B^n}\right)_T$

Susceptibilities: $\chi_B^{(n)} \equiv \frac{\partial^n (P/T^4)}{\partial(\mu_B/T)^n}$ $\Rightarrow$ $C_n = VT^3\chi_B^{(n)}$

$$\chi_2 = \frac{C_2}{T^3 V} \quad \Rightarrow \quad \chi_2(W, \mu_{\rm fo}) = \frac{C_2(W, \mu_{B,\rm fo})}{T_{\rm fo}^3 W dV_{\rm fo}/dy}$$

- We use rapidity bin width W as the subsystem size
- We use published thermal model fits for $T_{\rm fo}$ and $\mu_{B,\rm fo}$
- We parametrize $dV_{\rm fo}/dy$ from several publications. For 2.4 GeV, $T_{\rm fo}^3 V$ is highly uncertain, ranging from about 65 to 650
- Experiments can help by publishing $dV_{\rm fo}/dy$, $T_{\rm fo}$ and $\mu_{B,\rm fo}$ from thermal model fits for specific W

$\sqrt{s_{\rm NN}}$ (GeV)	$y_{\rm beam}$	$\mu_{\rm fo}$ (GeV)	$T_{\rm fo}$ (GeV)	$dV_{\rm fo}/dy$ (fm^3)
2.4	0.73	0.776	0.050	17157
3.0	1.05	0.720	0.080	4850
7.7	2.09	0.398	0.144	1044
11.5	2.50	0.287	0.149	1047
14.5	2.73	0.264	0.152	1080
19.6	3.04	0.188	0.154	1137
27	3.36	0.144	0.155	1218
39	3.73	0.103	0.156	1341
54.4	4.06	0.083	0.160	1487

J. Adamczewski-Musch et al. (HADES), Phys. Rev. C 102, 024914 (2020)
M. Abdallah *et al.* (STAR), Phys. Rev. C 104, 024902 (2021)
M. Abdallah *et al.* (STAR), Phys. Rev. C 107, 024908 (2023)
A. Andronic *et al.*, Acta Phys. Polon. B 40, 1005-1012 (2009)
A. Motornenko *et al.*, Phys. Lett. B 822, 136703 (2021)
S. Chatterjee *et al.*, Adv. High Energy Phys. 2015, 349013 (2015)

A. Sorensen, P. Sorensen, arXiv:2405.10278

Susceptibility as a function of rapidity bin W

$$\chi_2(W, \mu_{\rm fo}) = \frac{C_2(W, \mu_{B,\rm fo})}{T_{\rm fo}^3 W dV_{\rm fo}/dy}$$

- Grey band shows uncertainty from freeze-out ambiguities for the 2.4 GeV data

- Data do indicate a change in slope at higher μ_B and at small W:
  χ_2 decreases with increasing W for 7.7–54.4 GeV but changes slope at 2.4 GeV
  (3.0 GeV is ~flat)

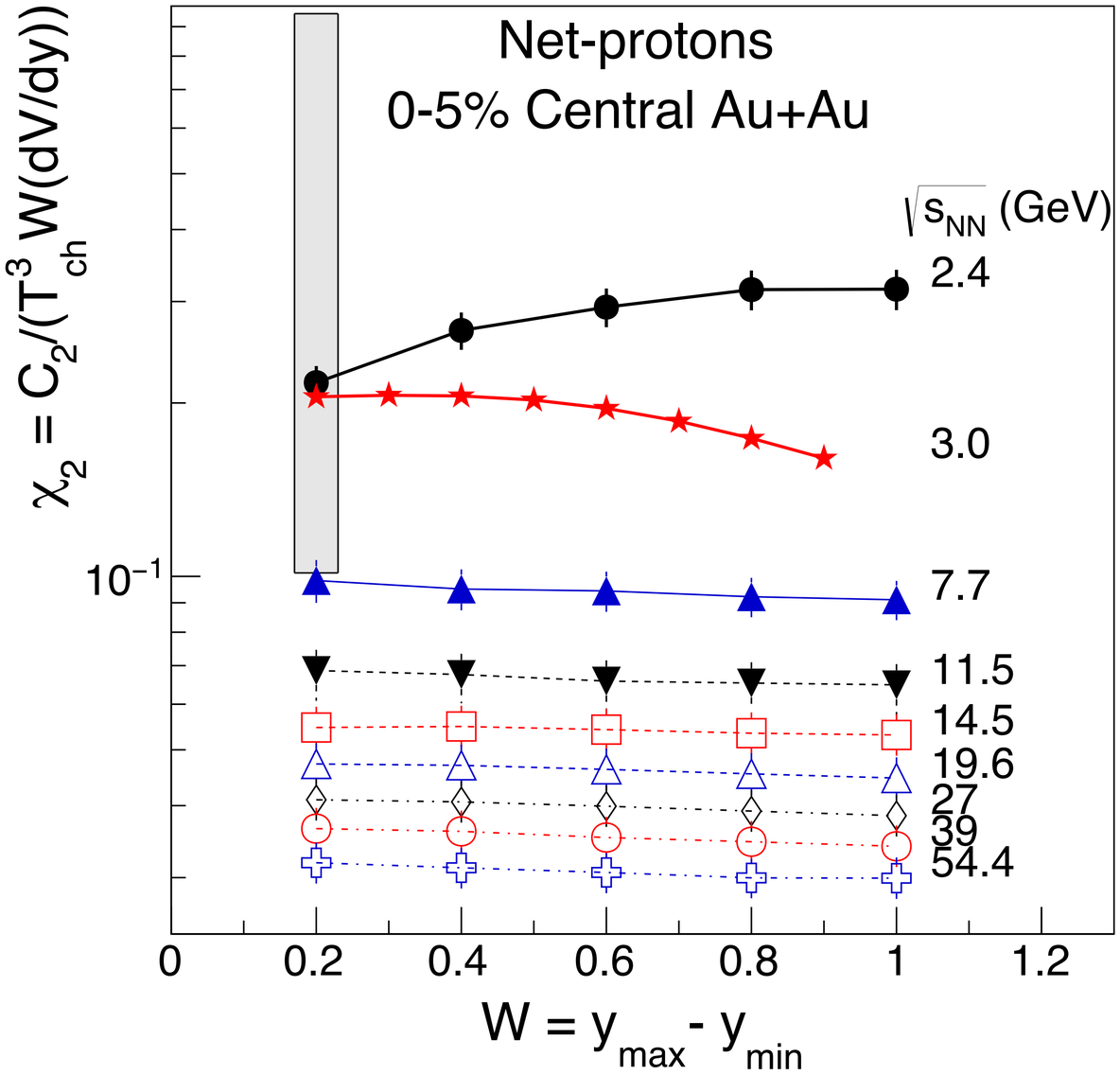

A. Sorensen, P. Sorensen, arXiv:2405.10278

Where can we expect scaling behavior?

- The system is scale-free if the data follows Taylor's law : $\sigma^2 = a\lambda^p$ $\Leftrightarrow$ $C_2 \sim C_1^p$

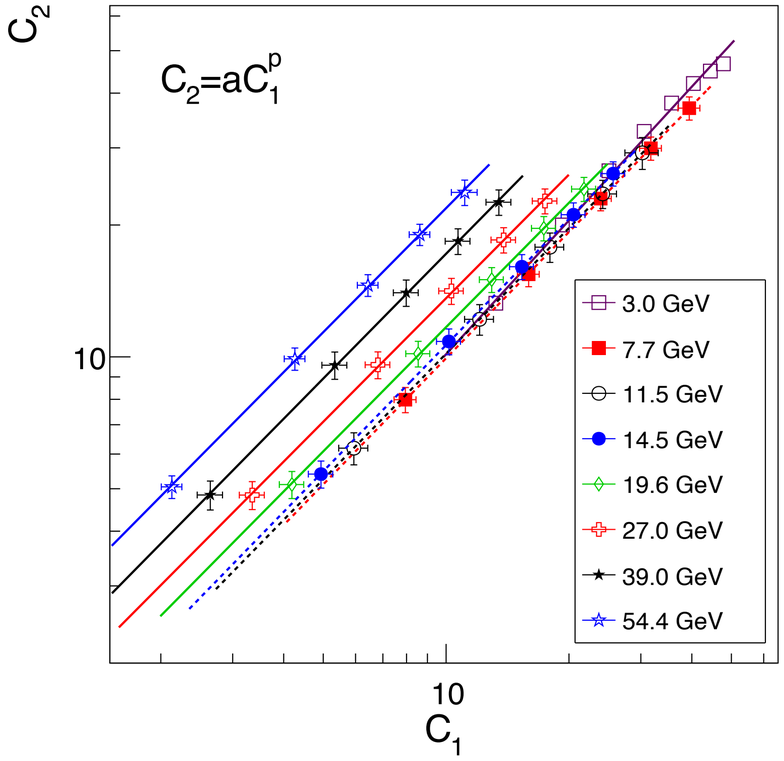

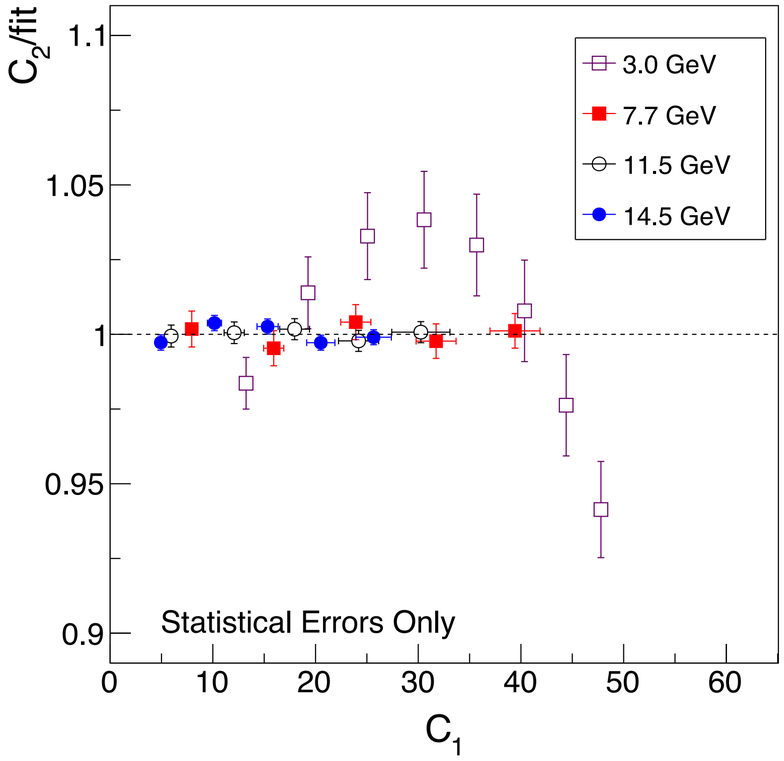

Following Taylor's law means it's scale-free:

$C_2 = aW^p$

$C_2 = a(xW)^p = ax^pW^p = a'W^p$

$C_1 \propto W$ in this energy range

Scale invariance supports the applicability of FSS

Where can we expect scaling behavior?

- The system is scale-free if the data follows Taylor's law : $\sigma^2 = a\lambda^p$ $\Leftrightarrow$ $C_2 \sim C_1^p$

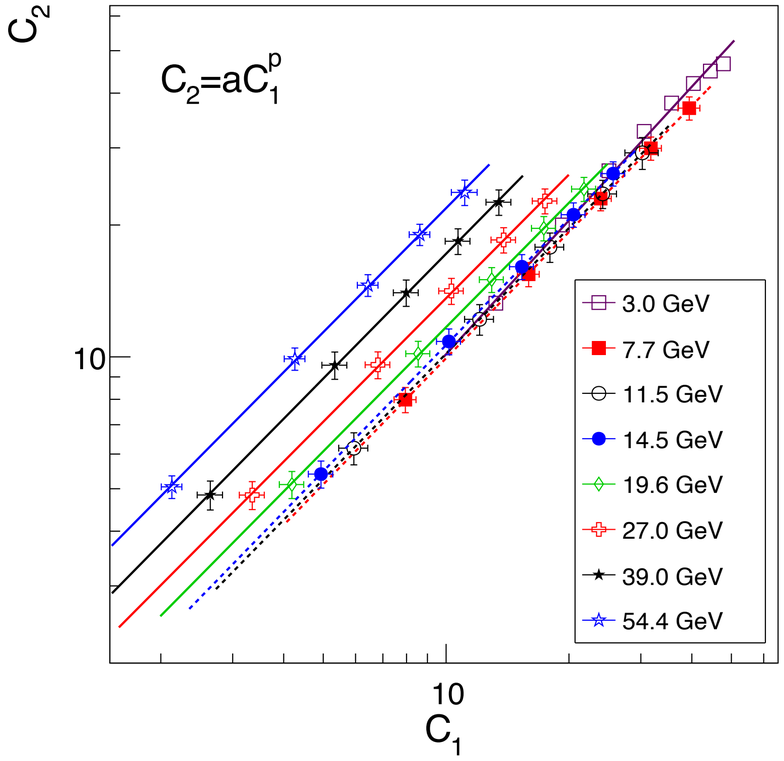

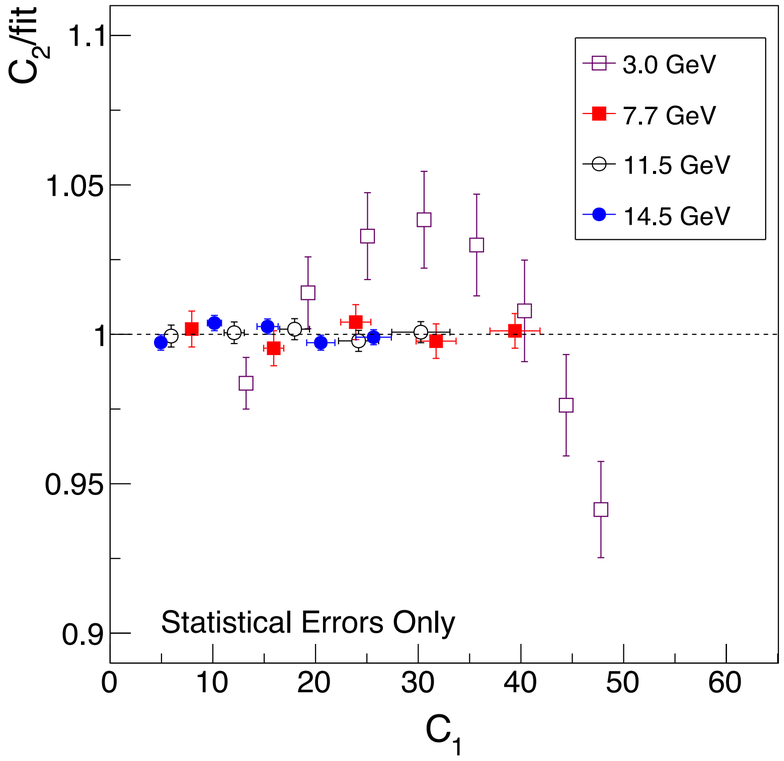

Following Taylor's law means it's scale-free:

$C_2 = aW^p$

$C_2 = a(xW)^p = ax^pW^p = a'W^p$

$C_1 \propto W$ in this energy range

Scale invariance supports the applicability of FSS

Note: the $\sqrt{s} = 3$ GeV data won't scale!

What to scale with?

$$\chi L^{-\frac{\sigma}{\nu}} = \phi(tL^{\frac{1}{\nu}})$$

one can find CP by plotting

$$\xi_\infty(t,0) \sim |t|^{-\nu}$$

$$\xi_\infty(0,h) \sim |h|^{-\nu_c}$$

$$t \equiv \frac{T - T_c}{T_c}$$

$$h \equiv \frac{H}{k_B T}$$

What to scale with?

$$\chi L^{-\frac{\sigma}{\nu}} = \phi(tL^{\frac{1}{\nu}})$$

one can find CP by plotting

$$\xi_\infty(t,0) \sim |t|^{-\nu}$$

$$\xi_\infty(0,h) \sim |h|^{-\nu_c}$$

$$t \equiv \frac{T - T_c}{T_c}$$

$$h \equiv \frac{H}{k_B T}$$

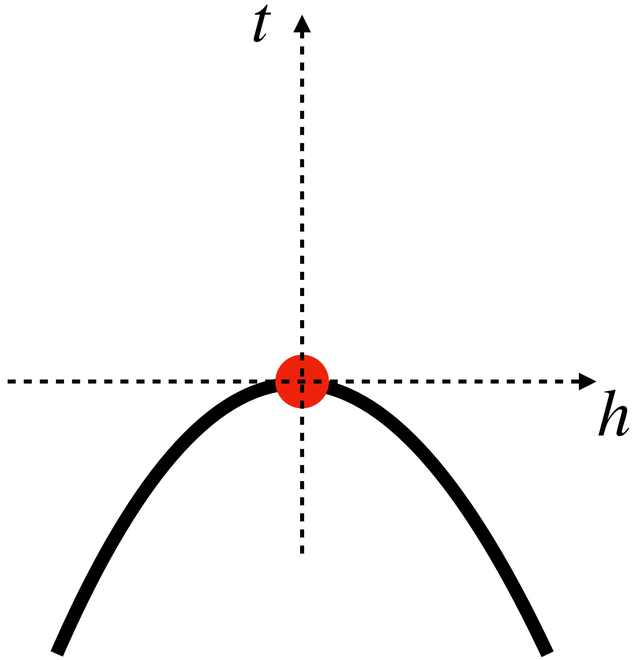

What to scale with?

$$\chi L^{-\frac{\sigma}{\nu}} = \phi(tL^{\frac{1}{\nu}})$$

one can find CP by plotting

$$\xi_\infty(t,0) \sim |t|^{-\nu}$$

$$\xi_\infty(0,h) \sim |h|^{-\nu_c}$$

$$t \equiv \frac{T - T_c}{T_c}$$

$$h \equiv \frac{H}{k_B T}$$

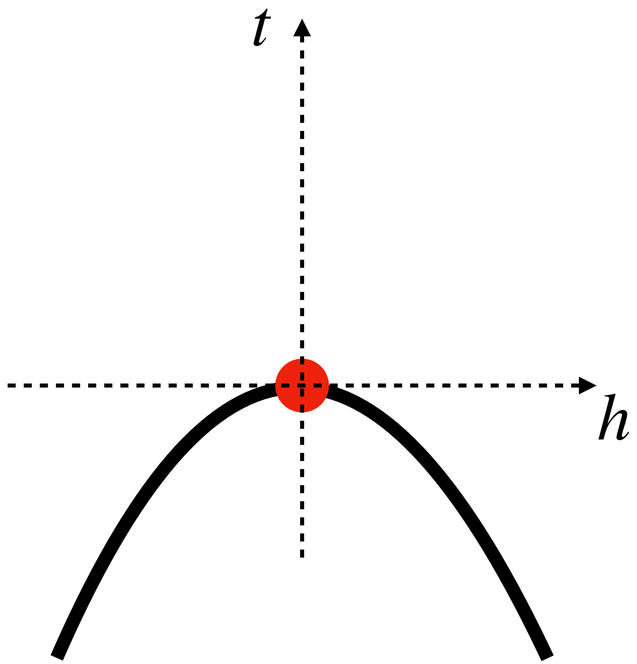

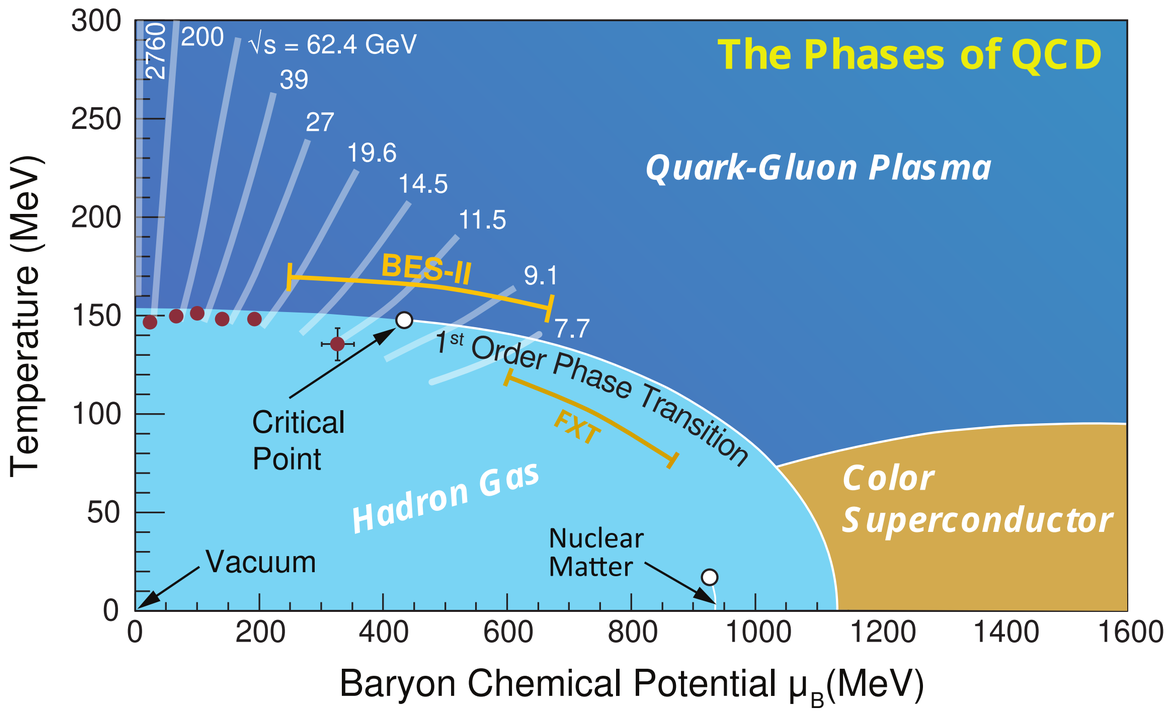

What to scale with?

$$\chi L^{-\frac{\sigma}{\nu}} = \phi(tL^{\frac{1}{\nu}})$$

one can find CP by plotting

$$\xi_\infty(t,0) \sim |t|^{-\nu}$$

$$\xi_\infty(0,h) \sim |h|^{-\nu_c}$$

$$t \equiv \frac{T - T_c}{T_c}$$

$$h \equiv \frac{H}{k_B T}$$

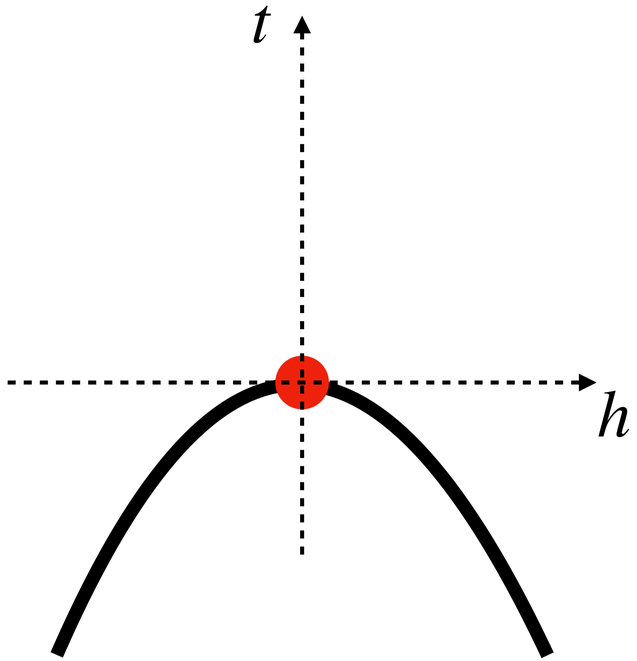

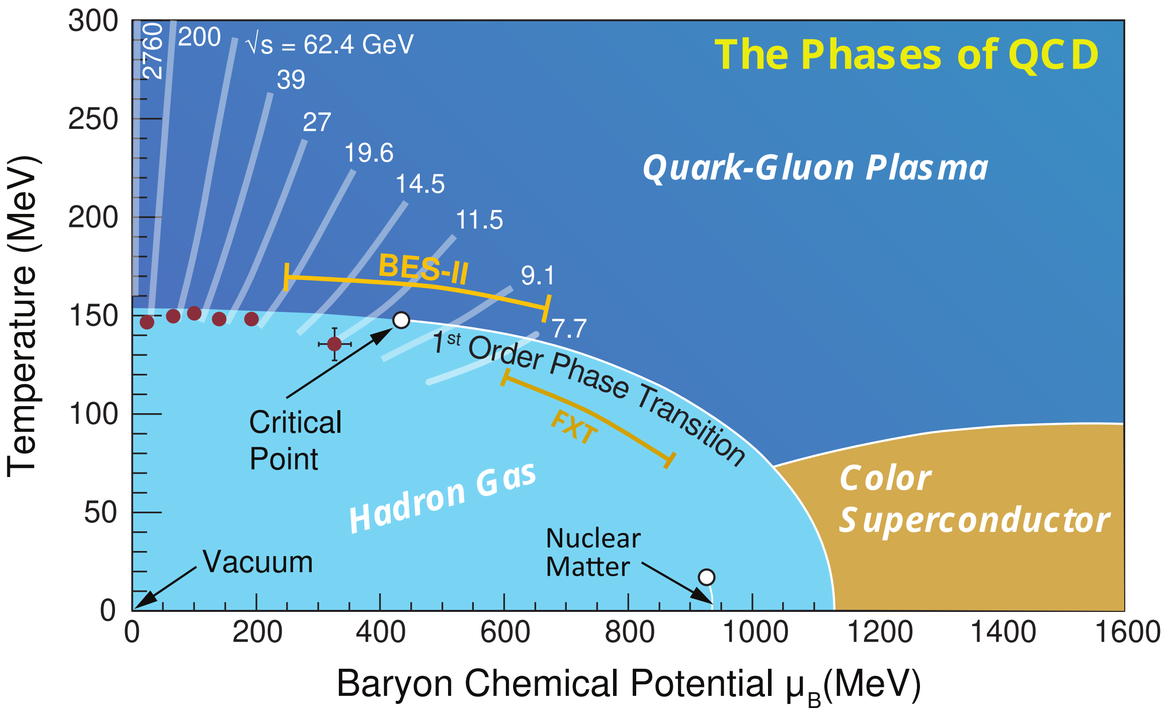

$$h(\mu, T) = -\frac{\cos\alpha_1 \Delta T + \sin\alpha_1 \Delta\mu}{wT_c \sin(\alpha_1 - \alpha_2)}$$

$$t(\mu, T) = \frac{\cos\alpha_2 \Delta T + \sin\alpha_2 \Delta\mu}{\rho w T_c \sin(\alpha_1 - \alpha_2)}$$

M.S. Pradeep, M. Stephanov, Phys. Rev. D **100** 5, 056003 (2019) arXiv:1905.13247

Scaling in 2-D

$$h(\mu, T) = -\frac{\cos\alpha_1 \Delta T + \sin\alpha_1 \Delta\mu}{wT_c \sin(\alpha_1 - \alpha_2)}$$

$$t(\mu, T) = \frac{\cos\alpha_2 \Delta T + \sin\alpha_2 \Delta\mu}{\rho w T_c \sin(\alpha_1 - \alpha_2)}$$

M.S. Pradeep, M. Stephanov, *Phys. Rev. D* **100** 5, 056003 (2019) arXiv:1905.13247

We map $\Delta\mu_B$ vs ΔT onto t and h with α_1 determined from a straight line between the candidate CP ($\mu_{B,c}$, T_c) and the 7.7 GeV freeze-out point.

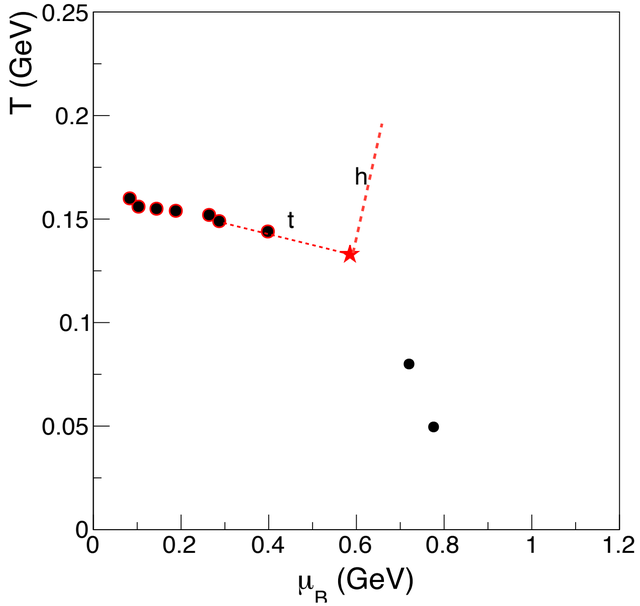

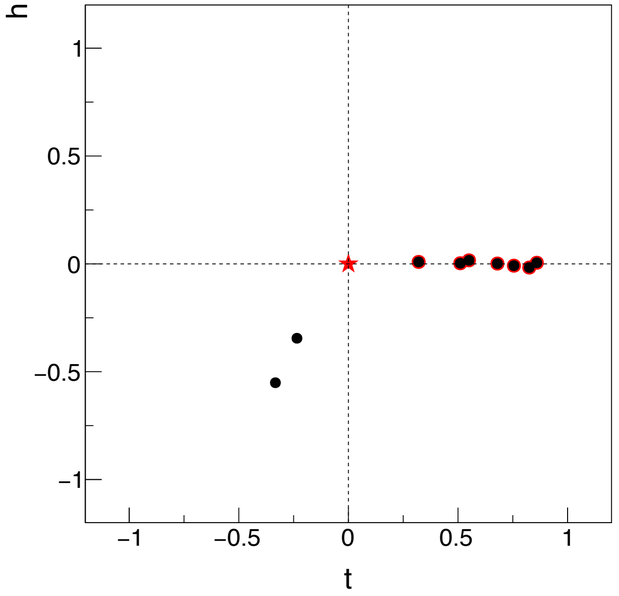

Scaling in 2-D

$$h(\mu, T) = -\frac{\cos\alpha_1 \Delta T + \sin\alpha_1 \Delta\mu}{wT_c \sin(\alpha_1 - \alpha_2)}$$

$$t(\mu, T) = \frac{\cos\alpha_2 \Delta T + \sin\alpha_2 \Delta\mu}{\rho w T_c \sin(\alpha_1 - \alpha_2)}$$

M.S. Pradeep, M. Stephanov, *Phys. Rev. D* **100** 5, 056003 (2019) arXiv:1905.13247

We map $\Delta\mu_B$ vs ΔT onto t and h with α_1 determined from a straight line between the candidate CP ($\mu_{B,c}$, T_c) and the 7.7 GeV freeze-out point.

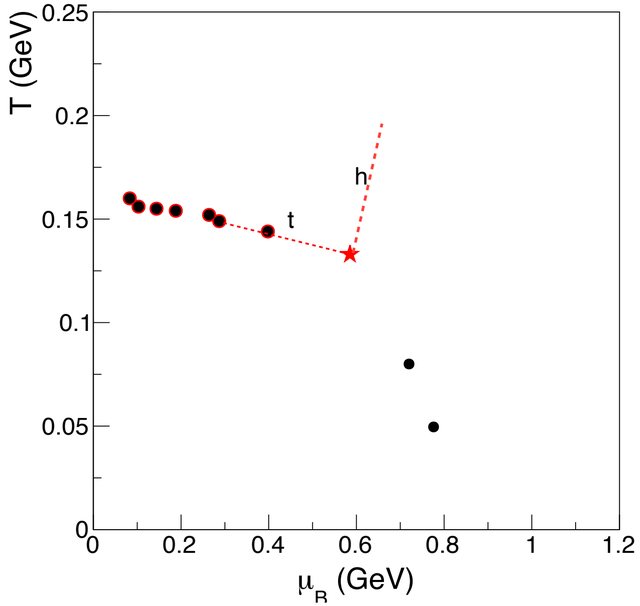

We checked that scaling in 1-D (only with μ_B) works well.
To make the 2-D scaling as similar to 1-D as possible, for the other parameters we take $\alpha_2 = \alpha_1 + \pi/2$, $w = 1$, and $\rho = \mu_{B,c}/T_c$.
With this, mapping of scaling fields simplifies to

$$h(\mu, T) = -\frac{\cos\alpha_1 \Delta T + \sin\alpha_1 \Delta\mu}{T_c}$$

$$t(\mu, T) = \frac{\cos\alpha_2 \Delta T + \sin\alpha_2 \Delta\mu}{\mu_{Bc}}$$

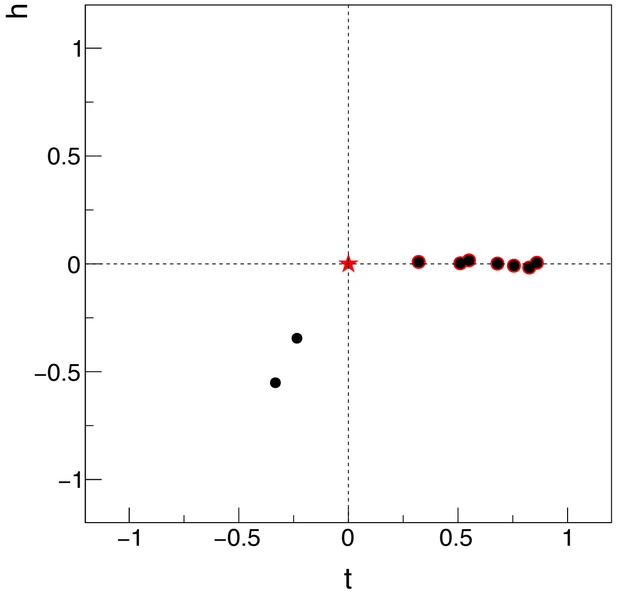

Scaled susceptibility: 2D fit w/ mean-field exponents

$\chi L^{-\frac{\sigma}{\nu}} = \phi(tL^{\frac{1}{\nu}})$

one can find CP by plotting

$$h(\mu, T) = -\frac{\cos\alpha_1 \Delta T + \sin\alpha_1 \Delta\mu}{T_c}$$

$$t(\mu, T) = \frac{\cos\alpha_2 \Delta T + \sin\alpha_2 \Delta\mu}{\mu_{Bc}}$$

Scaled susceptibility: 2D fit w/ mean-field exponents

$\chi L^{-\frac{\sigma}{\nu}} = \phi(tL^{\frac{1}{\nu}})$

one can find CP by plotting

$$h(\mu, T) = -\frac{\cos\alpha_1 \Delta T + \sin\alpha_1 \Delta\mu}{T_c}$$

$$t(\mu, T) = \frac{\cos\alpha_2 \Delta T + \sin\alpha_2 \Delta\mu}{\mu_{Bc}}$$

α_1 is usually small:

$$t \approx -\frac{\mu_B - \mu_{B,c}}{\mu_{B,c}}$$

Scaled susceptibility: 2D fit w/ mean-field exponents

$\chi L^{-\frac{\sigma}{\nu}} = \phi(tL^{\frac{1}{\nu}})$

one can find CP by plotting

$$h(\mu, T) = -\frac{\cos\alpha_1 \Delta T + \sin\alpha_1 \Delta\mu}{T_c}$$

$$t(\mu, T) = \frac{\cos\alpha_2 \Delta T + \sin\alpha_2 \Delta\mu}{\mu_{Bc}}$$

α_1 is usually small:

$$t \approx -\frac{\mu_B - \mu_{B,c}}{\mu_{B,c}}$$

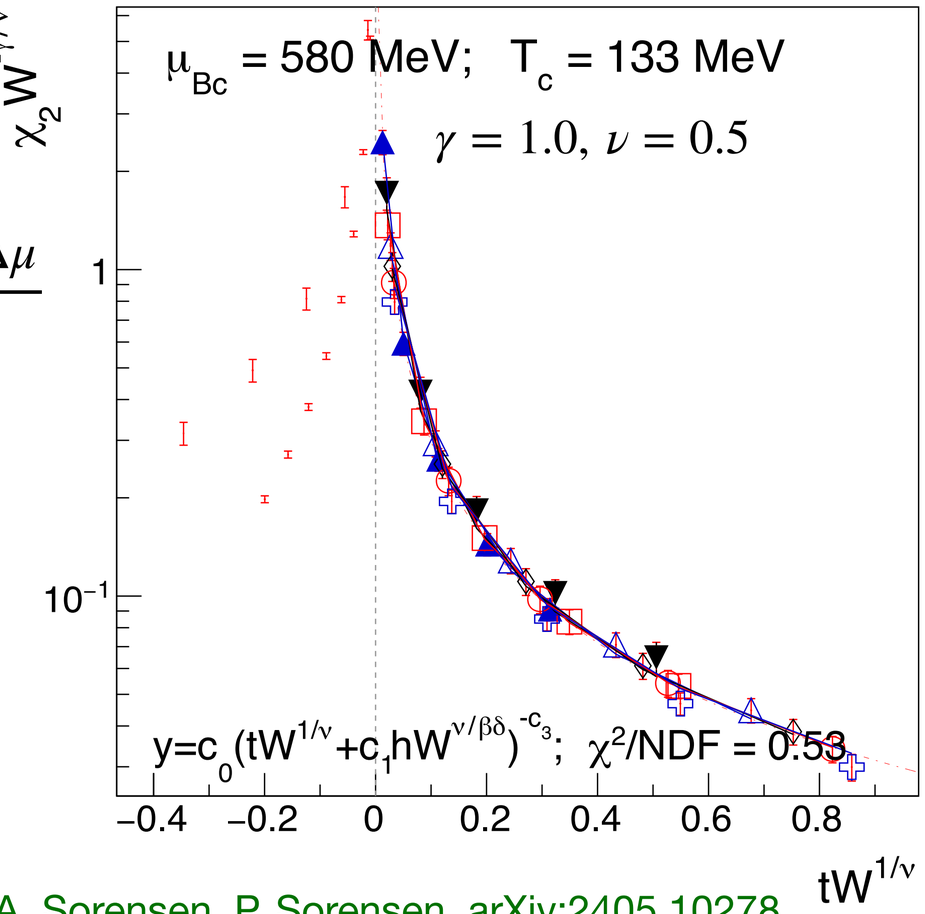

A. Sorensen, P. Sorensen, arXiv:2405.10278

With mean-field exponents, we find scaling for $555 < \mu_{B,c} < 610$ MeV;

T_c only constrained by "plausibility" (below $T_{pc,\mu_B=0}$ and above $T_{\rm fo}$)

Scaled susceptibility: 2D fit w/ mean-field exponents

$$\chi L^{-\frac{\sigma}{\nu}} = \phi(tL^{\frac{1}{\nu}})$$

one can find CP by plotting

$$h(\mu, T) = -\frac{\cos\alpha_1 \Delta T + \sin\alpha_1 \Delta\mu}{T_c}$$

$$t(\mu, T) = \frac{\cos\alpha_2 \Delta T + \sin\alpha_2 \Delta\mu}{\mu_{Bc}}$$

α_1 is usually small:

$$t \approx -\frac{\mu_B - \mu_{B,c}}{\mu_{B,c}}$$

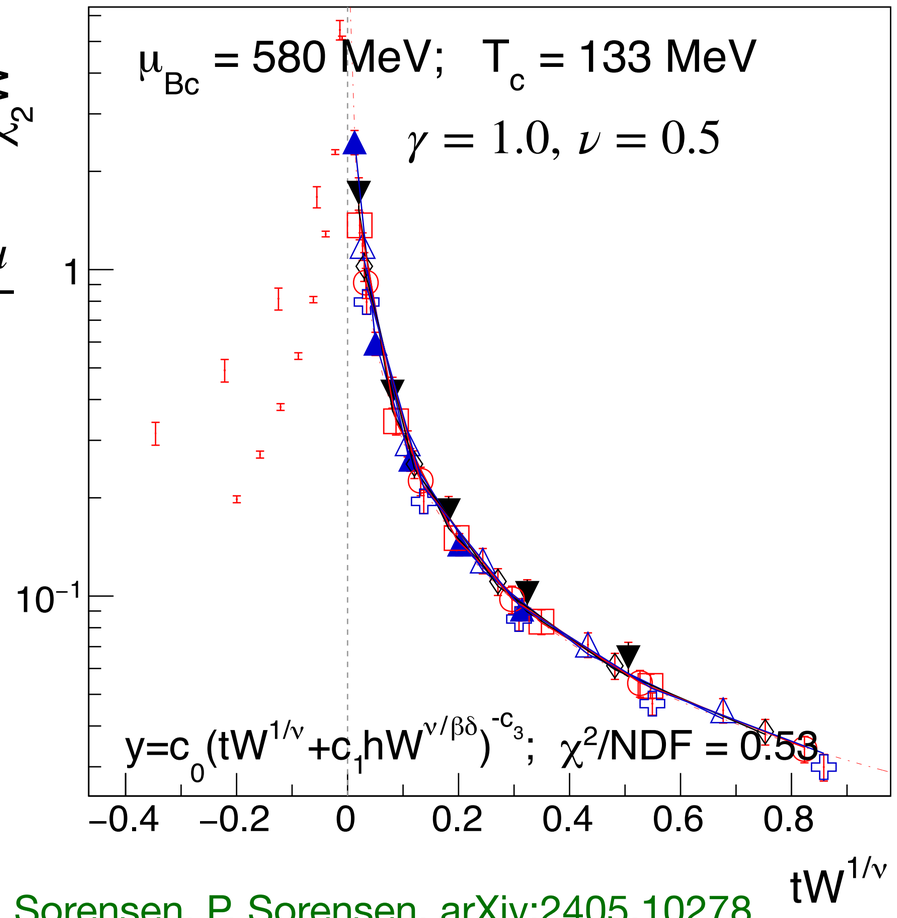

A. Sorensen, P. Sorensen, arXiv:2405.10278

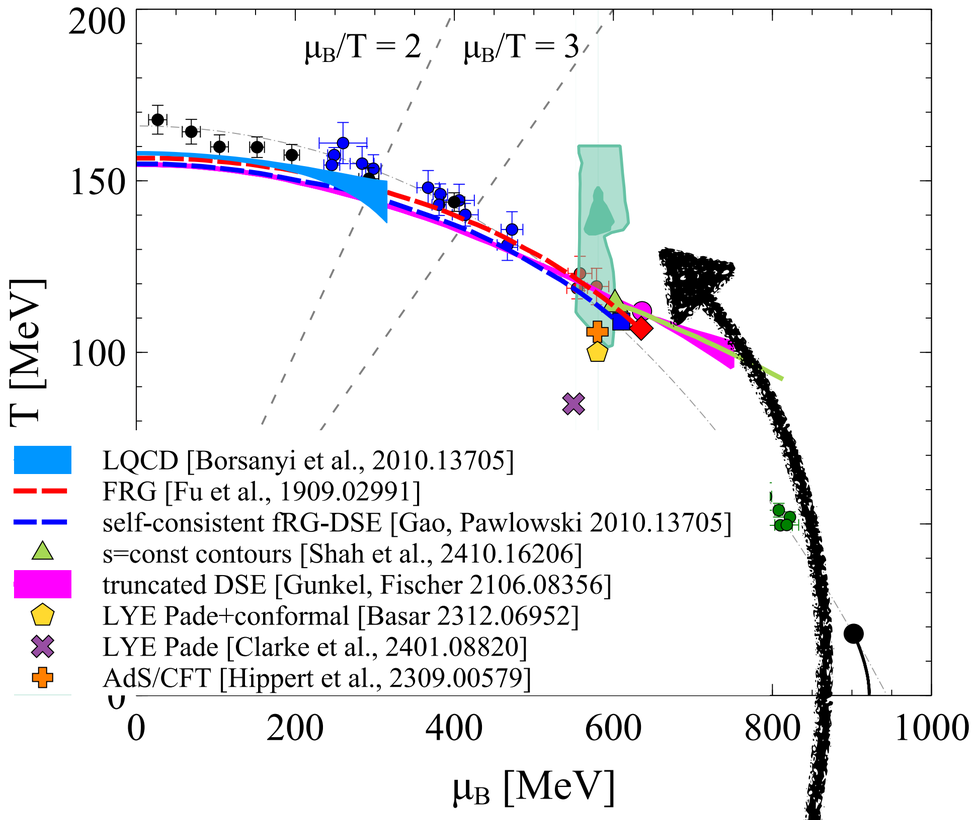

first extraction from experimental data?

With mean-field exponents, we find scaling for $555 < \mu_{B,c} < 610$ MeV;
T_c only constrained by "plausibility" (below $T_{pc,\mu_B=0}$ and above $T_{\rm fo}$)

Chi-square contours identify an allowed region in the phase diagram: $\mu_{B,c} = 580 \pm 30$ MeV

Scaled susceptibility: 2D fit w/ mean-field exponents

$$\chi L^{-\frac{\sigma}{\nu}} = \phi(tL^{\frac{1}{\nu}})$$

one can find CP by plotting

D. Oliinychenko, **A. Sorensen**, V. Koch, L. McLerran, Phys. Rev. C **108**, 3, 034908 (2023), arXiv:2208.11996

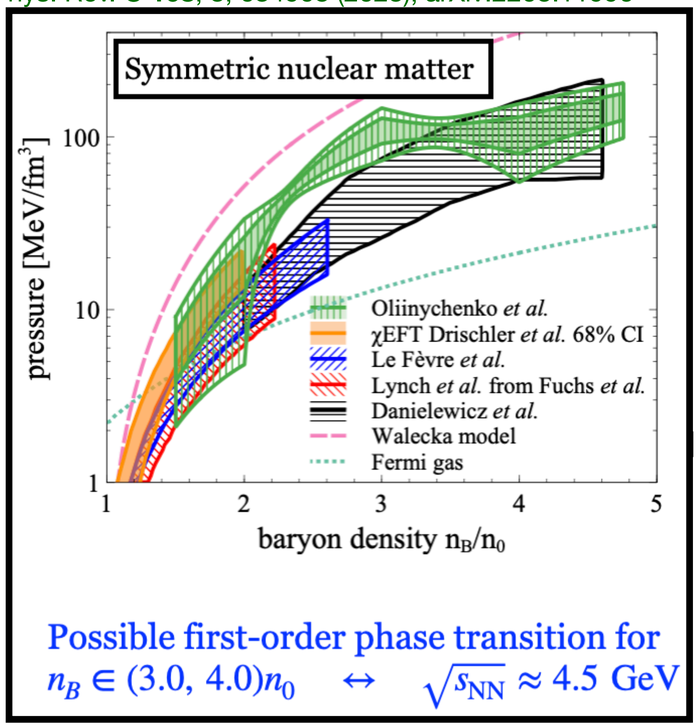

Possible first-order phase transition for $n_B \in (3.0, 4.0)n_0 \leftrightarrow \sqrt{s_{NN}} \approx 4.5$ GeV

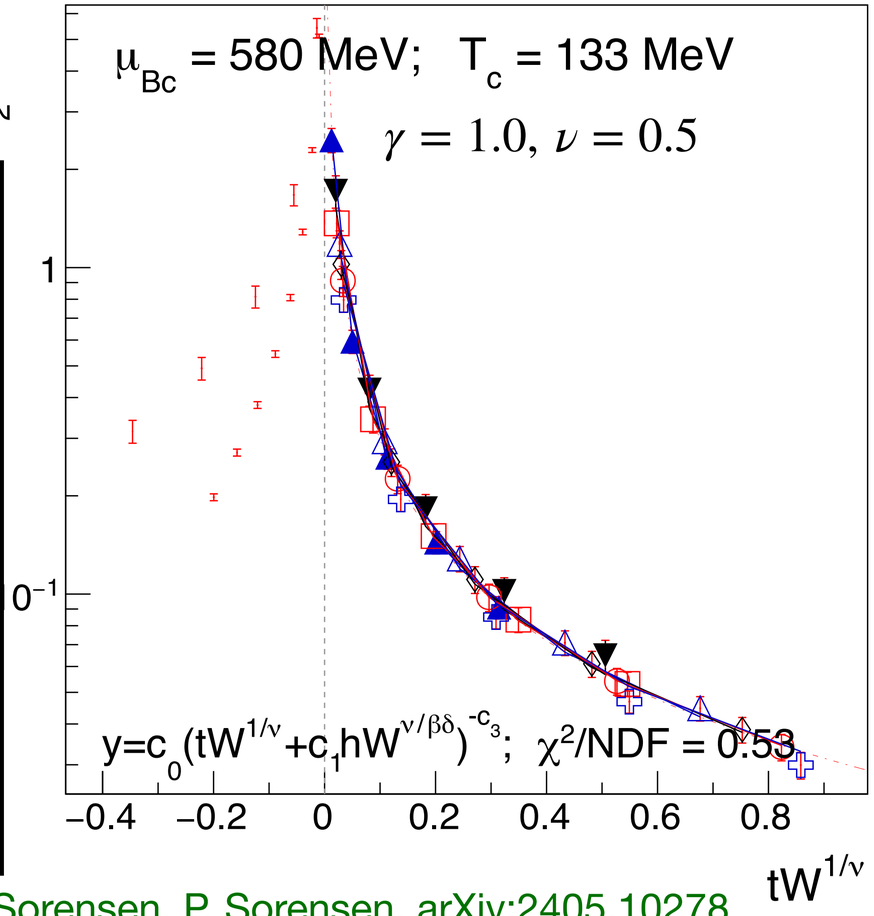

A. Sorensen, P. Sorensen, arXiv:2405.10278

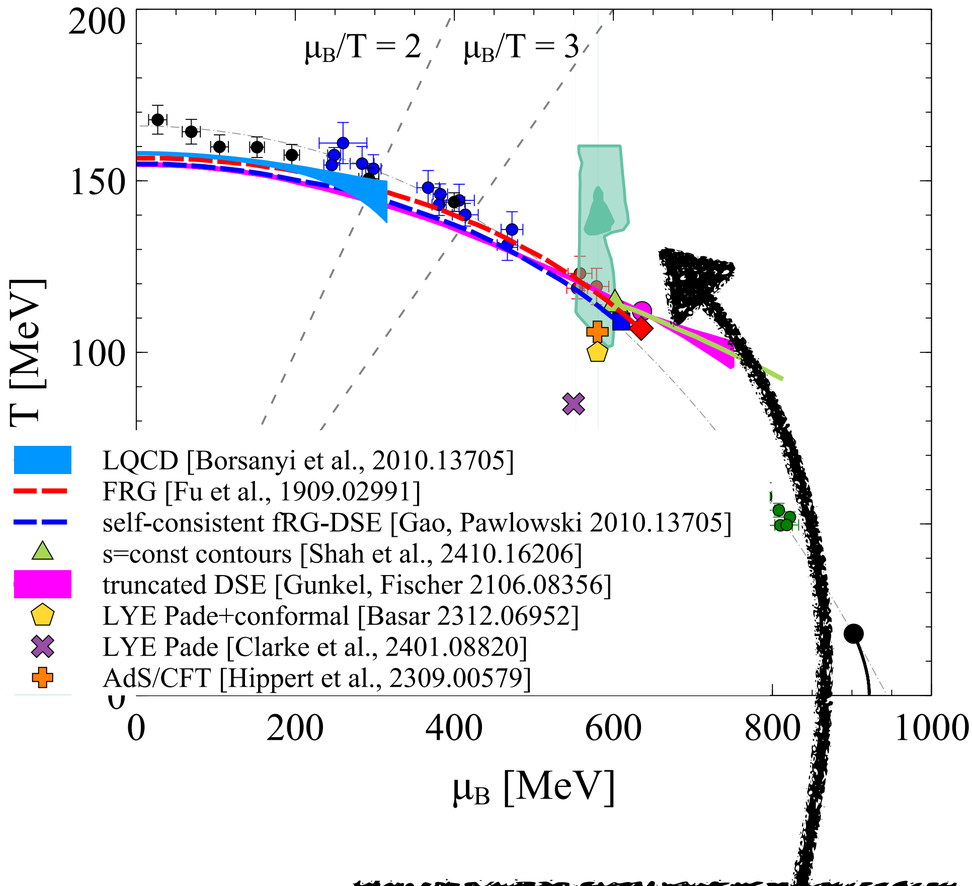

first extraction from experimental data?

With mean-field exponents, we find scaling for $555 < \mu_{B,c} < 610$ MeV;
T_c only constrained by "plausibility" (below $T_{pc,\mu_B=0}$ and above T_{fo})

Chi-square contours identify an allowed region in the phase diagram: $\mu_{B,c} = 580 \pm 30$ MeV

But is the scaling we see unique to CP physics?

Dynamic baseline

Let's compare to the simplest theory of QCD without a CP: the hadron resonance gas (HRG).

What about the dynamics? Simulations in SMASH transport code without mean-fields ~ HRG.

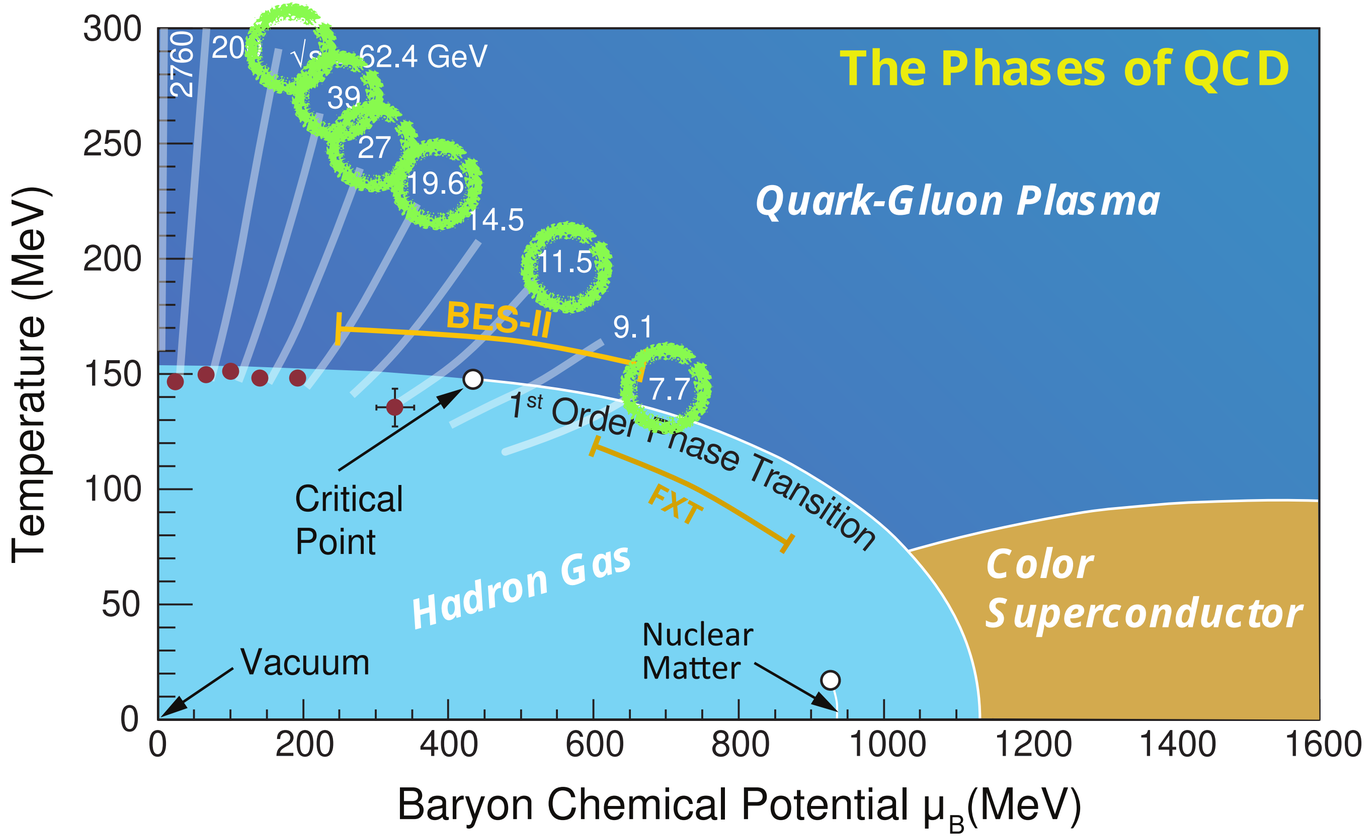

L. Du, A. Sorensen, M. Stephanov, *Int.J.Mod.Phys.E* 33 (2024) 07, 2430008, arXiv:2402.10183

J. Weil *et al.*, Phys.Rev.C 94 (2016) 5, 054905, arXiv:1606.06642

Unscaled plots: χ_2/L vs. μ_B

STAR result

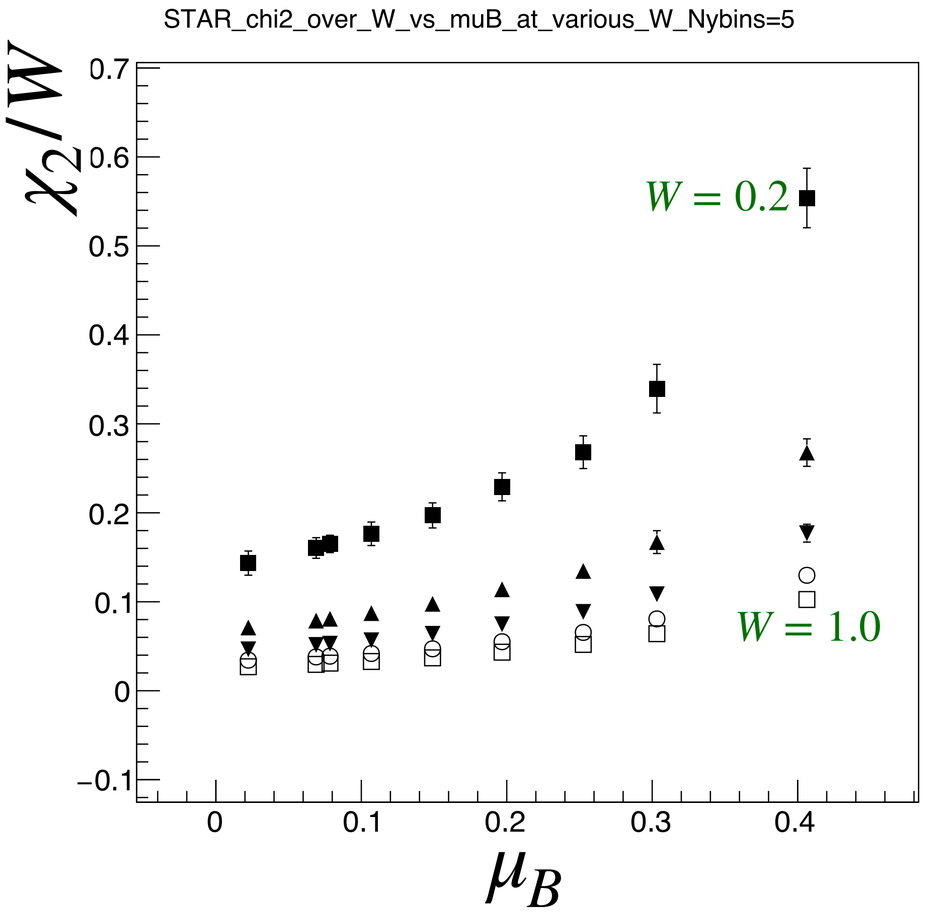

SMASH result

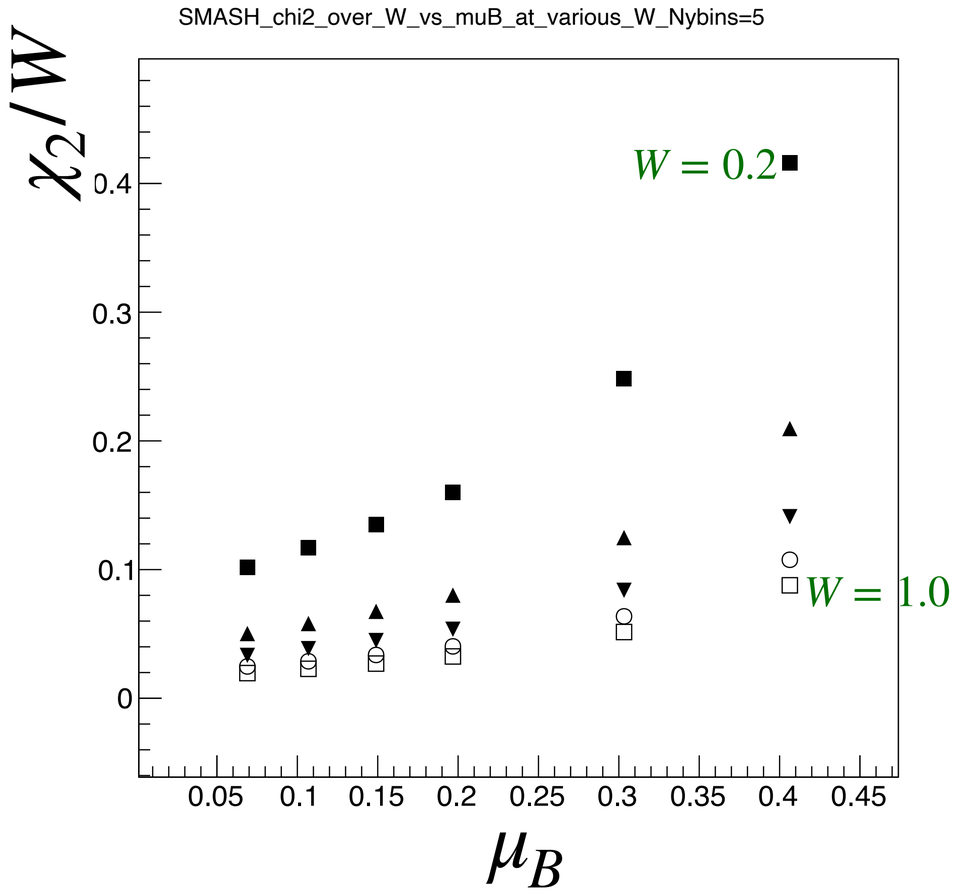

Unscaled plots: χ_2/L vs. μ_B

STAR result

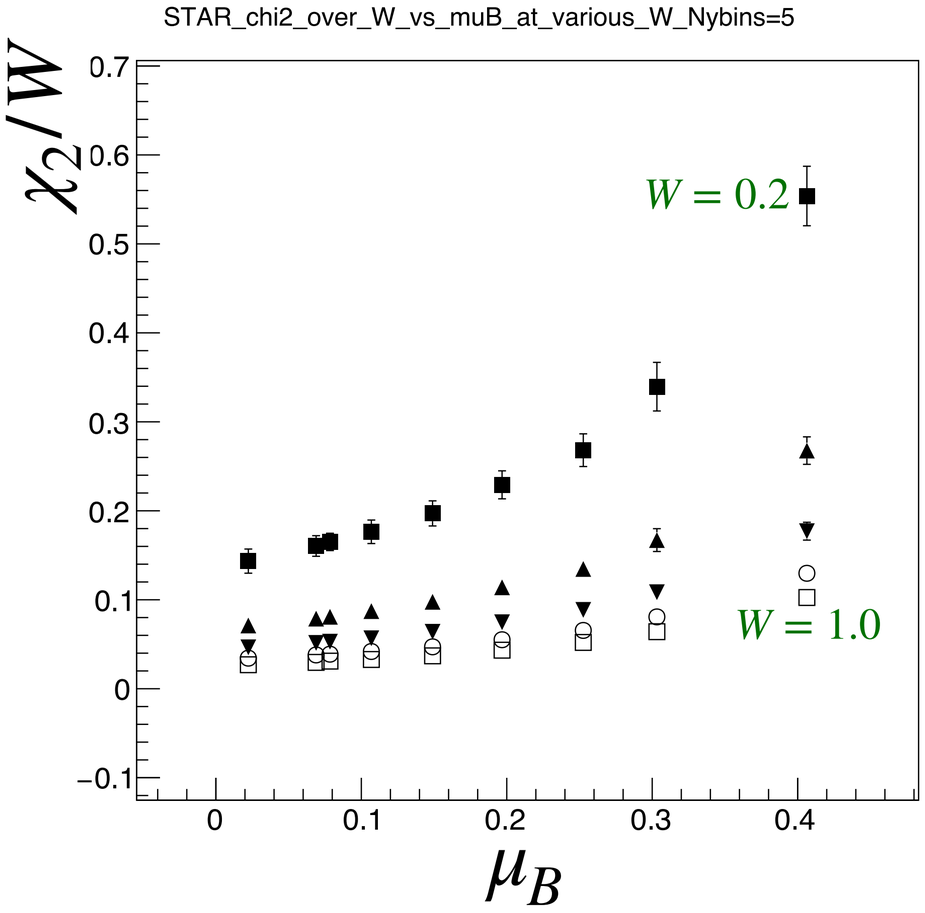

SMASH result

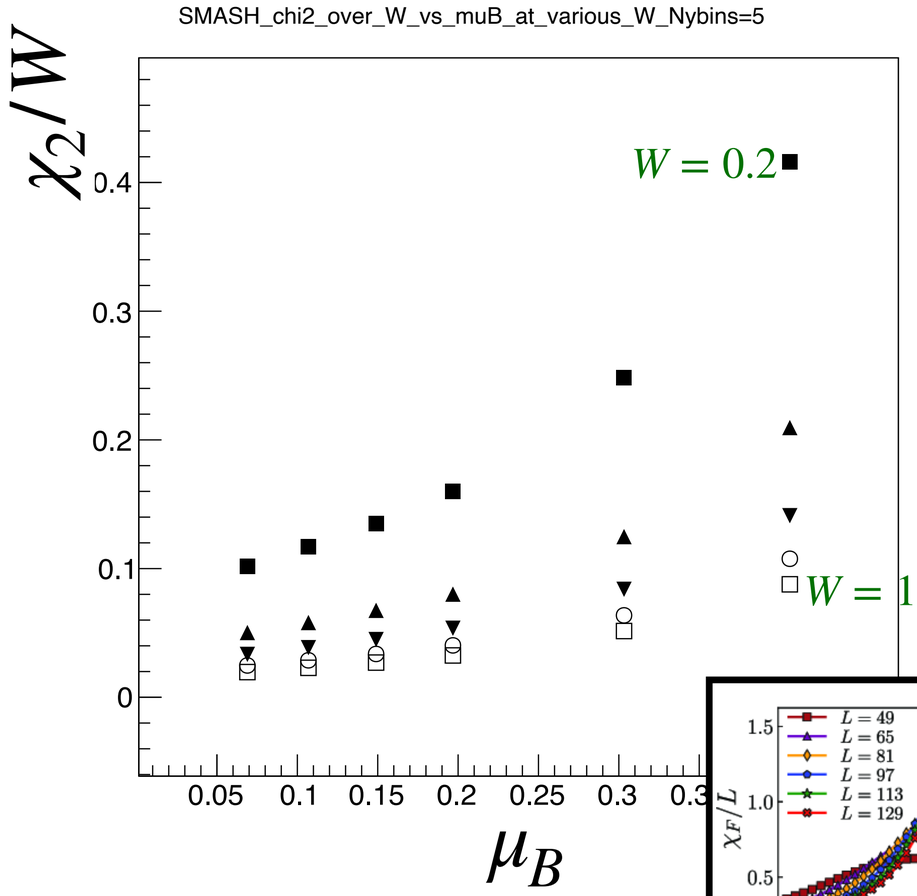

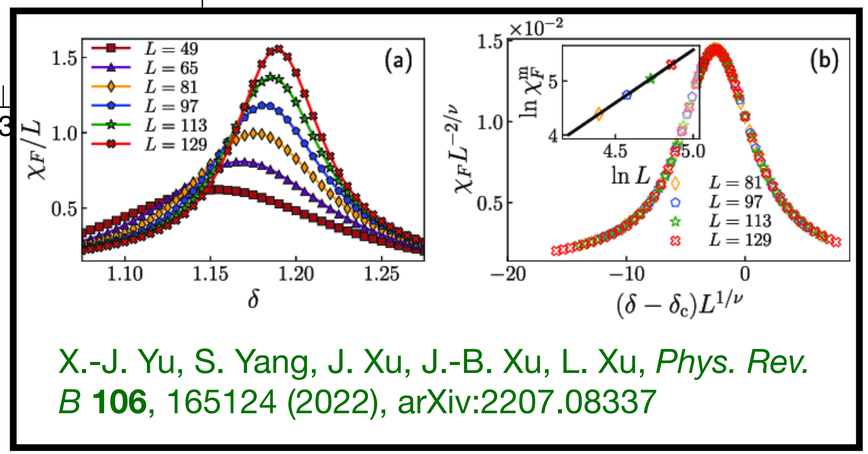

X.-J. Yu, S. Yang, J. Xu, J.-B. Xu, L. Xu, *Phys. Rev. B* **106**, 165124 (2022), arXiv:2207.08337

Unscaled plots: χ_2/L vs. μ_B

STAR result

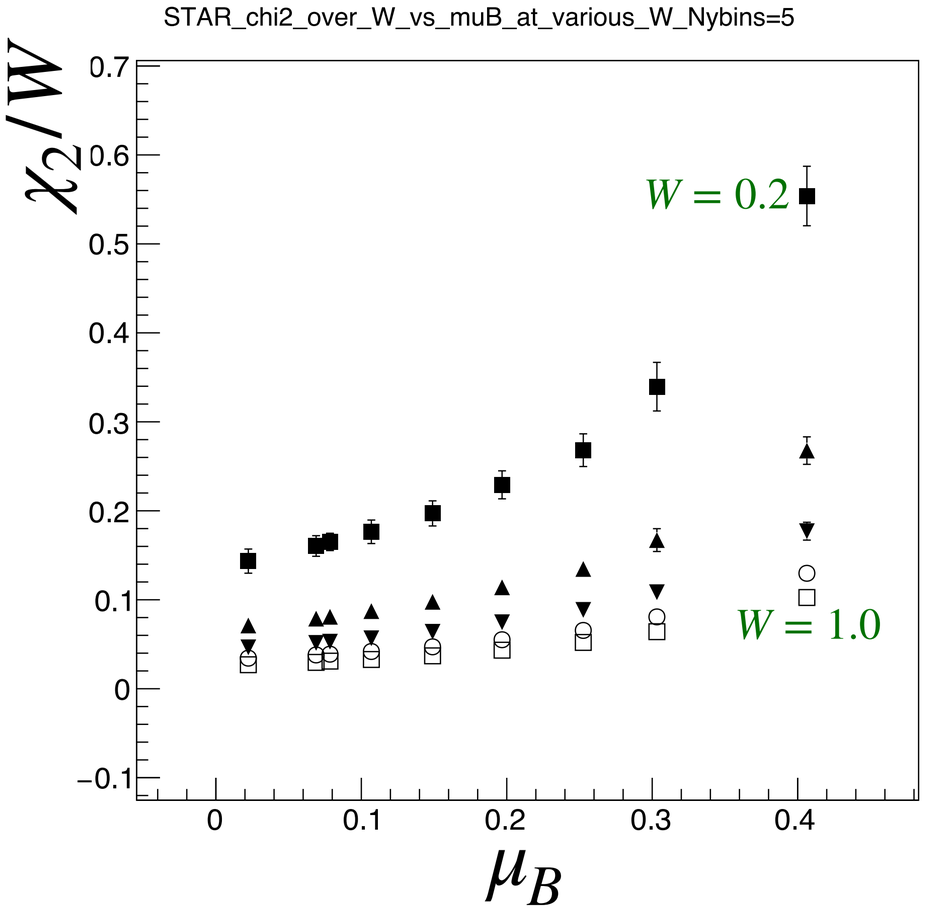

SMASH result

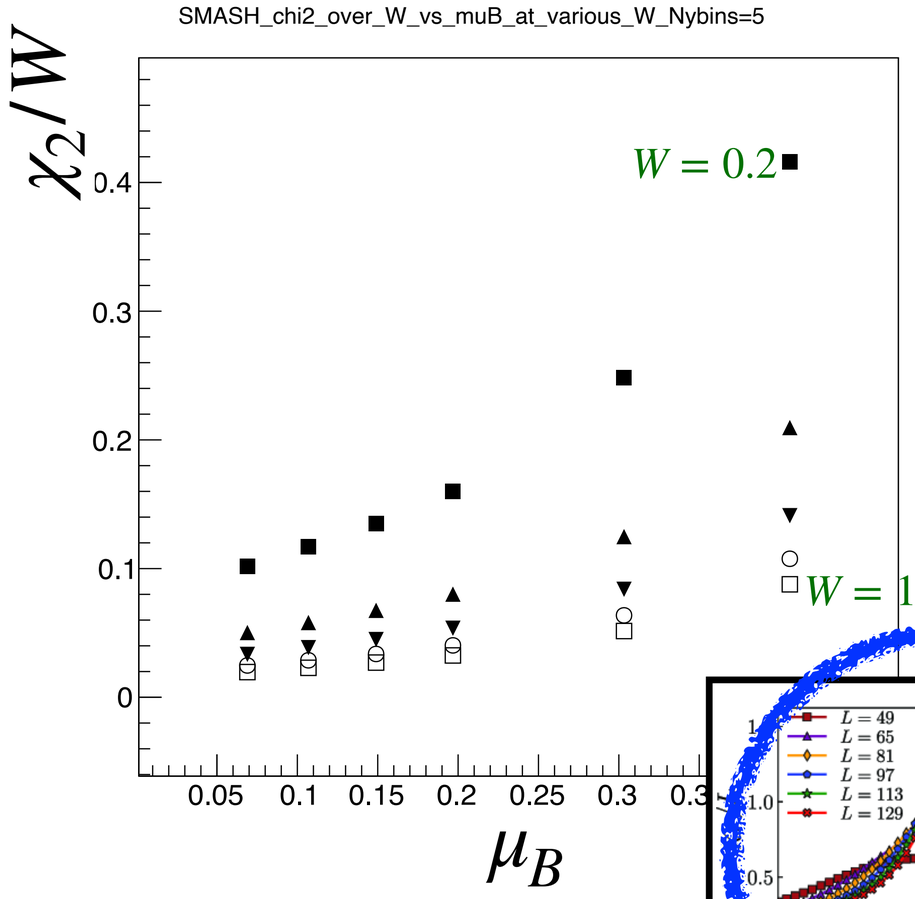

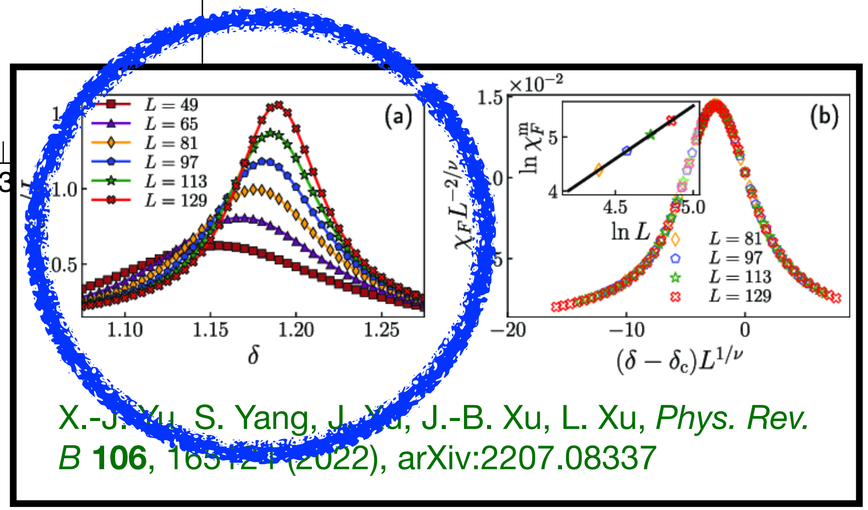

X.-J. Xu, S. Yang, J. Xu, J.-B. Xu, L. Xu, *Phys. Rev. B* **106**, 165124 (2022), arXiv:2207.08337

Scaled plots: $\chi_2 W^{-\gamma/\nu}$ vs. $|t|W^{1/\nu}$

STAR result

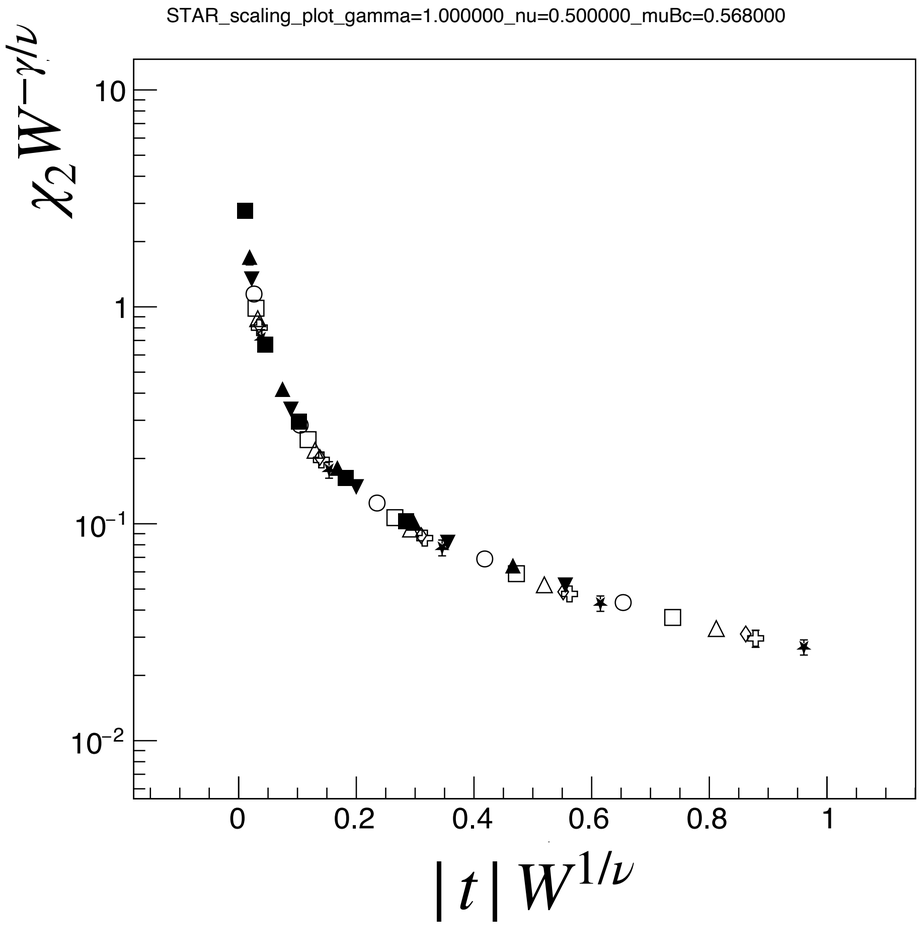

$\mu_{B,c} \approx 570$ MeV

SMASH result

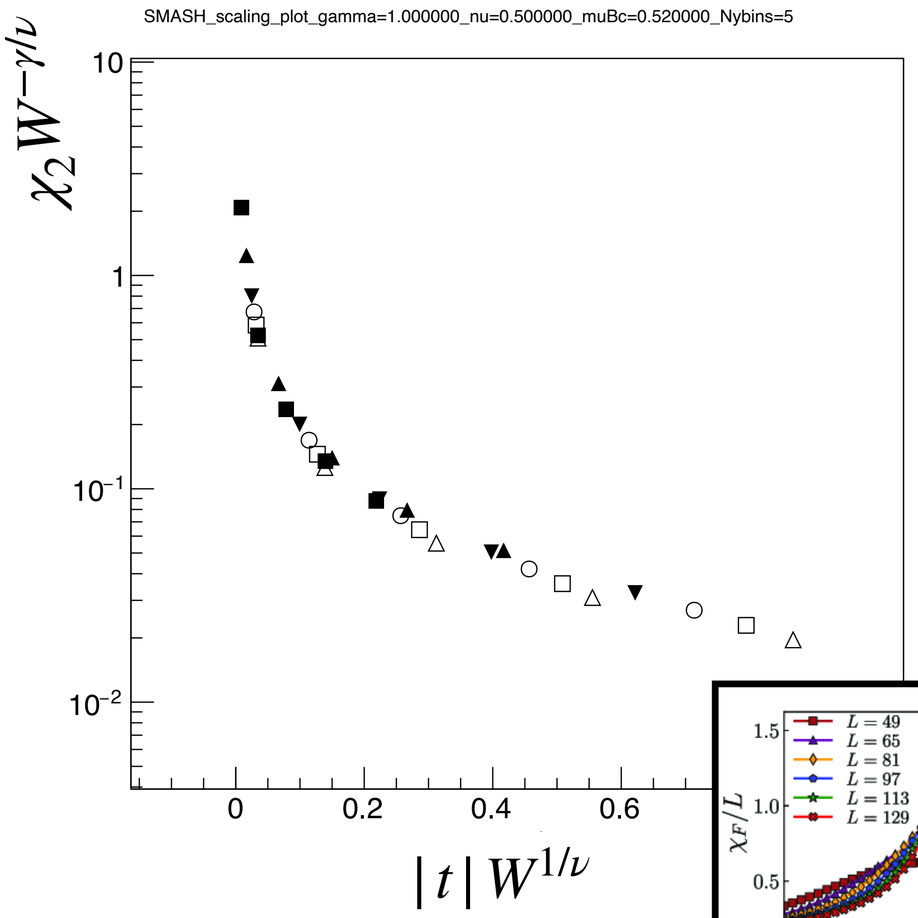

$\mu_{B,c} \approx 520$ MeV

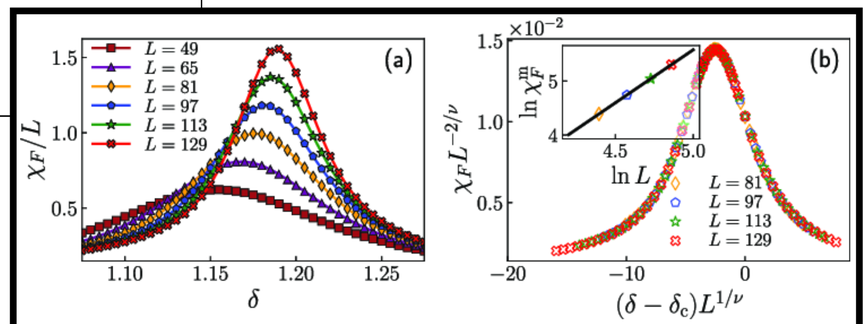

X.-J. Yu, S. Yang, J. Xu, J.-B. Xu, L. Xu, *Phys. Rev. B* **106**, 165124 (2022), arXiv:2207.08337

Scaled plots: $\chi_2 W^{-\gamma/\nu}$ vs. $|t|W^{1/\nu}$

STAR result

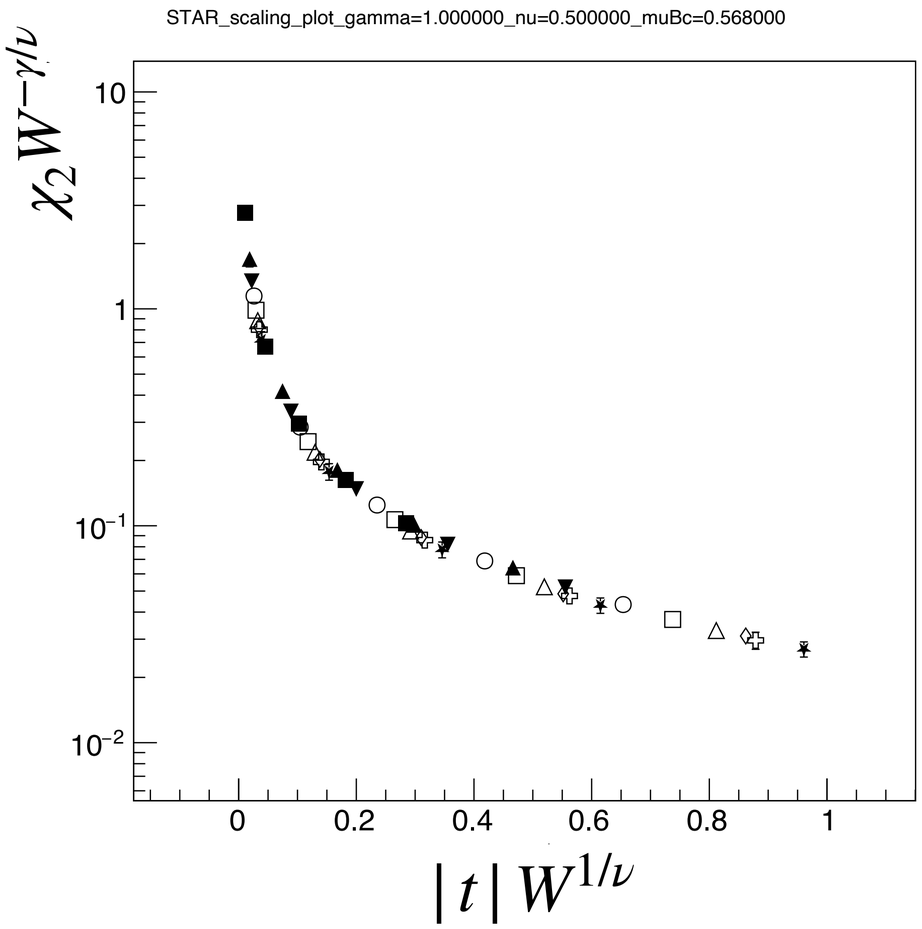

$\mu_{B,c} \approx 570$ MeV

SMASH result

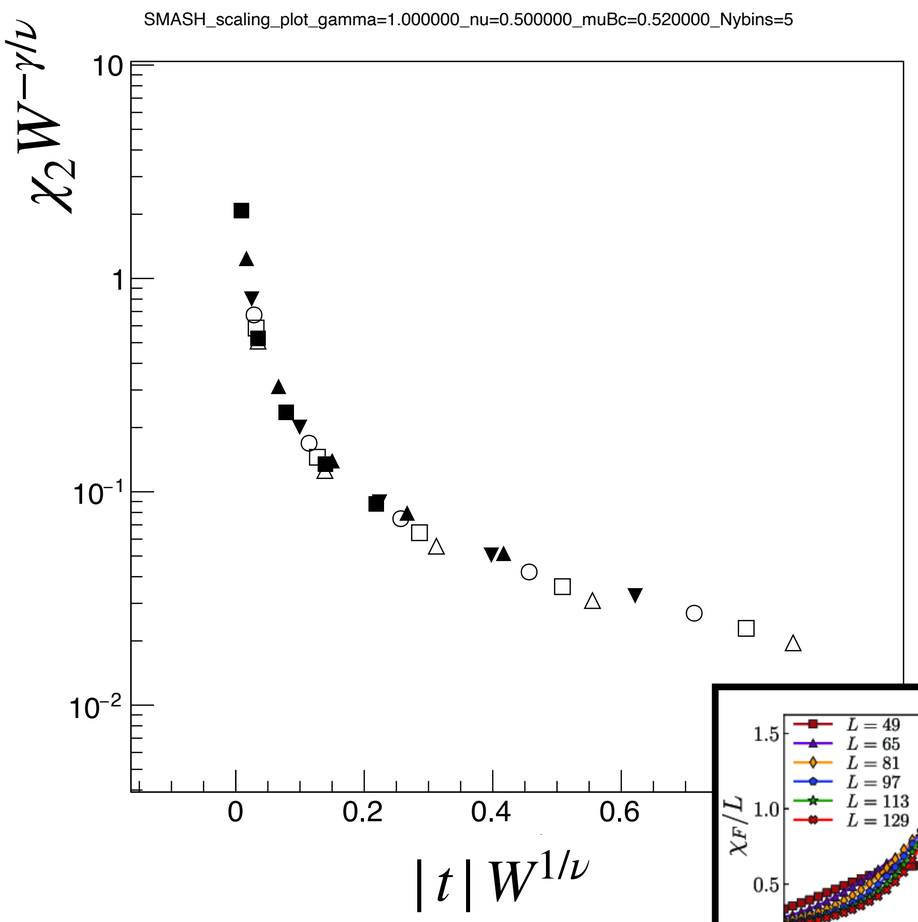

$\mu_{B,c} \approx 520$ MeV

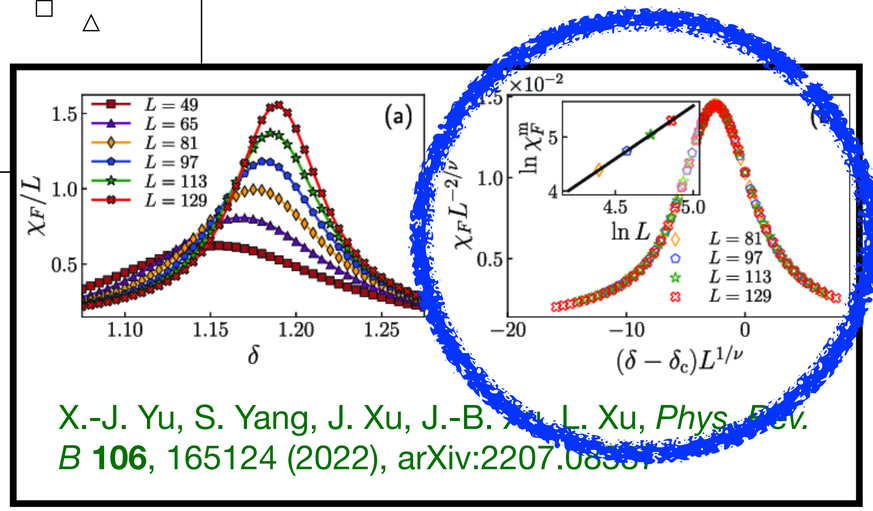

X.-J. Yu, S. Yang, J. Xu, J.-B. Xu, L. Xu, *Phys. Rev. B* **106**, 165124 (2022), arXiv:2207.08367

Scaled plots: $\chi_2 W^{-\gamma/\nu}$ vs. $|t|W^{1/\nu}$

STAR result

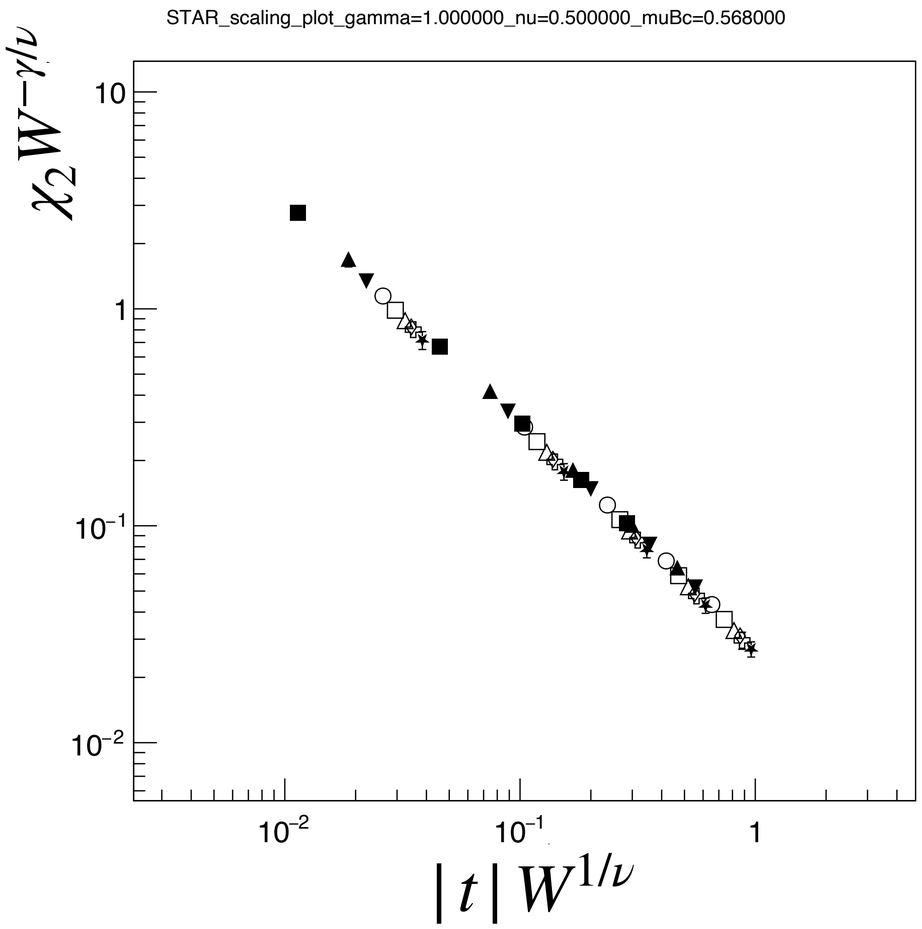

$\mu_{B,c} \approx 570$ MeV

SMASH result

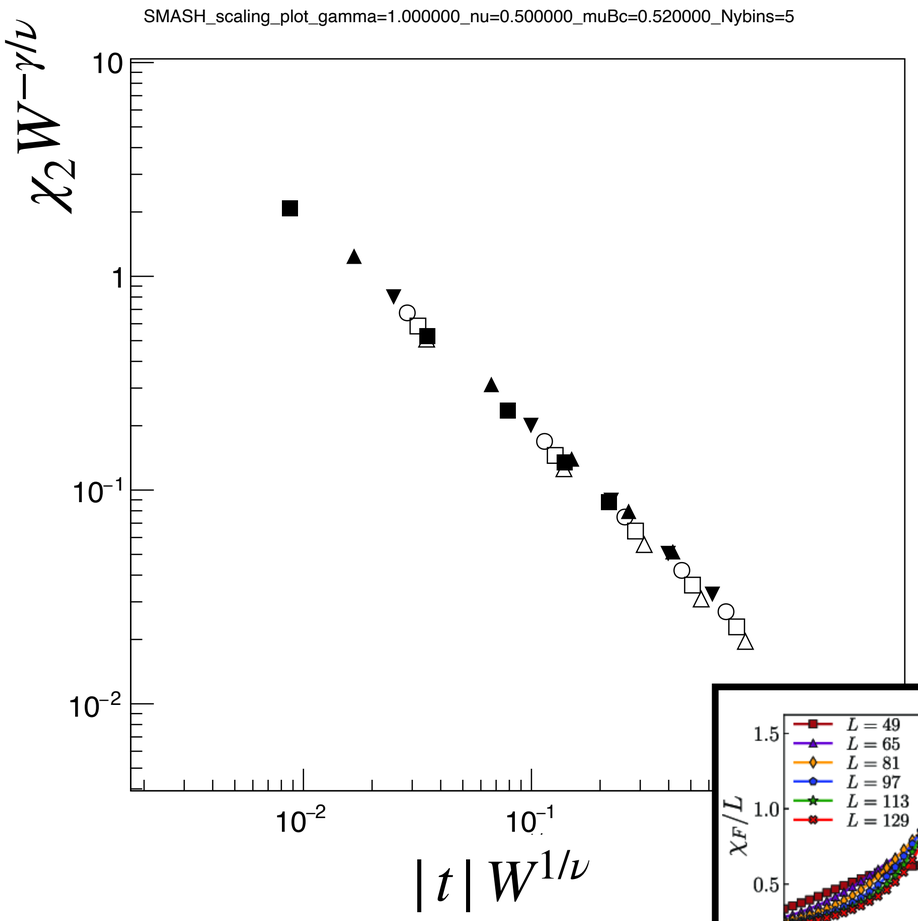

$\mu_{B,c} \approx 520$ MeV

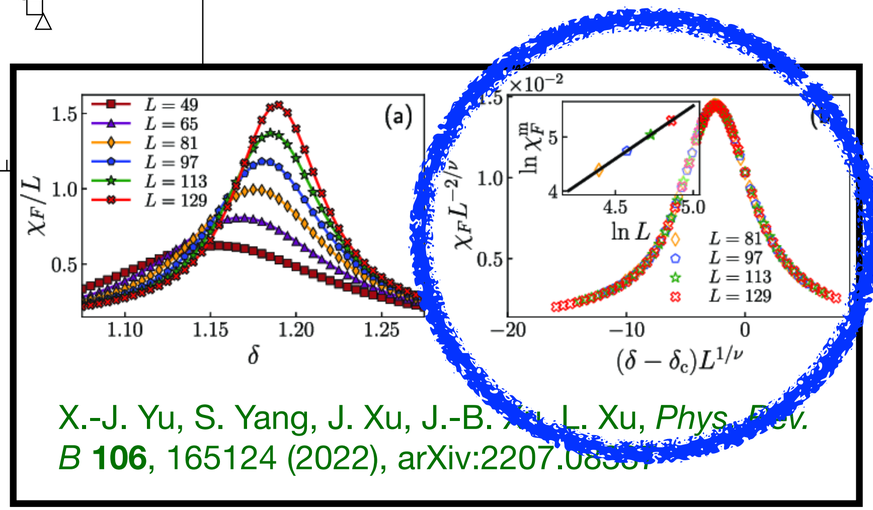

X.-J. Yu, S. Yang, J. Xu, J.-B. Xu, L. Xu, *Phys. Rev. B* **106**, 165124 (2022), arXiv:2207.08367

Scaled plots: $\chi_2 W^{-\gamma/\nu}$ vs. $|t|W^{1/\nu}$

STAR result

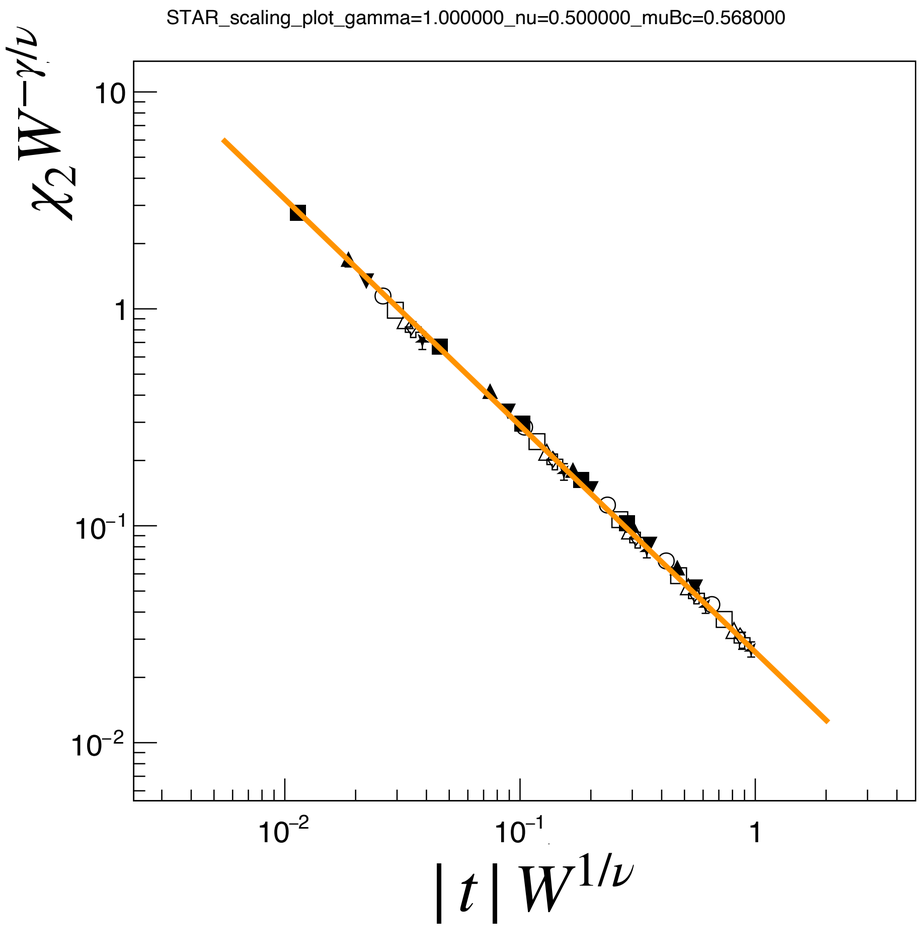

$\mu_{B,c} \approx 570$ MeV

SMASH result

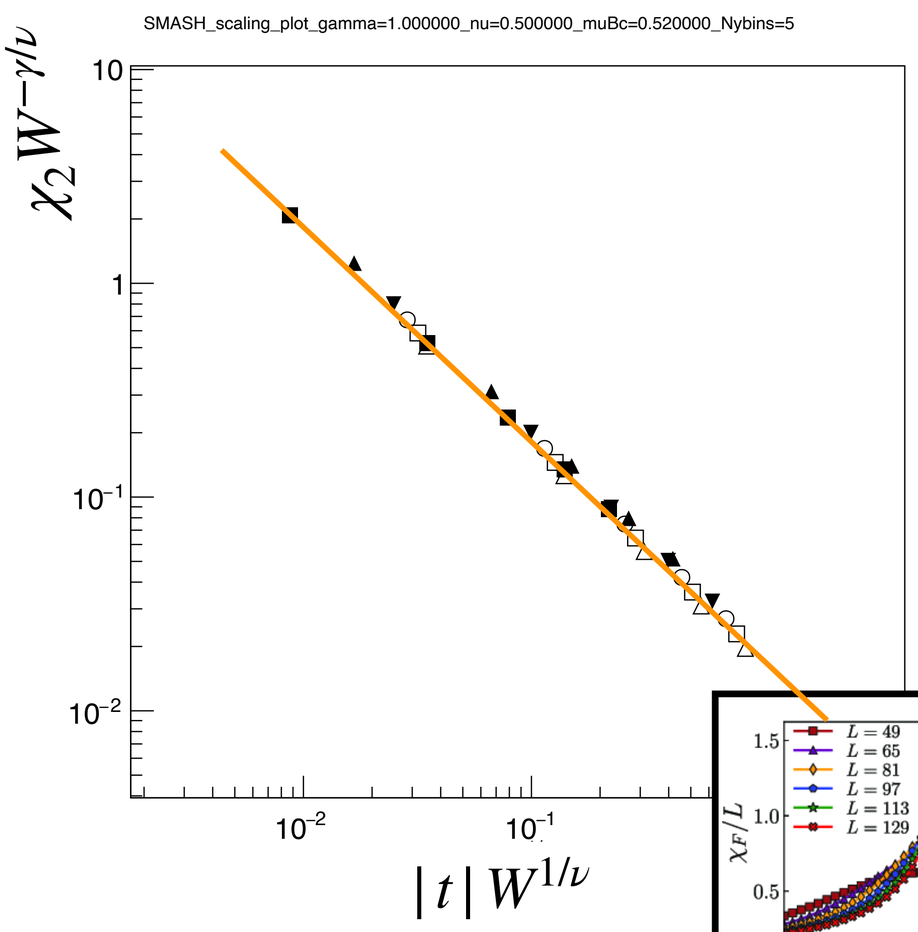

$\mu_{B,c} \approx 520$ MeV

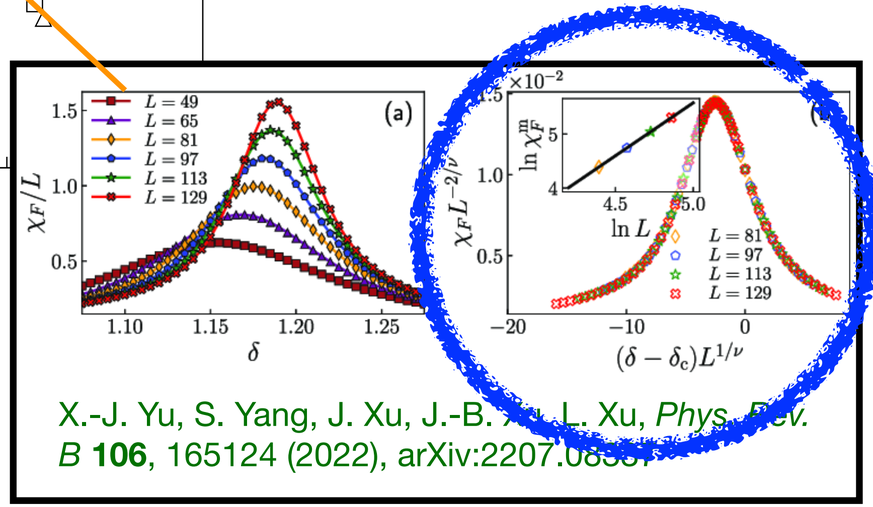

X.-J. Yu, S. Yang, J. Xu, J.-B. Xu, L. Xu, *Phys. Rev. B* **106**, 165124 (2022), arXiv:2207.08367

Scaled plots: $\chi_2 W^{-\gamma/\nu}$ vs. $|t|W^{1/\nu}$

STAR result

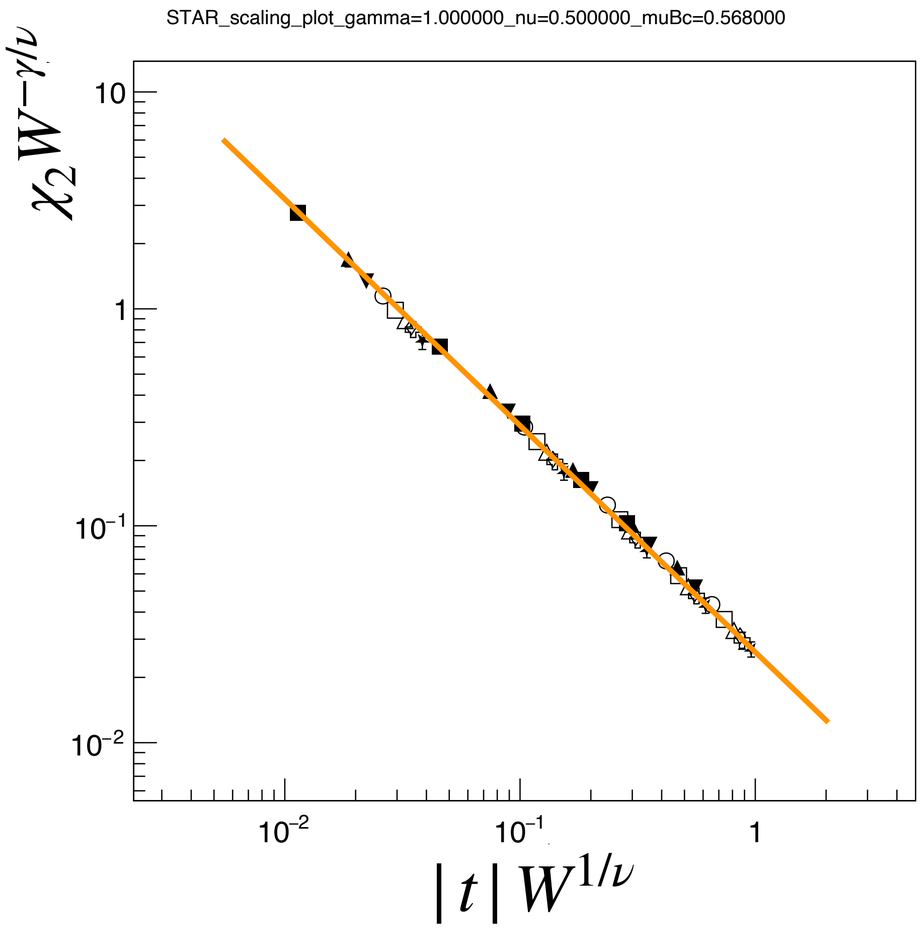

$\mu_{B,c} \approx 570$ MeV

SMASH result

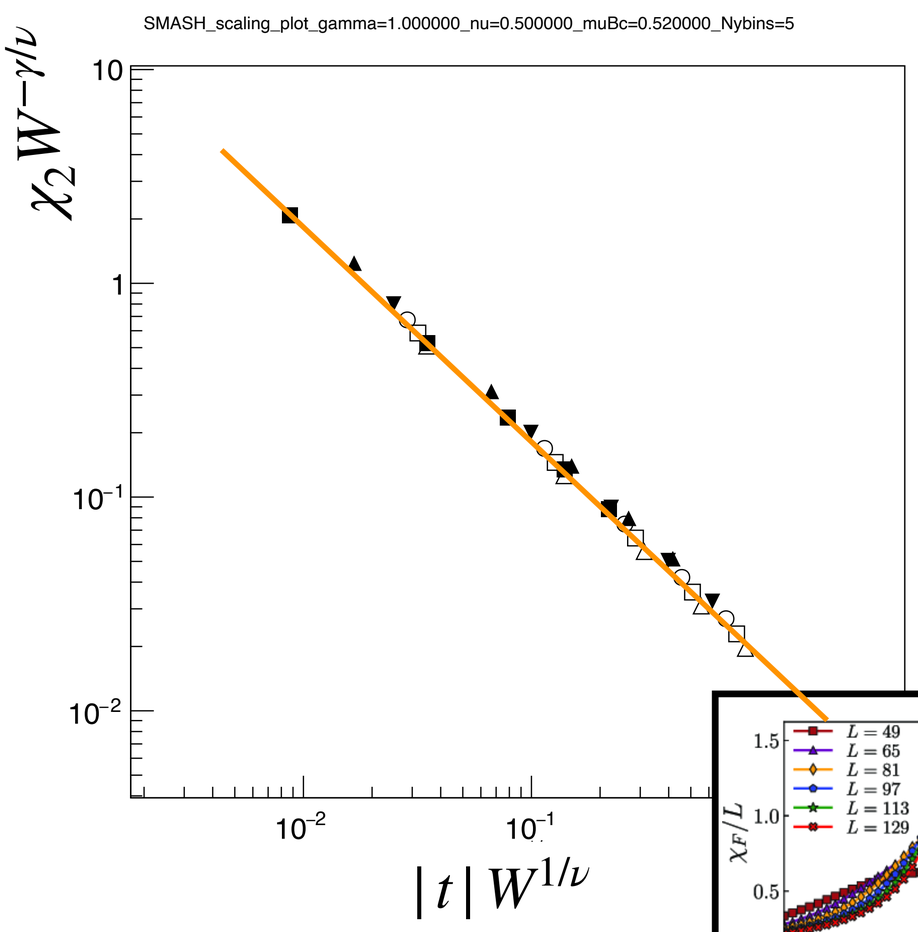

$\mu_{B,c} \approx 520$ MeV

Small difference in scalability — is it significant?

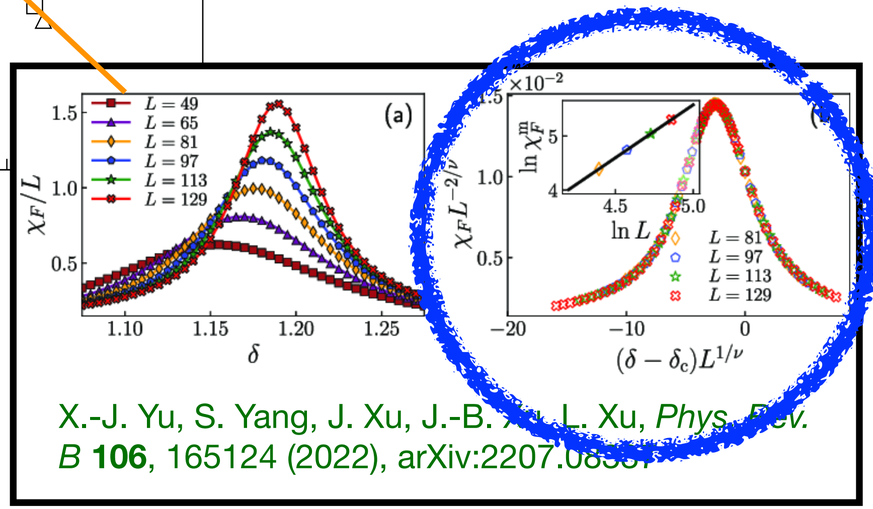

X.-J. Yu, S. Yang, J. Xu, J.-B. Xu, L. Xu, *Phys. Rev. B* **106**, 165124 (2022), arXiv:2207.08367

Remains to be done for SMASH results:

- Centrality bin width correction
- Freeze-out parameters from thermal fits (now: parametrization from Andronic *et al.*)
- Effects of baryon stopping / shape of multiplicity distribution
- …

Still: two QCD CP extractions in the same region of the phase diagram

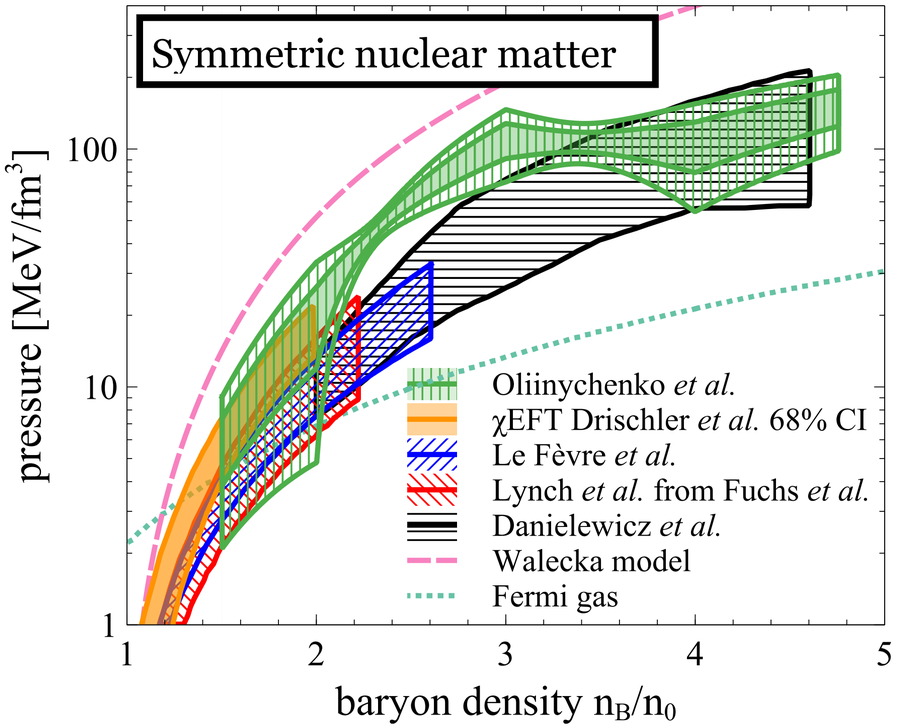

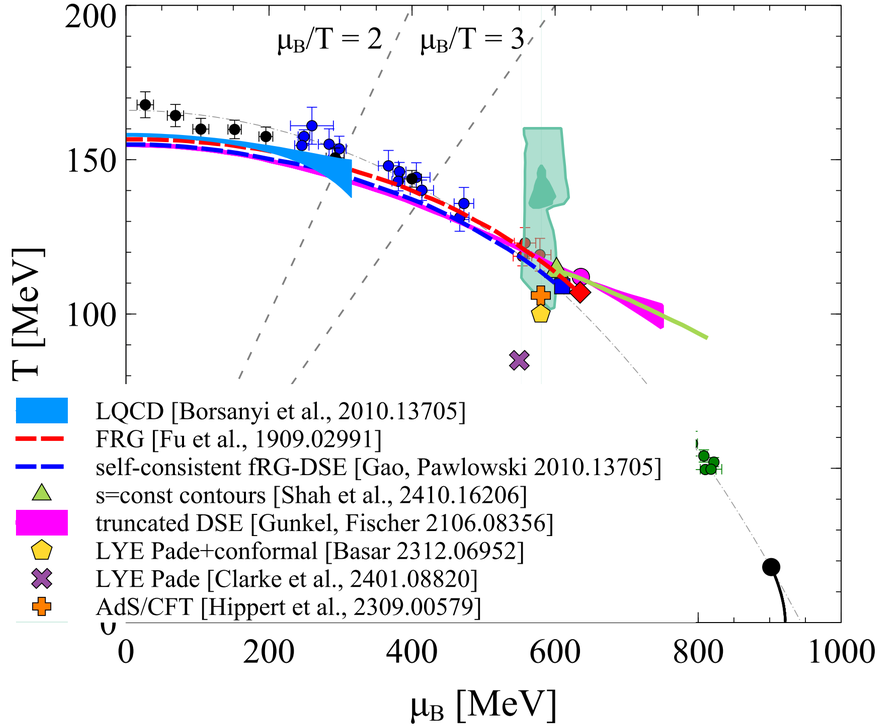

Still: two QCD CP extractions in the same region of the phase diagram

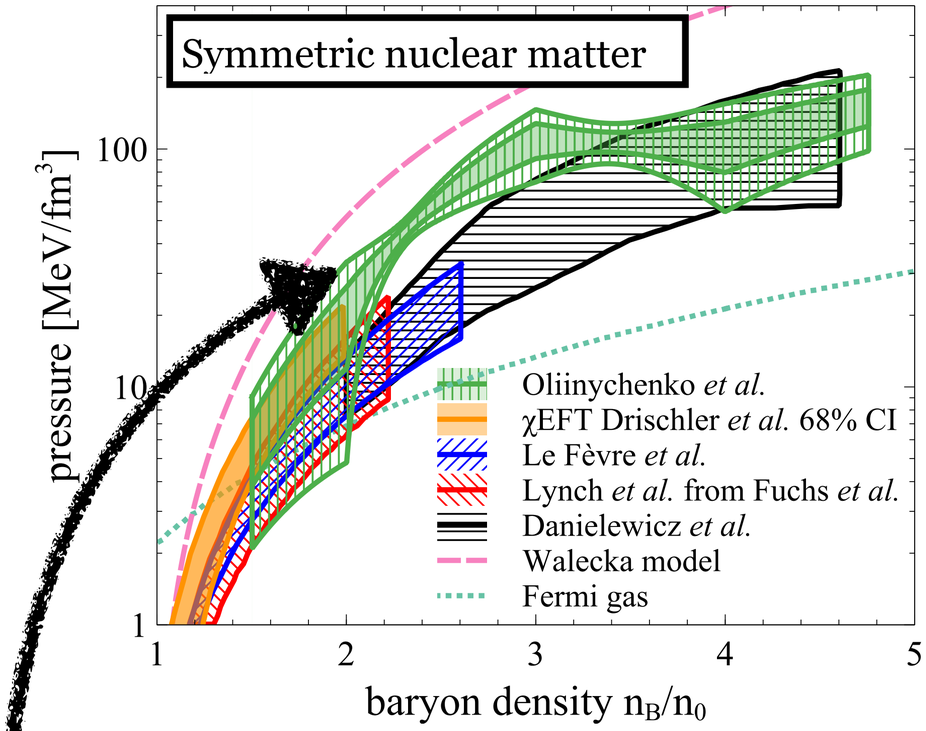

first modern EOS constraint from FXT data!

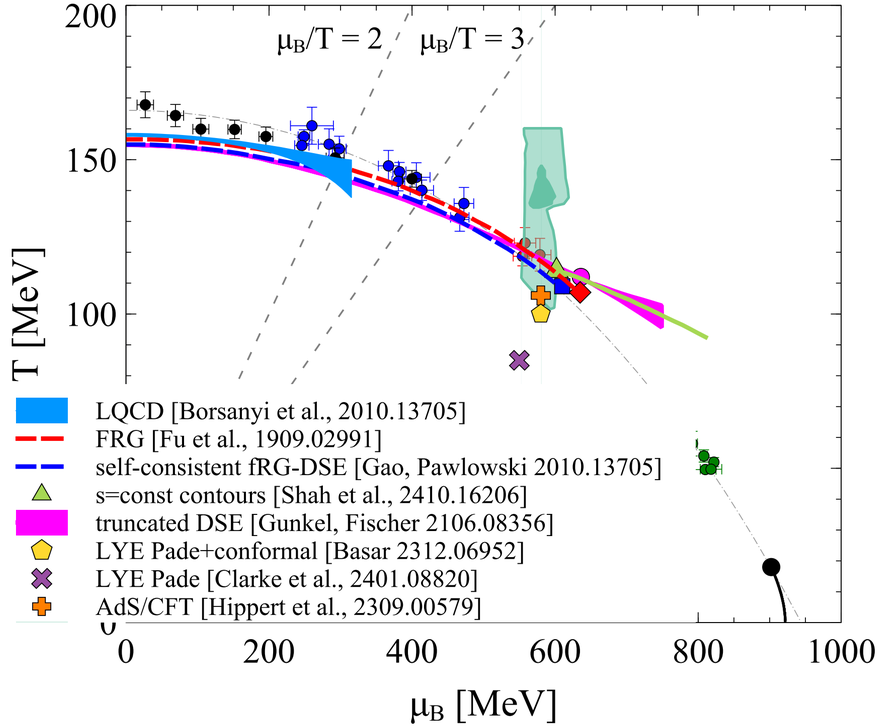

Still: two QCD CP extractions in the same region of the phase diagram

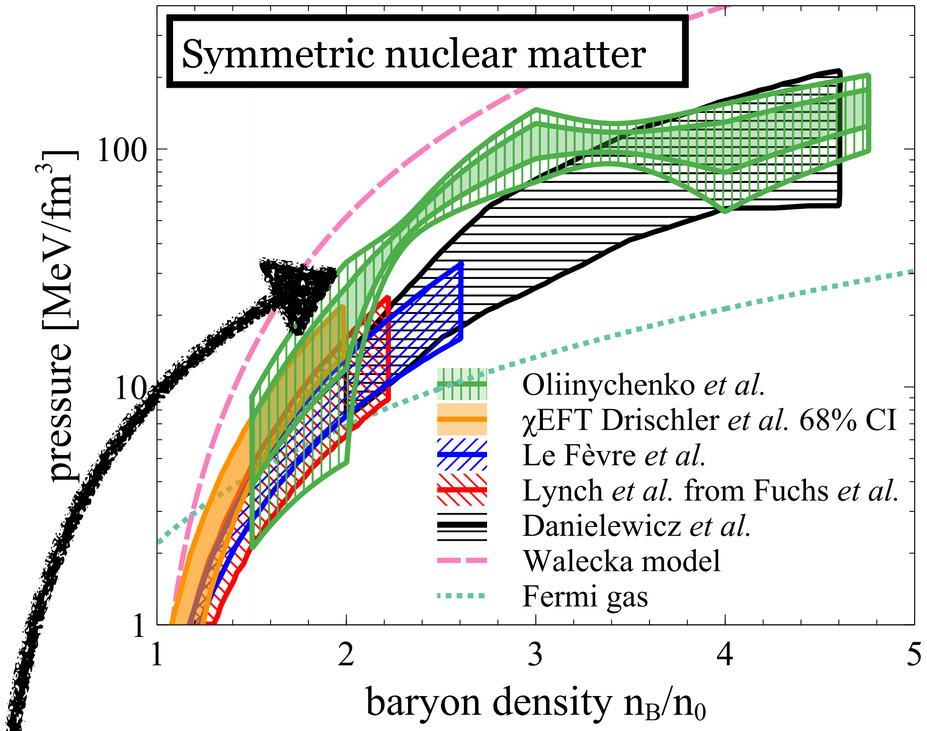

first modern EOS constraint from FXT data!

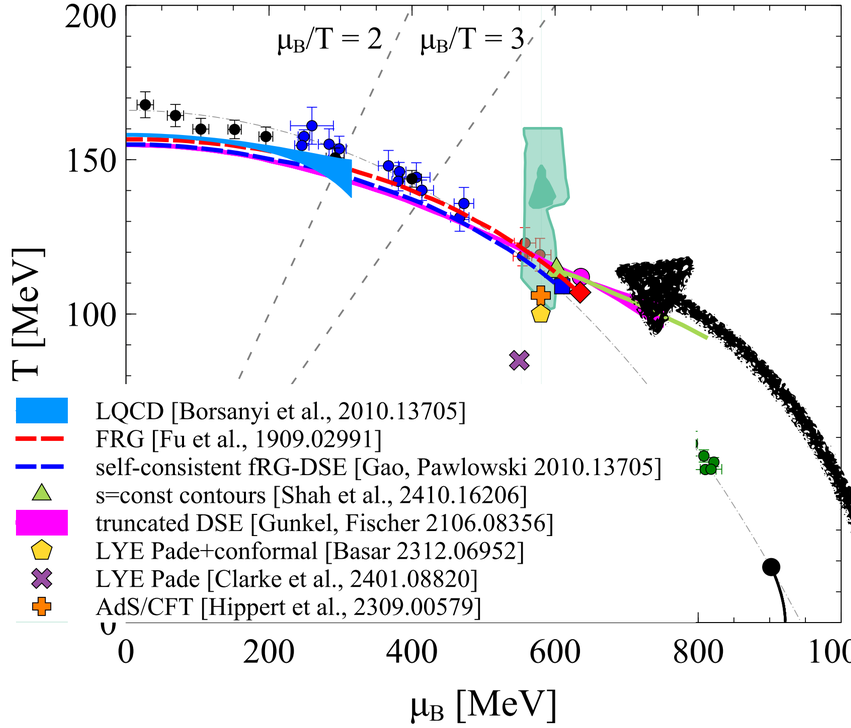

first extraction from experimental data!

Summary

- Theory studies find QCD CP in region probed by FXT: $\mu_B \in (525,625)$ MeV $\sim \sqrt{s_{NN}} \approx 4.5$ GeV

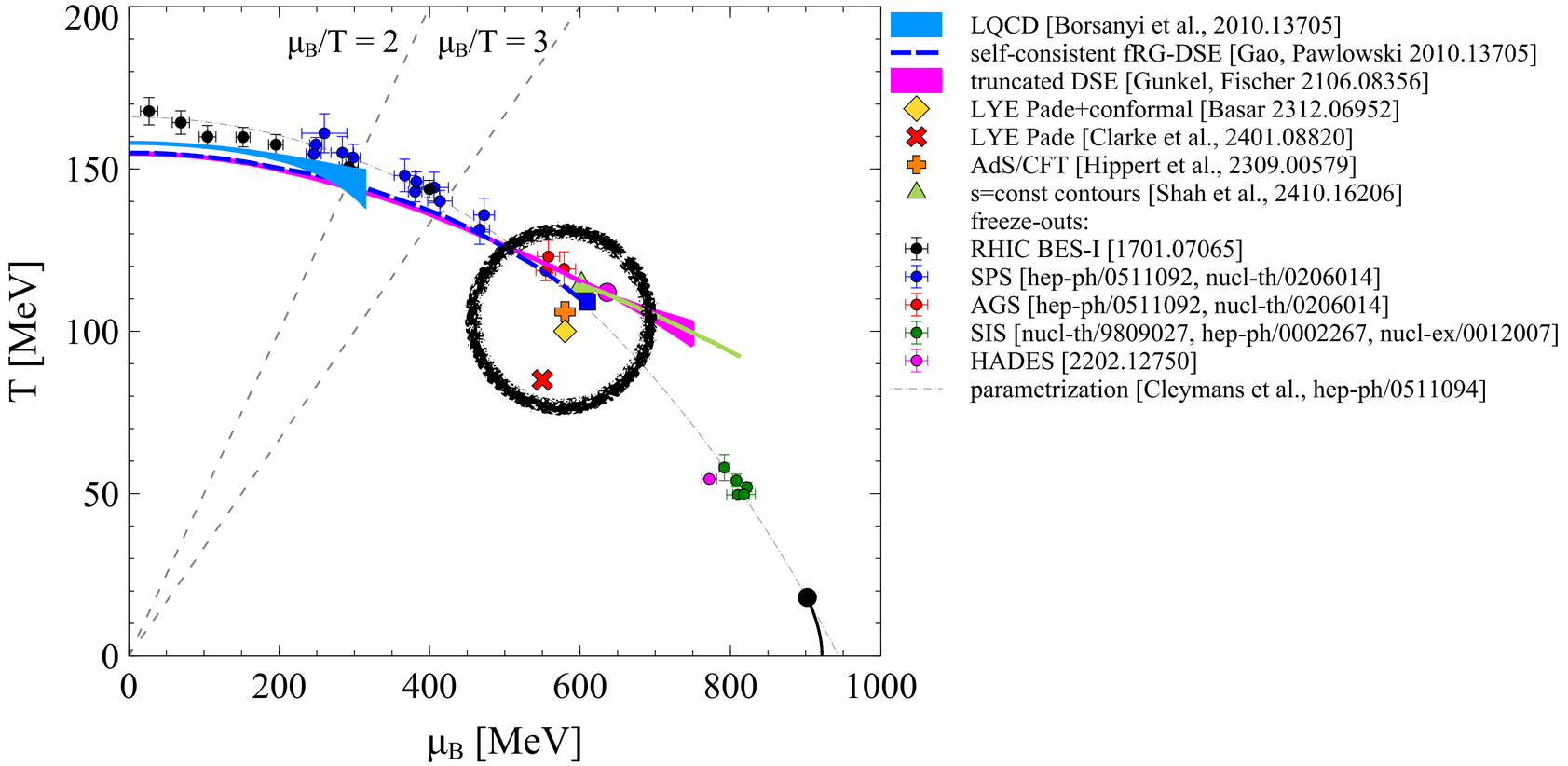

A. Sorensen, P. Sorensen, arXiv:2405.10278

Summary

- Theory studies find QCD CP in region probed by FXT: $\mu_B \in (525,625)$ MeV $\sim \sqrt{s_{NN}} \approx 4.5$ GeV
- FSS of C_2 finds the QCD CP as well: $\mu_B \approx 570$ MeV $\sim \sqrt{s_{NN}} \approx 4.5$ GeV

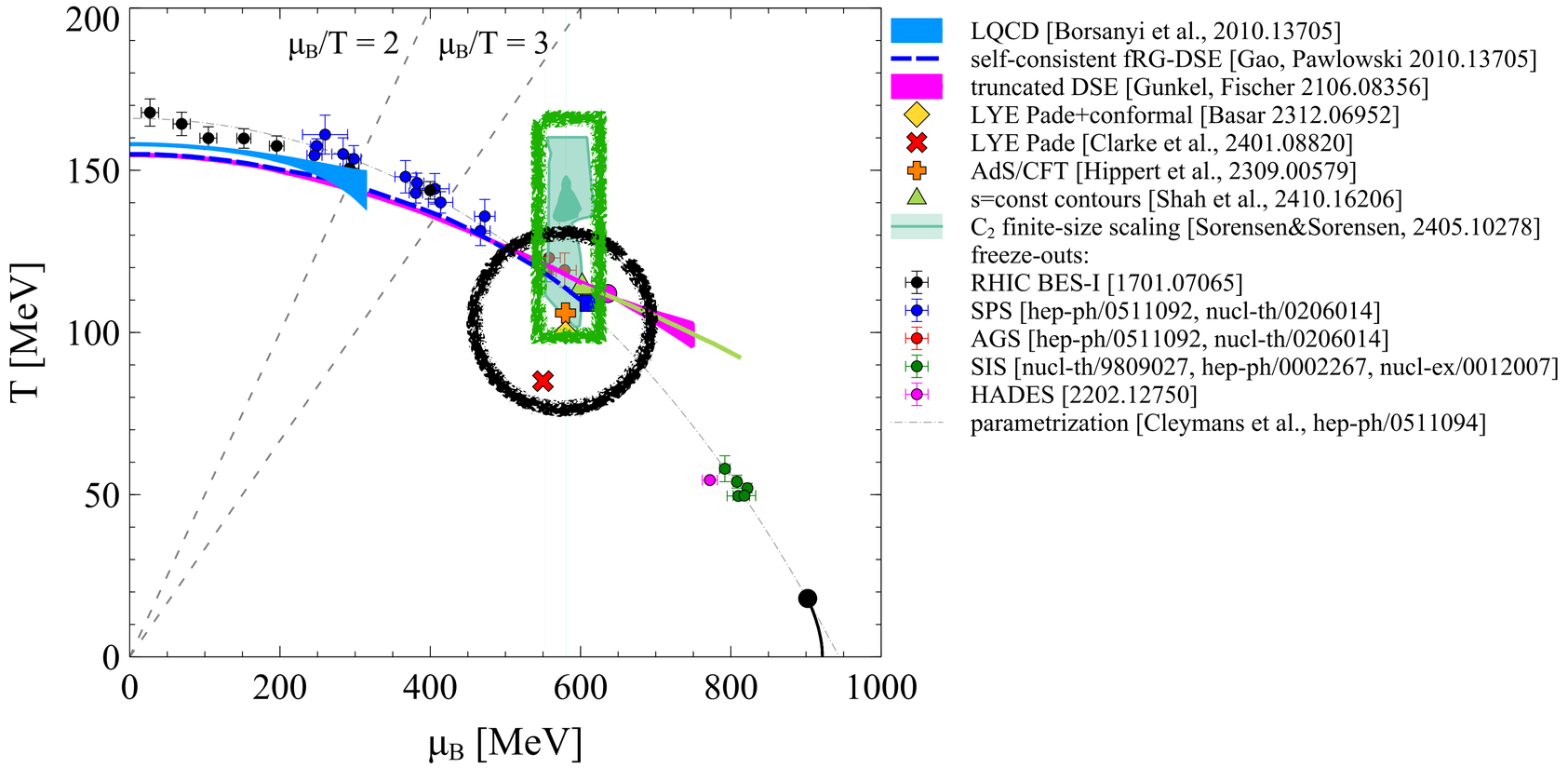

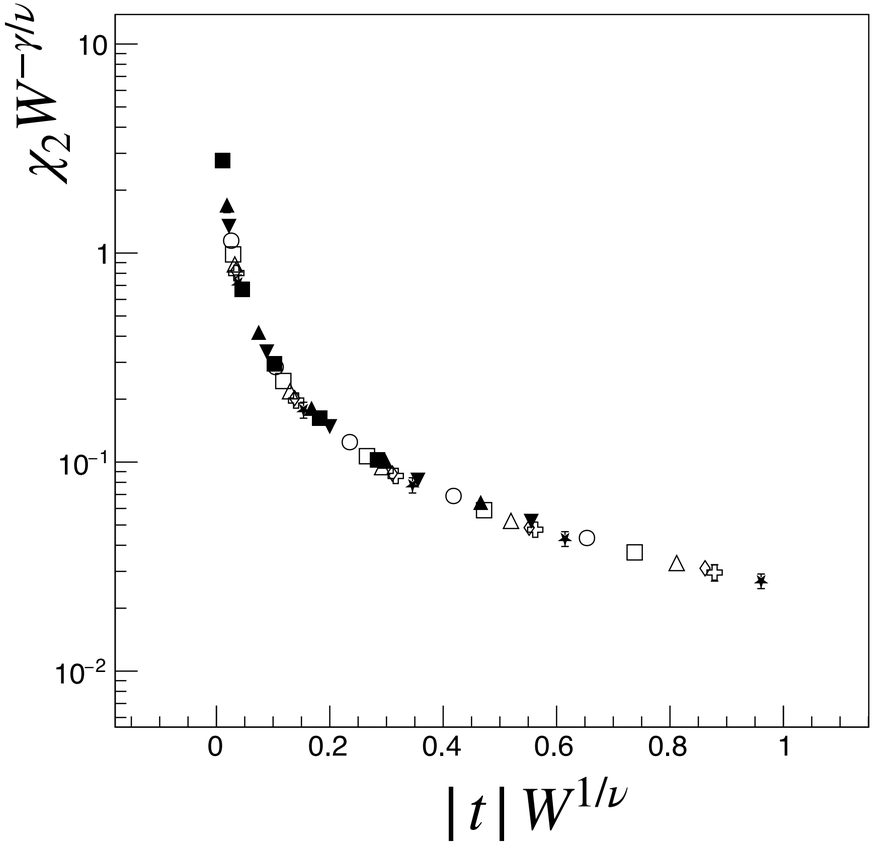

A. Sorensen, P. Sorensen, arXiv:2405.10278

Summary

- Theory studies find QCD CP in region probed by FXT: $\mu_B \in (525,625)$ MeV $\sim \sqrt{s_{NN}} \approx 4.5$ GeV
- FSS of C_2 finds the QCD CP as well: $\mu_B \approx 570$ MeV $\sim \sqrt{s_{NN}} \approx 4.5$ GeV
- C_2 from SMASH cascade does not scale as well (poorer power law fit with $\mu_B \approx 520$ MeV)

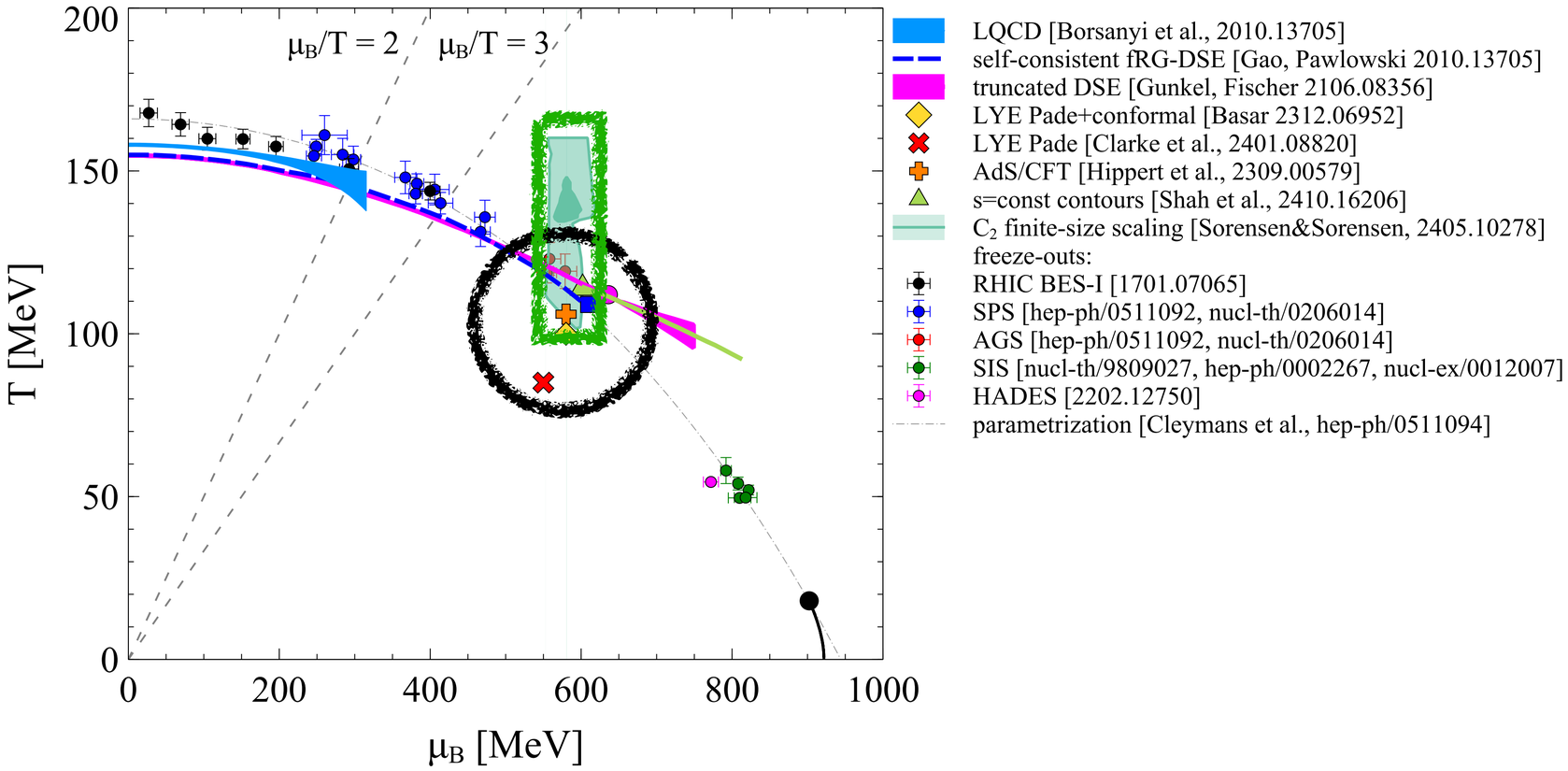

LQCD [Borsanyi et al., 2010.13705]
self-consistent fRG-DSE [Gao, Pawlowski 2010.13705]
truncated DSE [Gunkel, Fischer 2106.08356]
LYE Pade+conformal [Basar 2312.06952]
LYE Pade [Clarke et al., 2401.08820]
AdS/CFT [Hippert et al., 2309.00579]
s=const contours [Shah et al., 2410.16206]
C_2 finite-size scaling [Sorensen&Sorensen, 2405.10278]
freeze-outs:
RHIC BES-I [1701.07065]
SPS [hep-ph/0511092, nucl-th/0206014]
AGS [hep-ph/0511092, nucl-th/0206014]
SIS [nucl-th/9809027, hep-ph/0002267, nucl-ex/0012007]
HADES [2202.12750]
parametrization [Cleymans et al., hep-ph/0511094]

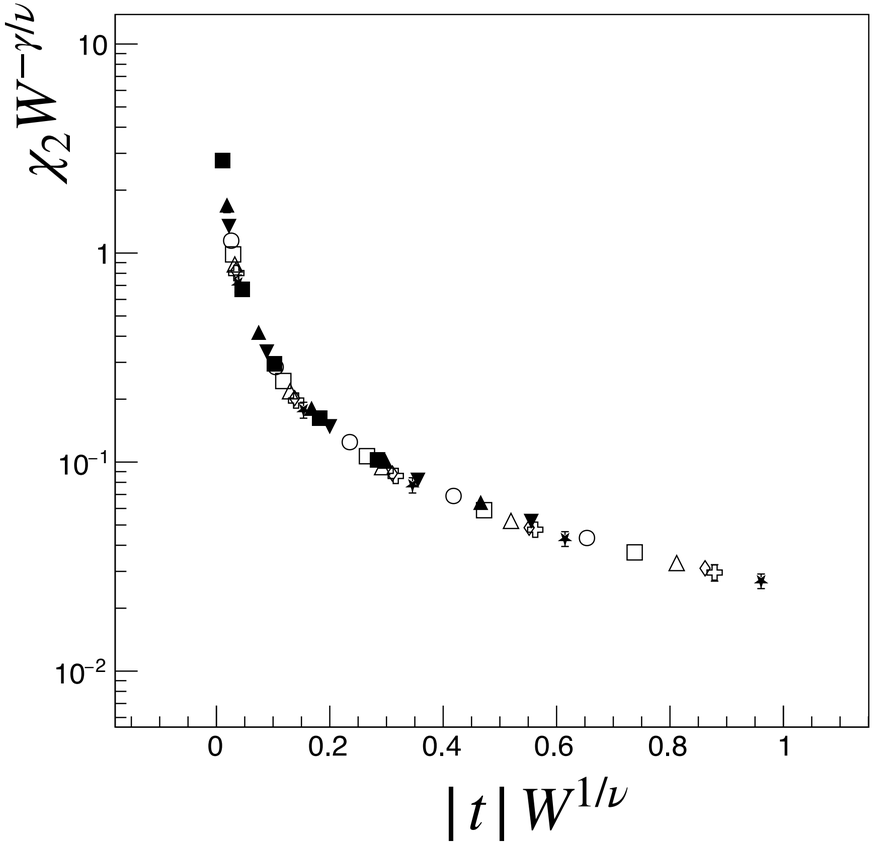

A. Sorensen, P. Sorensen, arXiv:2405.10278

Summary

- Theory studies find QCD CP in region probed by FXT: $\mu_B \in (525,625)$ MeV $\sim \sqrt{s_{NN}} \approx 4.5$ GeV
- FSS of C_2 finds the QCD CP as well: $\mu_B \approx 570$ MeV $\sim \sqrt{s_{NN}} \approx 4.5$ GeV
- C_2 from SMASH cascade does not scale as well (poorer power law fit with $\mu_B \approx 520$ MeV)

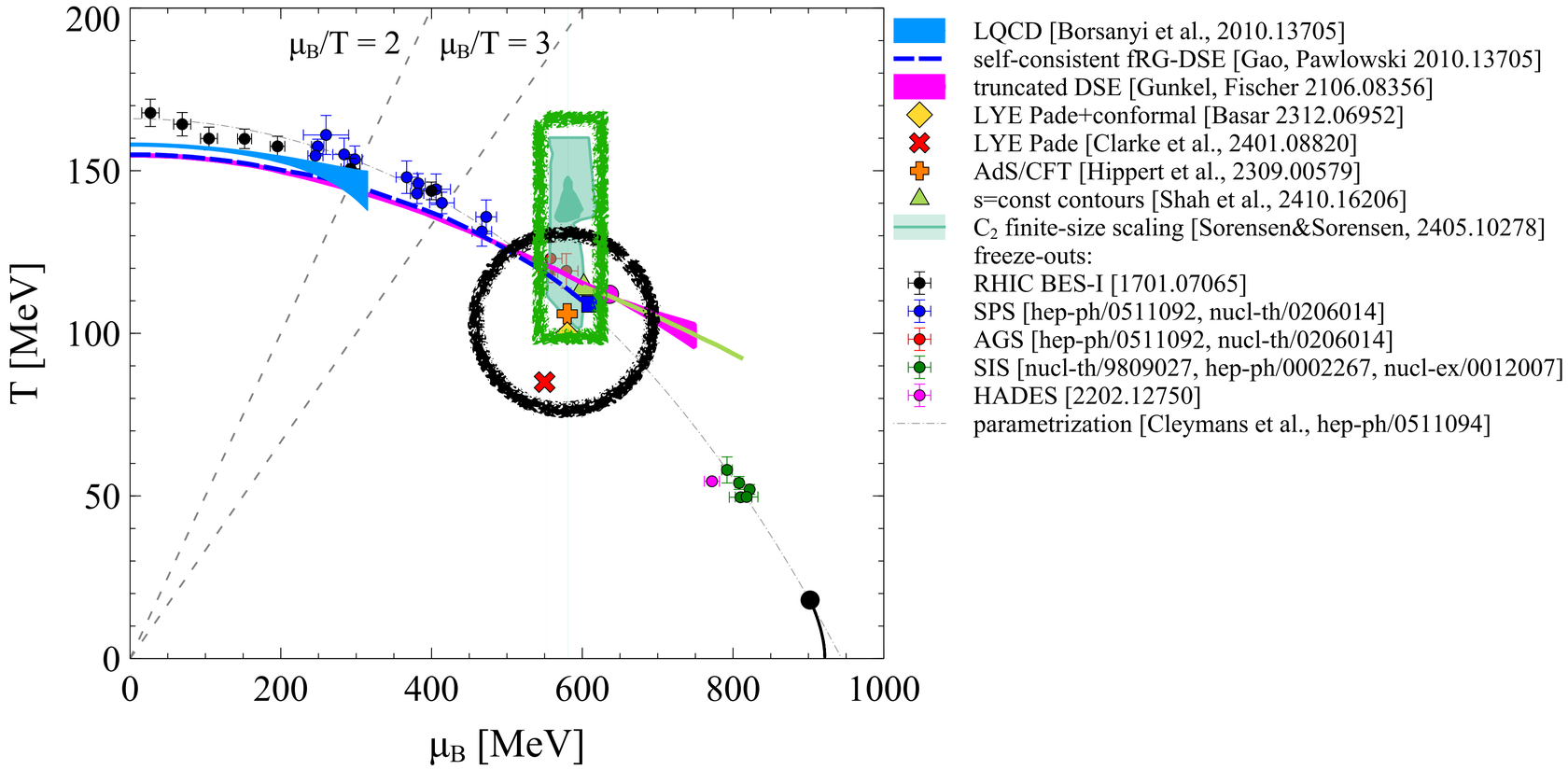

LQCD [Borsanyi et al., 2010.13705]
self-consistent fRG-DSE [Gao, Pawlowski 2010.13705]
truncated DSE [Gunkel, Fischer 2106.08356]
LYE Pade+conformal [Basar 2312.06952]
LYE Pade [Clarke et al., 2401.08820]
AdS/CFT [Hippert et al., 2309.00579]
s=const contours [Shah et al., 2410.16206]
C_2 finite-size scaling [Sorensen&Sorensen, 2405.10278]
freeze-outs:
RHIC BES-I [1701.07065]
SPS [hep-ph/0511092, nucl-th/0206014]
AGS [hep-ph/0511092, nucl-th/0206014]
SIS [nucl-th/9809027, hep-ph/0002267, nucl-ex/0012007]
HADES [2202.12750]
parametrization [Cleymans et al., hep-ph/0511094]

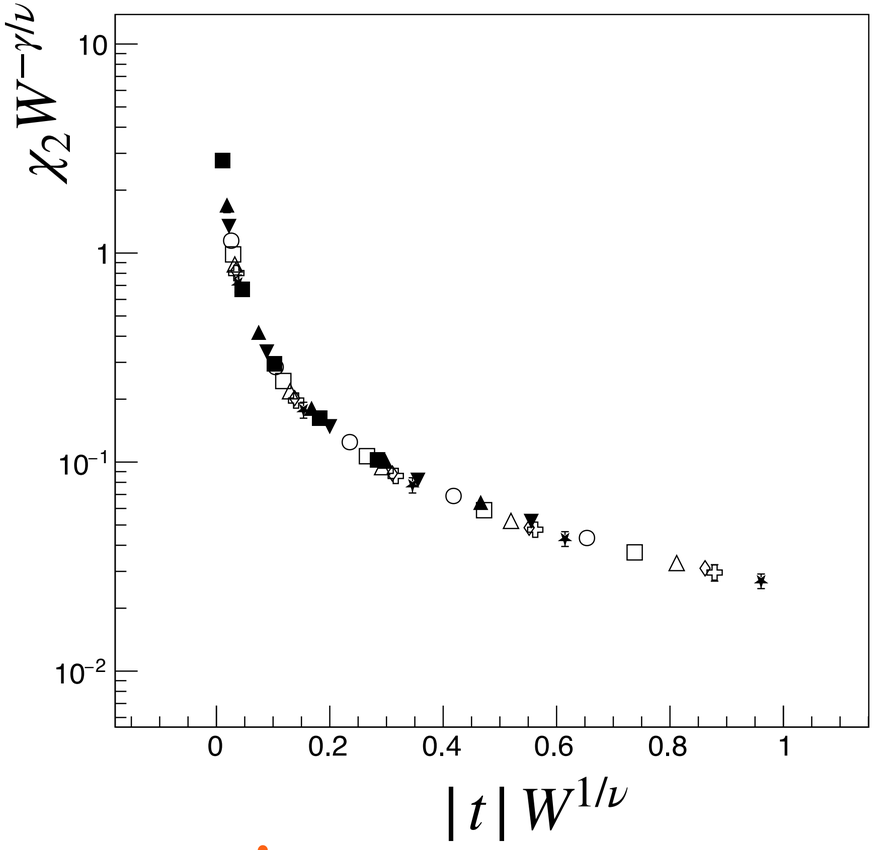

A. Sorensen, P. Sorensen, arXiv:2405.10278

Thank you for your attention

Backup slides

Scaled plots: $\chi_2 W^{-\gamma/\nu}$ divided by a fit vs. $|t|W^{1/\nu}$

STAR result

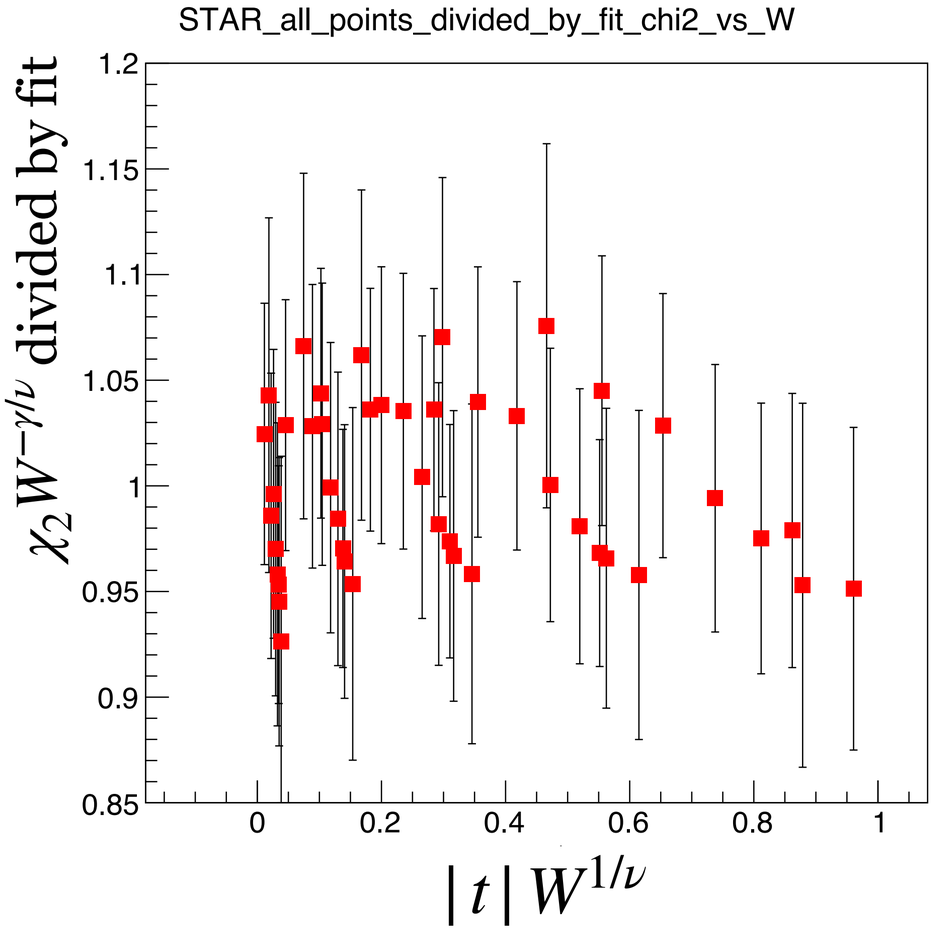

$\mu_{B,c} \approx 570$ MeV

SMASH result

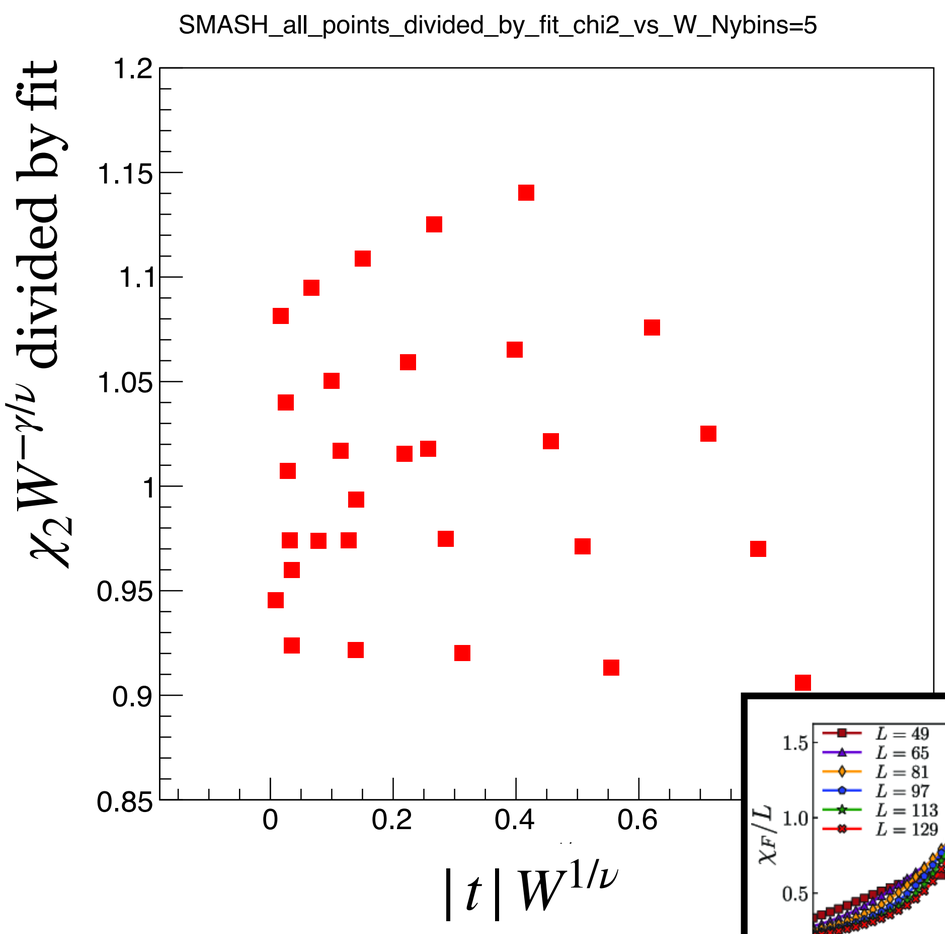

$\mu_{B,c} \approx 520$ MeV

Small difference in scalability — is it significant?

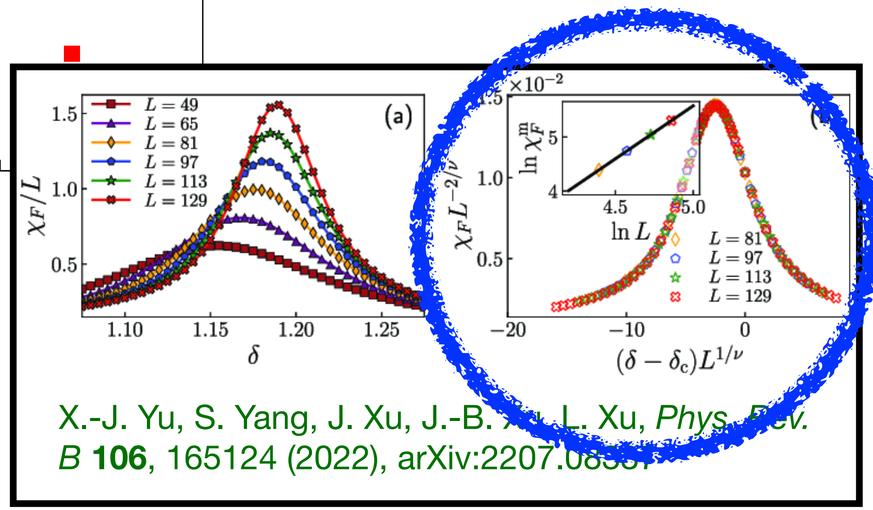

X.-J. Yu, S. Yang, J. Xu, J.-B. Xu, L. Xu, *Phys. Rev. B* **106**, 165124 (2022), arXiv:2207.08367

Divergence of second-order cumulant

Baryon number susceptibilities:

$$\chi_{(k)} \equiv \left(\frac{\partial^k P}{\partial \mu_B^k} \right)_T$$

Related to cumulants of N_B:

$$C_k = VT^{k-1}\chi_B^{(k)}$$

$$\chi_1 \equiv \left(\frac{\partial P}{\partial \mu_B} \right)_T = n_B \quad \text{because} \quad dP = Tds\Big|_{\mu_B} + n_B d\mu_B\Big|_s$$

Then $$\chi_2 \equiv \left(\frac{\partial n_B}{\partial \mu_B} \right)_T = \left(\frac{\partial \mu_B}{\partial n_B} \right)_T^{-1} = \left(\frac{\frac{1}{n_B}\partial P}{\partial n_B} \right)_T^{-1} = \frac{n_B}{\left(\frac{dP}{dn_B} \right)_T}$$

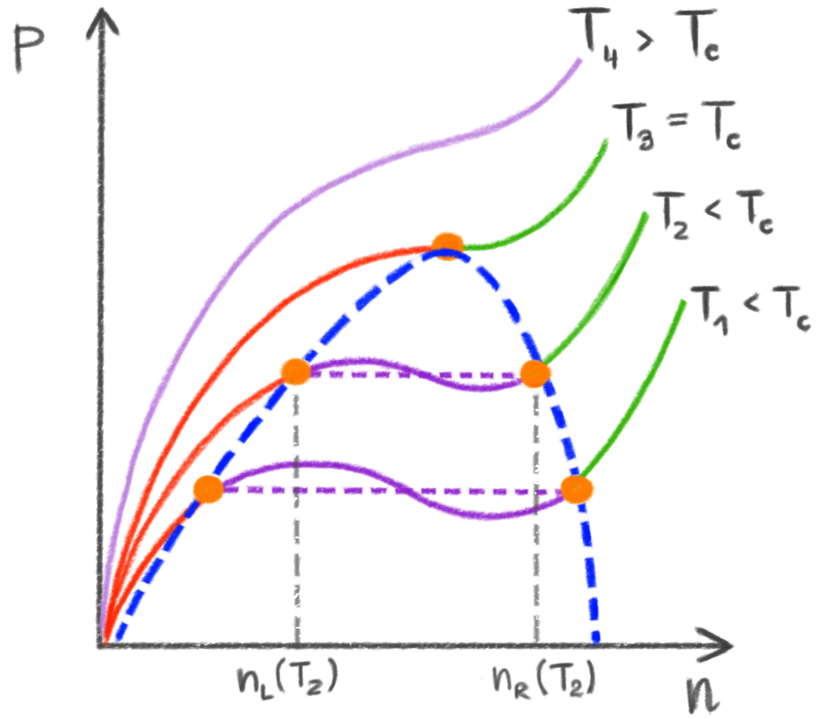

Divergence of second-order cumulant

Baryon number susceptibilities:

$$\chi_{(k)} \equiv \left(\frac{\partial^k P}{\partial \mu_B^k} \right)_T$$

Related to cumulants of N_B:

$$C_k = VT^{k-1}\chi_B^{(k)}$$

$$C_1 = \langle N \rangle$$
$$C_2 = \langle \left(N - \langle N \rangle \right)^2 \rangle = \sigma^2$$
$$C_3 = \langle \left(N - \langle N \rangle \right)^3 \rangle$$

measured in experiment!

$$\chi_1 \equiv \left(\frac{\partial P}{\partial \mu_B} \right)_T = n_B \quad \text{because} \quad dP = Tds\Big|_{\mu_B} + n_B d\mu_B\Big|_s$$

Then $$\chi_2 \equiv \left(\frac{\partial n_B}{\partial \mu_B} \right)_T = \left(\frac{\partial \mu_B}{\partial n_B} \right)_T^{-1} = \left(\frac{\frac{1}{n_B}\partial P}{\partial n_B} \right)_T^{-1} = \frac{n_B}{\left(\frac{dP}{dn_B} \right)_T}$$

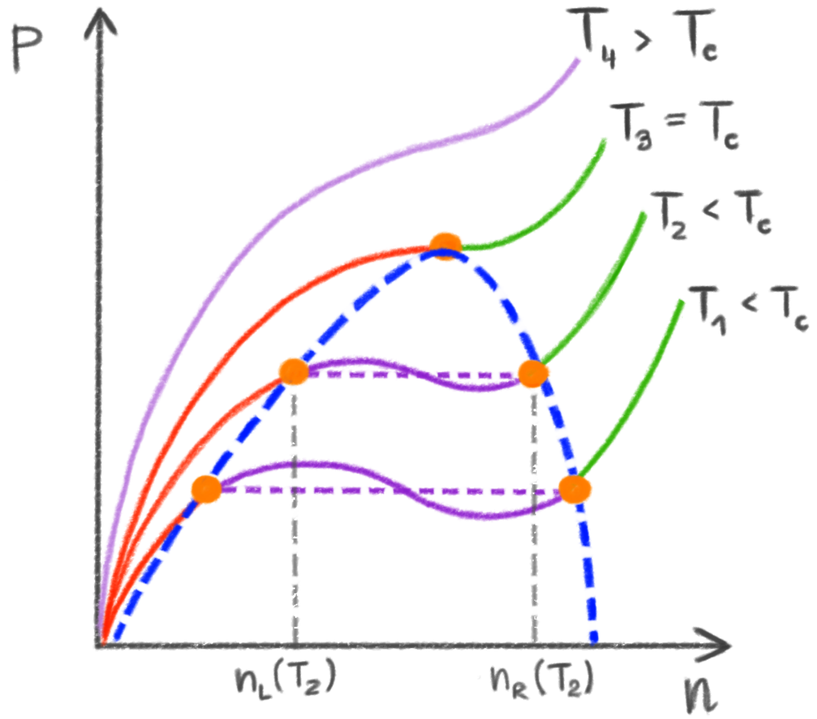

Universal scaling behavior

Scaling: any relationship in which one quantity goes like a power law of the other.

Universal scaling behavior

Scaling: any relationship in which one quantity goes like a power law of the other.

Example:
Random walk: the root-mean-square distance traveled by a random walker after N steps: $R \sim N^{\frac{1}{2}}$

$N \sim 10^2$

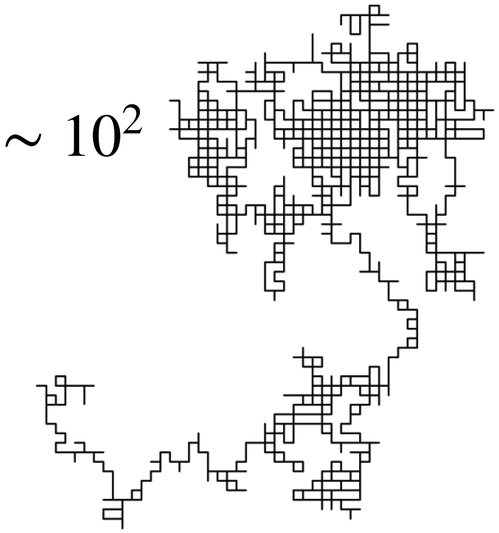

$N \sim 10^4$

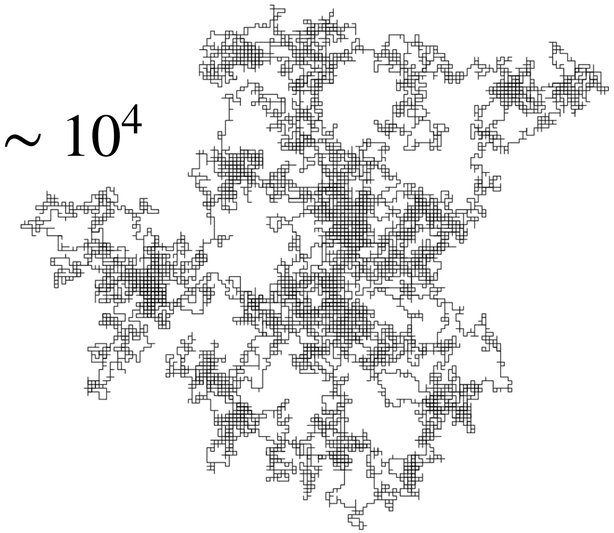

$N \sim 10^6$

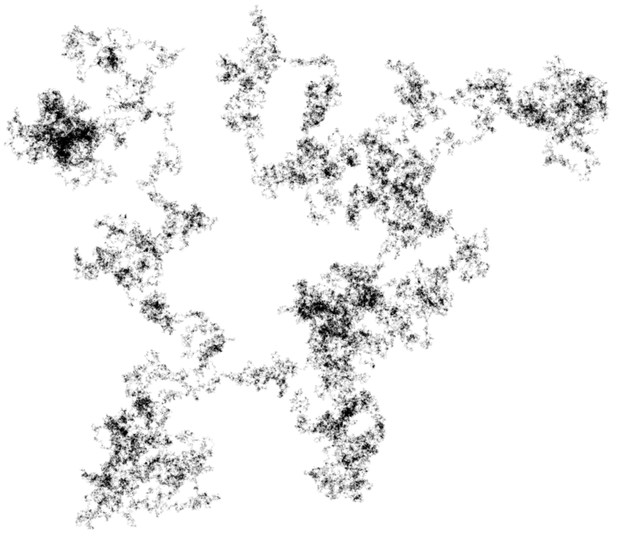

image source: Wikipedia

Universal scaling behavior

Scaling: any relationship in which one quantity goes like a power law of the other.

Example:

Random walk: the root-mean-square distance traveled by a random walker after N steps: $R \sim N^{\frac{1}{2}}$

$N \sim 10^2$

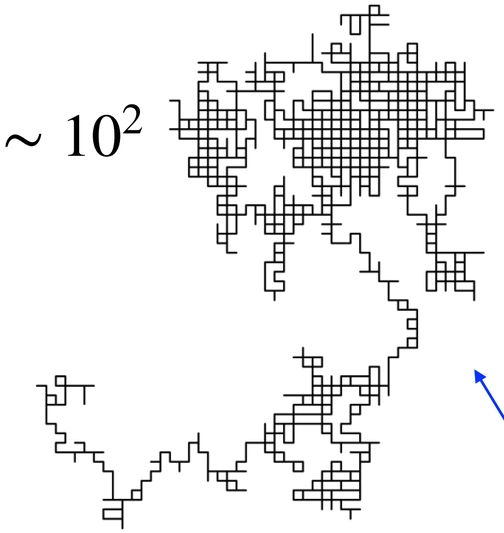

$N \sim 10^4$

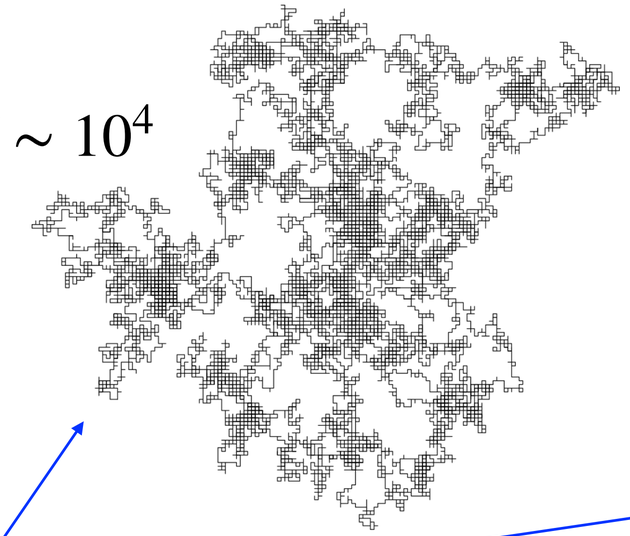

$N \sim 10^6$

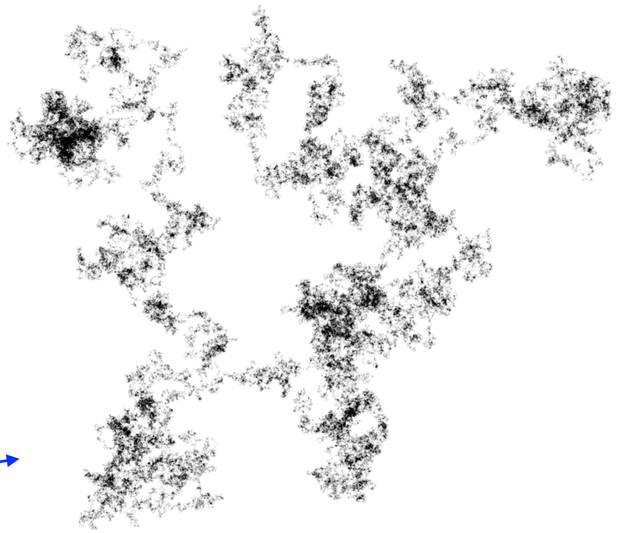

self-similarity

image source: Wikipedia

Universal scaling behavior

Scaling: any relationship in which one quantity goes like a power law of the other.

Example:
Random walk: the root-mean-square distance traveled by a random walker after N steps: $R \sim N^{\frac{1}{2}}$

$N \sim 10^2$

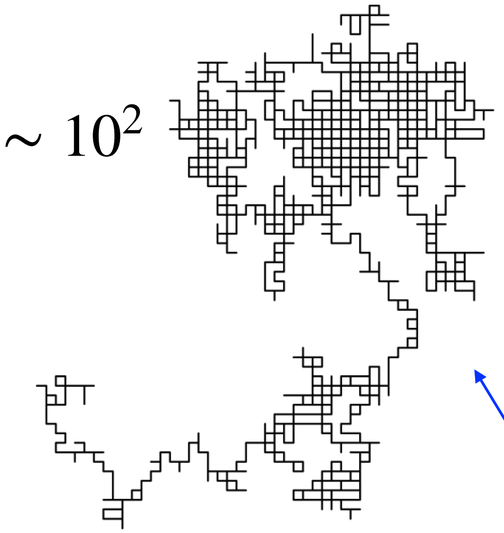

$N \sim 10^4$

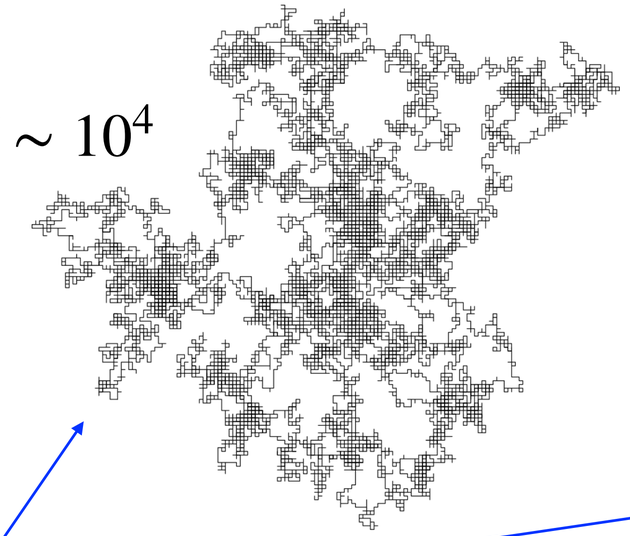

$N \sim 10^6$

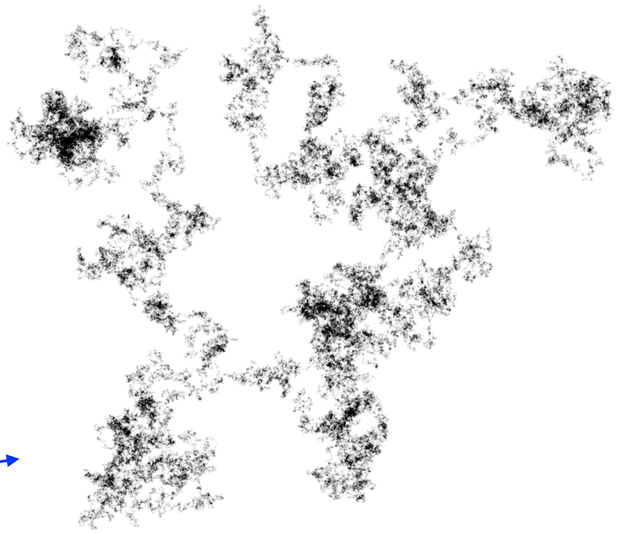

self-similarity

image source: Wikipedia

Example 2:
Self-avoiding random walk (SAW) - a minimal model for a polymer chain in a solution: $R \sim N^{0.586 \pm 0.004}$

Apparently, various interaction energies or the molecular structure do not influence the scaling behavior!

Universal scaling behavior near the CP

Example 3:
Liquid-gas phase transition:

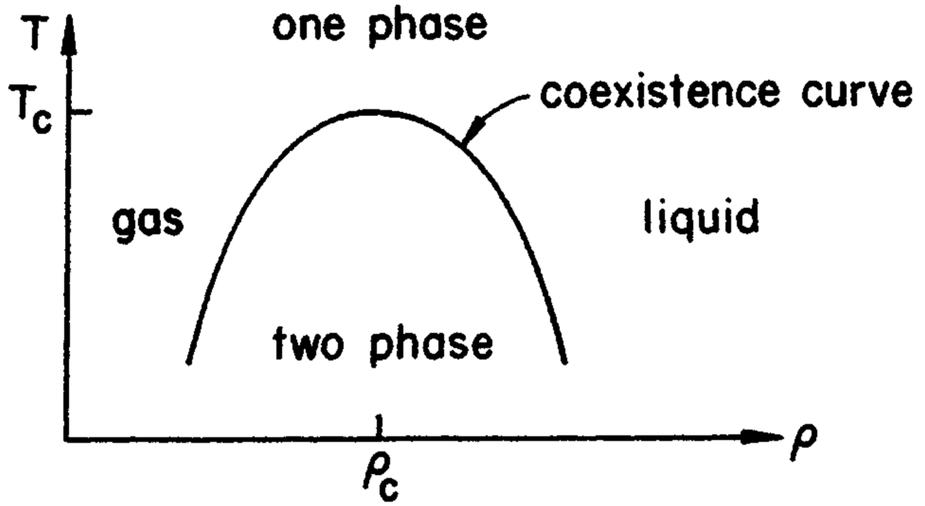

image source: N. Goldenfeld, *Lectures on Phase Transitions and the Renormalization Group*

Universal scaling behavior near the CP

Example 3:
Liquid-gas phase transition:

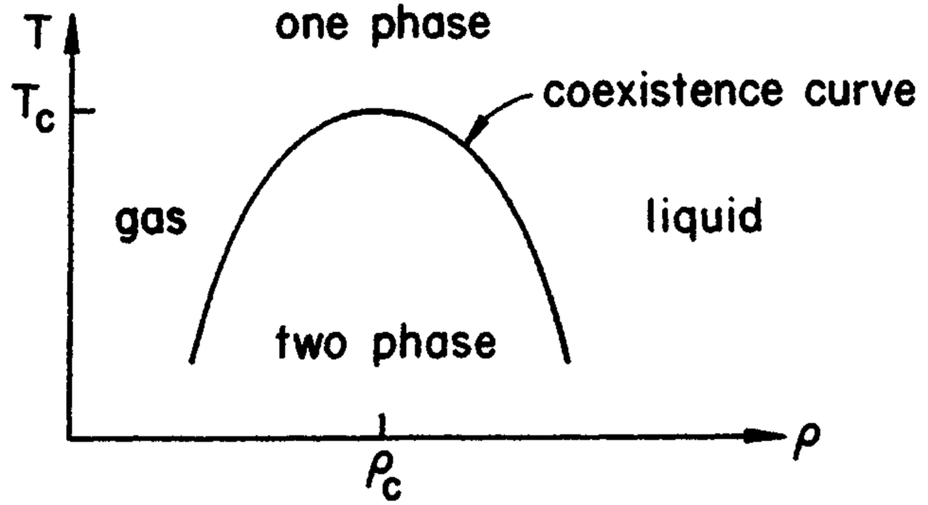

image source: N. Goldenfeld, *Lectures on Phase Transitions and the Renormalization Group*

You can assume that the curve is a parabola:
$f(\rho) = a\rho^2 + b\rho + c = T$

Apply conditions

$$1)\ f(\rho_c) = T_c \qquad 2)\ \left.\frac{df}{d\rho}\right|_{\rho=\rho_c} = 0$$

Obtain:

$$T - T_c = a(\rho - \rho_c)^2 \quad \Rightarrow \quad |\rho - \rho_c| \sim |T - T_c|^{\frac{1}{2}}$$

Universal scaling behavior near the CP

Example 3:
Liquid-gas phase transition:

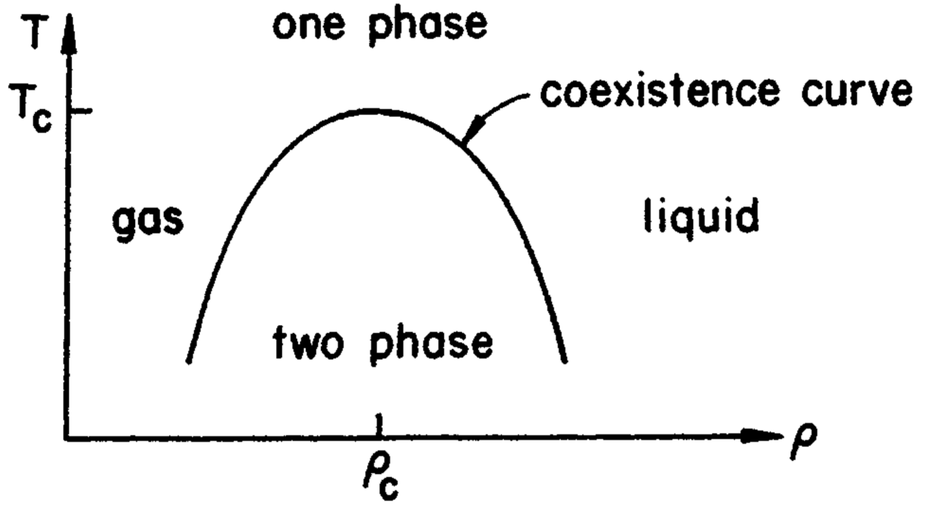

image source: N. Goldenfeld, *Lectures on Phase Transitions and the Renormalization Group*

You can assume that the curve is a parabola:
$f(\rho) = a\rho^2 + b\rho + c = T$

Apply conditions

$$1)\ f(\rho_c) = T_c \qquad 2)\ \left.\frac{df}{d\rho}\right|_{\rho=\rho_c} = 0$$

Obtain:

$$T - T_c = a(\rho - \rho_c)^2 \quad \Rightarrow \quad |\rho - \rho_c| \sim |T - T_c|^{\frac{1}{2}}$$

It turns out that
for sulphurhexafluoride $|\rho_+ - \rho_-| \sim |T - T_c|^{0.327\pm0.006}$

Universal scaling behavior near the CP

Example 3:
Liquid-gas phase transition:

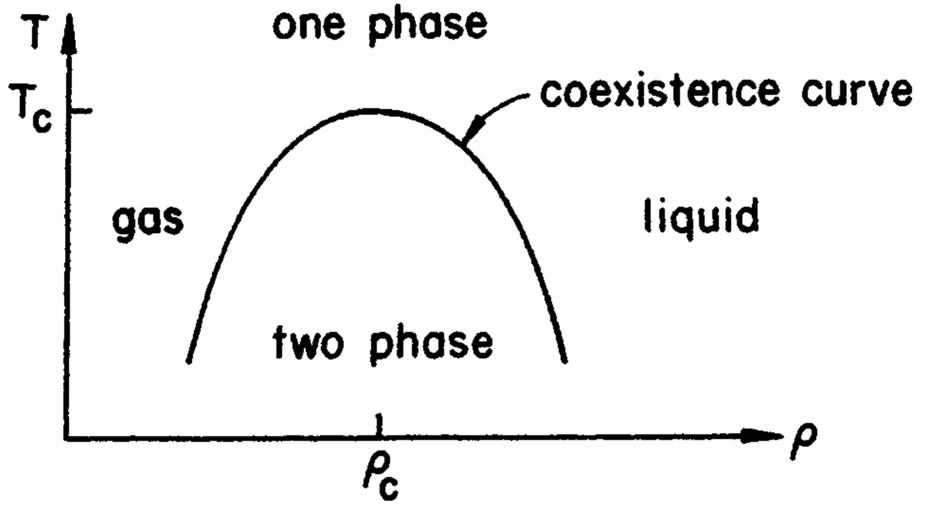

image source: N. Goldenfeld, *Lectures on Phase Transitions and the Renormalization Group*

You can assume that the curve is a parabola:
$f(\rho) = a\rho^2 + b\rho + c = T$

Apply conditions

$$1)\ f(\rho_c) = T_c \qquad 2)\ \left.\frac{df}{d\rho}\right|_{\rho=\rho_c} = 0$$

Obtain:

$$T - T_c = a(\rho - \rho_c)^2 \quad \Rightarrow \quad |\rho - \rho_c| \sim |T - T_c|^{\frac{1}{2}}$$

It turns out that
for sulphurhexafluoride $|\rho_+ - \rho_-| \sim |T - T_c|^{0.327\pm0.006}$

for ^{3}He: $|\rho_+ - \rho_-| \sim |T - T_c|^{0.321\pm0.006}$

Universal scaling behavior near the CP

Example 3:
Liquid-gas phase transition:

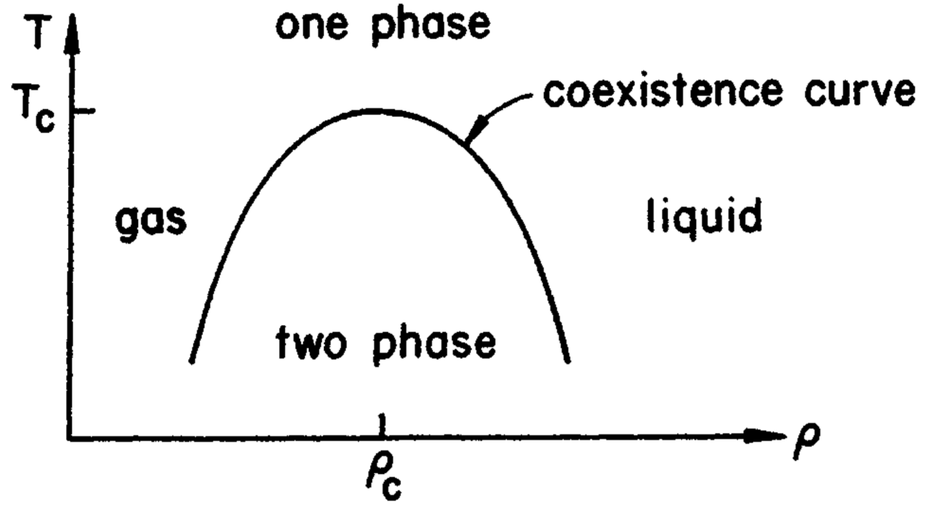

image source: N. Goldenfeld, *Lectures on Phase Transitions and the Renormalization Group*

You can assume that the curve is a parabola:
$f(\rho) = a\rho^2 + b\rho + c = T$

Apply conditions

$$1)\ f(\rho_c) = T_c \qquad 2)\ \left.\frac{df}{d\rho}\right|_{\rho=\rho_c} = 0$$

Obtain:

$$T - T_c = a(\rho - \rho_c)^2 \quad \Rightarrow \quad |\rho - \rho_c| \sim |T - T_c|^{\frac{1}{2}}$$

It turns out that
for sulphurhexafluoride $|\rho_+ - \rho_-| \sim |T - T_c|^{0.327\pm0.006}$

for ^{3}He: $|\rho_+ - \rho_-| \sim |T - T_c|^{0.321\pm0.006}$

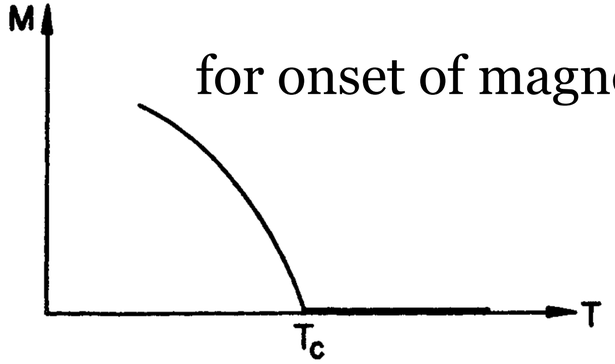

for onset of magnetization in an Ising ferromagnet: $M \sim |T - T_c|^{0.311\pm0.005}$

Universal scaling behavior near the CP

Example 3:
Liquid-gas phase transition:

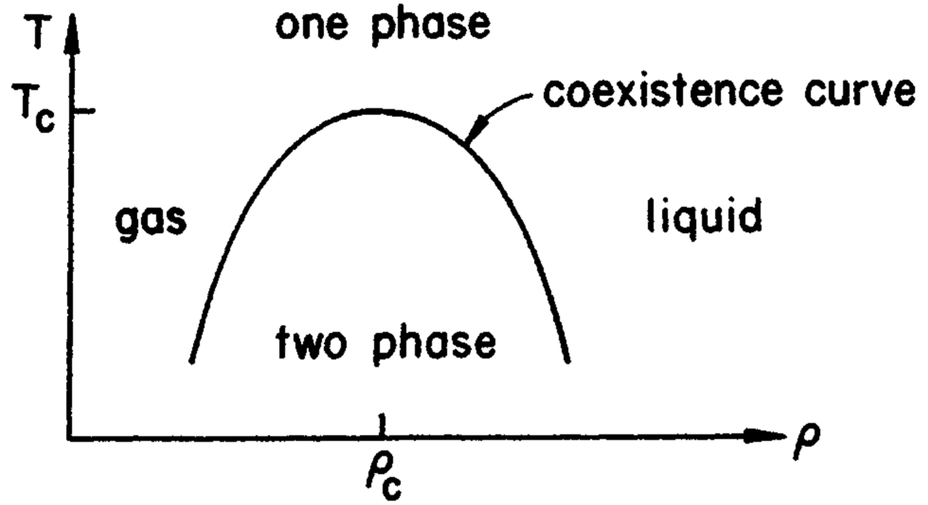

image source: N. Goldenfeld, *Lectures on Phase Transitions and the Renormalization Group*

You can assume that the curve is a parabola:
$f(\rho) = a\rho^2 + b\rho + c = T$

Apply conditions

$$1)\ f(\rho_c) = T_c \qquad 2)\ \left.\frac{df}{d\rho}\right|_{\rho=\rho_c} = 0$$

Obtain:

$$T - T_c = a(\rho - \rho_c)^2 \quad \Rightarrow \quad |\rho - \rho_c| \sim |T - T_c|^{\frac{1}{2}}$$

It turns out that
for sulphurhexafluoride $|\rho_+ - \rho_-| \sim |T - T_c|^{0.327\pm0.006}$

for ^{3}He: $|\rho_+ - \rho_-| \sim |T - T_c|^{0.321\pm0.006}$

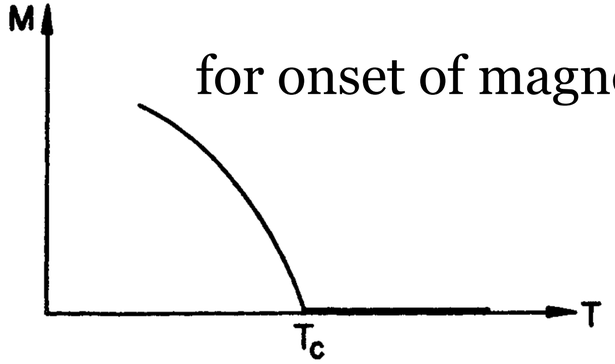

for onset of magnetization in an Ising ferromagnet: $M \sim |T - T_c|^{0.311\pm0.005}$

universality = different systems exhibit the same scaling

Finite-size scaling: use the limits to universal behavior to find the CP

The important question for scaling is: what is the scale relevant to the problem?

Near CP: $\chi_\infty(t,0) \sim |t|^{-\gamma}$ $\xi_\infty(t,0) \sim |t|^{-\nu}$ $t \equiv \frac{T - T_c}{T_c}$

For a thermodynamic quantity $Q \sim |t|^{-\sigma}$: $Q_\infty(t) \sim |t|^{-\sigma} \sim \left[\xi_\infty(t)\right]^{\frac{\sigma}{\nu}}$

Finite-size scaling: use the limits to universal behavior to find the CP

The important question for scaling is: what is the scale relevant to the problem?

Near CP: $\chi_\infty(t,0) \sim |t|^{-\gamma}$ $\xi_\infty(t,0) \sim |t|^{-\nu}$ $t \equiv \frac{T - T_c}{T_c}$

For a thermodynamic quantity $Q \sim |t|^{-\sigma}$: $Q_\infty(t) \sim |t|^{-\sigma} \sim \left[\xi_\infty(t)\right]^{\frac{\sigma}{\nu}}$

CP: infinite volume concept
In the real world ξ does not go to infinity = thermodynamic functions do not exhibit singularities

ξ is bound by the size of the system L

Finite-size scaling: use the limits to universal behavior to find the CP

The important question for scaling is: what is the scale relevant to the problem?

Near CP: $\chi_\infty(t,0) \sim |t|^{-\gamma}$ $\xi_\infty(t,0) \sim |t|^{-\nu}$ $t \equiv \frac{T - T_c}{T_c}$

For a thermodynamic quantity $Q \sim |t|^{-\sigma}$: $Q_\infty(t) \sim |t|^{-\sigma} \sim \left[\xi_\infty(t)\right]^{\frac{\sigma}{\nu}}$

CP: infinite volume concept
In the real world ξ does not go to infinity = thermodynamic functions do not exhibit singularities

ξ is bound by the size of the system L $\Rightarrow$ $Q_L(t_L) \sim L^{\frac{\sigma}{\nu}}$

Finite-size scaling: use the limits to universal behavior to find the CP

The important question for scaling is: what is the scale relevant to the problem?

Near CP: $\chi_\infty(t,0) \sim |t|^{-\gamma}$ $\xi_\infty(t,0) \sim |t|^{-\nu}$ $t \equiv \frac{T - T_c}{T_c}$

For a thermodynamic quantity $Q \sim |t|^{-\sigma}$: $Q_\infty(t) \sim |t|^{-\sigma} \sim \left[\xi_\infty(t)\right]^{\frac{\sigma}{\nu}}$

CP: infinite volume concept
In the real world ξ does not go to infinity = thermodynamic functions do not exhibit singularities

ξ is bound by the size of the system L $\Rightarrow$ $Q_L(t_L) \sim L^{\frac{\sigma}{\nu}}$

$\Rightarrow$ $Q_L(t_L) = L^{\frac{\sigma}{\nu}}\phi(t, L) = L^{\frac{\sigma}{\nu}}\phi(tL^{\frac{1}{\nu}})$

Finite-size scaling: use the limits to universal behavior to find the CP

The important question for scaling is: what is the scale relevant to the problem?

Near CP: $\chi_\infty(t,0) \sim |t|^{-\gamma}$ $\xi_\infty(t,0) \sim |t|^{-\nu}$ $t \equiv \frac{T - T_c}{T_c}$

For a thermodynamic quantity $Q \sim |t|^{-\sigma}$: $Q_\infty(t) \sim |t|^{-\sigma} \sim \left[\xi_\infty(t)\right]^{\frac{\sigma}{\nu}}$

CP: infinite volume concept
In the real world ξ does not go to infinity = thermodynamic functions do not exhibit singularities

ξ is bound by the size of the system L $\Rightarrow$ $Q_L(t_L) \sim L^{\frac{\sigma}{\nu}}$

$$\Rightarrow \quad Q_L(t_L) = L^{\frac{\sigma}{\nu}}\phi(t, L) = L^{\frac{\sigma}{\nu}}\phi(tL^{\frac{1}{\nu}})$$

$$\Rightarrow \quad Q_L(t_L)L^{-\frac{\sigma}{\nu}} = \phi(tL^{\frac{1}{\nu}})$$

Finite-size scaling: use the limits to universal behavior to find the CP

The important question for scaling is: what is the scale relevant to the problem?

Near CP: $\chi_\infty(t,0) \sim |t|^{-\gamma}$ $\xi_\infty(t,0) \sim |t|^{-\nu}$ $t \equiv \frac{T - T_c}{T_c}$

For a thermodynamic quantity $Q \sim |t|^{-\sigma}$: $Q_\infty(t) \sim |t|^{-\sigma} \sim \left[\xi_\infty(t)\right]^{\frac{\sigma}{\nu}}$

CP: infinite volume concept
In the real world ξ does not go to infinity = thermodynamic functions do not exhibit singularities

ξ is bound by the size of the system L

$$\Rightarrow \quad Q_L(t_L) \sim L^{\frac{\sigma}{\nu}}$$

$$\Rightarrow \quad Q_L(t_L) = L^{\frac{\sigma}{\nu}}\phi(t, L) = L^{\frac{\sigma}{\nu}}\phi(tL^{\frac{1}{\nu}})$$

$$\Rightarrow \quad Q_L(t_L)L^{-\frac{\sigma}{\nu}} = \phi(tL^{\frac{1}{\nu}})$$

one can find CP by plotting

Modern EOS constraint from HICs

Flow observables in HICs

Flow $v_n \equiv \langle \cos(n\phi) \rangle$

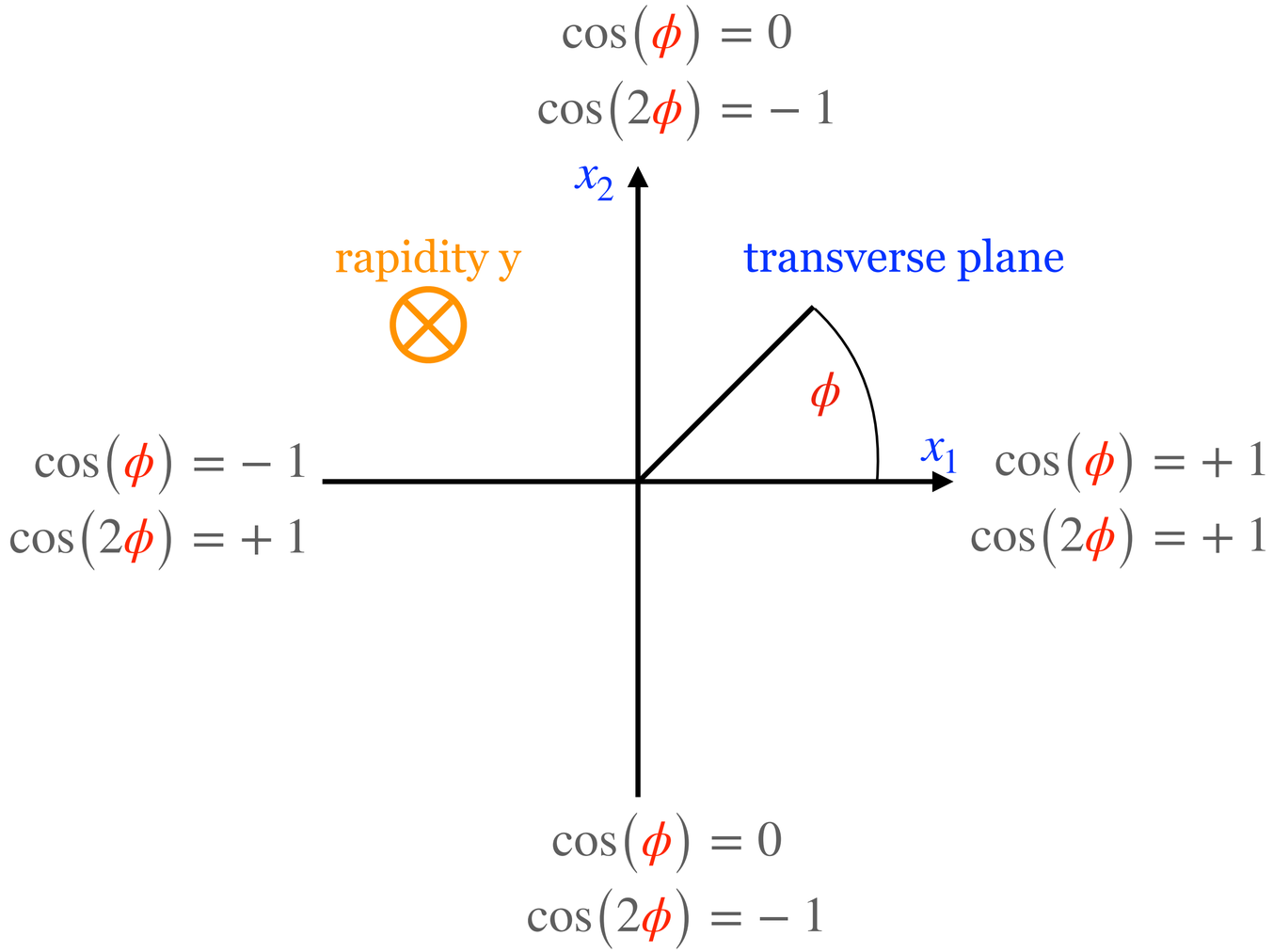

Flow observables in HICs

Flow $v_n \equiv \langle \cos(n\phi) \rangle$

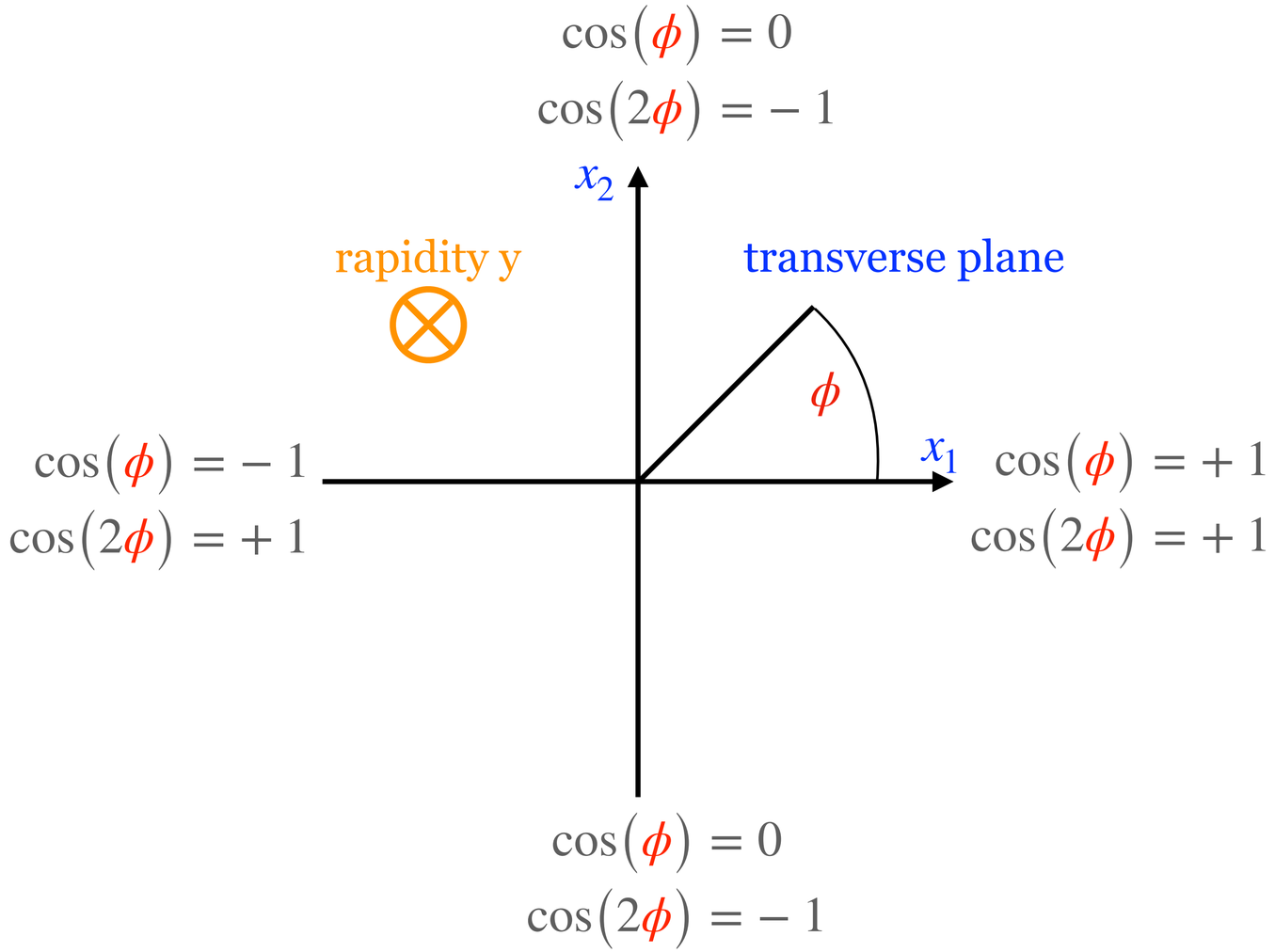

directed flow $v_1(y)$, slope $dv_1/dy(y \approx 0)$

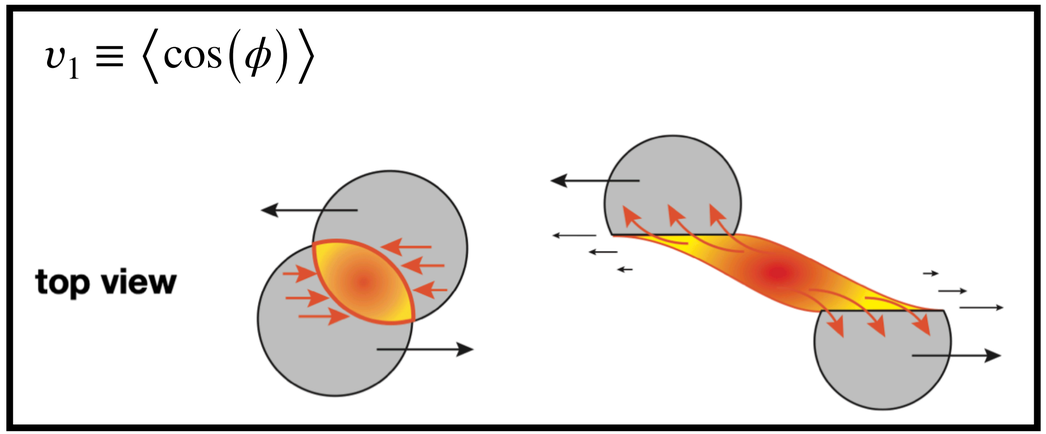

illustrations from a presentation by B. Kardan (HADES)

Flow observables in HICs

Flow $v_n \equiv \langle \cos(n\phi) \rangle$

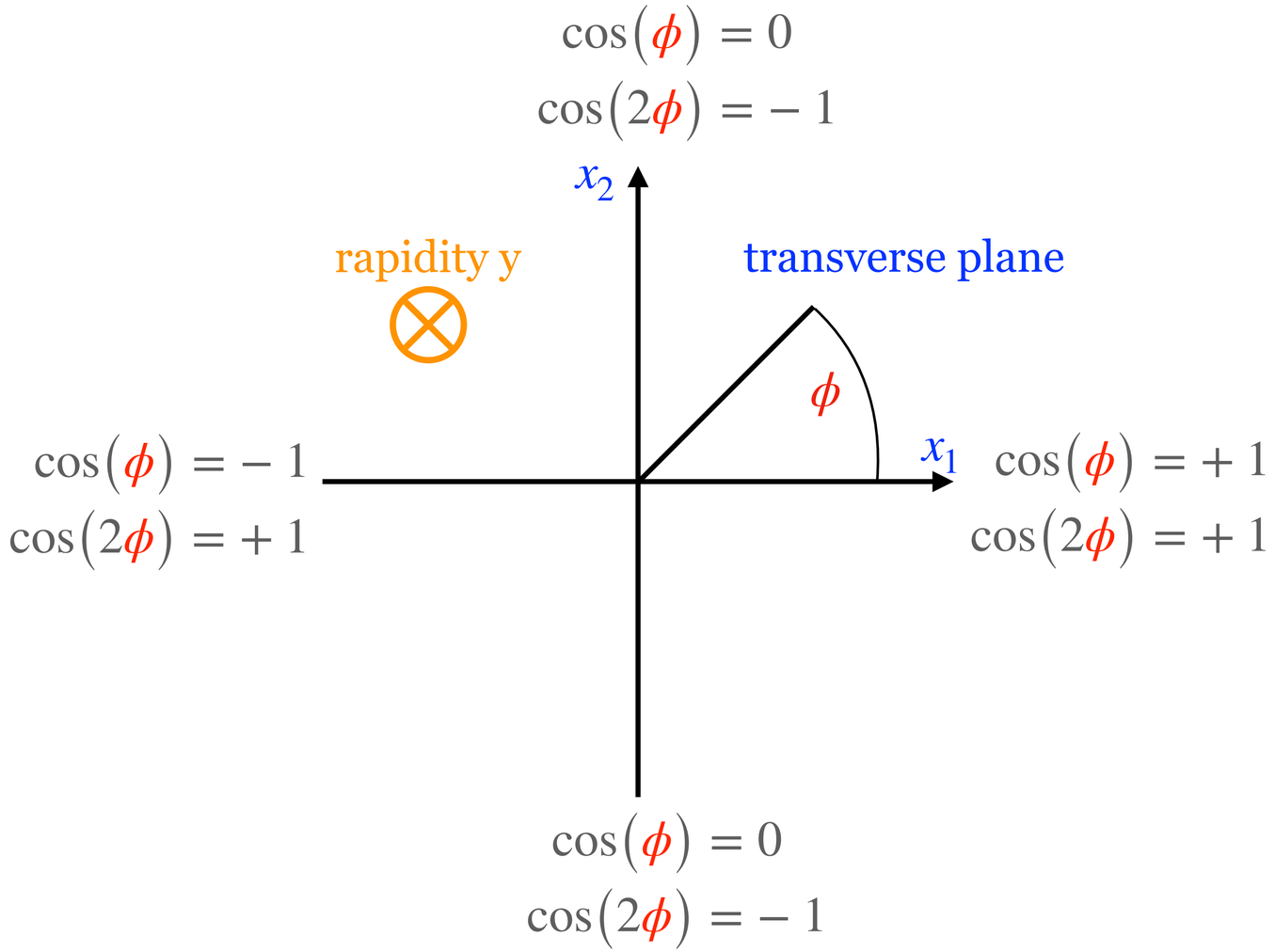

directed flow $v_1(y)$, slope $dv_1/dy(y \approx 0)$

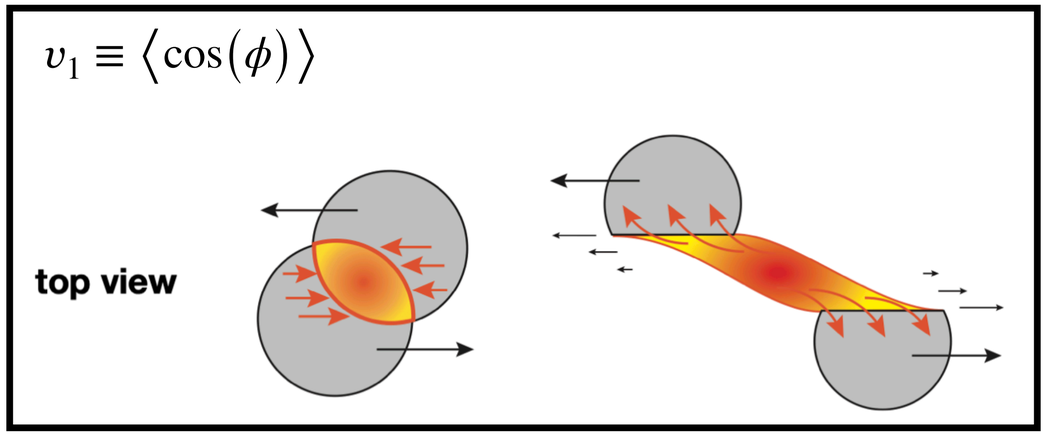

elliptic flow $v_2(y)$, at midrapidity $v_2(y \approx 0)$

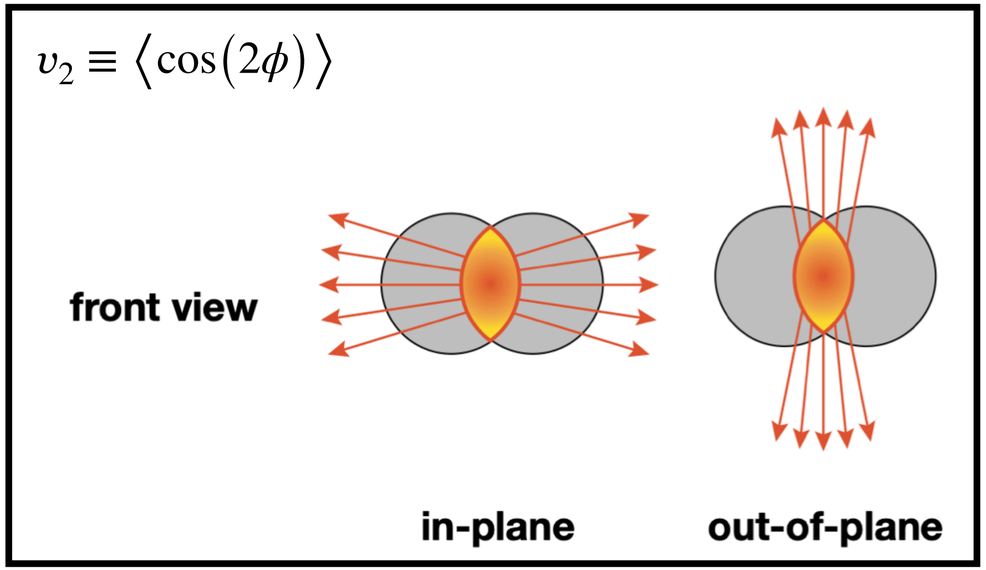

illustrations from a presentation by B. Kardan (HADES)

Flow observables in HICs

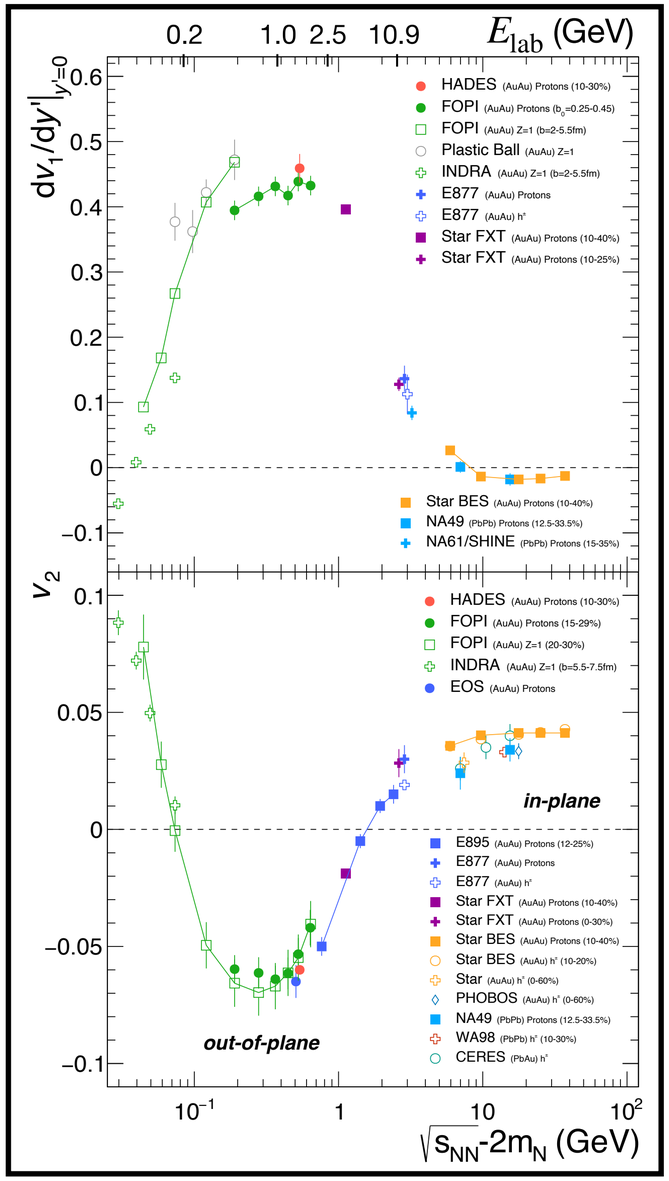

directed flow $v_1(y)$, slope $dv_1/dy(y \approx 0)$

$$v_1 \equiv \langle \cos(\phi) \rangle$$

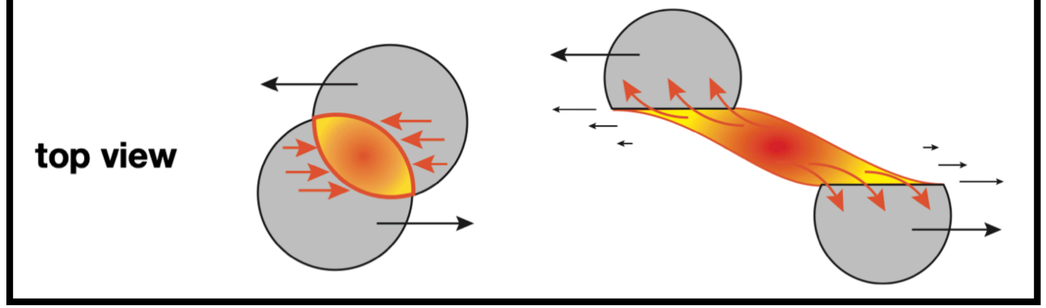

elliptic flow $v_2(y)$, at midrapidity $v_2(y \approx 0)$

$$v_2 \equiv \langle \cos(2\phi) \rangle$$

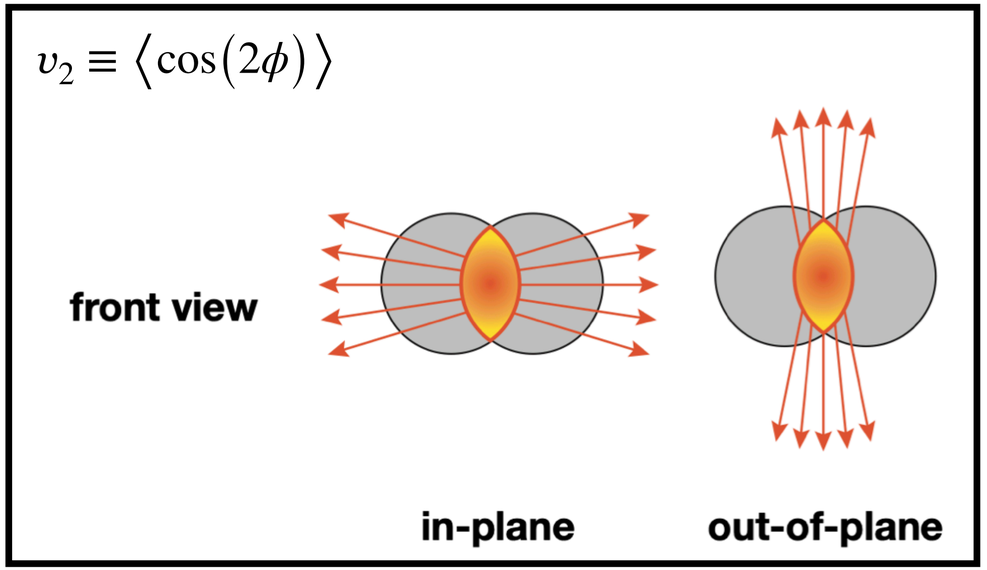

illustrations from a presentation by B. Kardan (HADES)

Flow observables in HICs

Experiments:
BES FXT,
FRIB & FRIB400,
HADES, CBM, ...

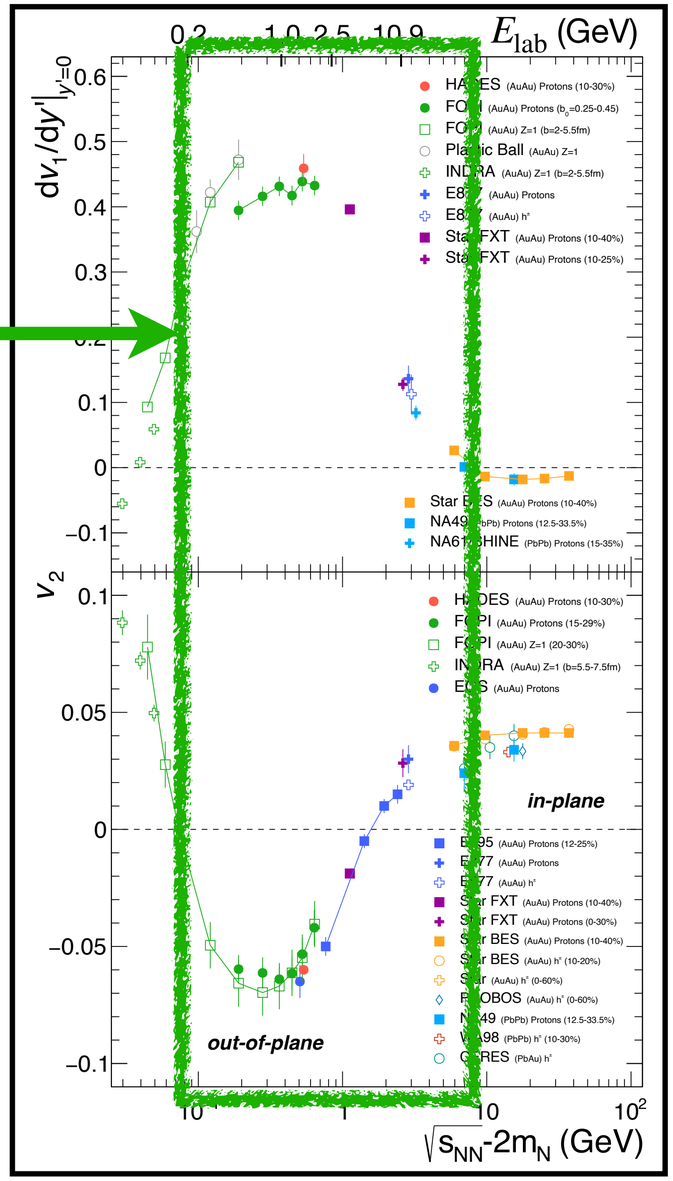

directed flow $v_1(y)$, slope $dv_1/dy(y \approx 0)$

$v_1 \equiv \langle \cos(\phi) \rangle$

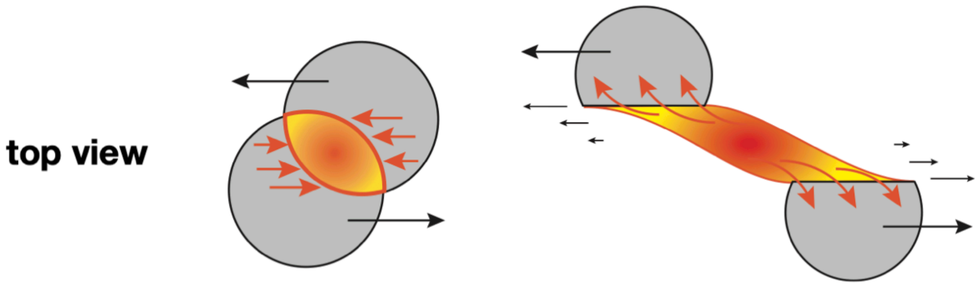

elliptic flow $v_2(y)$, at midrapidity $v_2(y \approx 0)$

$v_2 \equiv \langle \cos(2\phi) \rangle$

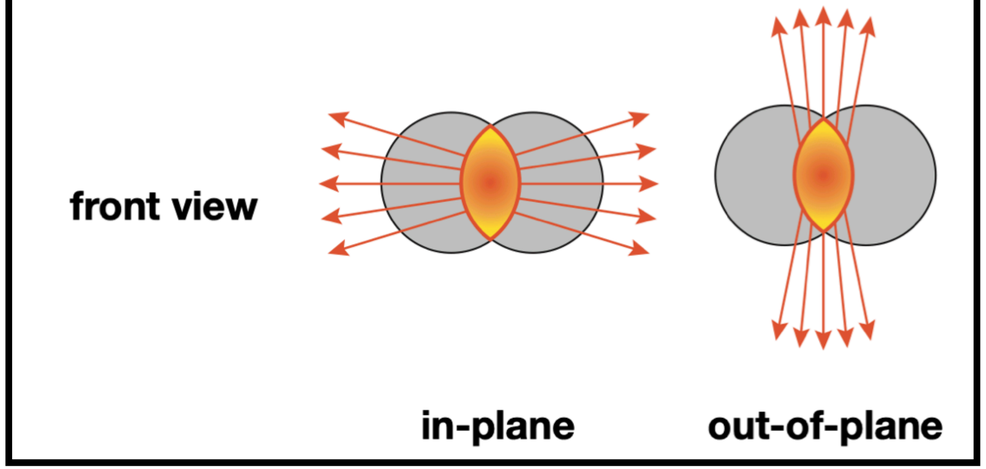

illustrations from a presentation by B. Kardan (HADES)

Flow observables in HICs

Experiments:
BES FXT,
FRIB & FRIB400,
HADES, CBM, ...

These observables are extremely sensitive to the EOS

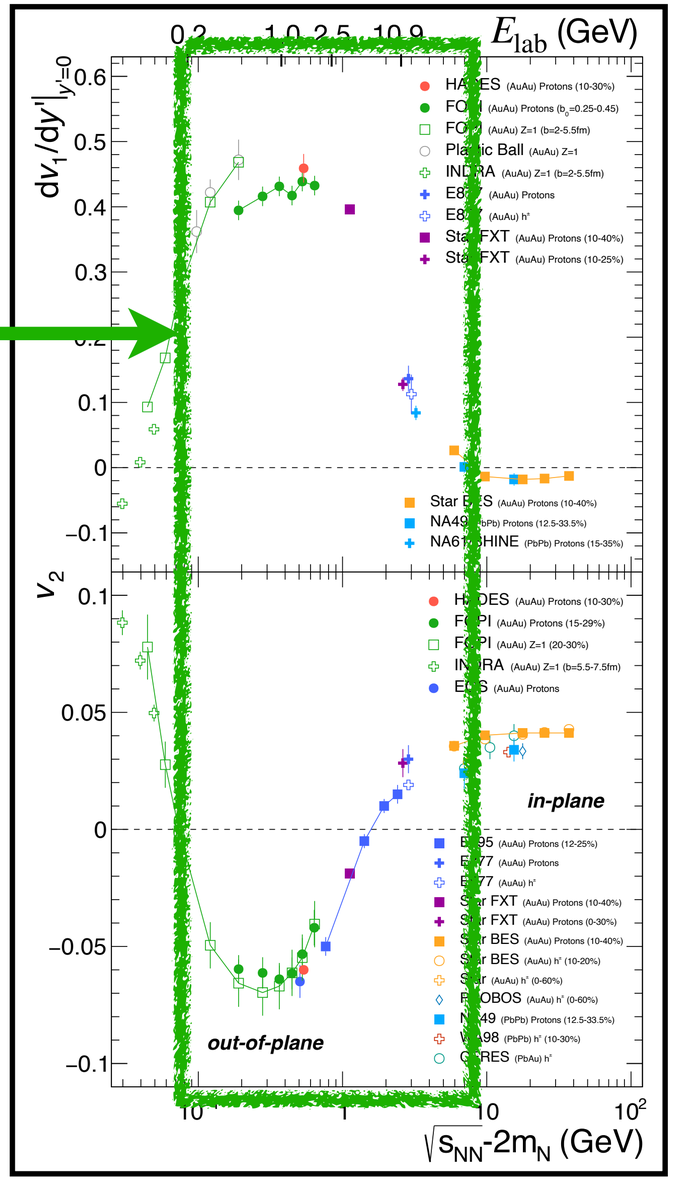

directed flow $v_1(y)$, slope $dv_1/dy(y \approx 0)$

$v_1 \equiv \langle \cos(\phi) \rangle$

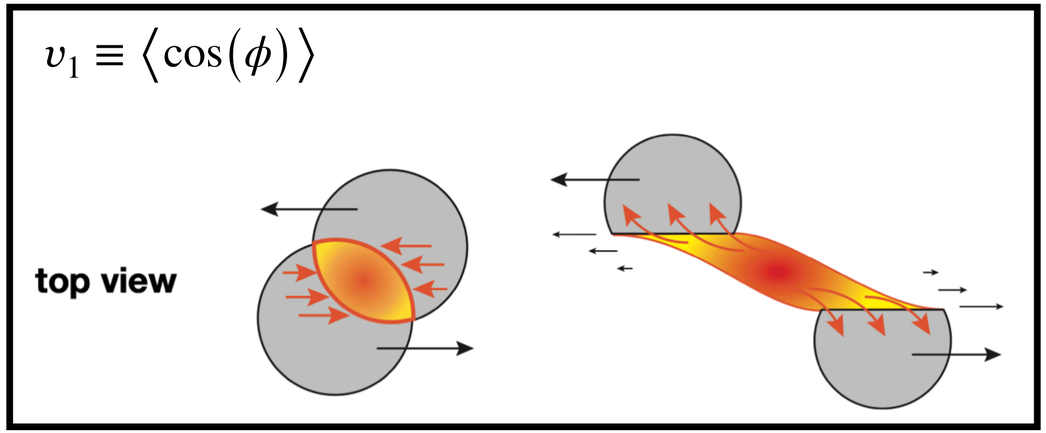

elliptic flow $v_2(y)$, at midrapidity $v_2(y \approx 0)$

$v_2 \equiv \langle \cos(2\phi) \rangle$

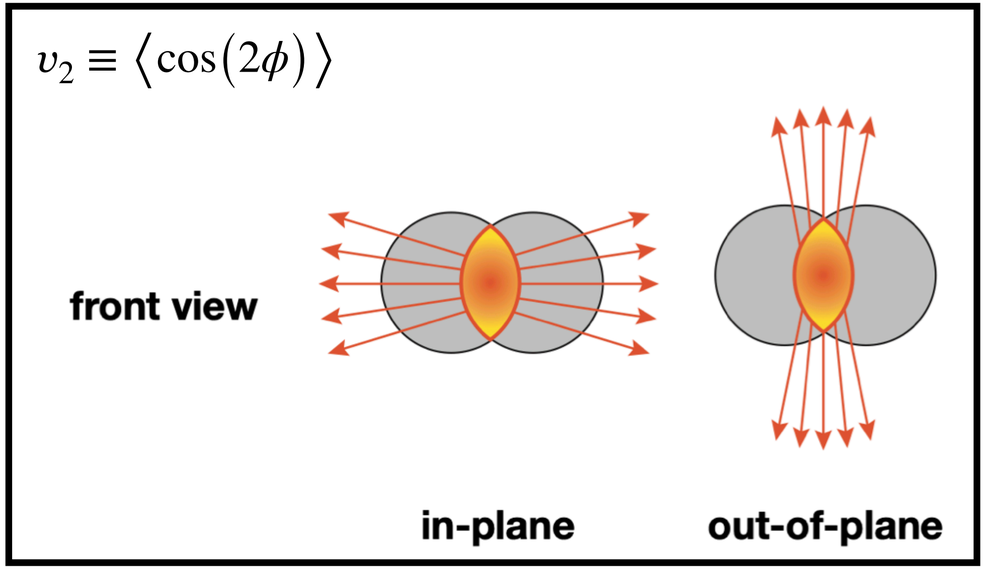

illustrations from a presentation by B. Kardan (HADES)

New approach to the EOS: piecewise parametrization of c_s^2

Piecewise parametrization of $c_s^2(n_B)$:

$$c_s^2(n_B) = \begin{cases} c_s^2(\text{Skyrme}), & n_B < n_1 = 2n_0 \\ c_1^2, & n_1 < n_B < n_2 \\ c_2^2, & n_2 < n_B < n_3 \\ \dots & \\ c_m^2, & n_m < n_B \end{cases}$$

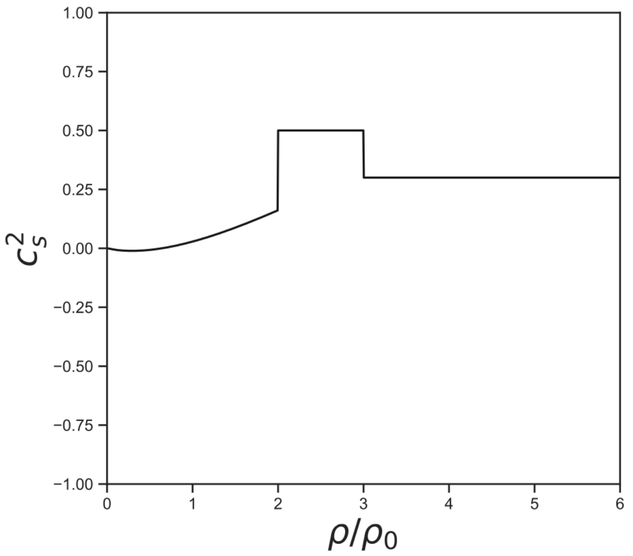

D. Oliinychenko, **A. Sorensen**, V. Koch, L. McLerran,
Phys. Rev. C **108**, 3, 034908 (2023), arXiv:2208.11996

New approach to the EOS: piecewise parametrization of c_s^2

Piecewise parametrization of $c_s^2(n_B)$:

$$c_s^2(n_B) = \begin{cases} c_s^2(\text{Skyrme}), & n_B < n_1 = 2n_0 \\ c_1^2, & n_1 < n_B < n_2 \\ c_2^2, & n_2 < n_B < n_3 \\ \dots & \\ c_m^2, & n_m < n_B \end{cases}$$

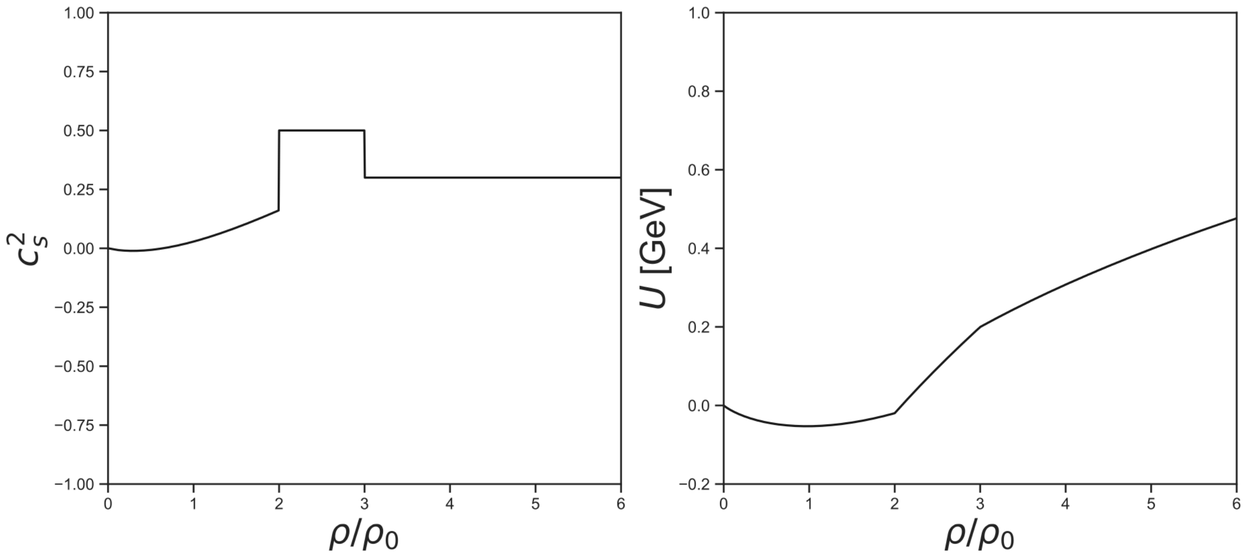

1-to-1 relation to the single-particle potential $U(n_B)$:

$$U(n_B) = \begin{cases} U_{\text{Sk}}(n_B) & n_B < n_1 = 2n_0 \\ U_1(n_B) & n_1 < n_B < n_2 \\ \dots & \\ U_k(n_B) & n_k < n_B < n_{k+1} \end{cases}$$

D. Oliinychenko, **A. Sorensen**, V. Koch, L. McLerran,
Phys. Rev. C **108**, 3, 034908 (2023), arXiv:2208.11996

New approach to the EOS: piecewise parametrization of c_s^2

Piecewise parametrization of $c_s^2(n_B)$:

$$c_s^2(n_B) = \begin{cases} c_s^2(\text{Skyrme}), & n_B < n_1 = 2n_0 \\ c_1^2, & n_1 < n_B < n_2 \\ c_2^2, & n_2 < n_B < n_3 \\ \dots & \\ c_m^2, & n_m < n_B \end{cases}$$

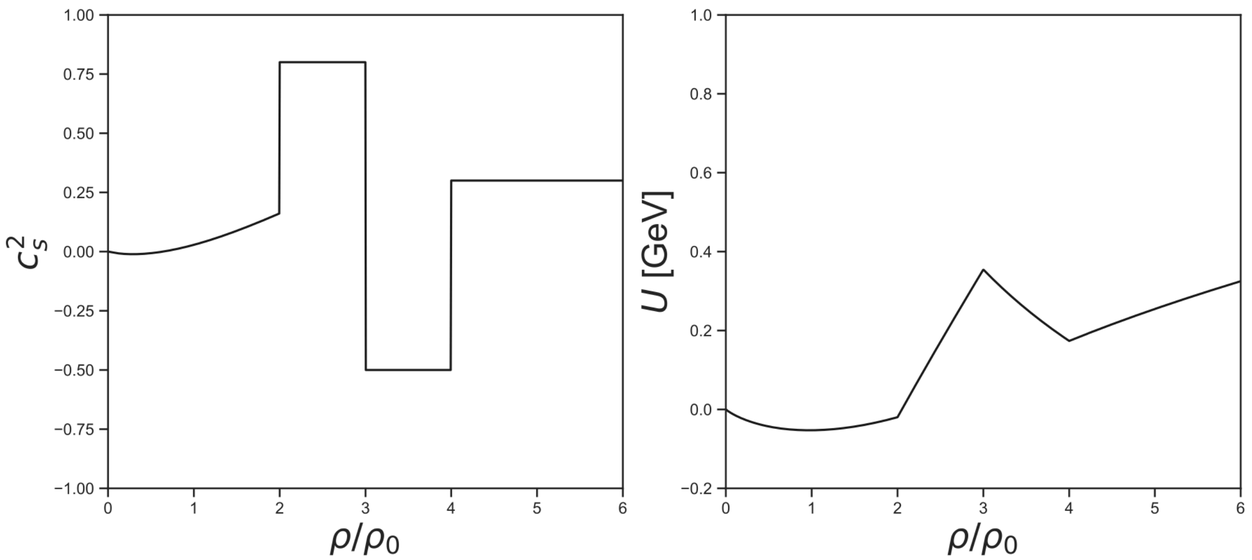

1-to-1 relation to the single-particle potential $U(n_B)$:

$$U(n_B) = \begin{cases} U_{\text{Sk}}(n_B) & n_B < n_1 = 2n_0 \\ U_1(n_B) & n_1 < n_B < n_2 \\ \dots & \\ U_k(n_B) & n_k < n_B < n_{k+1} \end{cases}$$

D. Oliinychenko, **A. Sorensen**, V. Koch, L. McLerran,
Phys. Rev. C **108**, 3, 034908 (2023), arXiv:2208.11996

New approach to the EOS: piecewise parametrization of c_s^2

Piecewise parametrization of $c_s^2(n_B)$:

$$c_s^2(n_B) = \begin{cases} c_s^2(\text{Skyrme}), & n_B < n_1 = 2n_0 \\ c_1^2, & n_1 < n_B < n_2 \\ c_2^2, & n_2 < n_B < n_3 \\ \dots & \\ c_m^2, & n_m < n_B \end{cases}$$

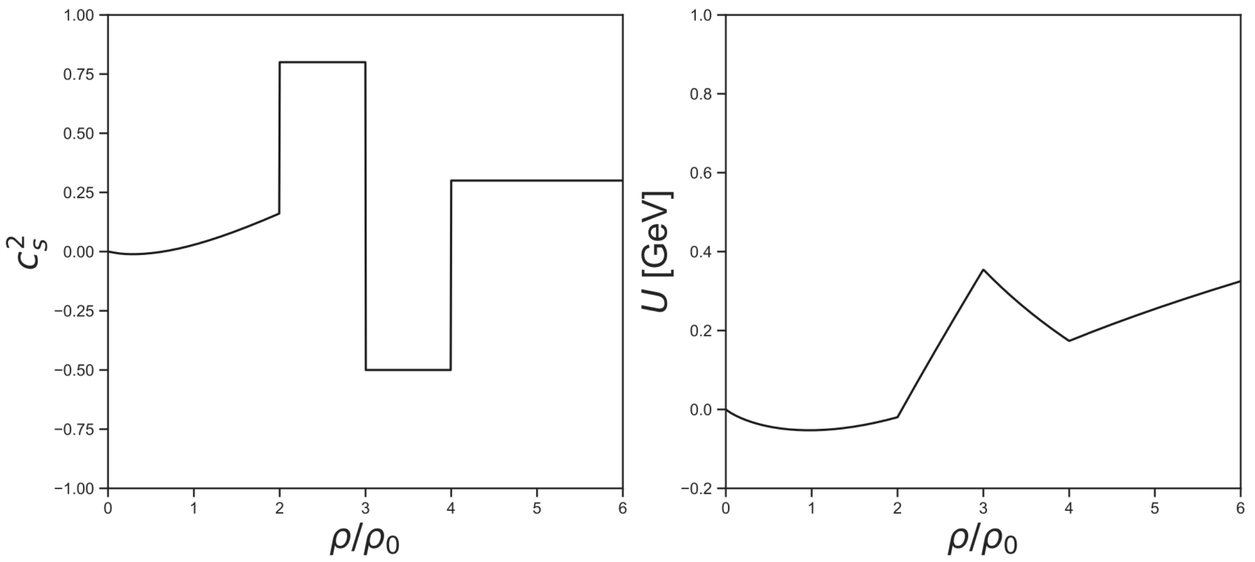

1-to-1 relation to the single-particle potential $U(n_B)$:

$$U(n_B) = \begin{cases} U_{\text{Sk}}(n_B) & n_B < n_1 = 2n_0 \\ U_1(n_B) & n_1 < n_B < n_2 \\ \dots & \\ U_k(n_B) & n_k < n_B < n_{k+1} \end{cases}$$

Gradients of $U(n_B)$ enter the EOMs
= directly affect the evolution in simulations

D. Oliinychenko, **A. Sorensen**, V. Koch, L. McLerran,
Phys. Rev. C **108**, 3, 034908 (2023), arXiv:2208.11996

New approach to the EOS: piecewise parametrization of c_s^2

Piecewise parametrization of $c_s^2(n_B)$:

$$c_s^2(n_B) = \begin{cases} c_s^2(\text{Skyrme}), & n_B < n_1 = 2n_0 \\ c_1^2, & n_1 < n_B < n_2 \\ c_2^2, & n_2 < n_B < n_3 \\ \dots & \\ c_m^2, & n_m < n_B \end{cases}$$

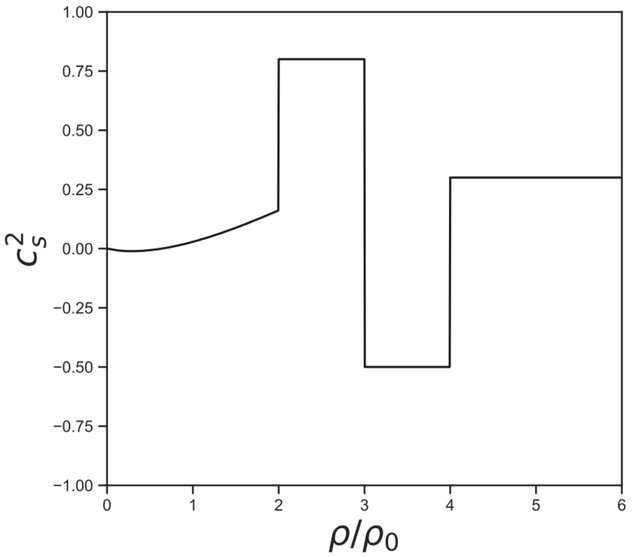

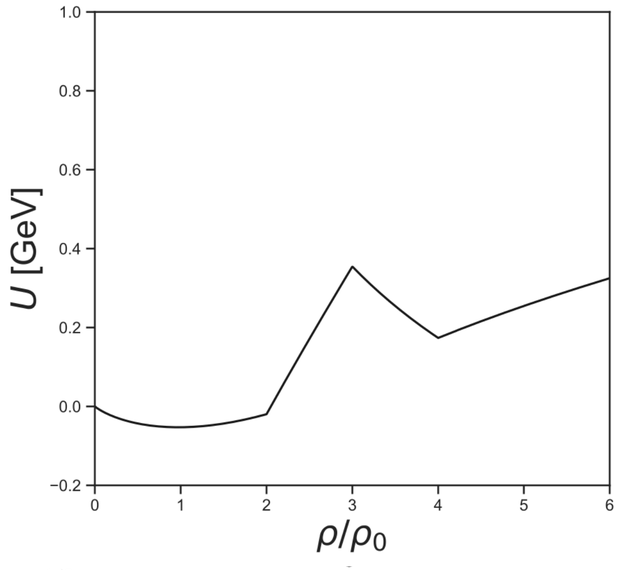

1-to-1 relation to the single-particle potential $U(n_B)$:

$$U(n_B) = \begin{cases} U_{\text{Sk}}(n_B) & n_B < n_1 = 2n_0 \\ U_1(n_B) & n_1 < n_B < n_2 \\ \dots & \\ U_k(n_B) & n_k < n_B < n_{k+1} \end{cases}$$

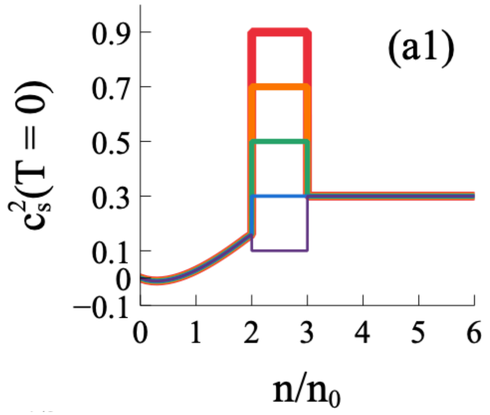

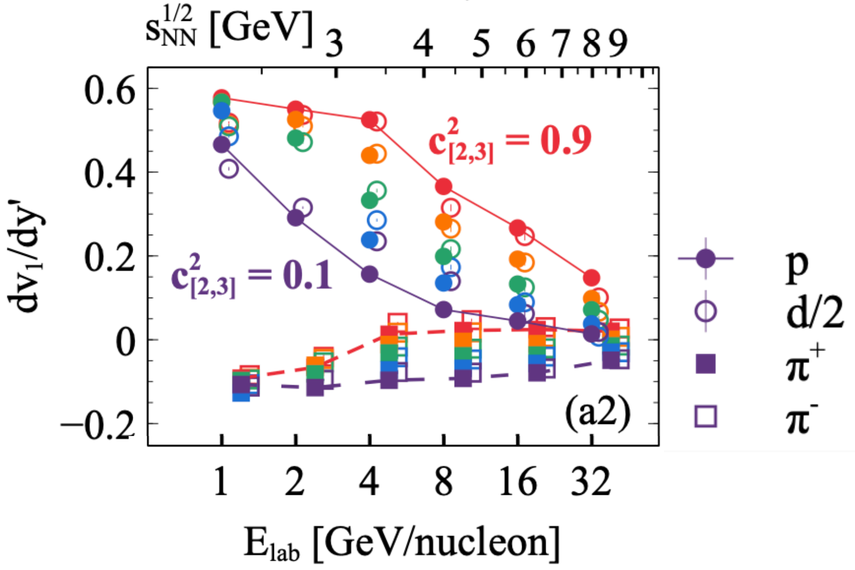

D. Oliinychenko, **A. Sorensen**, V. Koch, L. McLerran,
Phys. Rev. C **108**, 3, 034908 (2023), arXiv:2208.11996

Bayesian analysis of STAR flow data with varying K_0, $c^2_{[2,3]n_0}$, $c^2_{[3,4]n_0}$

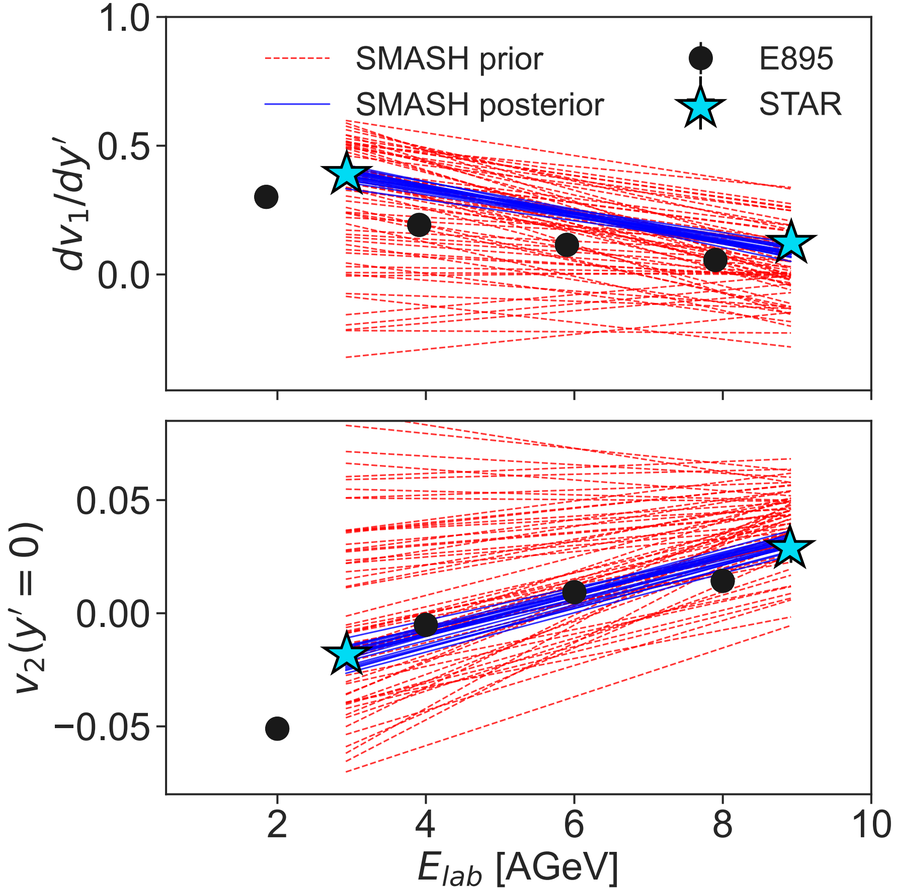

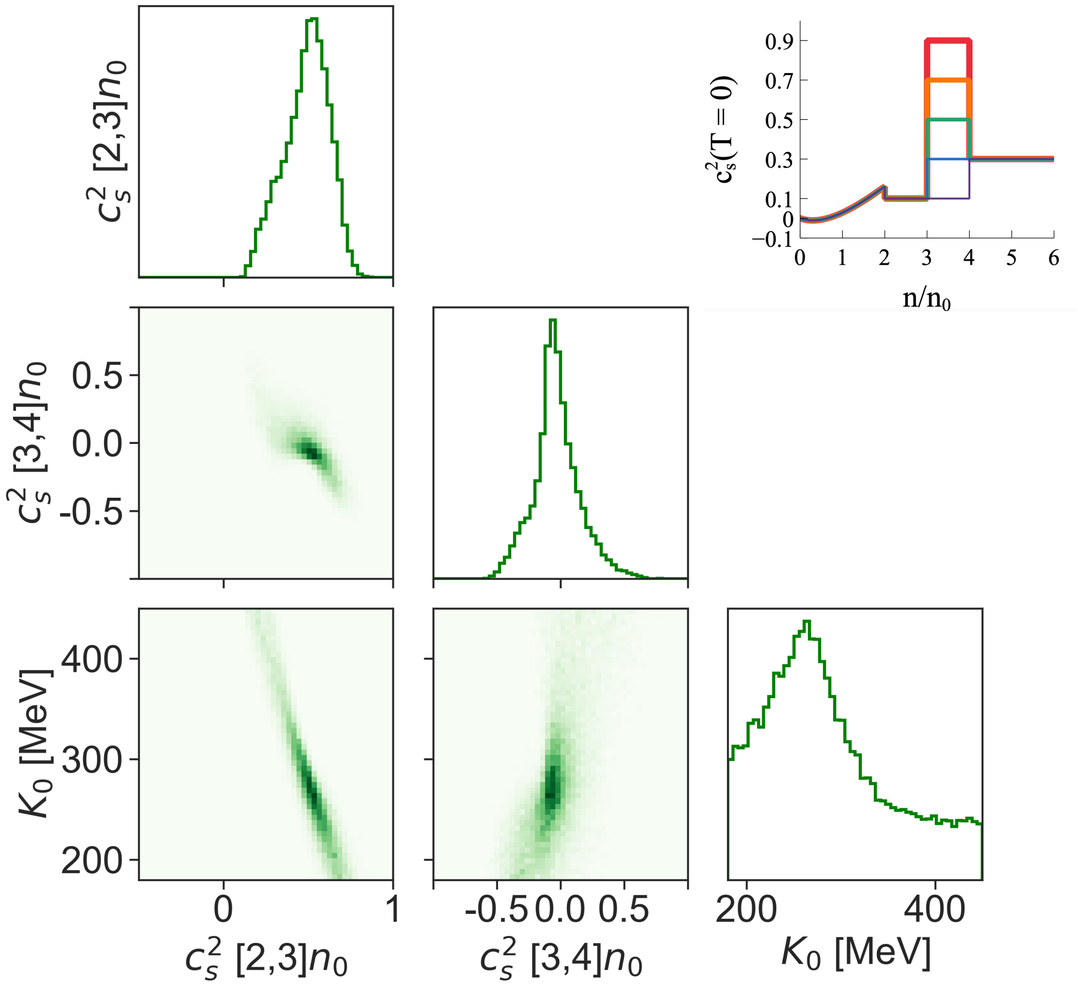

The maximum a posteriori probability (MAP) parameters are

$K_0 = 285 \pm 67$ MeV, $c^2_{[2,3]n_0} = 0.49 \pm 0.13$, $c^2_{[3,4]n_0} = -0.03 \pm 0.15$

D. Oliinychenko, **A. Sorensen**, V. Koch, L. McLerran, Phys. Rev. C **108**, 3, 034908 (2023), arXiv:2208.11996

Bayesian analysis of STAR flow data with varying K_0, $c^2_{[2,3]n_0}$, $c^2_{[3,4]n_0}$

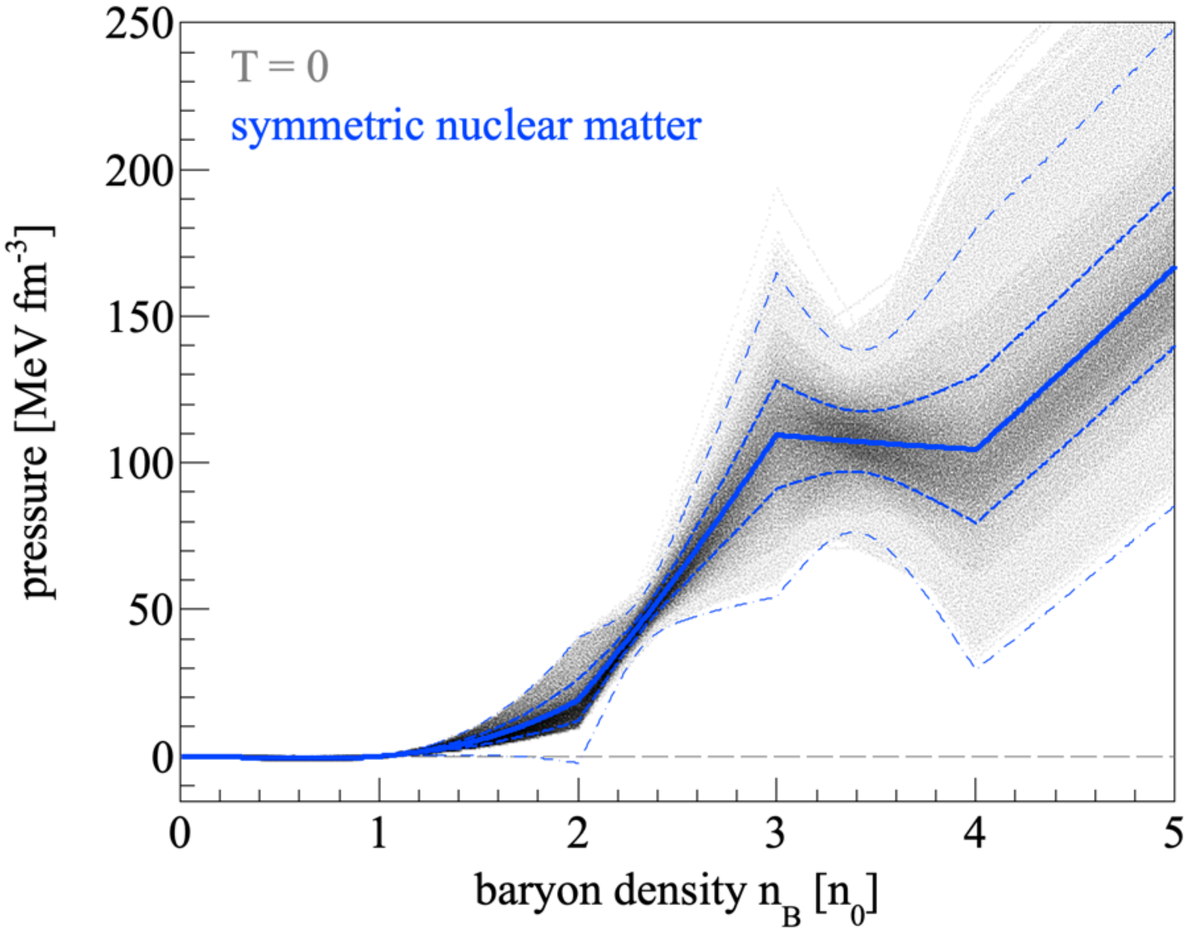

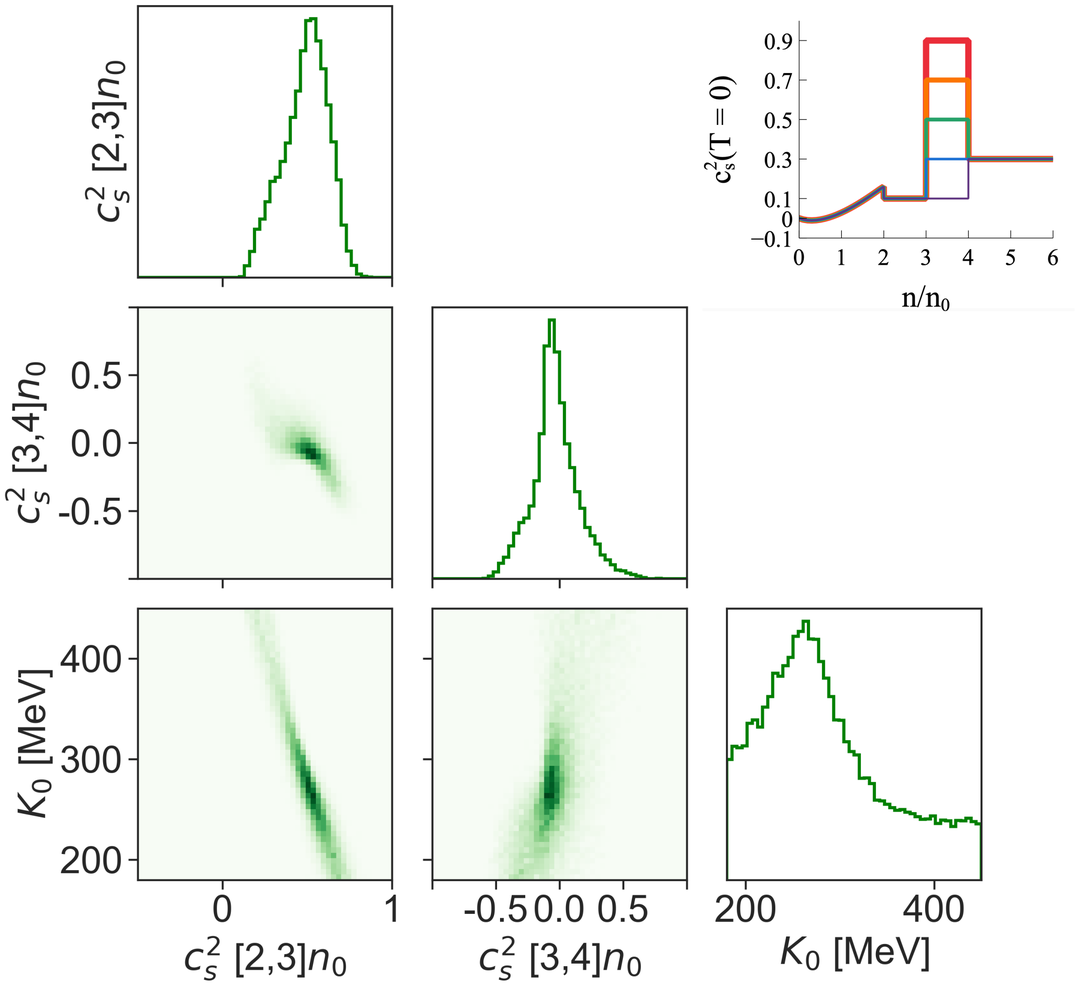

The maximum a posteriori probability (MAP) parameters are

$K_0 = 285 \pm 67$ MeV, $\quad c^2_{[2,3]n_0} = 0.49 \pm 0.13$, $\quad c^2_{[3,4]n_0} = -0.03 \pm 0.15$

D. Oliinychenko, **A. Sorensen**, V. Koch, L. McLerran, Phys. Rev. C **108**, 3, 034908 (2023), arXiv:2208.11996

Bayesian analysis of STAR flow data with varying K_0, $c^2_{[2,3]n_0}$, $c^2_{[3,4]n_0}$

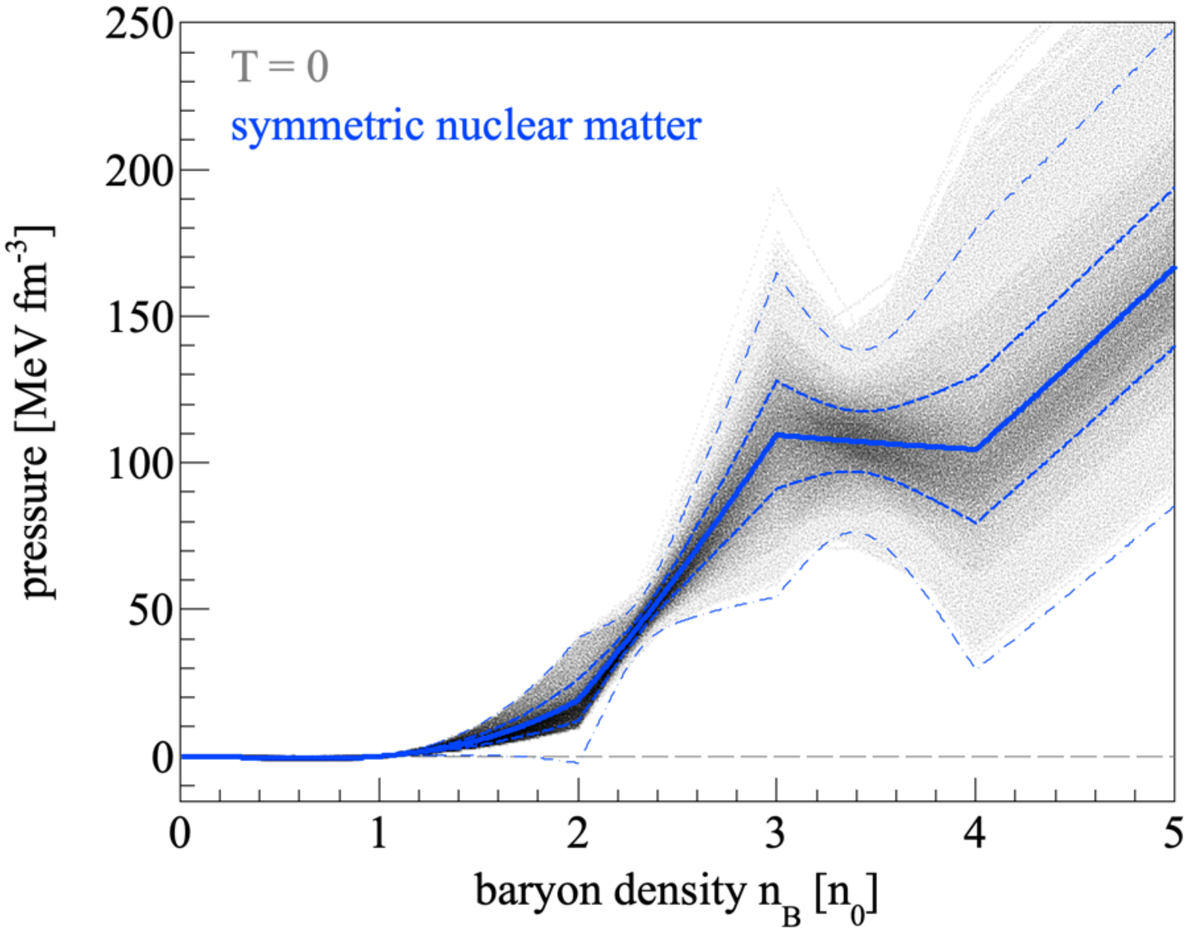

The constrained EOS is very stiff at $n_B \in (2,3)n_0$ and very soft at $n_B \in (3,4)n_0$

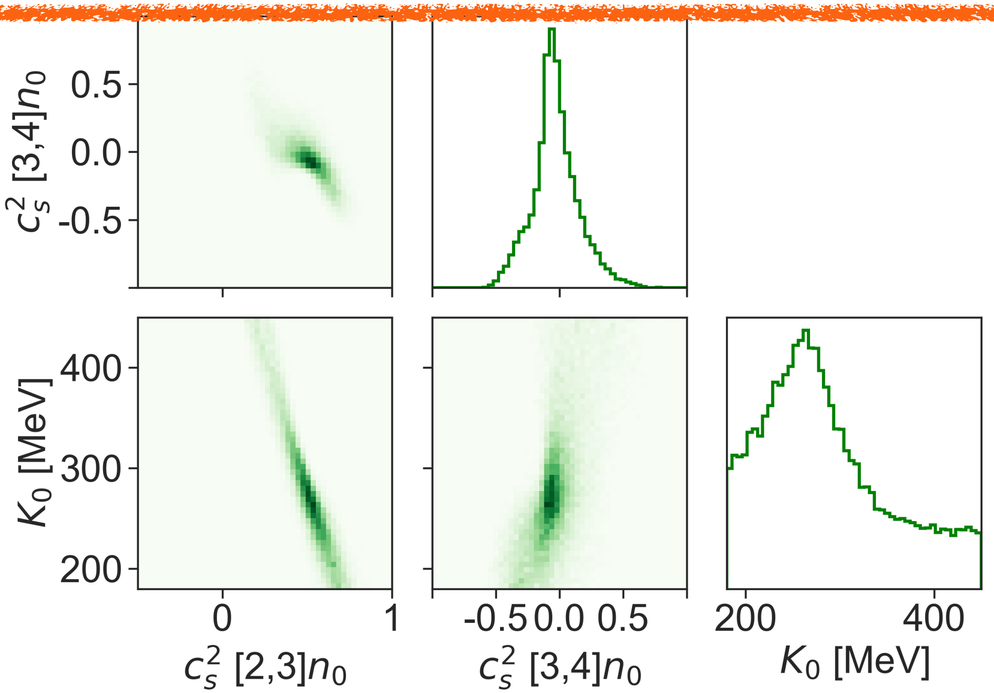

The maximum a posteriori probability (MAP) parameters are

$K_0 = 285 \pm 67$ MeV, $c^2_{[2,3]n_0} = 0.49 \pm 0.13$, $c^2_{[3,4]n_0} = -0.03 \pm 0.15$

D. Oliinychenko, **A. Sorensen**, V. Koch, L. McLerran, Phys. Rev. C **108**, 3, 034908 (2023), arXiv:2208.11996

Bayesian analysis of STAR flow data with varying K_0, $c^2_{[2,3]n_0}$, $c^2_{[3,4]n_0}$

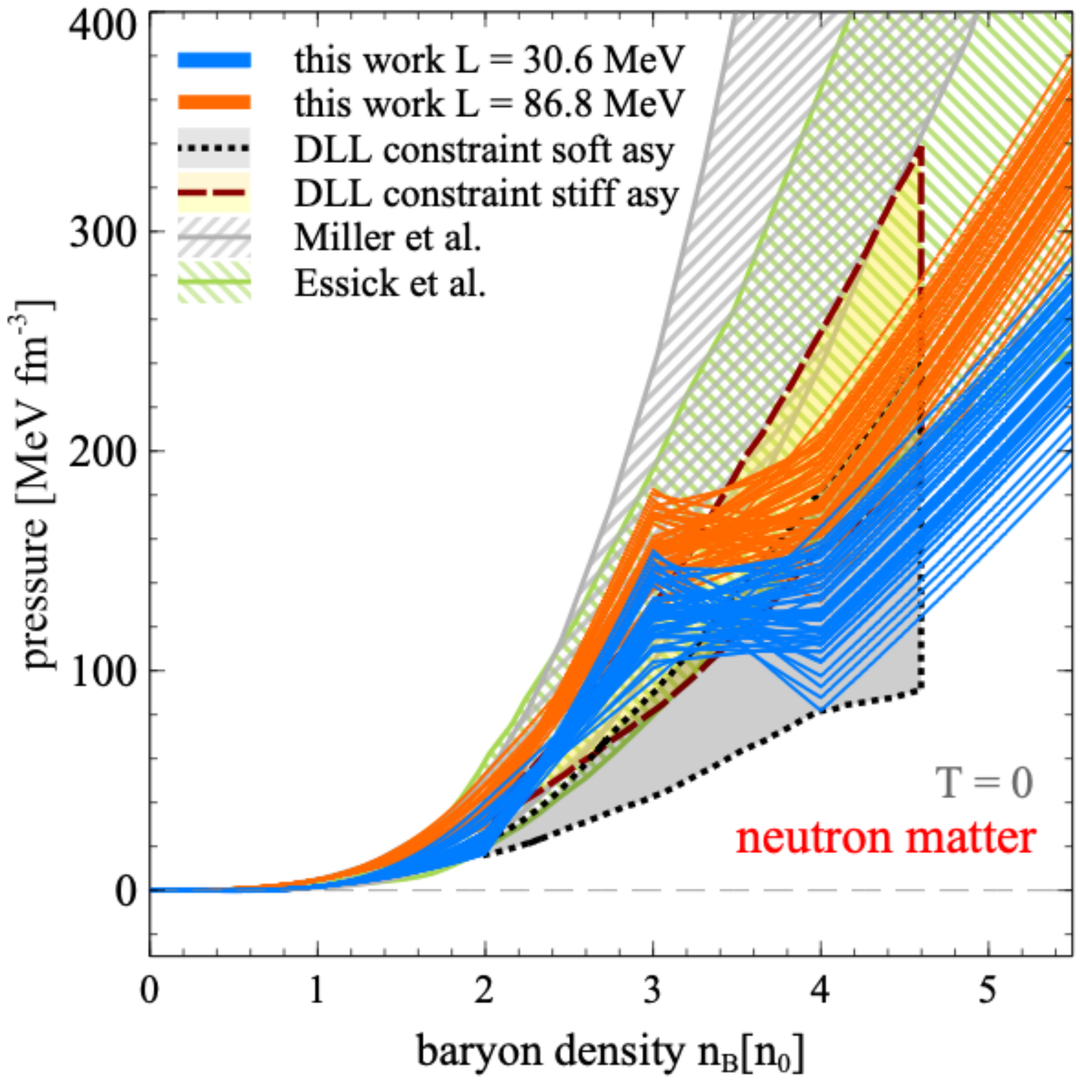

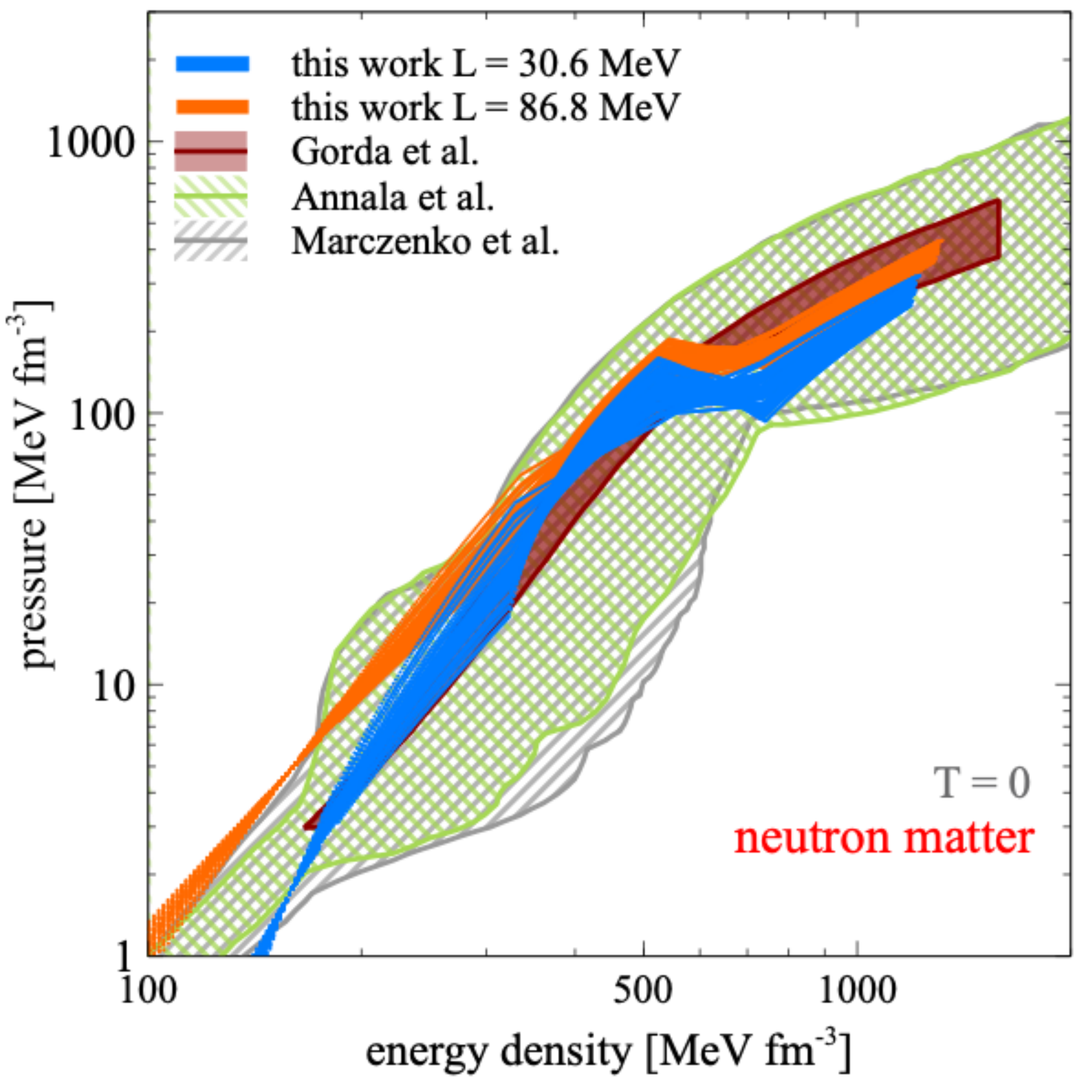

D. Oliinychenko, **A. Sorensen**, V. Koch, L. McLerran, Phys. Rev. C **108**, 3, 034908 (2023), arXiv:2208.11996

Still needed: momentum-dependence of nuclear matter interactions

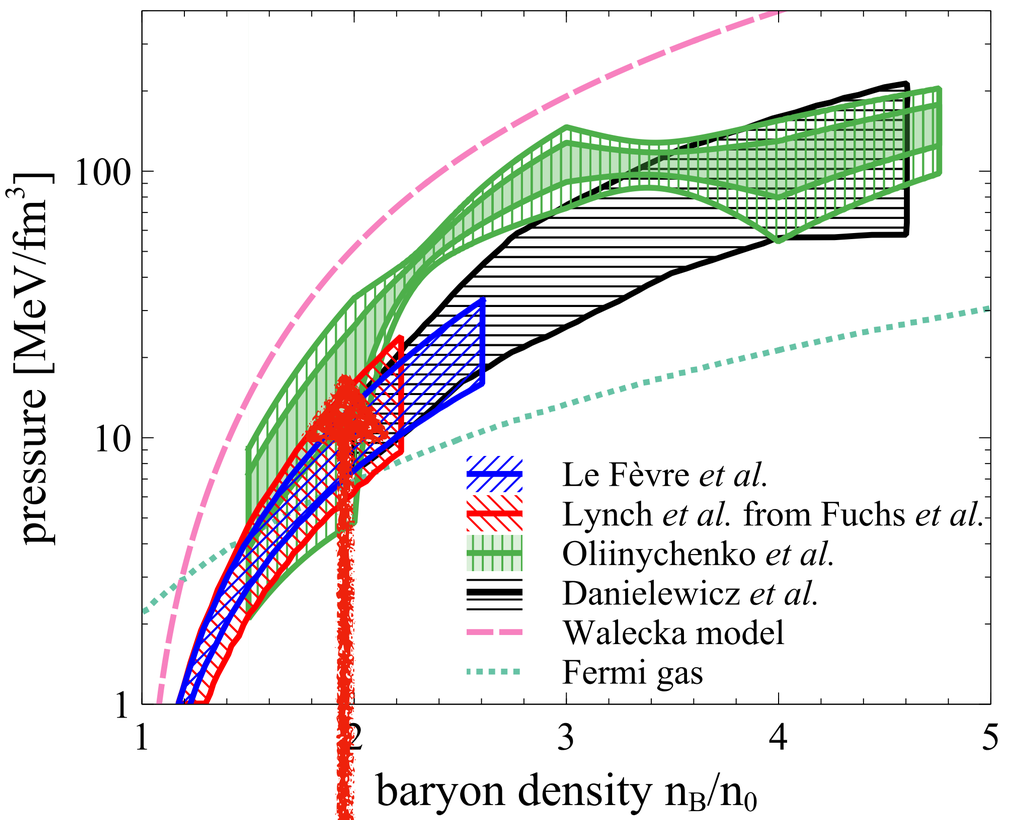

A. Sorensen *et al.*, Prog. Part. Nucl. Phys. **134**, 104080 (2024)
arXiv:2301.13253

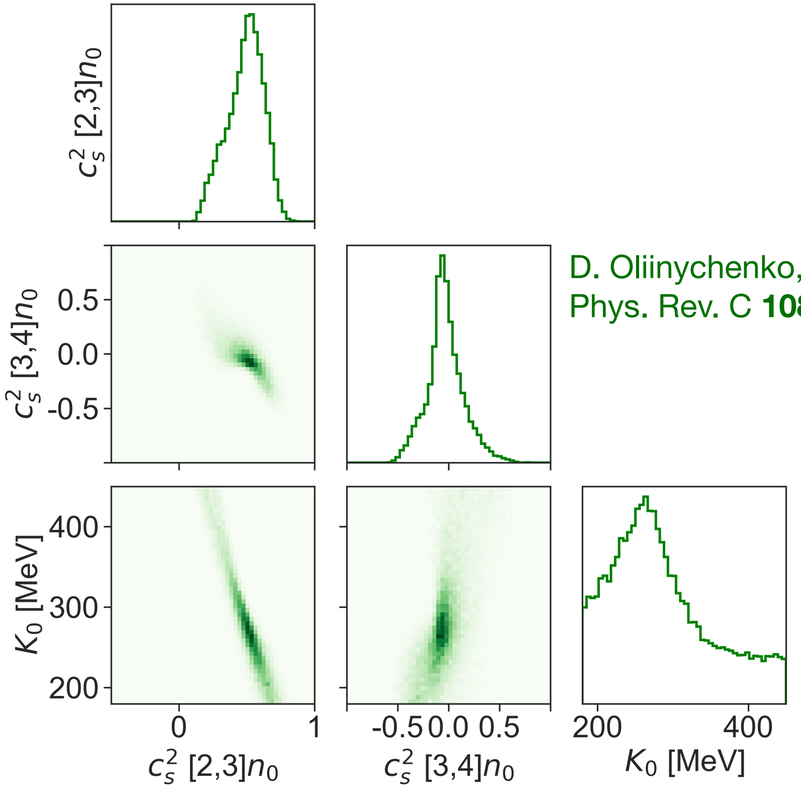

D. Oliinychenko, **A. Sorensen**, V. Koch, L. McLerran,
Phys. Rev. C **108**, 3, 034908 (2023), arXiv:2208.11996

Without momentum dependence, "artificial" additional source of repulsion is needed = the extracted EOS is too stiff?

Still needed: momentum-dependence of nuclear matter interactions

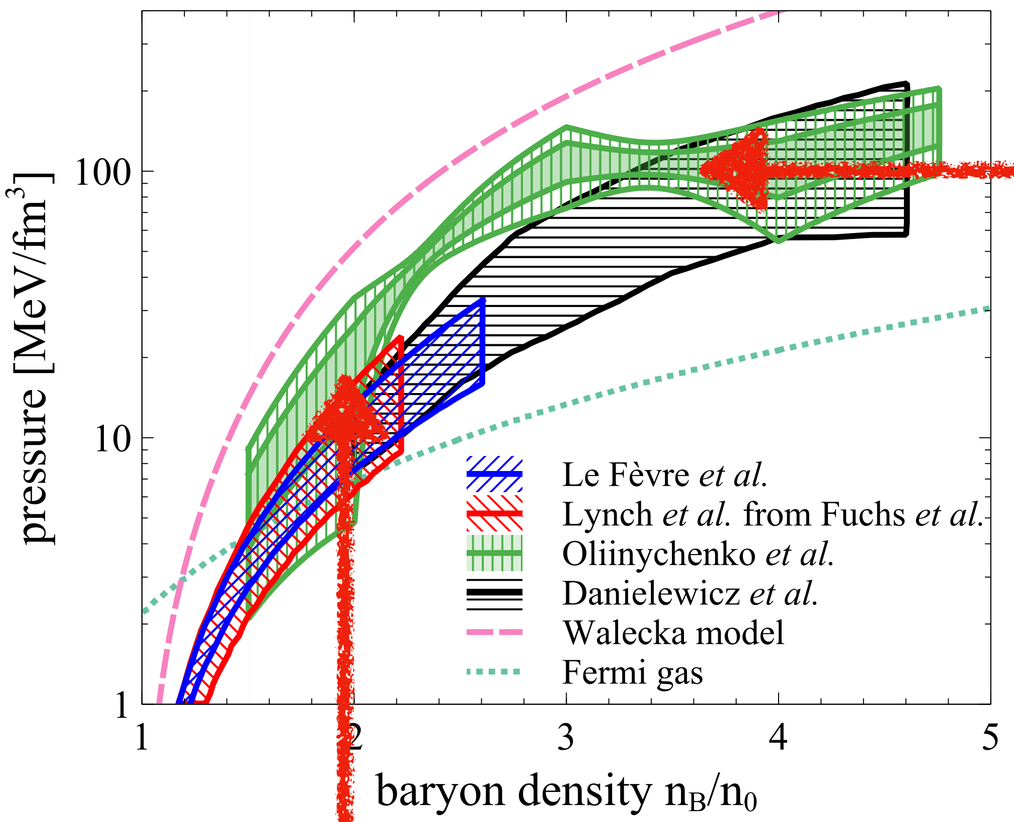

A. Sorensen *et al.*, Prog. Part. Nucl. Phys. **134**, 104080 (2024)
arXiv:2301.13253

Without momentum dependence, "artificial" additional source of repulsion is needed = the extracted EOS is too stiff?

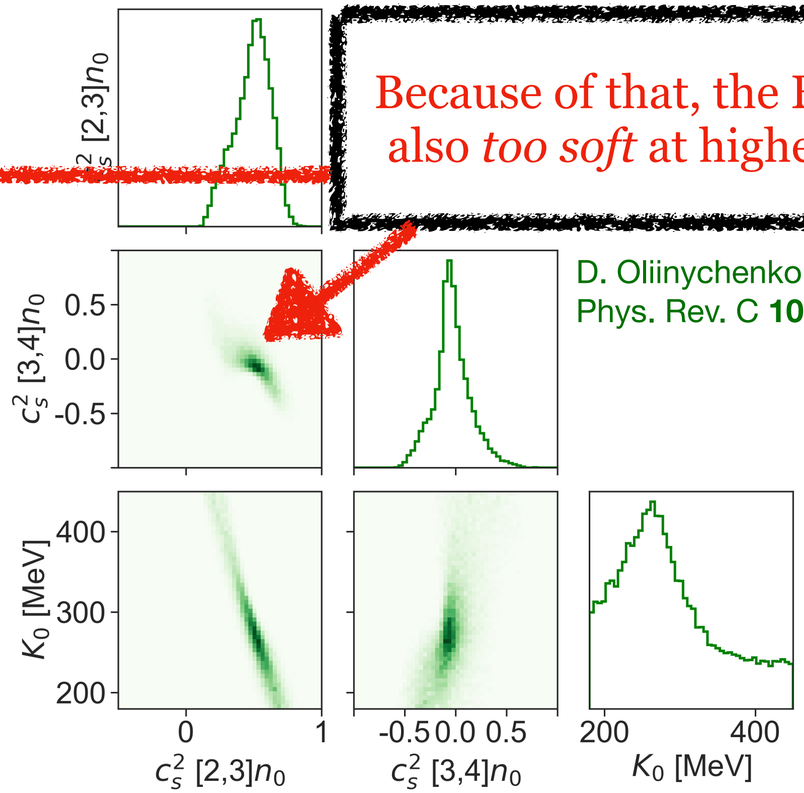

Because of that, the EOS may be also *too soft* at higher densities

D. Oliinychenko, **A. Sorensen**, V. Koch, L. McLerran, Phys. Rev. C **108**, 3, 034908 (2023), arXiv:2208.11996

Still needed: momentum-dependence of nuclear matter interactions

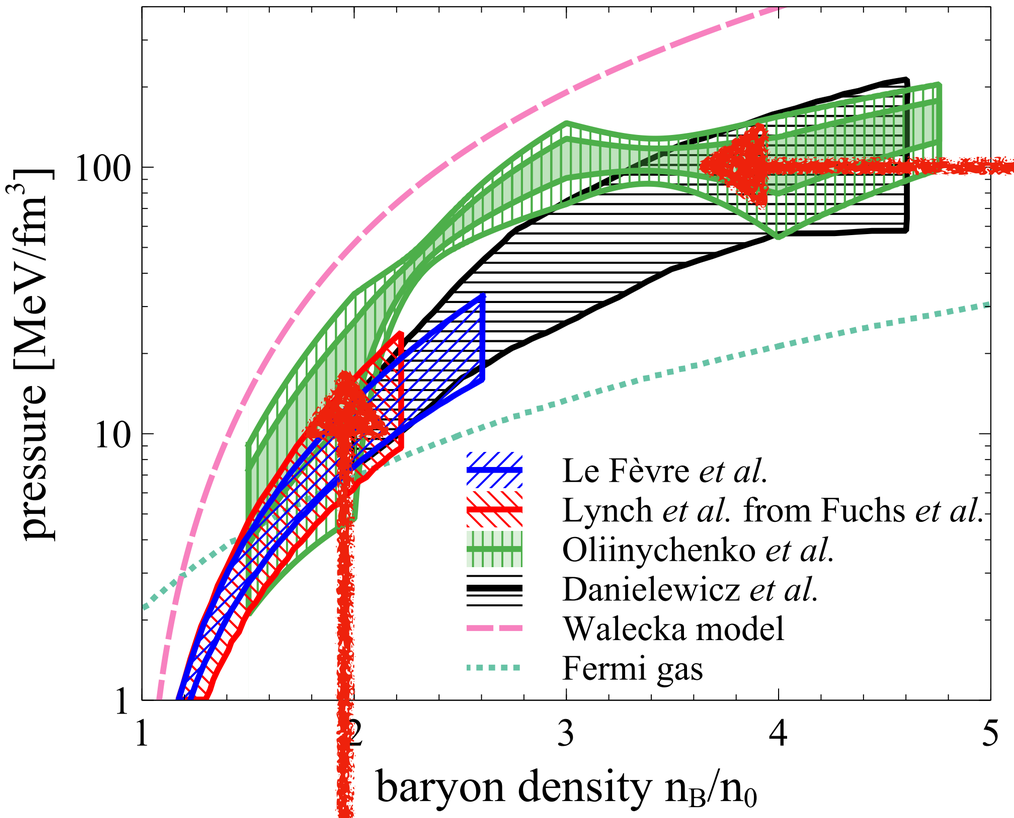

A. Sorensen *et al.*, Prog. Part. Nucl. Phys. **134**, 104080 (2024) arXiv:2301.13253

Without momentum dependence, "artificial" additional source of repulsion is needed = the extracted EOS is too stiff?

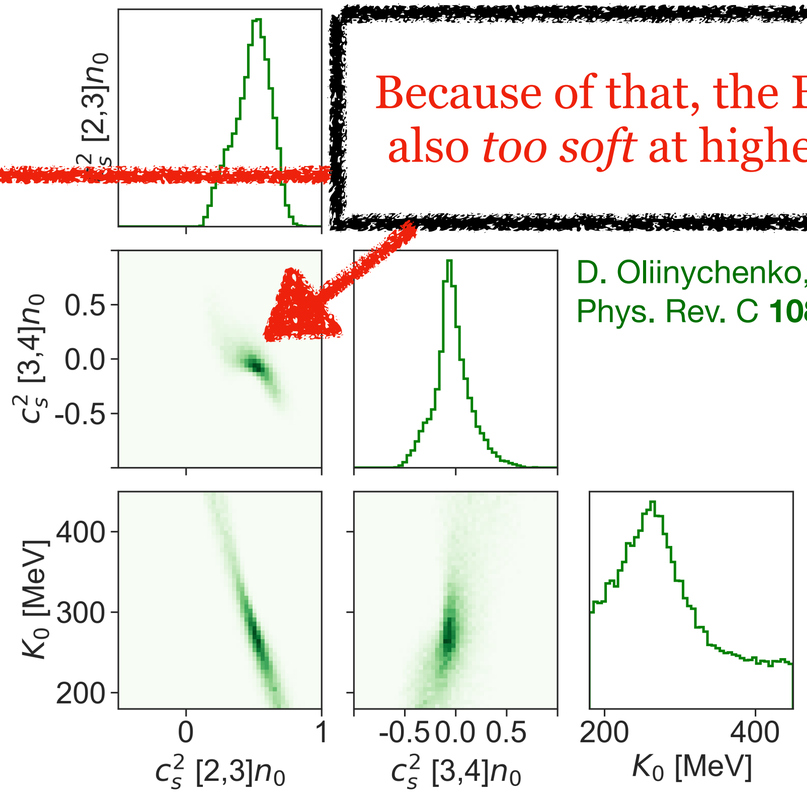

Because of that, the EOS may be also *too soft* at higher densities

D. Oliinychenko, **A. Sorensen**, V. Koch, L. McLerran, Phys. Rev. C **108**, 3, 034908 (2023), arXiv:2208.11996

P. Danielewicz, R. Lacey, and W. G. Lynch, Science **298**, 1592 (2002), arXiv:0208016

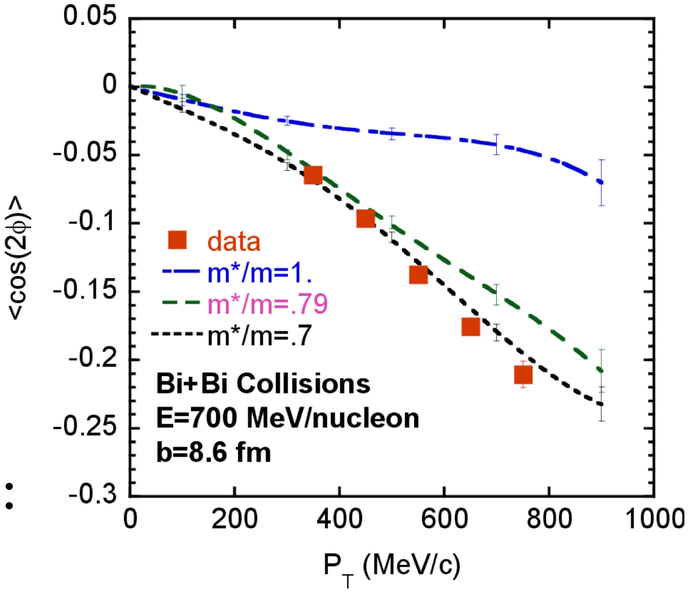

Use peripheral collisions to constrain the *p*-dependence:

Objective: the EOS and the phase diagram

Use heavy-ion collisions to study the QCD EOS = extract equilibrium bulk properties
from an extremely small ($\sim 10^{-14}$ m across)
and extremely short-lived ($\sim 10^{-22}$ s) system
using phenomenological simulations

Is it even possible???

Objective: the EOS and the phase diagram

Use heavy-ion collisions to study the QCD EOS = extract equilibrium bulk properties
from an extremely small ($\sim 10^{-14}$ m across)
and extremely short-lived ($\sim 10^{-22}$ s) system
using phenomenological simulations

Is it even possible??? What we learned at top RHIC energies suggests YES!

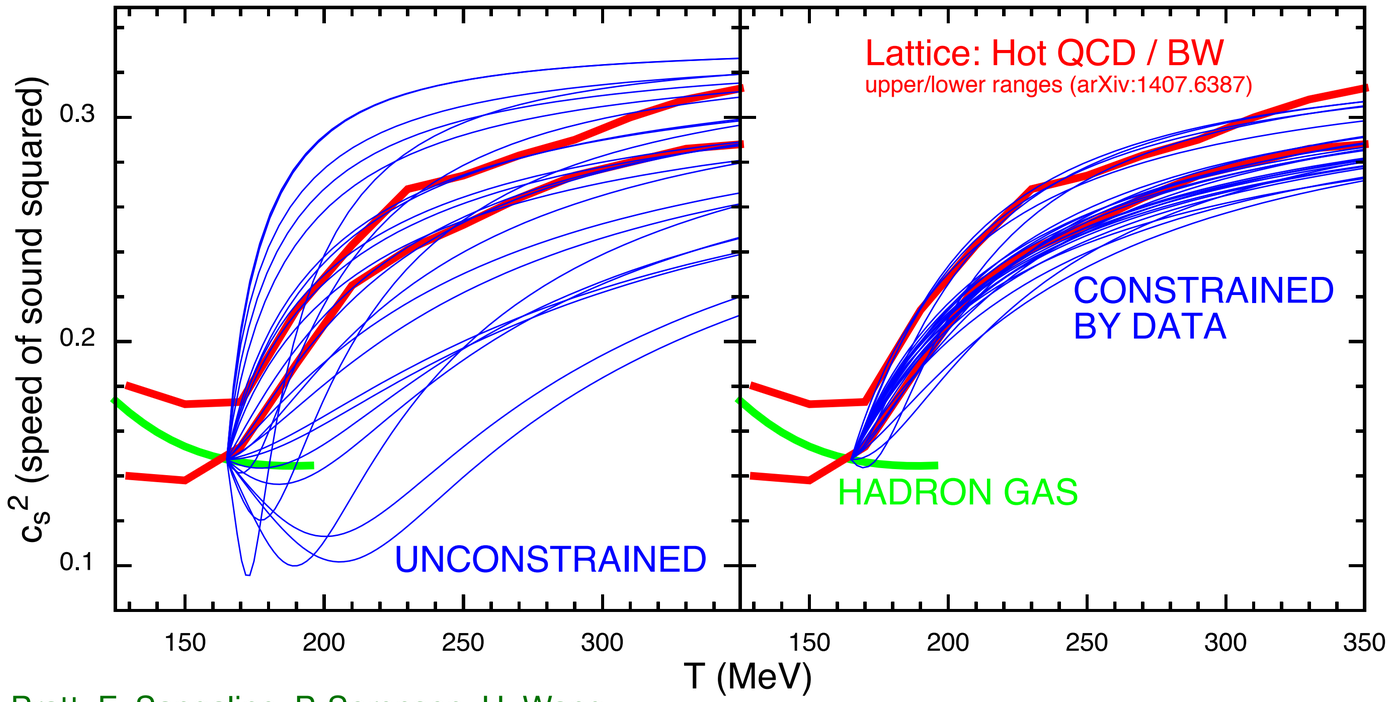

EOS constrained by Bayesian analysis of heavy-ion collisions at top RHIC energy ($\mu_B \approx 0$) agrees with LQCD

S. Pratt, E. Sangaline, P. Sorensen, H. Wang,
Phys. Rev. Lett. **114** 202301 (2015), arXiv:1501.04042

Objective: the EOS and the phase diagram

Use heavy-ion collisions to study the QCD EOS = extract equilibrium bulk properties
from an extremely small ($\sim 10^{-14}$ m across)
and extremely short-lived ($\sim 10^{-22}$ s) system
using phenomenological simulations

Is it even possible??? What we learned at top RHIC energies suggests YES!

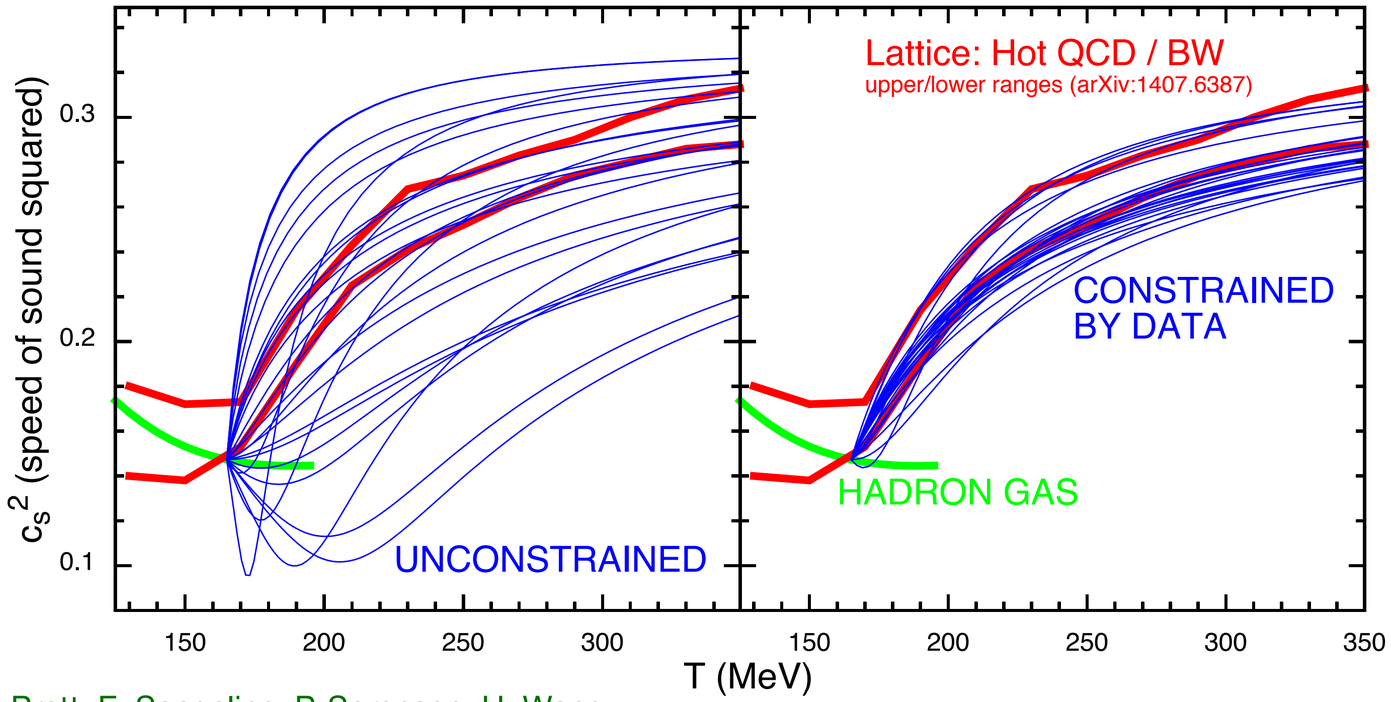

S. Pratt, E. Sangaline, P. Sorensen, H. Wang,
Phys. Rev. Lett. **114** 202301 (2015), arXiv:1501.04042

EOS constrained by Bayesian analysis of heavy-ion collisions at top RHIC energy ($\mu_B \approx 0$) agrees with LQCD

No/Scarce theory predictions at finite μ_B
=
Unique occasion to guide theory and understanding of QCD by extracting the EOS from new experimental data

Part 2: Historical constraints on the EOS from HICs

Constraints on the EOS come from comparisons to transport models

197Au+197Au @ 0.4—1.5 GeV/u
($\sqrt{s_{NN}}$ = 2.07 — 2.52 GeV)
observables: proton flow (FOPI)
model used: **isospin QMD (IQMD)** w/ nucleons, Δ, N*(1440), deuterons, tritons;
EOS parametrized by K_0;
momentum dependence
A. Le Fèvre, Y. Leifels, W. Reisdorf, J. Aichelin, C. Hartnack, Nucl. Phys. A 945, 112 (2016), arXiv:1501.05246

197Au+197Au & 12C+12C @ < 1.5 GeV/u
($\sqrt{s_{NN}}$ < 2.5 GeV)
observables: subthreshold kaon production (KaoS)
model used: **QMD** w/ nucleons, Δ, N*(1440), pions, kaons;
EOS parametrized by K_0;
kaon potentials, momentum dependence
C. Fuchs *et al.*, Prog. Part. Nucl. Phys. **53**, 113–124 (2004) arXiv:nucl-th/0312052

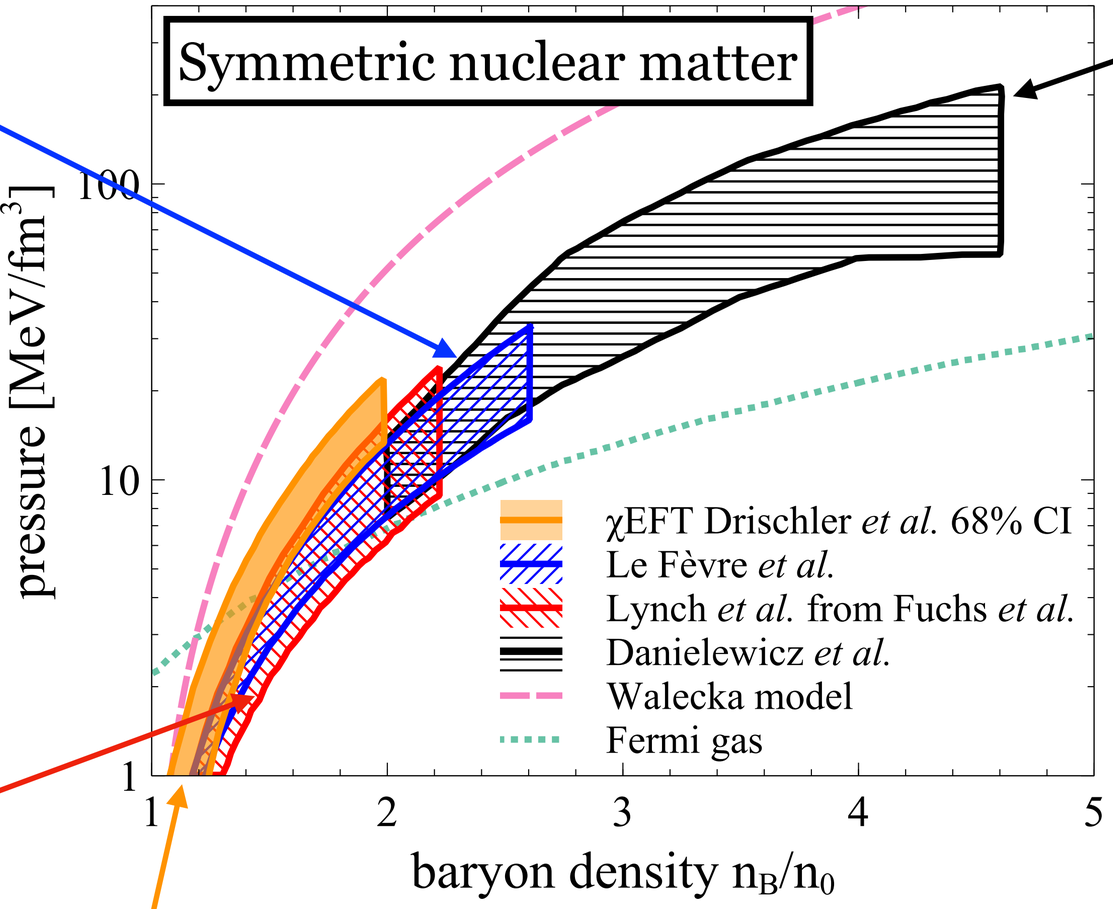

A. Sorensen *et al.*, Prog. Part. Nucl. Phys. **134**, 104080 (2024) arXiv:2301.13253

χEFT
C. Drischler *et al.*, Phys. Rev. C **102** 5, 054315 (2020) arXiv:2004.07805

197Au+197Au @ 0.15—10 GeV/u
($\sqrt{s_{NN}}$ = 1.95 — 4.72 GeV)
observables: proton flow (Plastic Ball, EOS, E877, E895)
model used: **pBUU** w/ nucleons, Δ, N*(1440), pions;
EOS parametrized by K_0;
momentum dependence
P. Danielewicz, R. Lacey, W. G. Lynch, Science **298**,1592–1596 (2002)

Standard way of modeling the EOS: Skyrme potential

The most common form of the EOS is the "Skyrme potential": $U(n_B) = A\left(\frac{n_B}{n_0}\right) + B\left(\frac{n_B}{n_0}\right)^{\tau}$

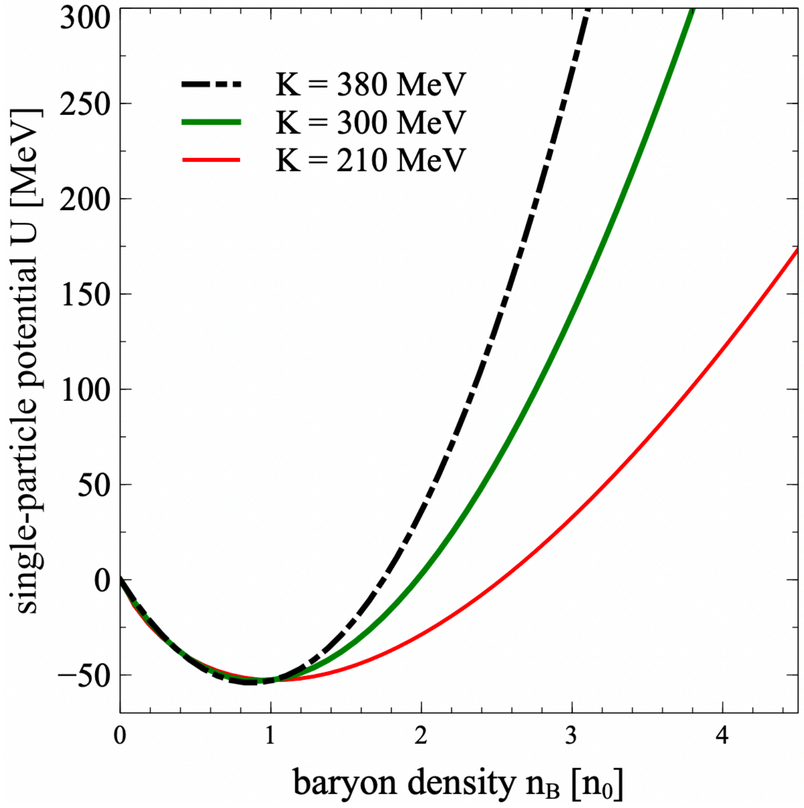

$$F = \left.\frac{d\langle p_x/A\rangle}{d(y/y_{cm})}\right|_{y/y_{cm}=1} \sim \frac{dv_1}{dy}$$

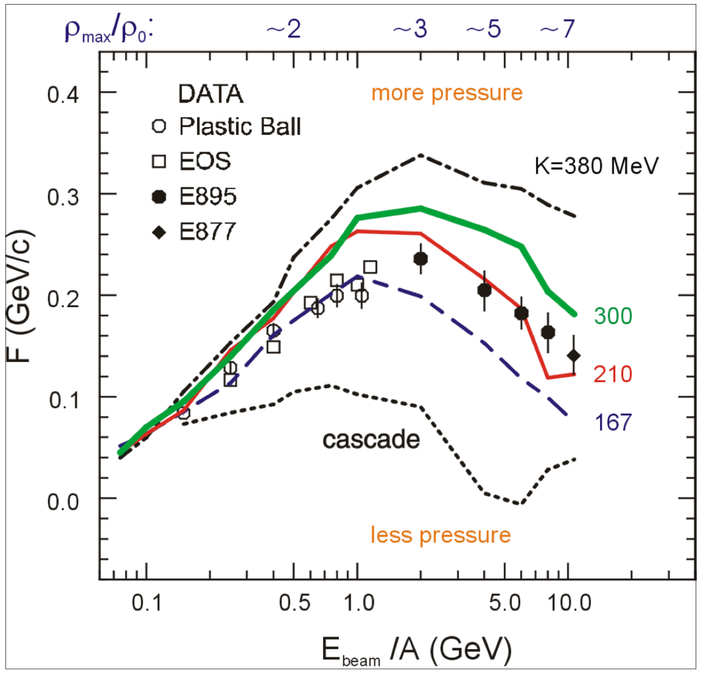

v_2

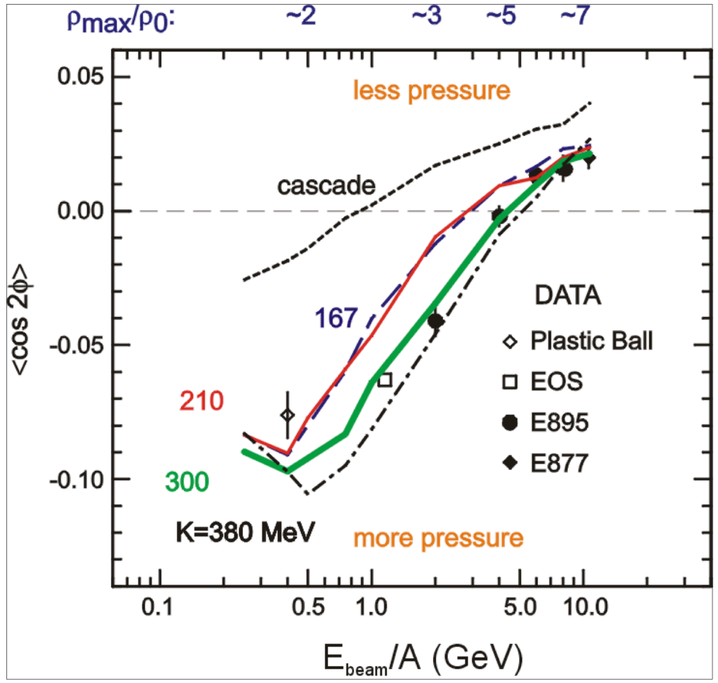

P. Danielewicz, R. Lacey, W. G. Lynch,
Science **298**, 1592–1596 (2002), arXiv:nucl-th/0208016

Standard way of modeling the EOS: Skyrme potential

P. Danielewicz, R. Lacey, W. G. Lynch,
Science **298**, 1592–1596 (2002), arXiv:nucl-th/0208016

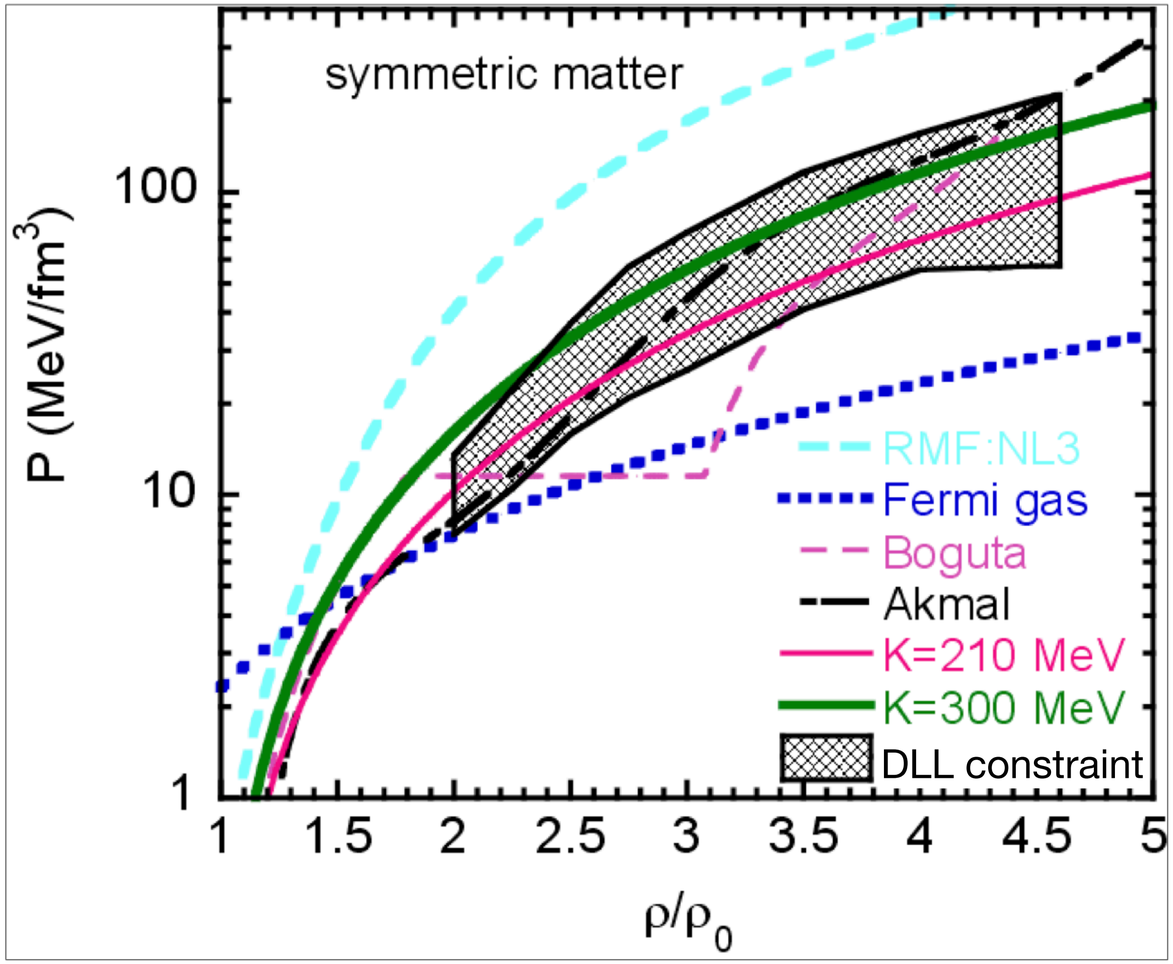

"the heavy-ion constraint"

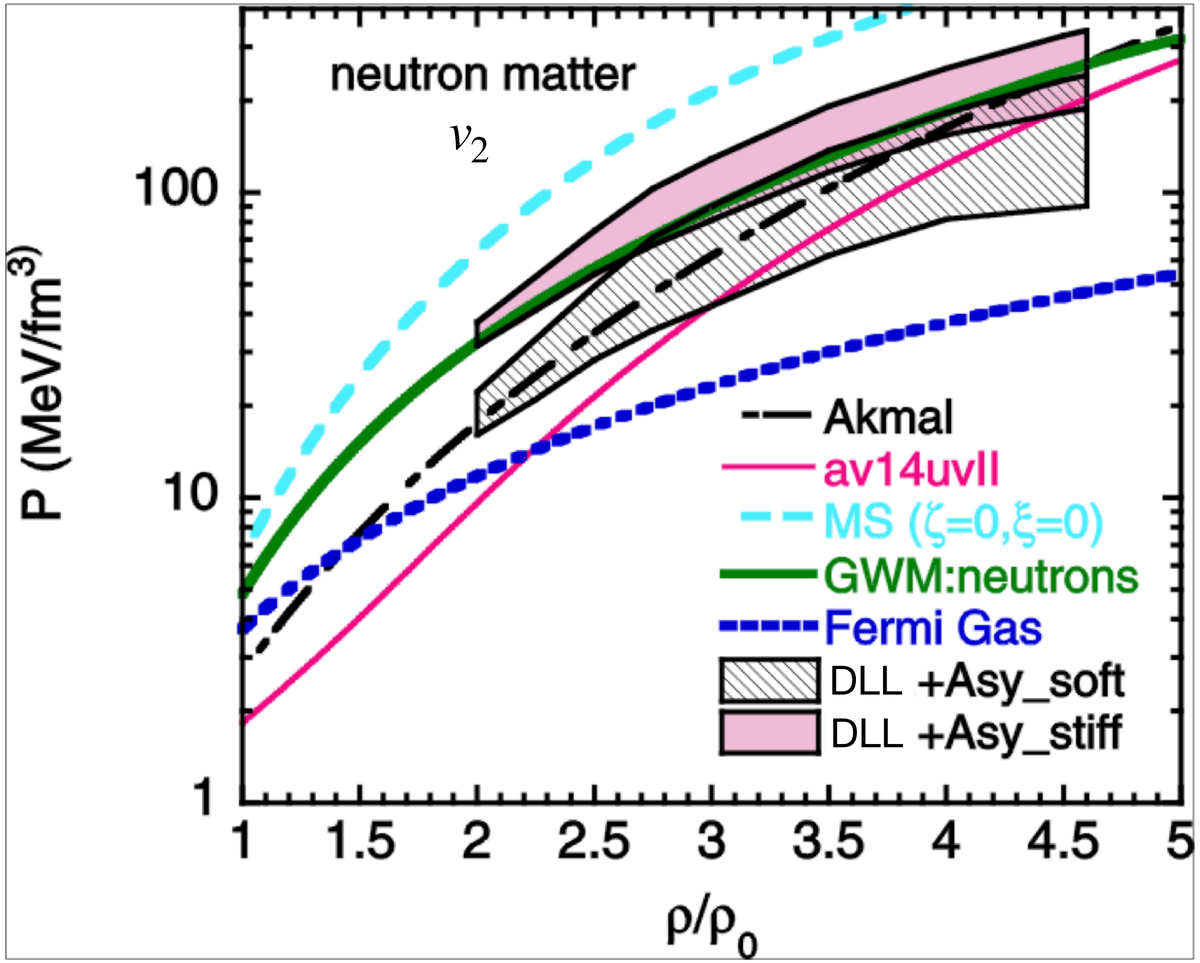

Standard way of modeling the EOS: Skyrme potential

P. Danielewicz, R. Lacey, W. G. Lynch,
Science **298**, 1592–1596 (2002), arXiv:nucl-th/0208016

"the heavy-ion constraint"

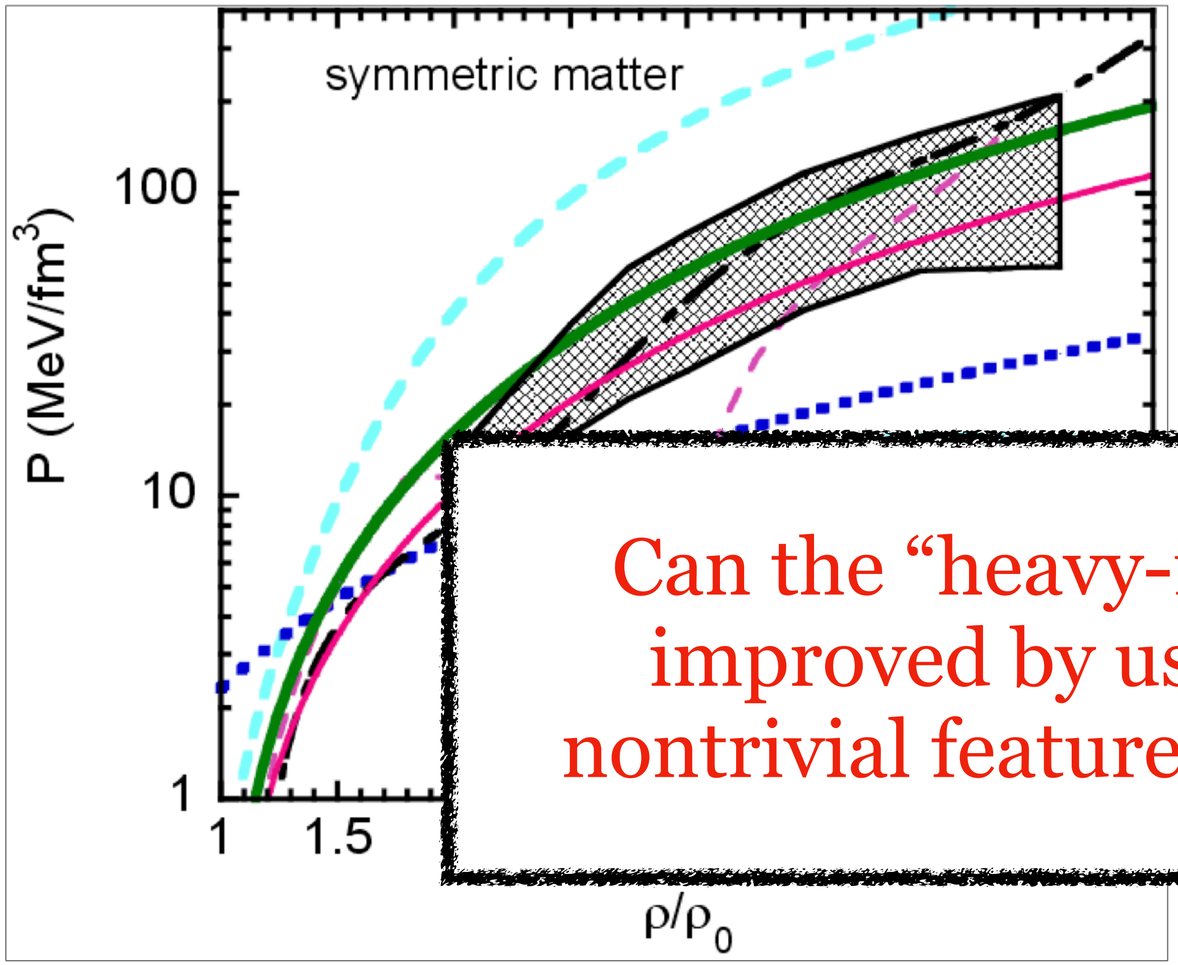

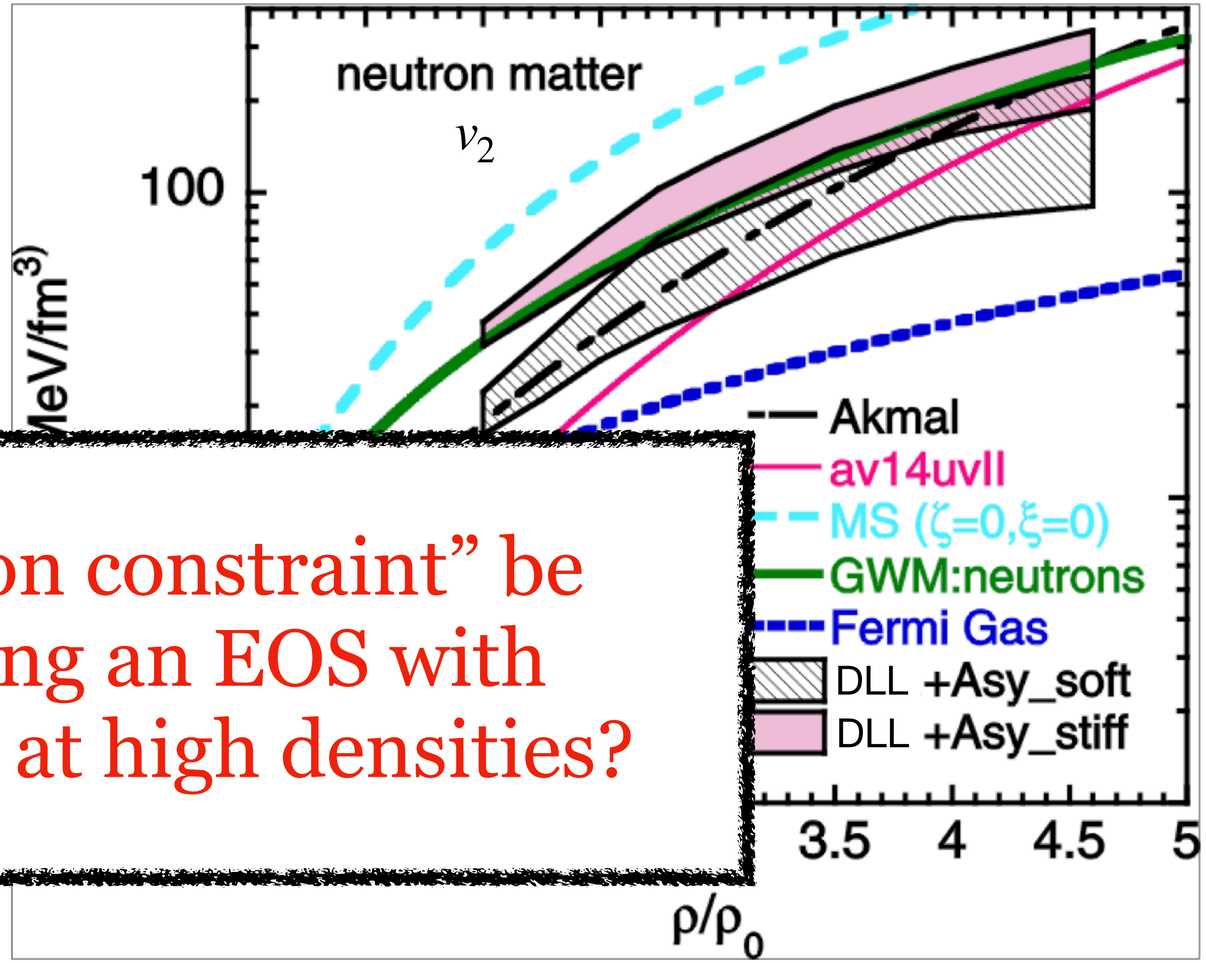

Can the "heavy-ion constraint" be improved by using an EOS with nontrivial features at high densities?

EOS of symmetric nuclear matter: selected (*few*) results

197Au+197Au @ 0.4—1.5 GeV/u
($\sqrt{s_{NN}}$ = 2.07 — 2.52 GeV)
observables: proton flow (FOPI)
model used: **isospin QMD (IQMD)** w/ nucleons, Δ, N*(1440), deuterons, tritons;
EOS parametrized by K_0;
momentum dependence
A. Le Fèvre, Y. Leifels, W. Reisdorf, J. Aichelin, C. Hartnack, Nucl. Phys. A 945, 112 (2016), arXiv:1501.05246

197Au+197Au & 12C+12C @ < 1.5 GeV/u
($\sqrt{s_{NN}}$ < 2.5 GeV)
observables: subthreshold kaon production (KaoS)
model used: **QMD** w/ nucleons, Δ, N*(1440), pions, kaons;
EOS parametrized by K_0;
kaon potentials, momentum dependence
C. Fuchs *et al.*, Prog. Part. Nucl. Phys. **53**, 113–124 (2004) arXiv:nucl-th/0312052

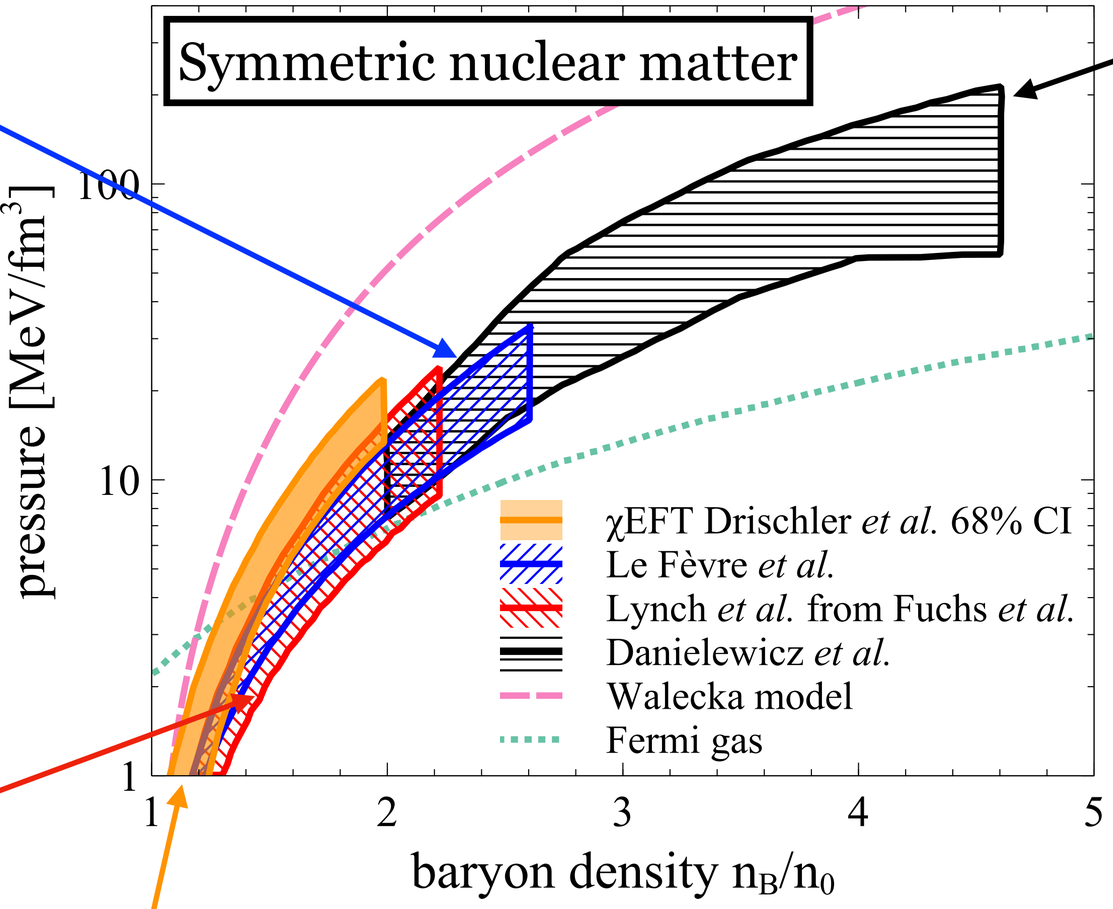

197Au+197Au @ 0.15—10 GeV/u
($\sqrt{s_{NN}}$ = 1.95 — 4.72 GeV)
observables: proton flow
(Plastic Ball, EOS, E877, E895)
model used: **pBUU** w/ nucleons, Δ, N*(1440), pions;
EOS parametrized by K_0;
momentum dependence
P. Danielewicz, R. Lacey, W. G. Lynch, Science **298**,1592–1596 (2002)

A. Sorensen *et al.*, Prog. Part. Nucl. Phys. **134**, 104080 (2024) arXiv:2301.13253

χEFT
C. Drischler *et al.*, Phys. Rev. C **102** 5, 054315 (2020) arXiv:2004.07805

EOS of symmetric nuclear matter: selected (*few*) results

197Au+197Au @ 0.4—1.5 GeV/u
($\sqrt{s_{NN}}$ = 2.07 — 2.52 GeV)
observables: proton flow (FOPI)
model used: **isospin QMD (IQMD)** w/ nucleons, Δ, N*(1440), deuterons, tritons;
EOS parametrized by K_0;
momentum dependence
A. Le Fèvre, Y. Leifels, W. Reisdorf, J. Aichelin, C. Hartnack, Nucl. Phys. A 945, 112 (2016), arXiv:1501.05246

197Au+197Au & 12C+12C @ < 1.5 GeV/u
($\sqrt{s_{NN}}$ < 2.5 GeV)
observables: subthreshold kaon production (KaoS)
model used: **QMD** w/ nucleons, Δ, N*(1440), pions, kaons;
EOS parametrized by K_0;
kaon potentials, momentum dependence
C. Fuchs *et al.*, Prog. Part. Nucl. Phys. **53**, 113–124 (2004) arXiv:nucl-th/0312052

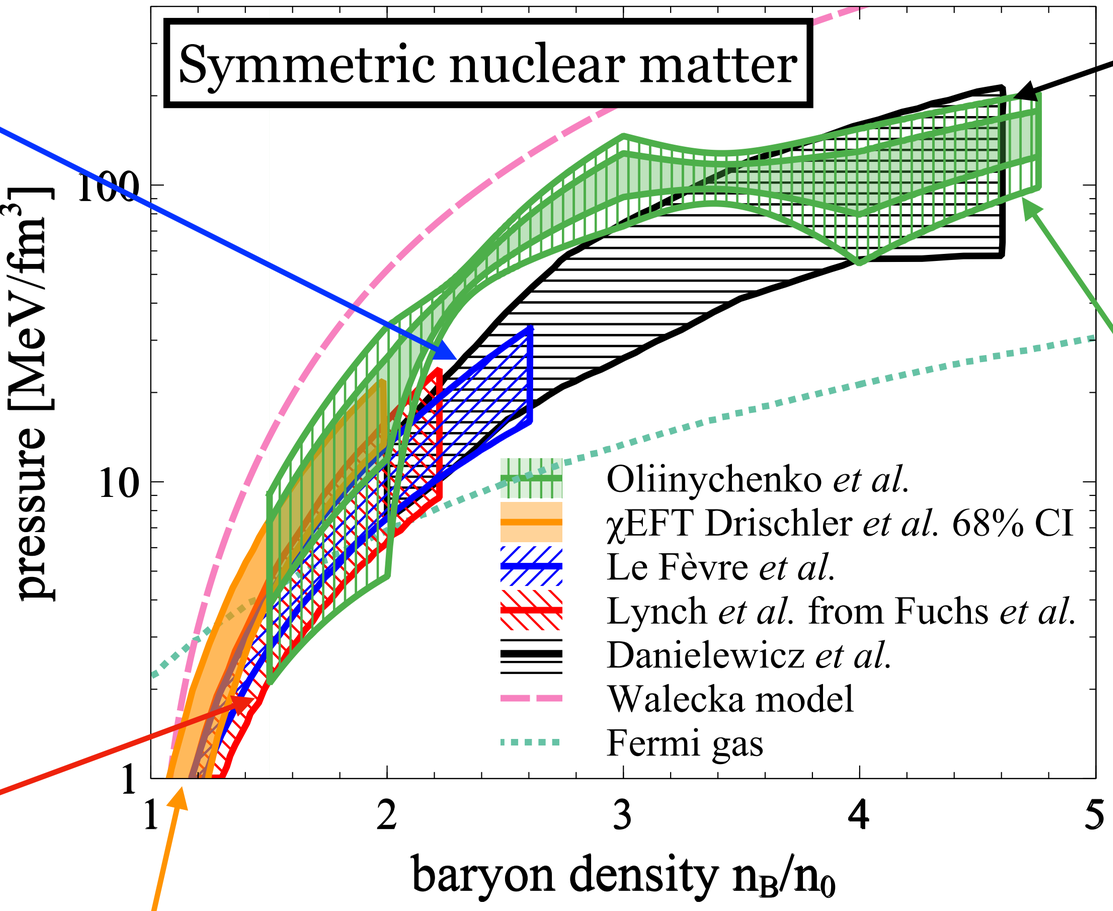

A. Sorensen *et al.*, Prog. Part. Nucl. Phys. **134**, 104080 (2024) arXiv:2301.13253

χEFT
C. Drischler *et al.*, Phys. Rev. C **102** 5, 054315 (2020) arXiv:2004.07805

197Au+197Au @ 0.15—10 GeV/u
($\sqrt{s_{NN}}$ = 1.95 — 4.72 GeV)
observables: proton flow (Plastic Ball, EOS, E877, E895)
model used: **pBUU** w/ nucleons, Δ, N*(1440), pions;
EOS parametrized by K_0;
momentum dependence
P. Danielewicz, R. Lacey, W. G. Lynch, Science **298**,1592–1596 (2002)

197Au+197Au @ 2.9—9 GeV/u
($\sqrt{s_{NN}}$ = 3 — 4.5 GeV)
observables: proton flow (STAR)
model used: SMASH w/ over 120 hadronic species, including deuterons;
relativistic EOS parametrized independently in different density regions;
NO momentum dependence
D. Oliinychenko, **A. Sorensen**, V. Koch, L. McLerran, Phys. Rev. C **108**, 3, 034908 (2023), arXiv:2208.11996

The way forward for EOS constraints

Calculations with momentum dependence are *extremely* computationally expensive:
by far, access to HPC is not enough.
The path forward will rely heavily on AI/ML: 1) emulators, 2) active learning, 3) transfer learning, …

The way forward for EOS constraints

Calculations with momentum dependence are *extremely* computationally expensive:
by far, access to HPC is not enough.
The path forward will rely heavily on AI/ML: 1) emulators, 2) active learning, 3) transfer learning, …

Exciting opportunities for constraining the isospin-dependence of the EOS with
1) experiments at GSI (*ASY-EOS II has just taken data!*),
2) experiments at FRIB (*later this year!*),
3) multi-messenger astronomy (*LVK Observing Run 4, Einstein Telescope/Cosmic Explorer*).

The way forward for EOS constraints

Calculations with momentum dependence are *extremely* computationally expensive:
by far, access to HPC is not enough.
The path forward will rely heavily on AI/ML: 1) emulators, 2) active learning, 3) transfer learning, …

Exciting opportunities for constraining the isospin-dependence of the EOS with
1) experiments at GSI (*ASY-EOS II has just taken data!*),
2) experiments at FRIB (*later this year!*),
3) multi-messenger astronomy (*LVK Observing Run 4, Einstein Telescope/Cosmic Explorer*).

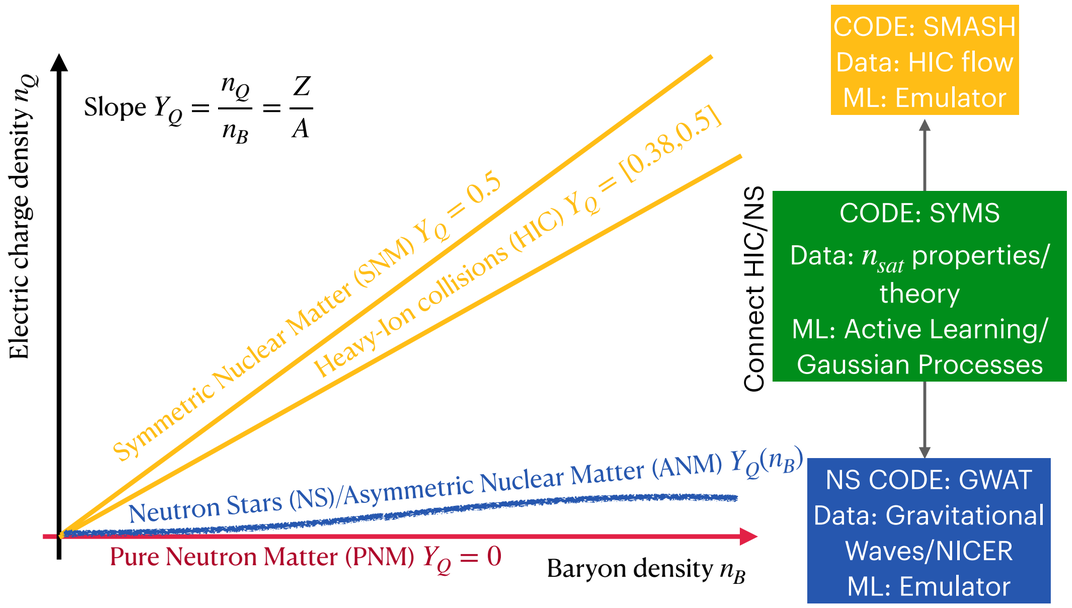

State-of-the-art joint constraints from HIC & NS data only possible with AI/ML

project w/ J. Noronha-Hostler & N. Yunes (UIUC), K. Godbey (FRIB)

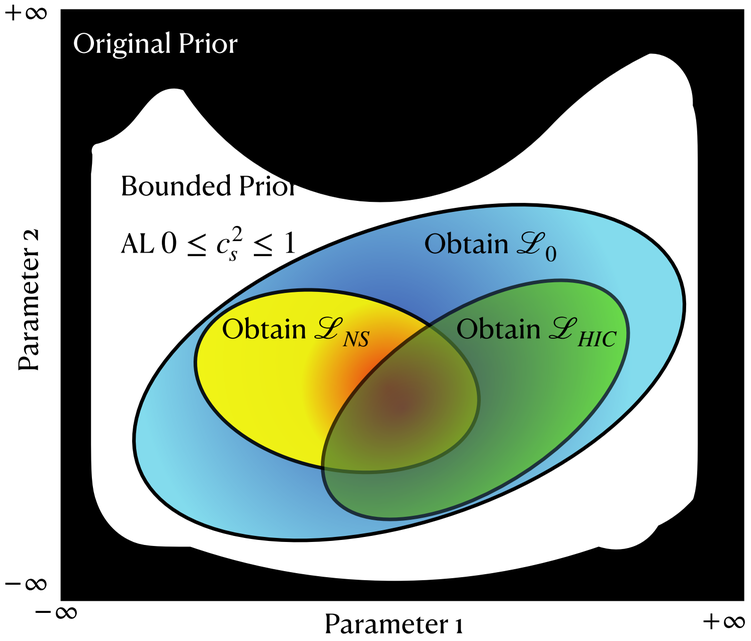

The way forward for EOS constraints

Calculations with momentum dependence are *extremely* computationally expensive:
by far, access to HPC is not enough.
The path forward will rely heavily on AI/ML: 1) emulators, 2) active learning, 3) transfer learning, …

Exciting opportuniti
1) experiments at GS
2) experiments at FR
3) multi-messenger

xplorer).

All of this is a LOT of work…

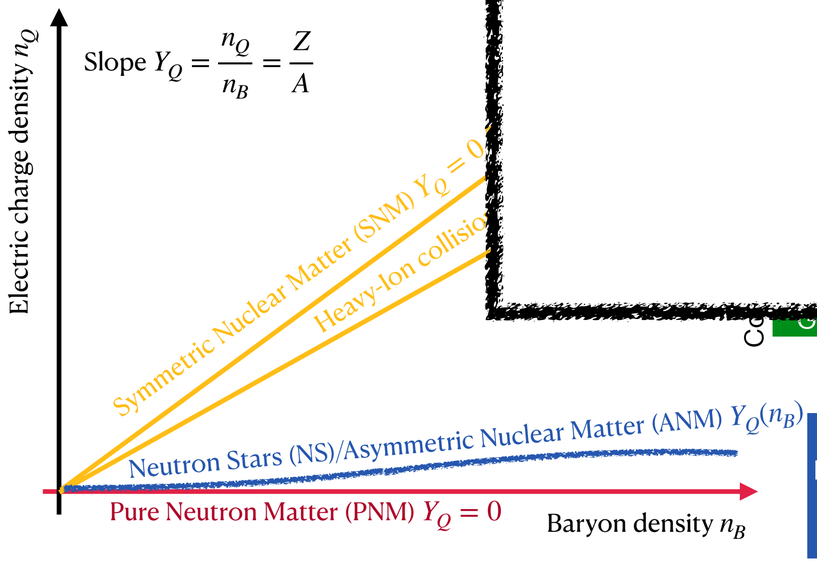

Gaussian Processes

NS CODE: GWAT
Data: Gravitational Waves/NICER
ML: Emulator

project w/ J. Noronha-Hostler &
N. Yunes (UIUC), K. Godbey (FRIB)

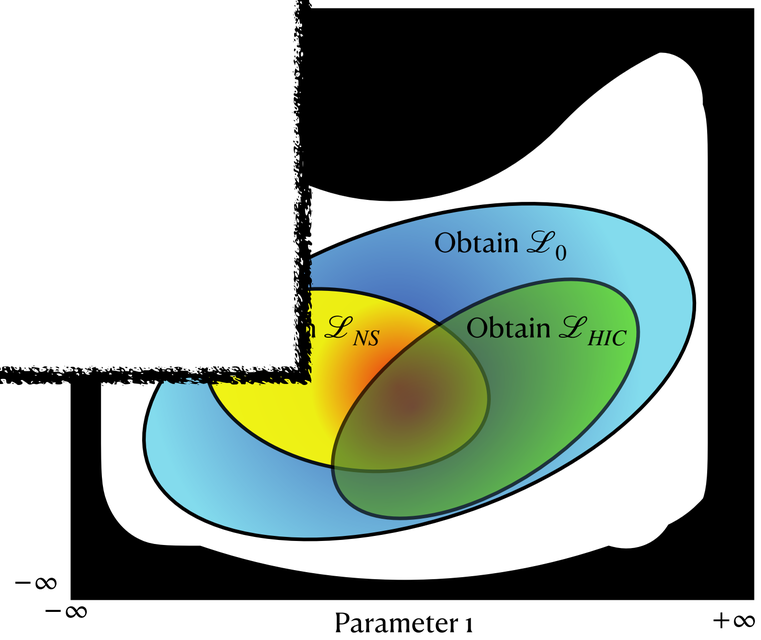

Part 4.2: Results using data from BES-I

The idea to probe the QCD phase diagram with heavy-ins is not new...

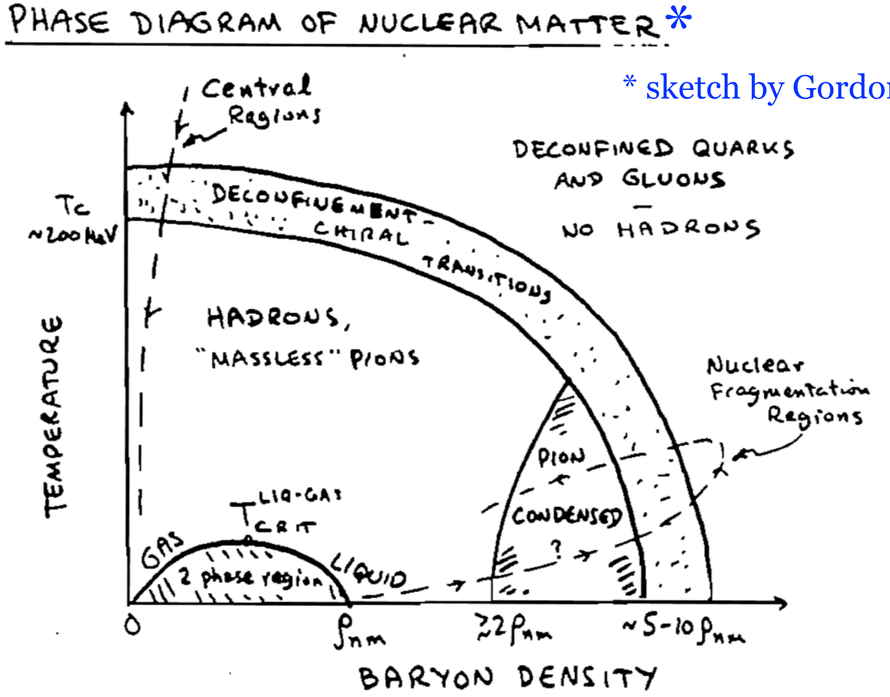

* sketch by Gordon Baym, LRP 1983

The idea to probe the QCD phase diagram with heavy-ions is not new...

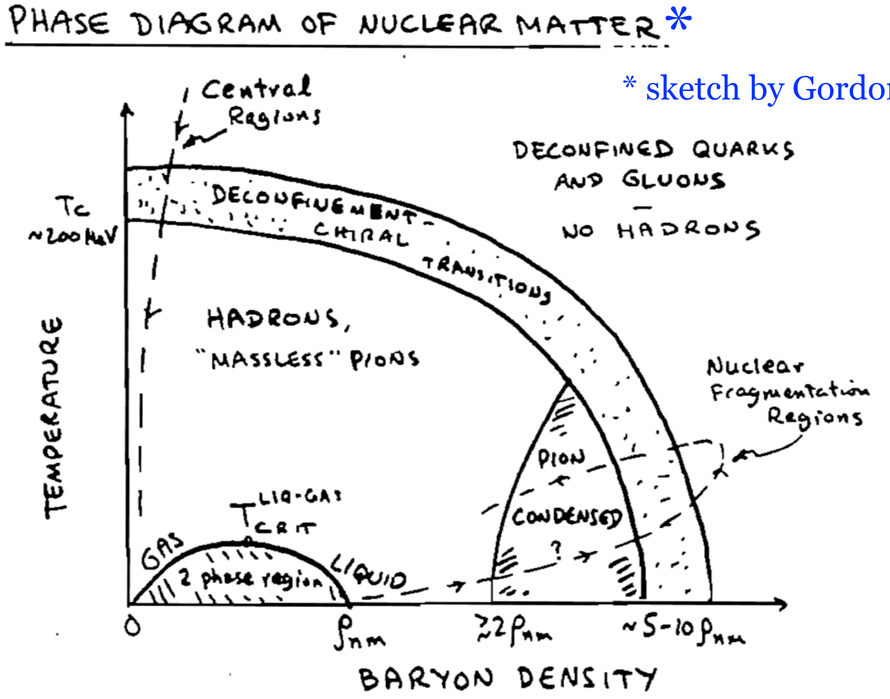

* sketch by Gordon Baym, LRP 1983

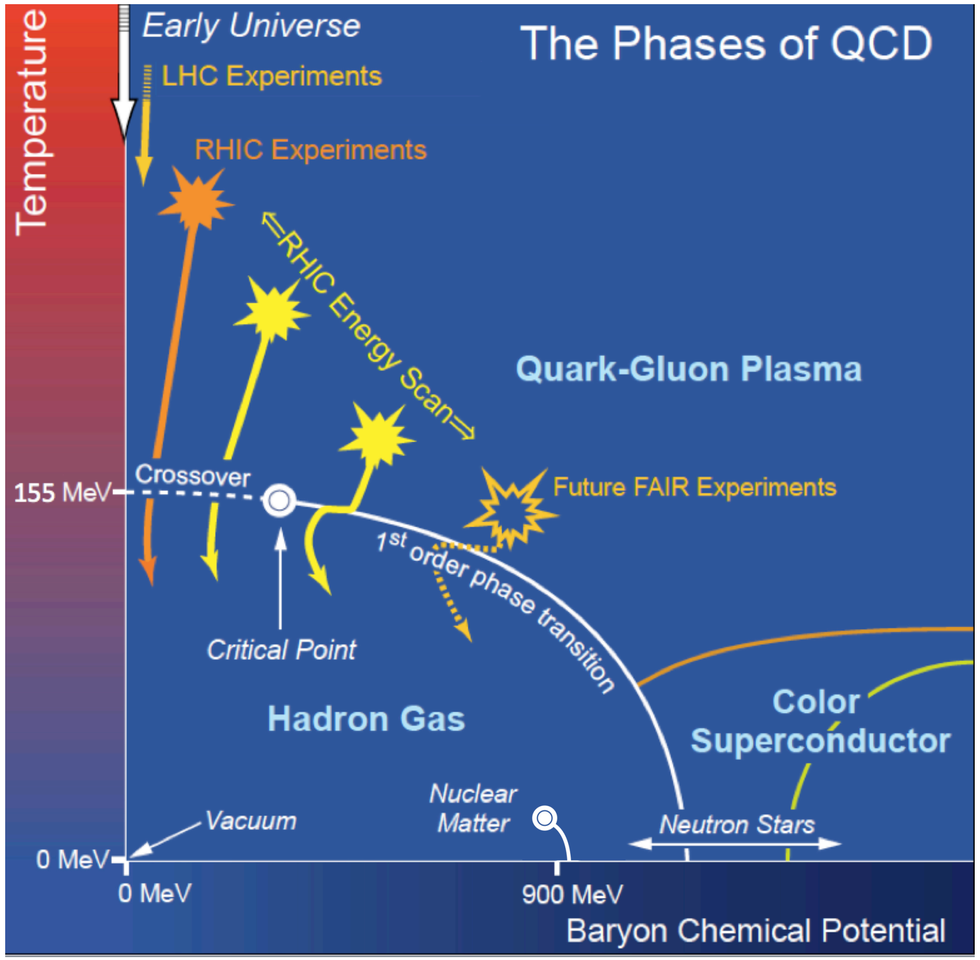

LRP 2007

The idea to probe the QCD phase diagram with heavy-ions is not new…

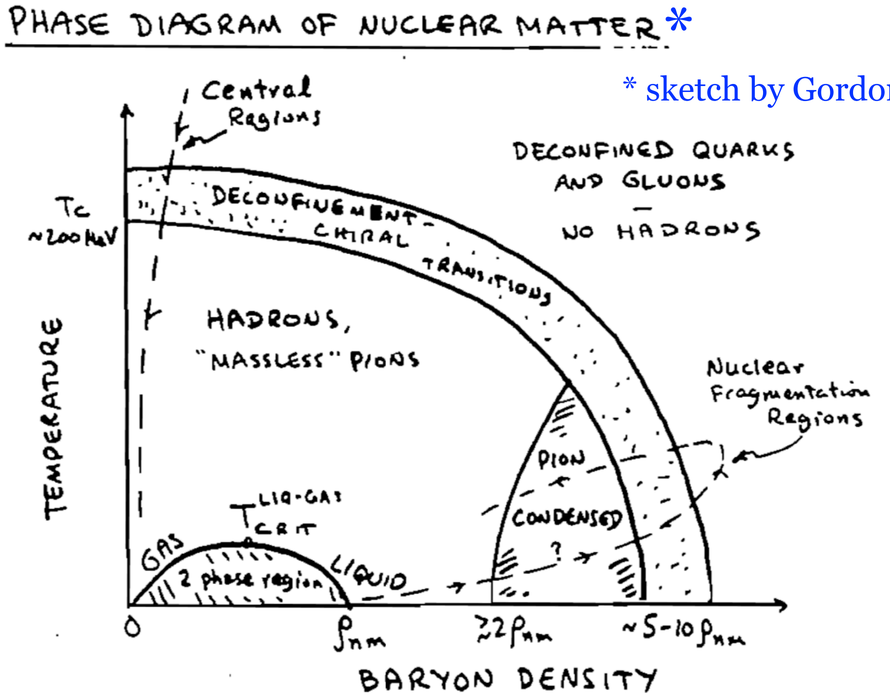

* sketch by Gordon Baym, LRP 1983

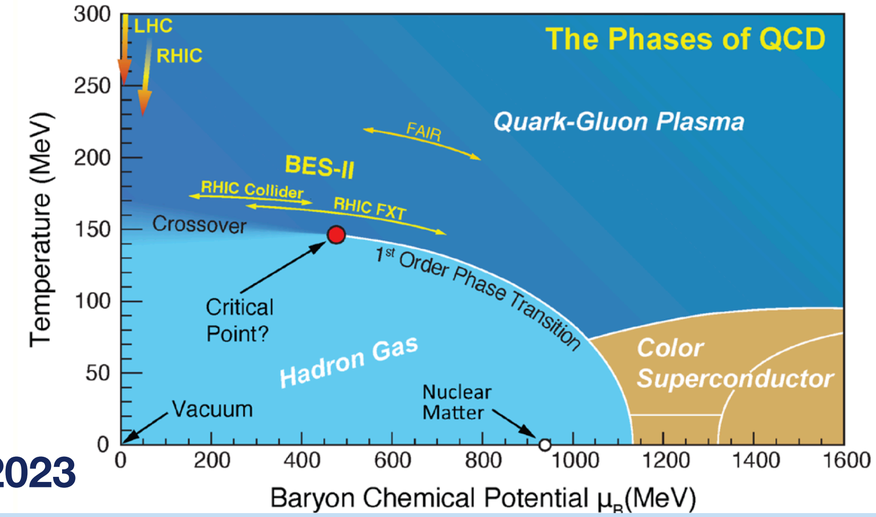

LRP 2023

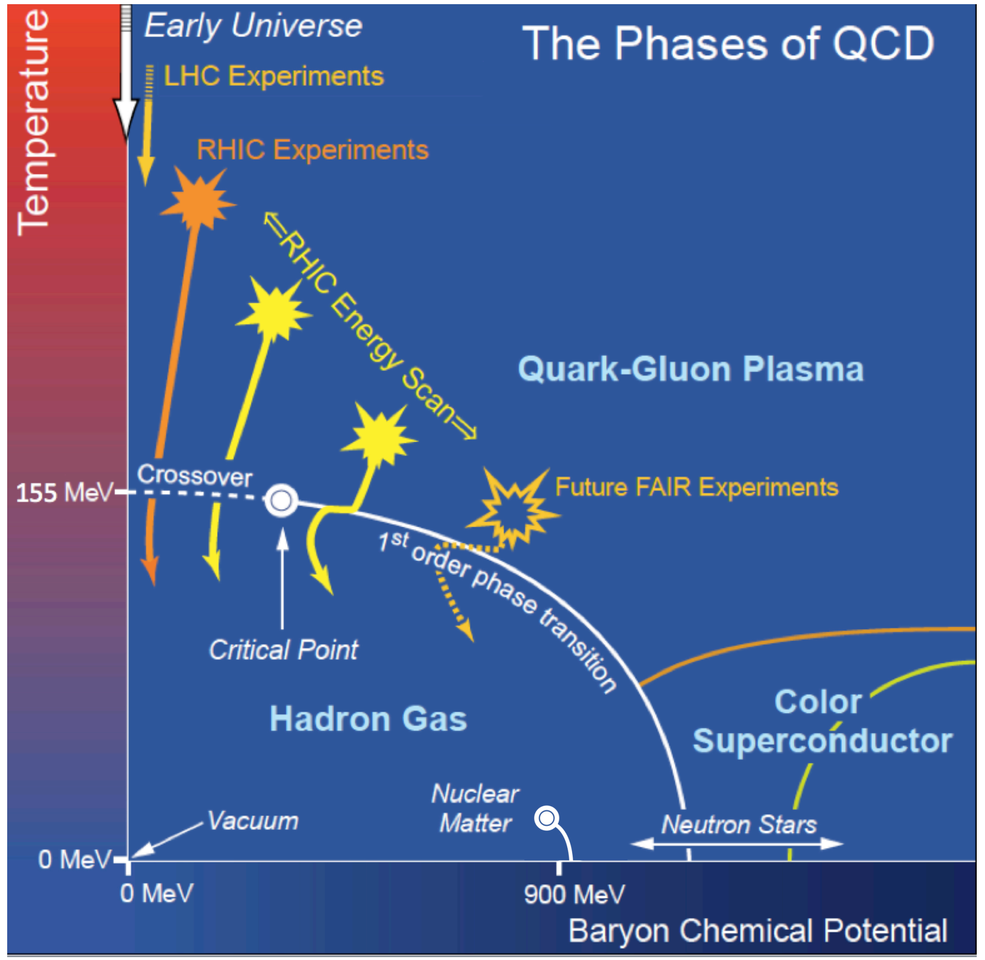

LRP 2007

The EOS of dense nuclear matter in heavy-ion collisions

Models predict a 1st order phase transition
at large μ_B ~ large n_B

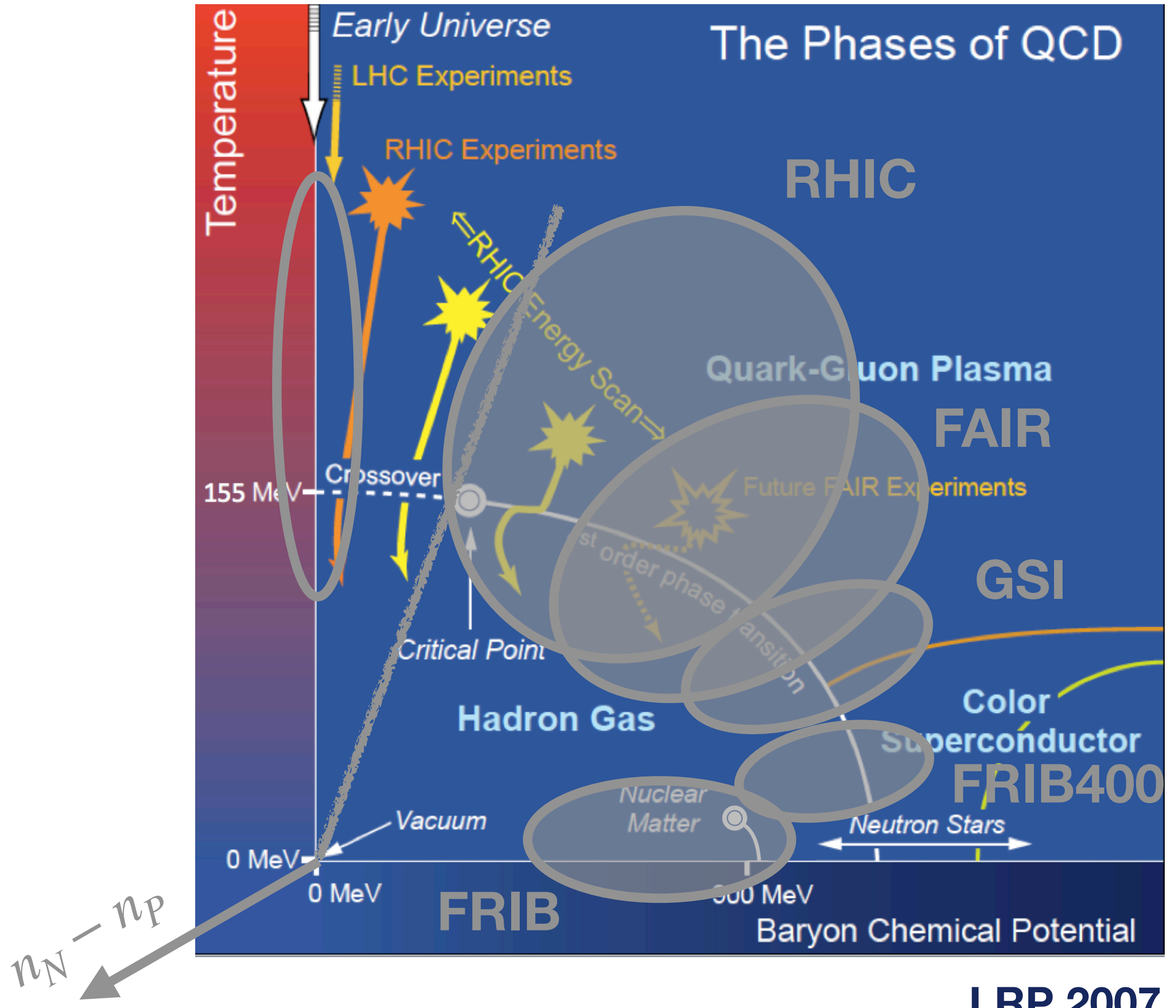

LRP 2007

The EOS of dense nuclear matter in heavy-ion collisions

Relativistic viscous hydrodynamic simulations with LQCD EOS: amazing agreement with data from high-energy collisions

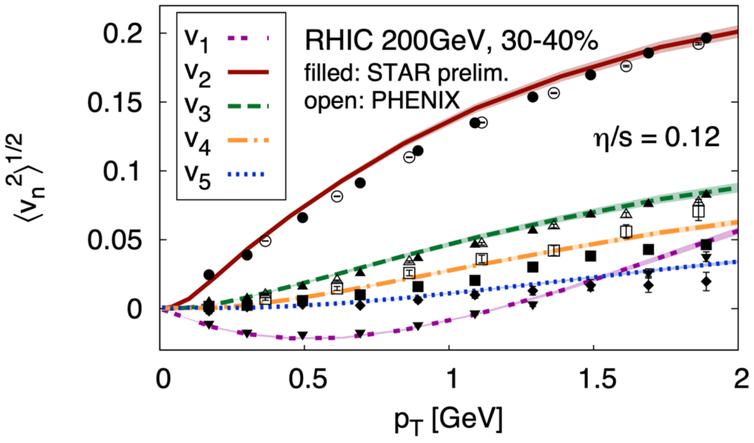

C. Gale, S. Jeon, B. Schenke, P. Tribedy, R. Venugopalan, Phys. Rev. Lett. **110** (2013) 1, 012302, arXiv:1209.6330

systems equilibrate fast* = hydro applies

* and even if they don't, hydrodynamic attractors lead to hydro solutions

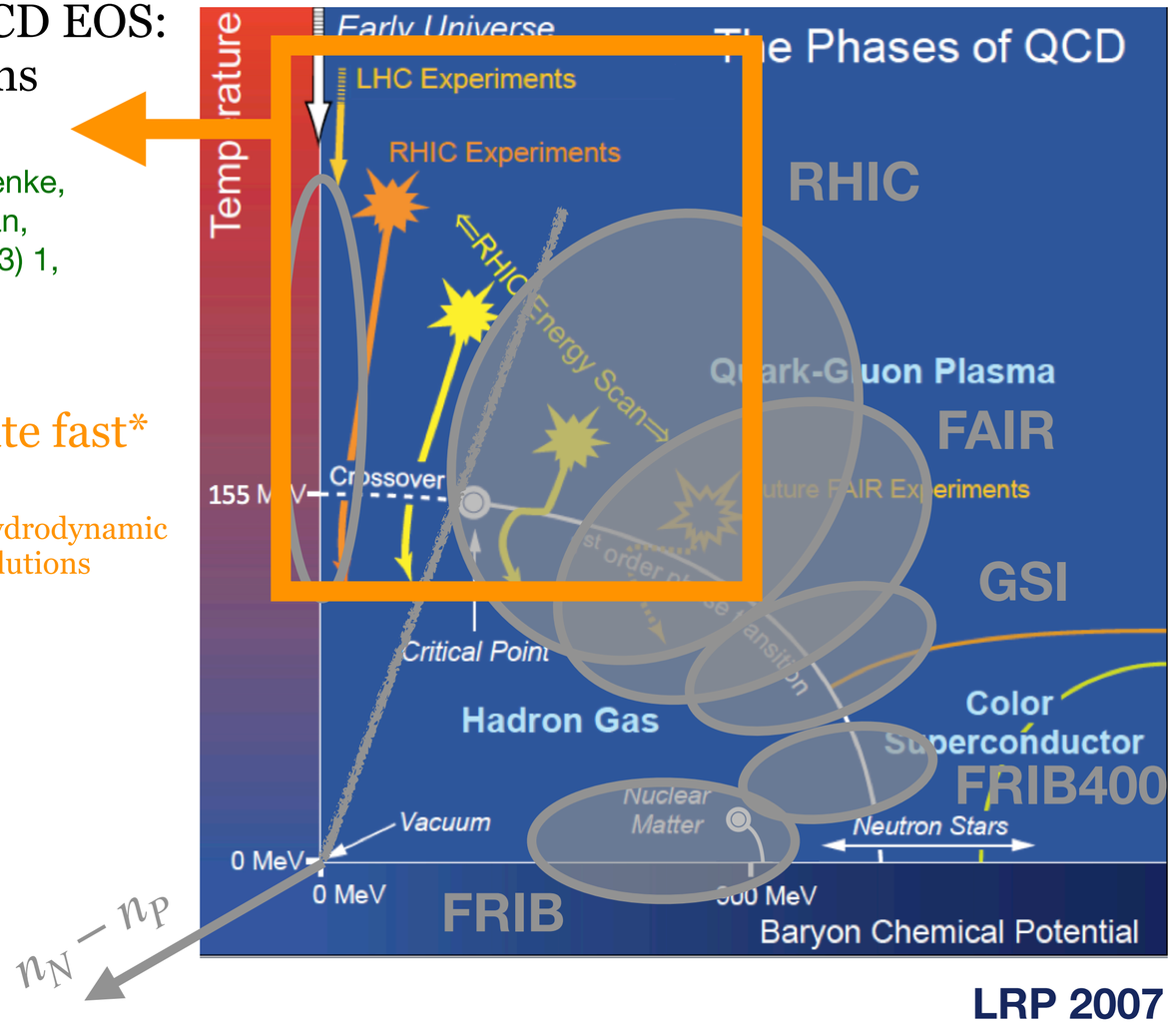

LRP 2007

The EOS of dense nuclear matter in heavy-ion collisions

Relativistic viscous hydrodynamic simulations with LQCD EOS: amazing agreement with data from high-energy collisions

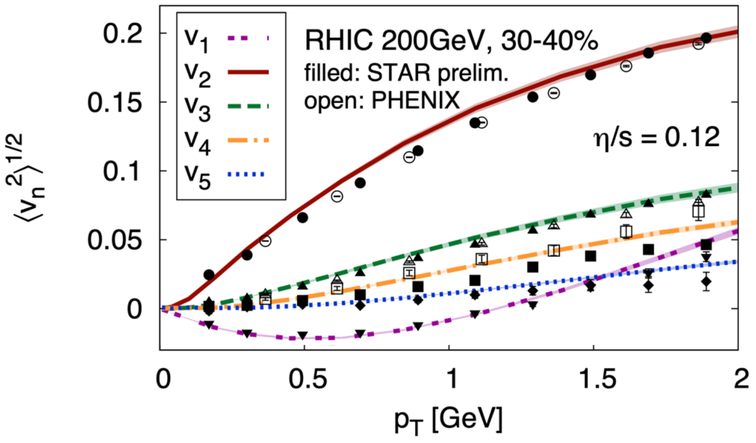

C. Gale, S. Jeon, B. Schenke, P. Tribedy, R. Venugopalan, Phys. Rev. Lett. **110** (2013) 1, 012302, arXiv:1209.6330

systems equilibrate fast* = hydro applies

* and even if they don't, hydrodynamic attractors lead to hydro solutions

Hadronic transport simulations:

systems out of equilibrium = microscopic approach needed

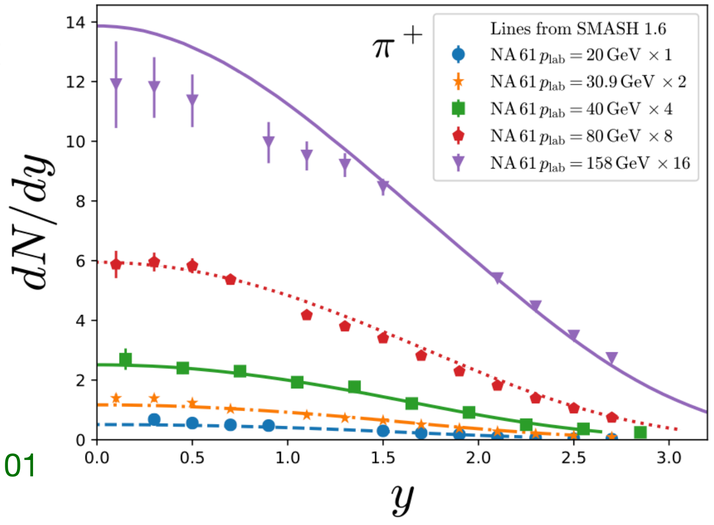

J. Mohs, S. Ryu, H. Elfner, J. Phys. G **47** (2020) 6, 065101 arXiv:1909.05586

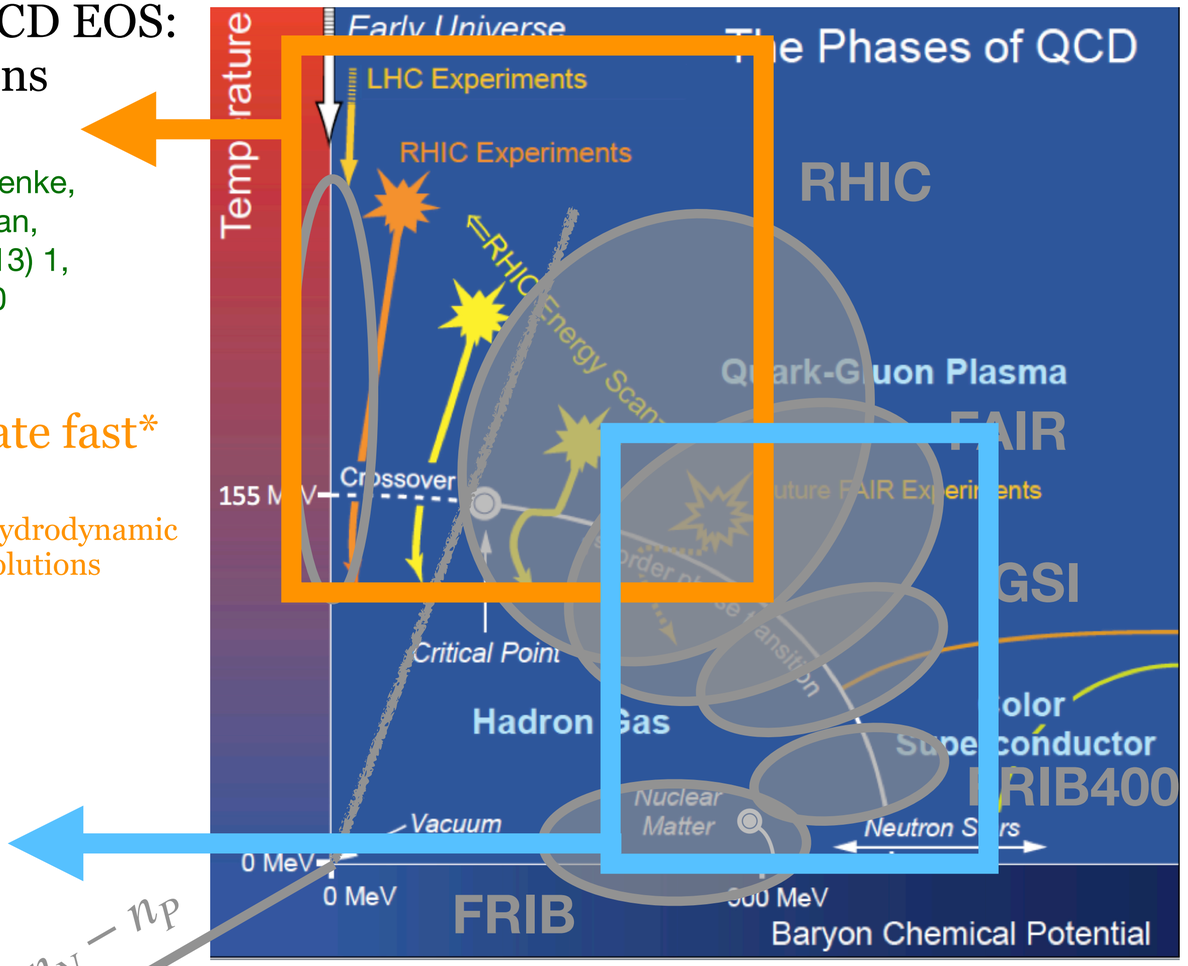

LRP 2007

Stages of a heavy-ion collision: rich physics to explore

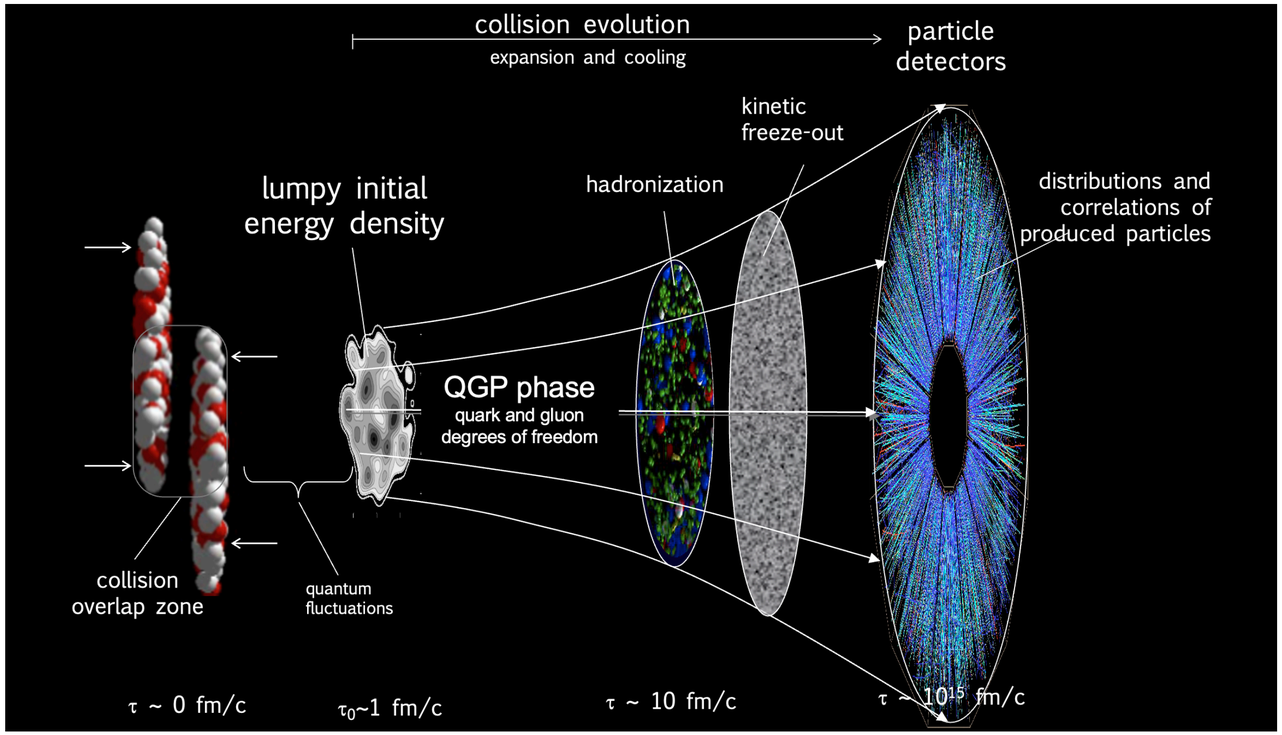

P. Sorensen, Quark-gluon plasma 4, 323–374 (2010) arXiv:0905.0174

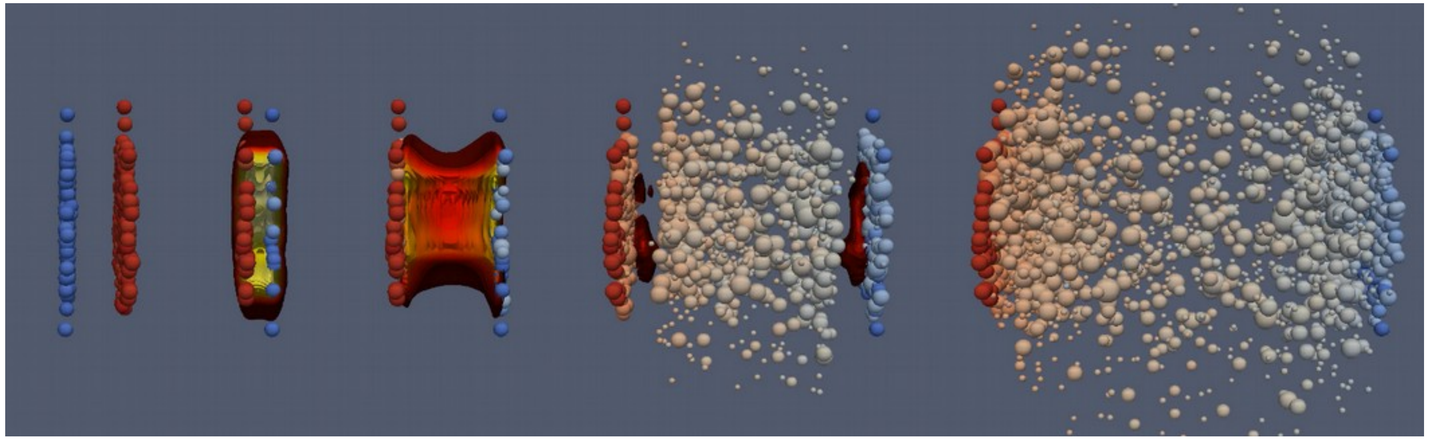

MADAI collaboration, http://madai.us

Stages of a heavy-ion collision: rich physics to explore

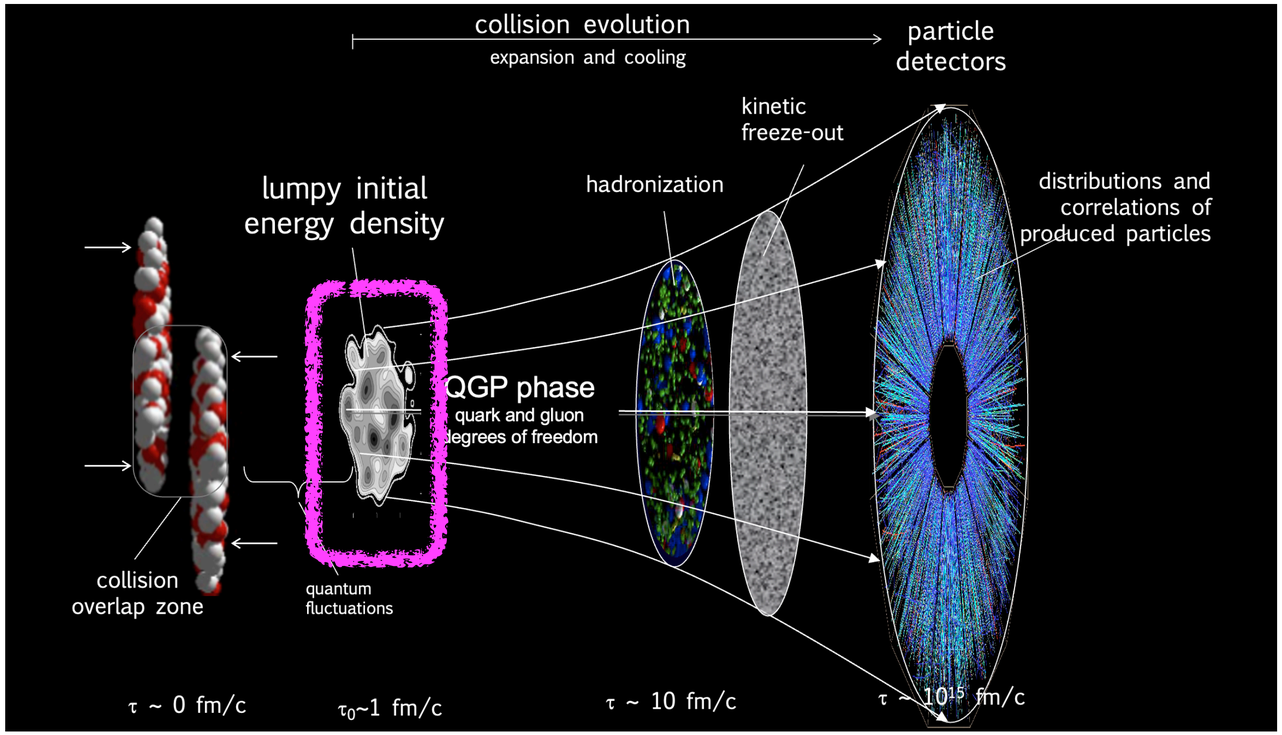

P. Sorensen, Quark-gluon plasma 4, 323–374 (2010) arXiv:0905.0174

impact ~ initial state

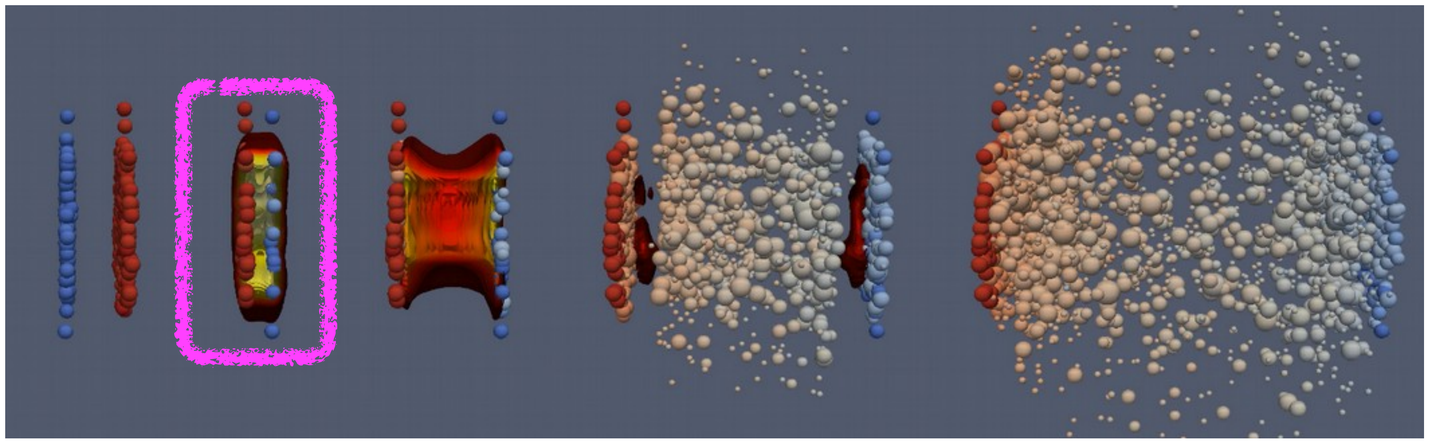

MADAI collaboration, http://madai.us

Stages of a heavy-ion collision: rich physics to explore

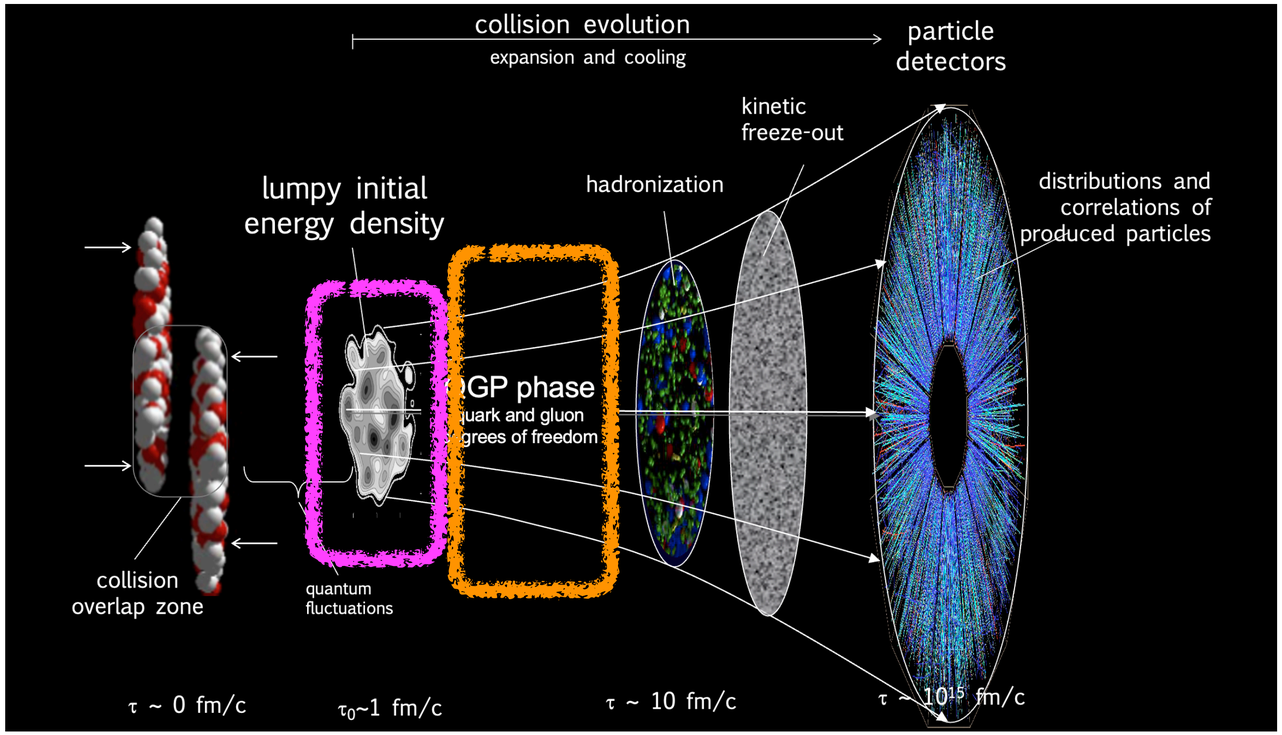

P. Sorensen, Quark-gluon plasma 4, 323–374 (2010) arXiv:0905.0174

impact ~ initial state

expansion

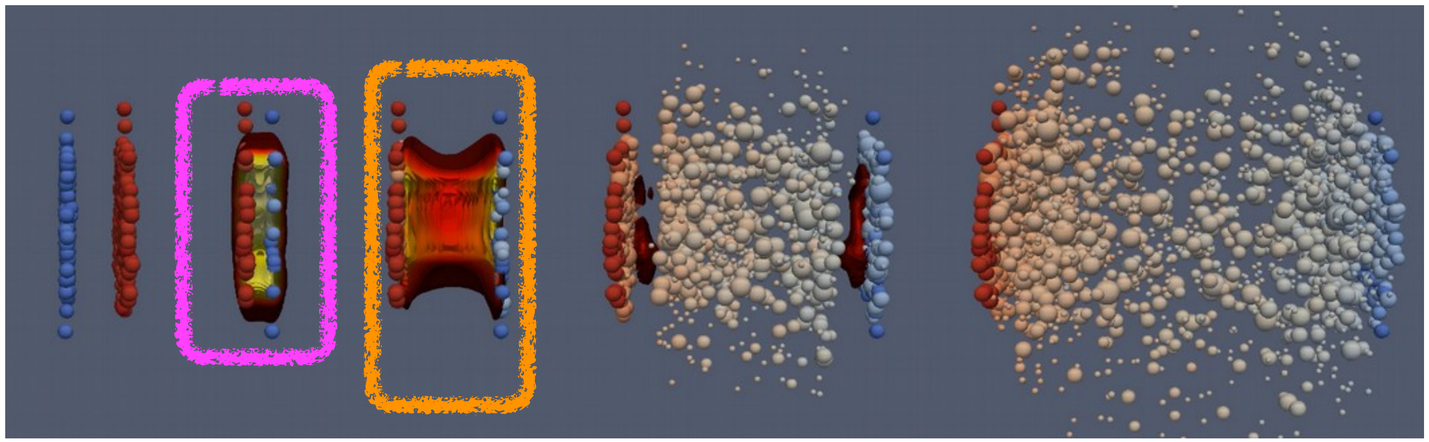

MADAI collaboration, http://madai.us

Stages of a heavy-ion collision: rich physics to explore

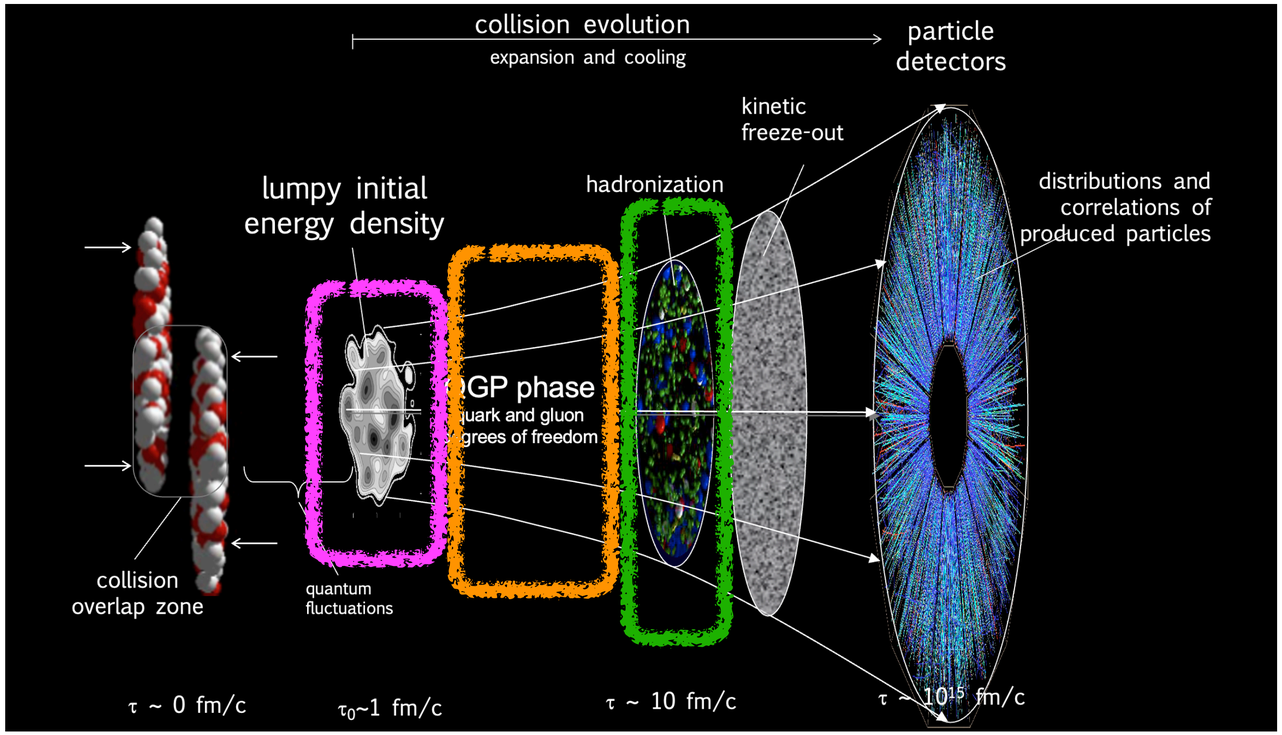

P. Sorensen, Quark-gluon plasma 4, 323–374 (2010) arXiv:0905.0174

impact ~ initial state

expansion

hadronization (if applicable)

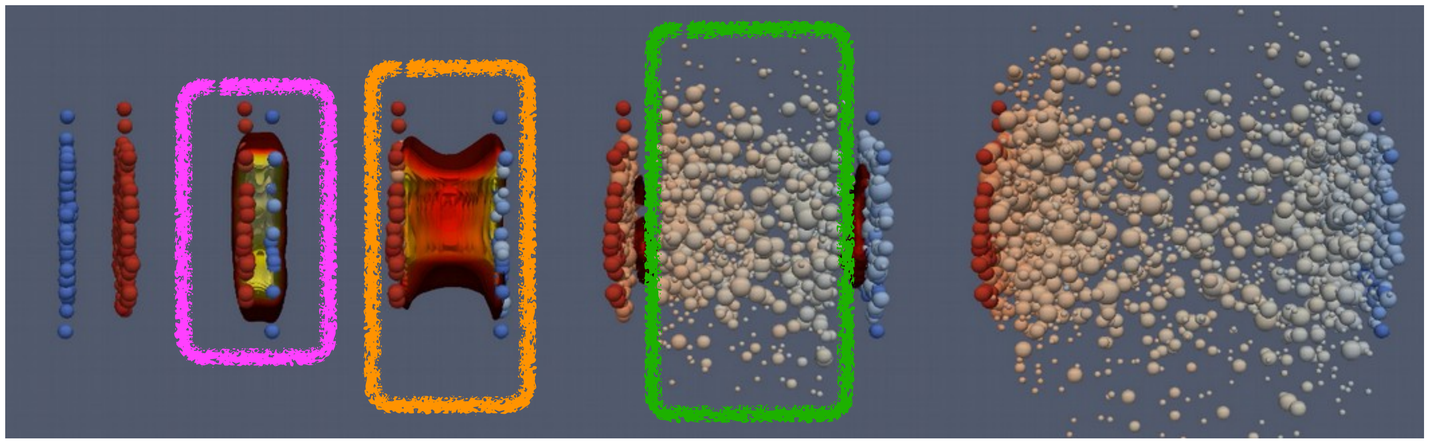

MADAI collaboration, http://madai.us

Stages of a heavy-ion collision: rich physics to explore

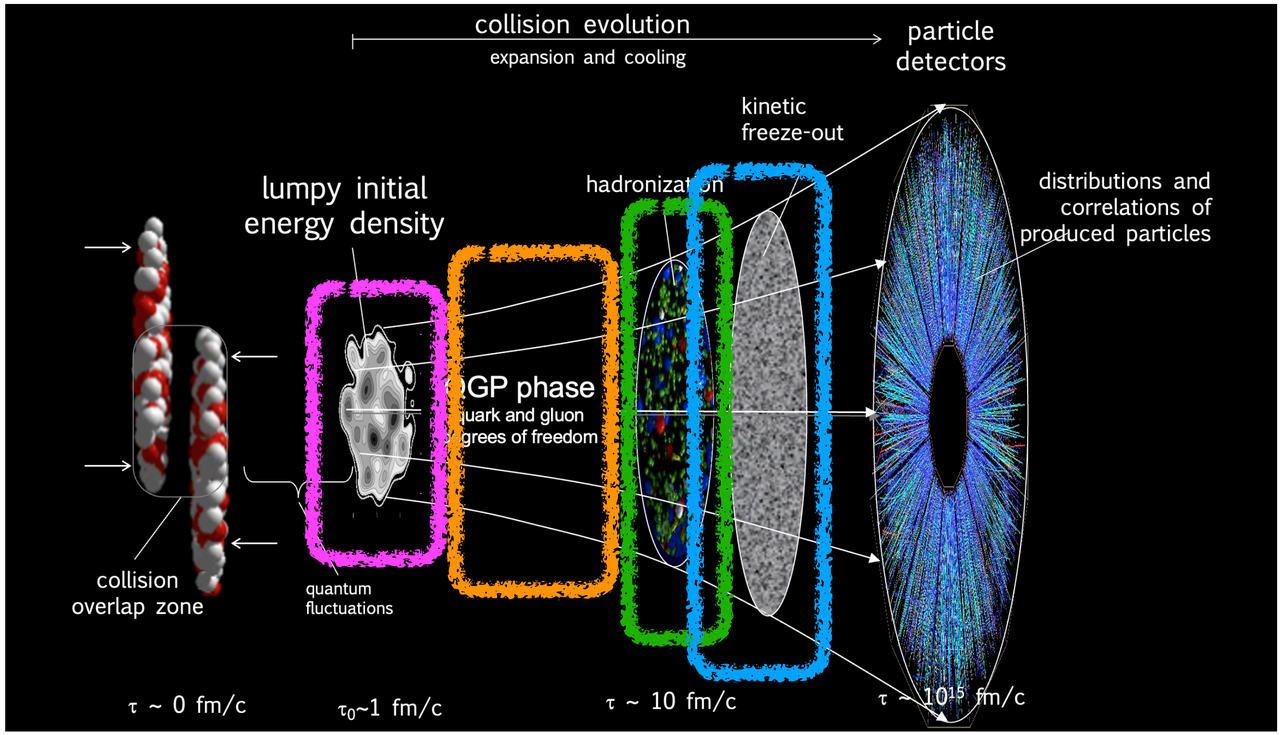

P. Sorensen, Quark-gluon plasma 4, 323–374 (2010) arXiv:0905.0174

impact ~ initial state

expansion

hadronization (if applicable)

hadronic evolution & freeze-out

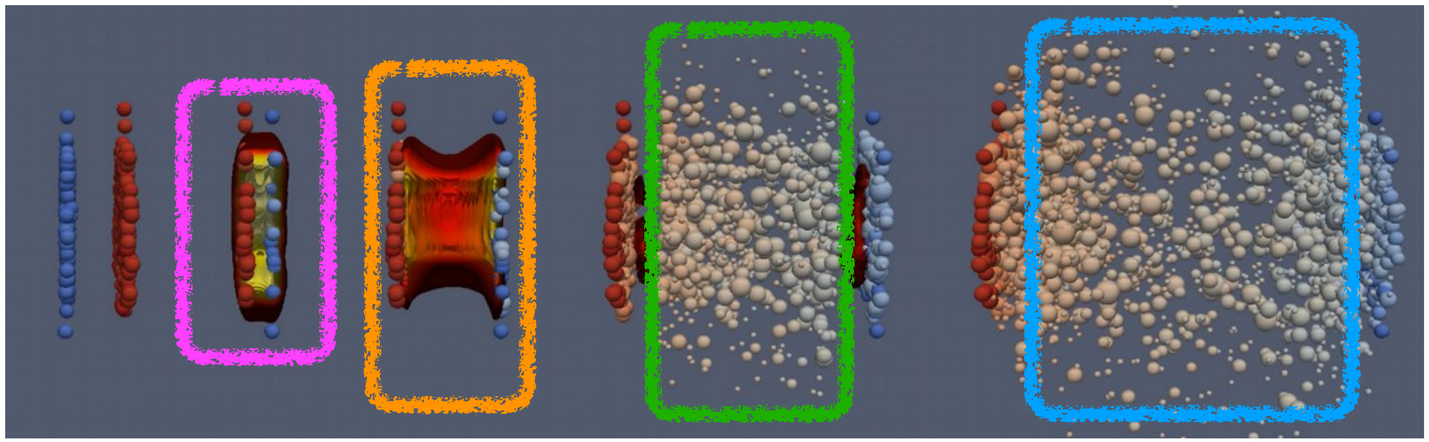

MADAI collaboration, http://madai.us

Stages of a heavy-ion collision: rich physics to explore

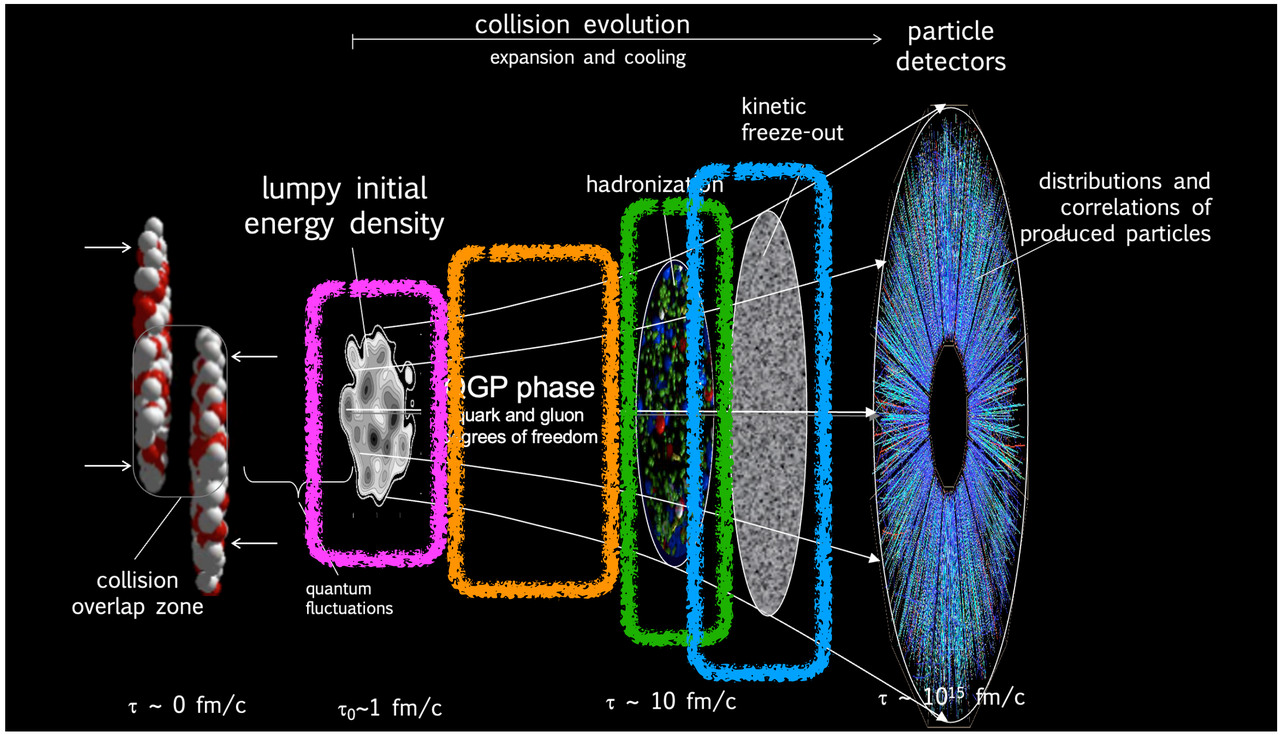

P. Sorensen, Quark-gluon plasma 4, 323–374 (2010) arXiv:0905.0174

impact ~ initial state

collision geometry
collision energy
nuclear structure

expansion

hadronization (if applicable)

hadronic evolution & freeze-out

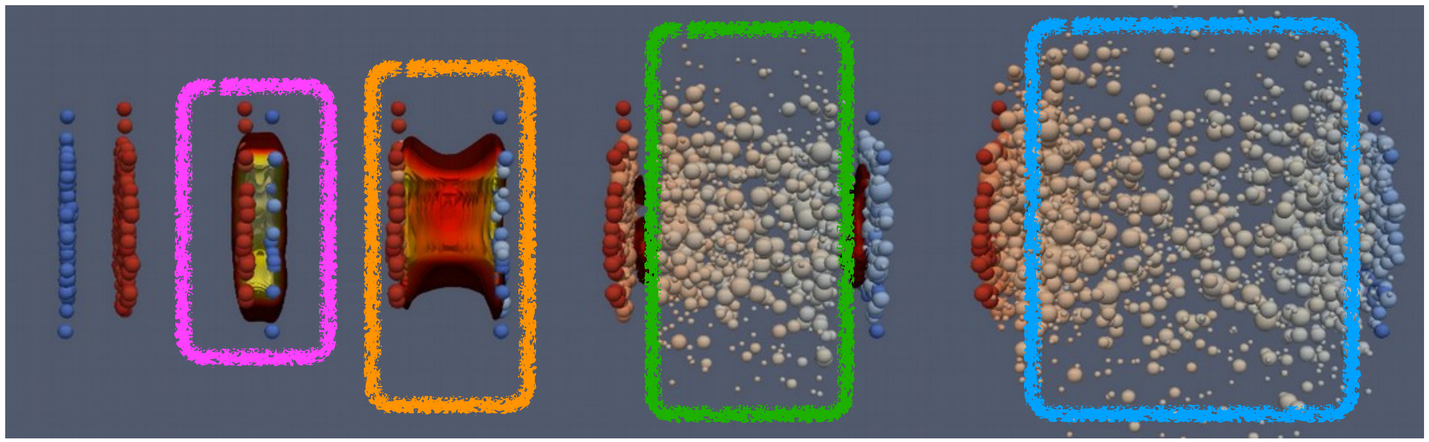

MADAI collaboration, http://madai.us

Stages of a heavy-ion collision: rich physics to explore

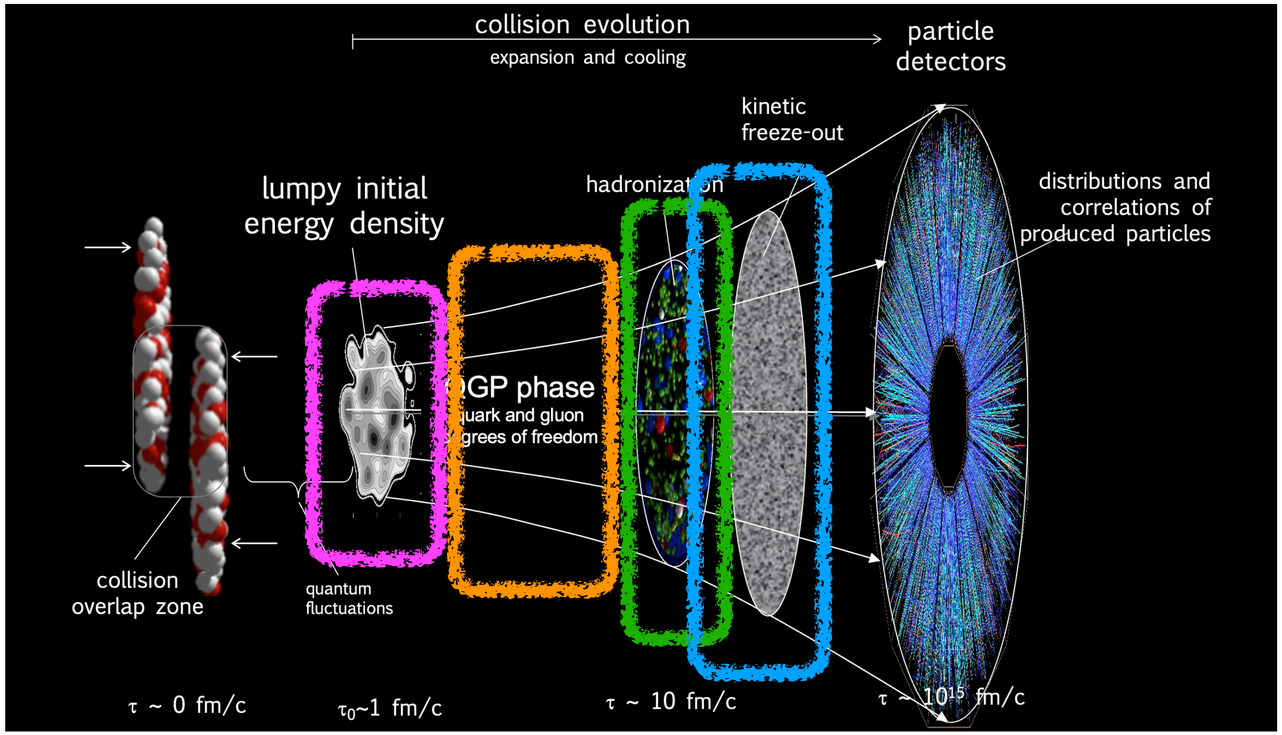

P. Sorensen, Quark-gluon plasma 4, 323–374 (2010) arXiv:0905.0174

impact ~ initial state — collision geometry, collision energy, nuclear structure

expansion — high energy: hydrodynamics (driven by the EOS & transport coefficients); low energy: transport (driven by the EOS & scatterings)

hadronization (if applicable)

hadronic evolution & freeze-out

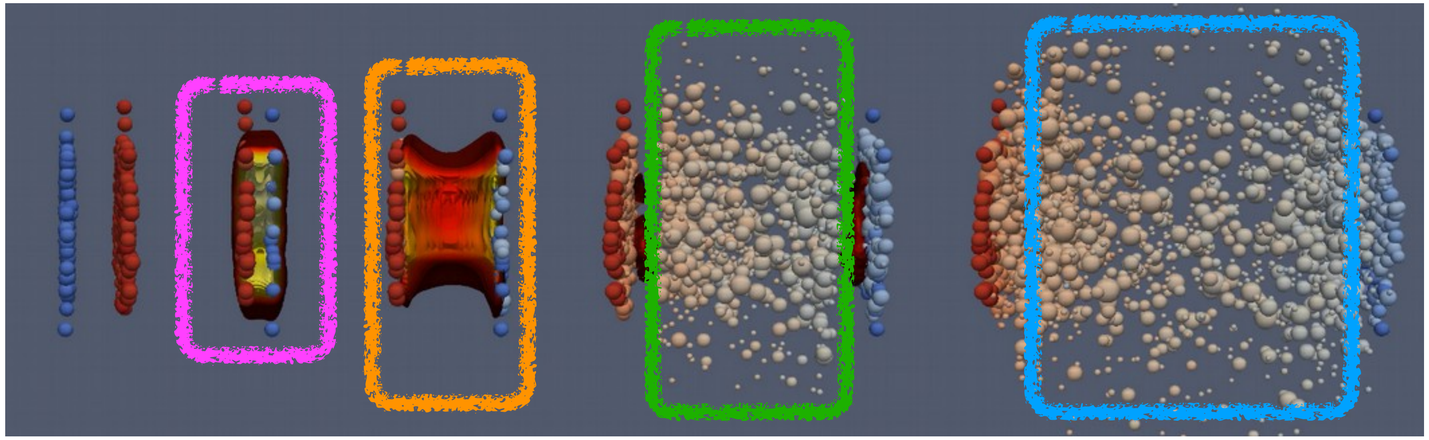

MADAI collaboration, http://madai.us

Stages of a heavy-ion collision: rich physics to explore

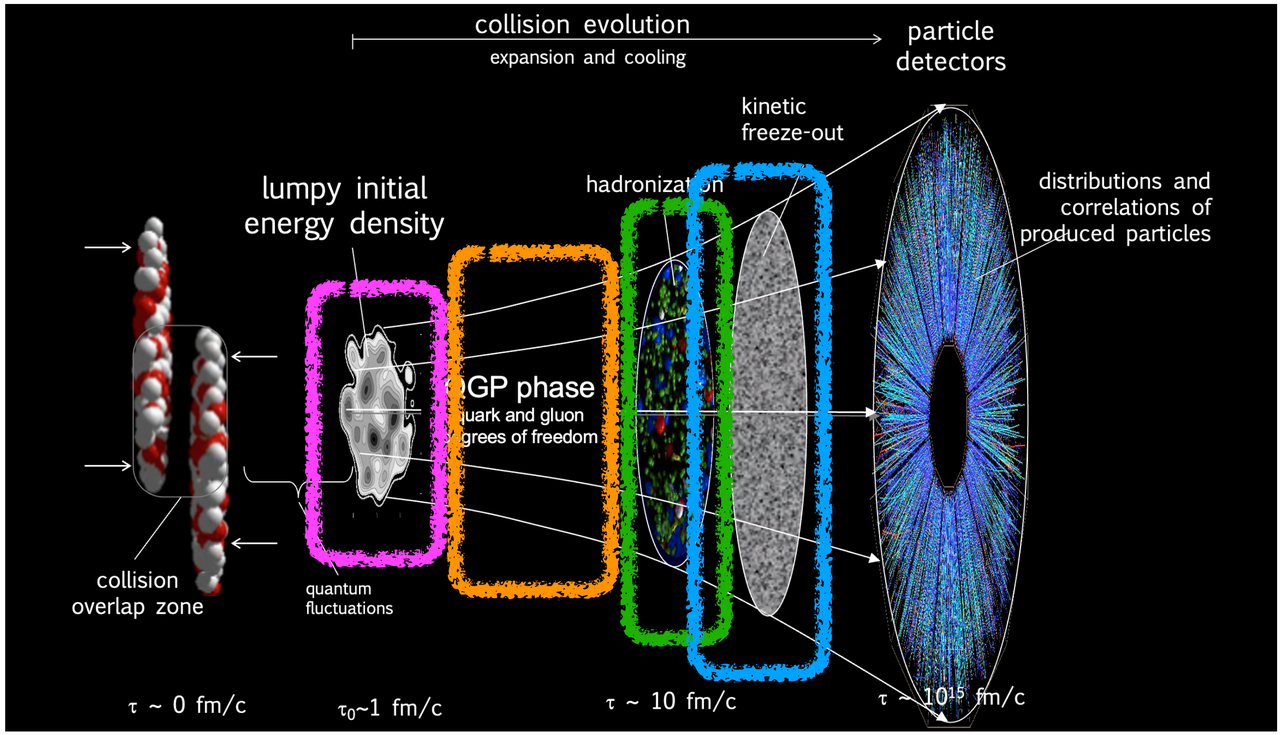

P. Sorensen, Quark-gluon plasma 4, 323–374 (2010) arXiv:0905.0174

impact ~ initial state — collision geometry, collision energy, nuclear structure

expansion — high energy: hydrodynamics (driven by the EOS & transport coefficients); low energy: transport (driven by the EOS & scatterings)

hadronization (if applicable) — loss of information?

hadronic evolution & freeze-out

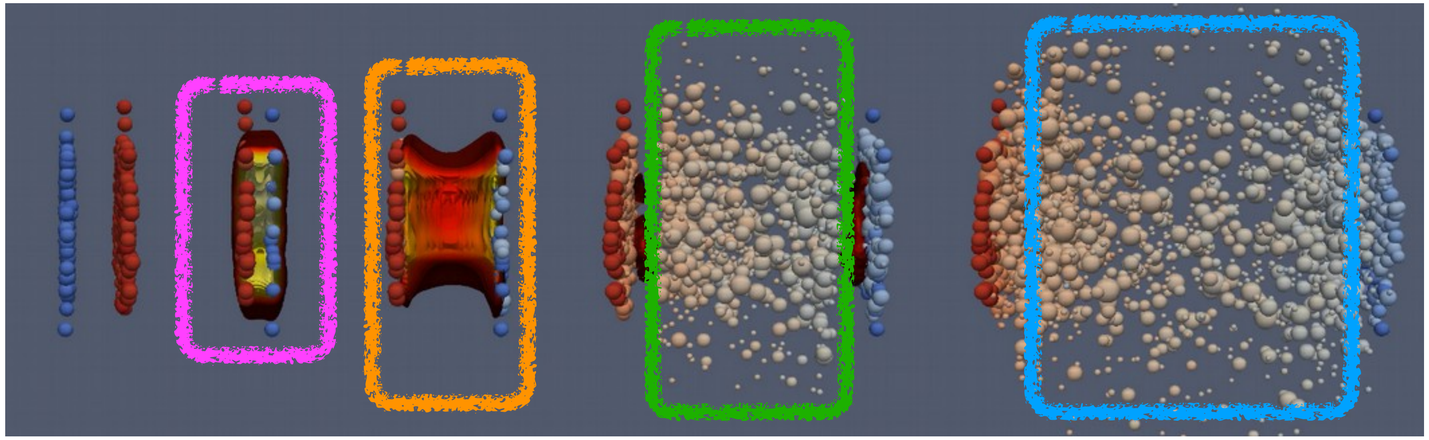

MADAI collaboration, http://madai.us

Stages of a heavy-ion collision: rich physics to explore

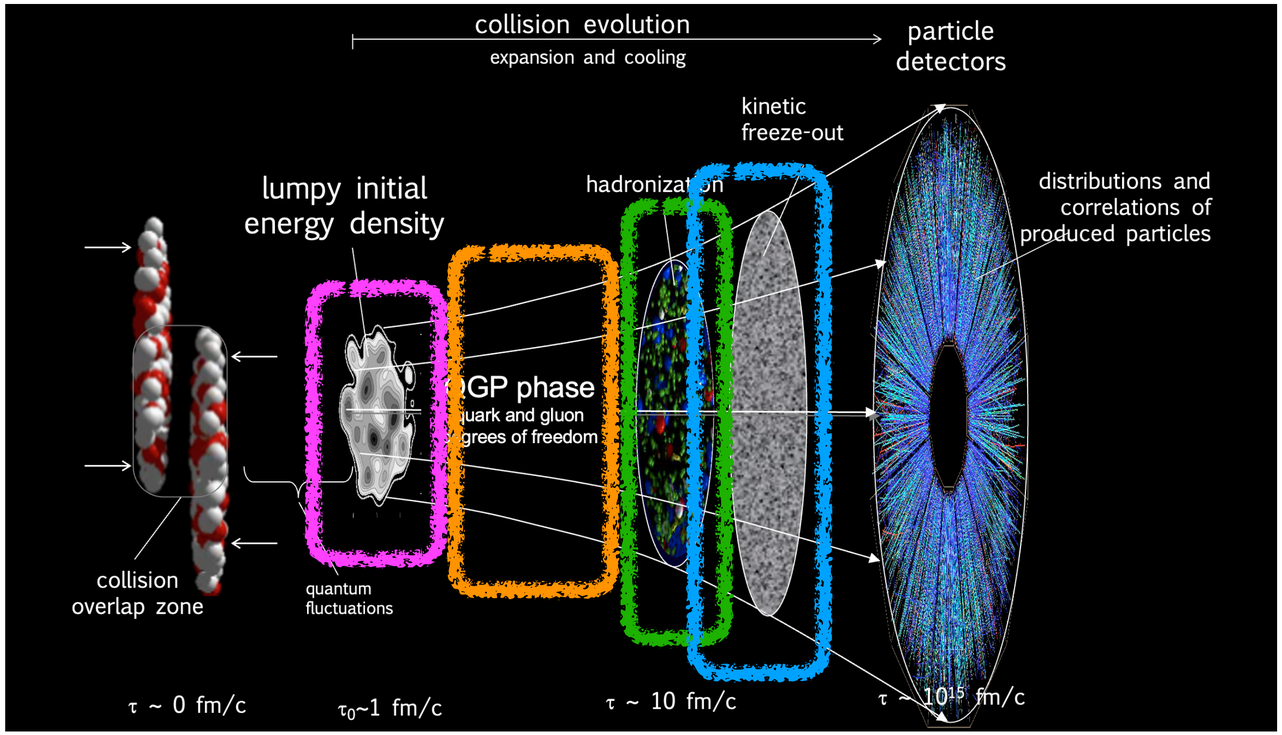

P. Sorensen, Quark-gluon plasma 4, 323–374 (2010) arXiv:0905.0174

impact ~ initial state — collision geometry, collision energy, nuclear structure

expansion — high energy: hydrodynamics (driven by the EOS & transport coefficients); low energy: transport (driven by the EOS & scatterings)

hadronization (if applicable) — loss of information?

hadronic evolution & freeze-out — essential to reproduce spectra

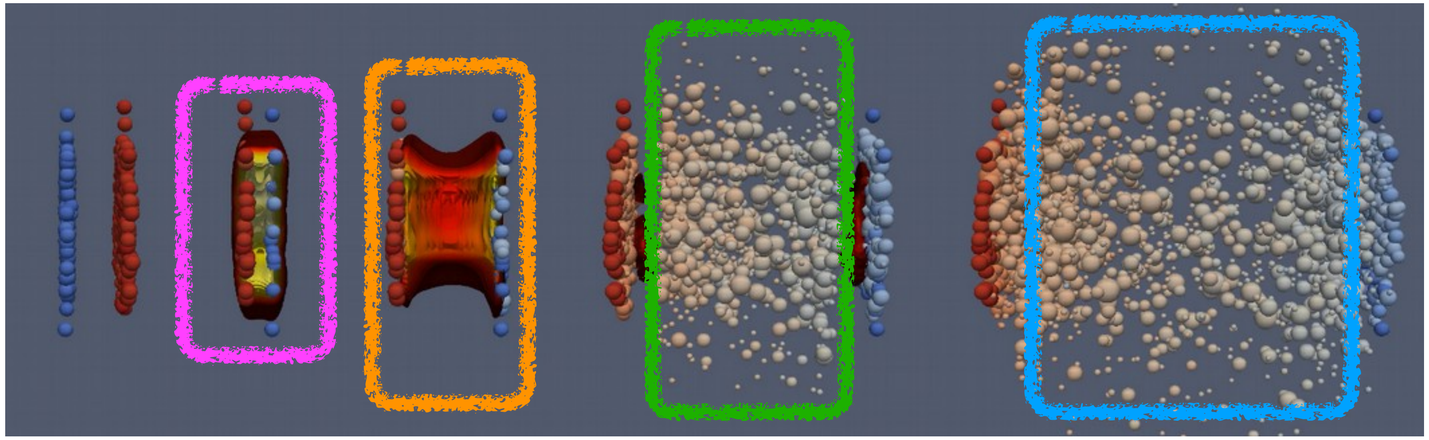

MADAI collaboration, http://madai.us

Stages of a heavy-ion collision: rich physics to explore

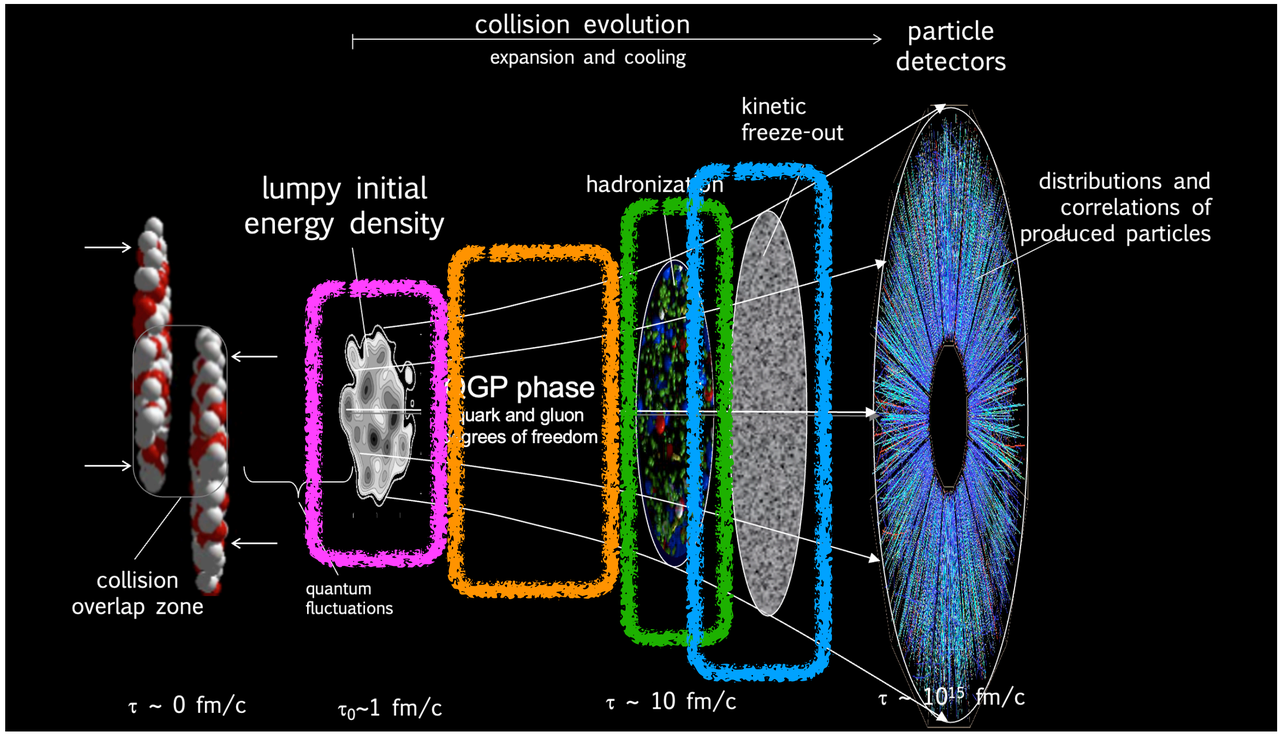

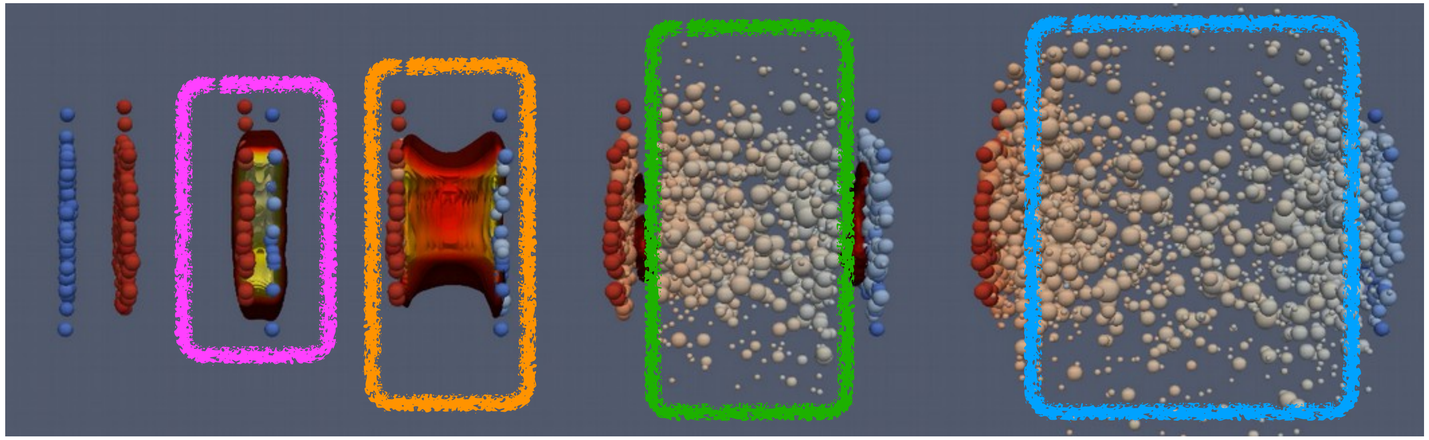

P. Sorensen, Quark-gluon plasma 4, 323–374 (2010) arXiv:0905.0174

impact ~ initial state — collision geometry, collision energy, nuclear structure

expansion — high energy: hydrodynamics (driven by the EOS & transport coefficients); low energy: transport (driven by the EOS & scatterings)

hadronization (if applicable) — loss of information?

hadronic evolution & freeze-out — essential to reproduce spectra

Comparisons to dynamical simulations essential for interpreting measurements

MADAI collaboration, http://madai.us

VDF model: relativistic potentials with two 1st order phase transitions

A. Sorensen, V. Koch, Phys. Rev. C **104** (2021) 3, 034904, arXiv:2011.06635

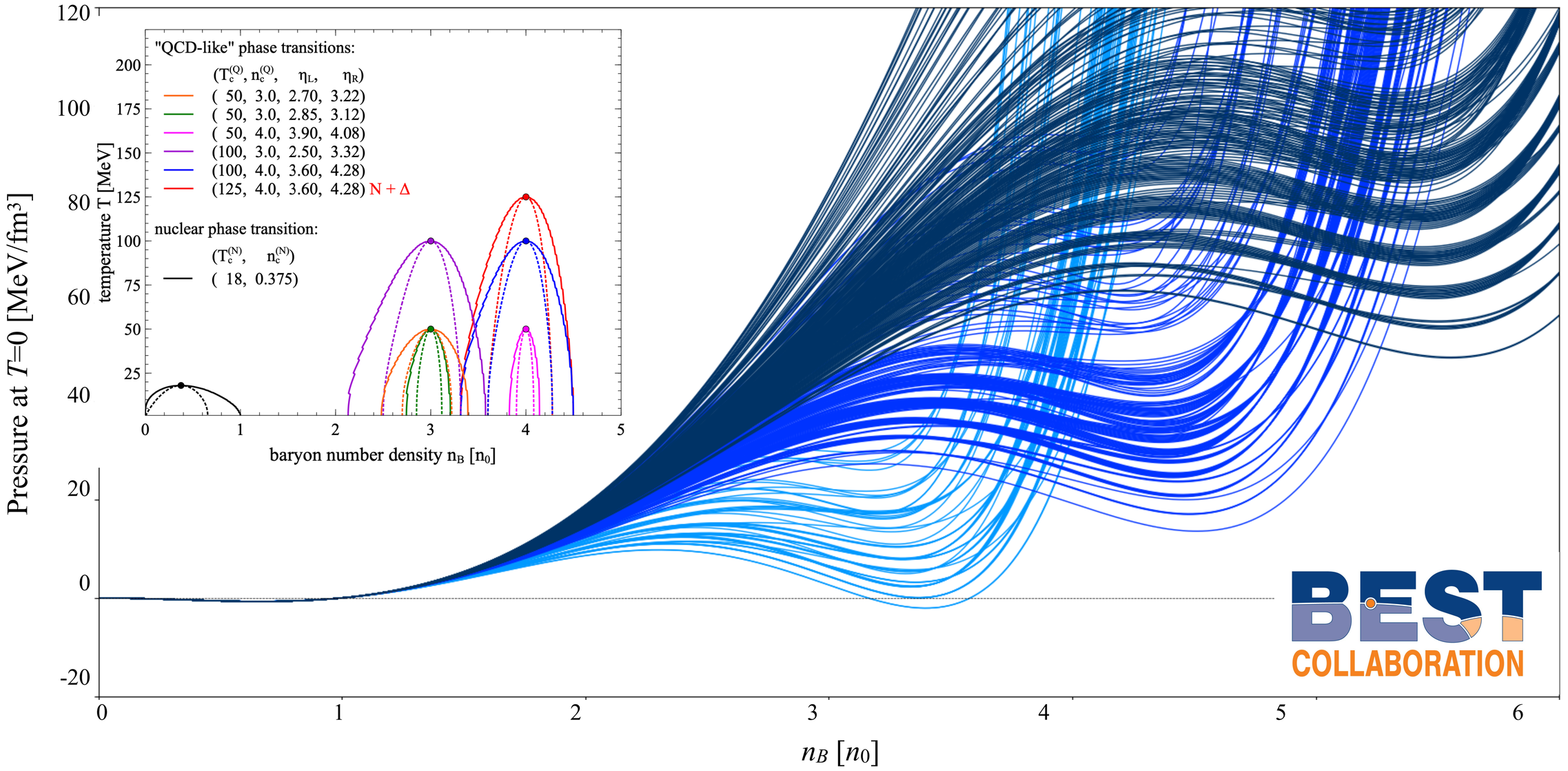

VDF model: relativistic potentials with two 1st order phase transitions

A. Sorensen, V. Koch, Phys. Rev. C **104** (2021) 3, 034904, arXiv:2011.06635

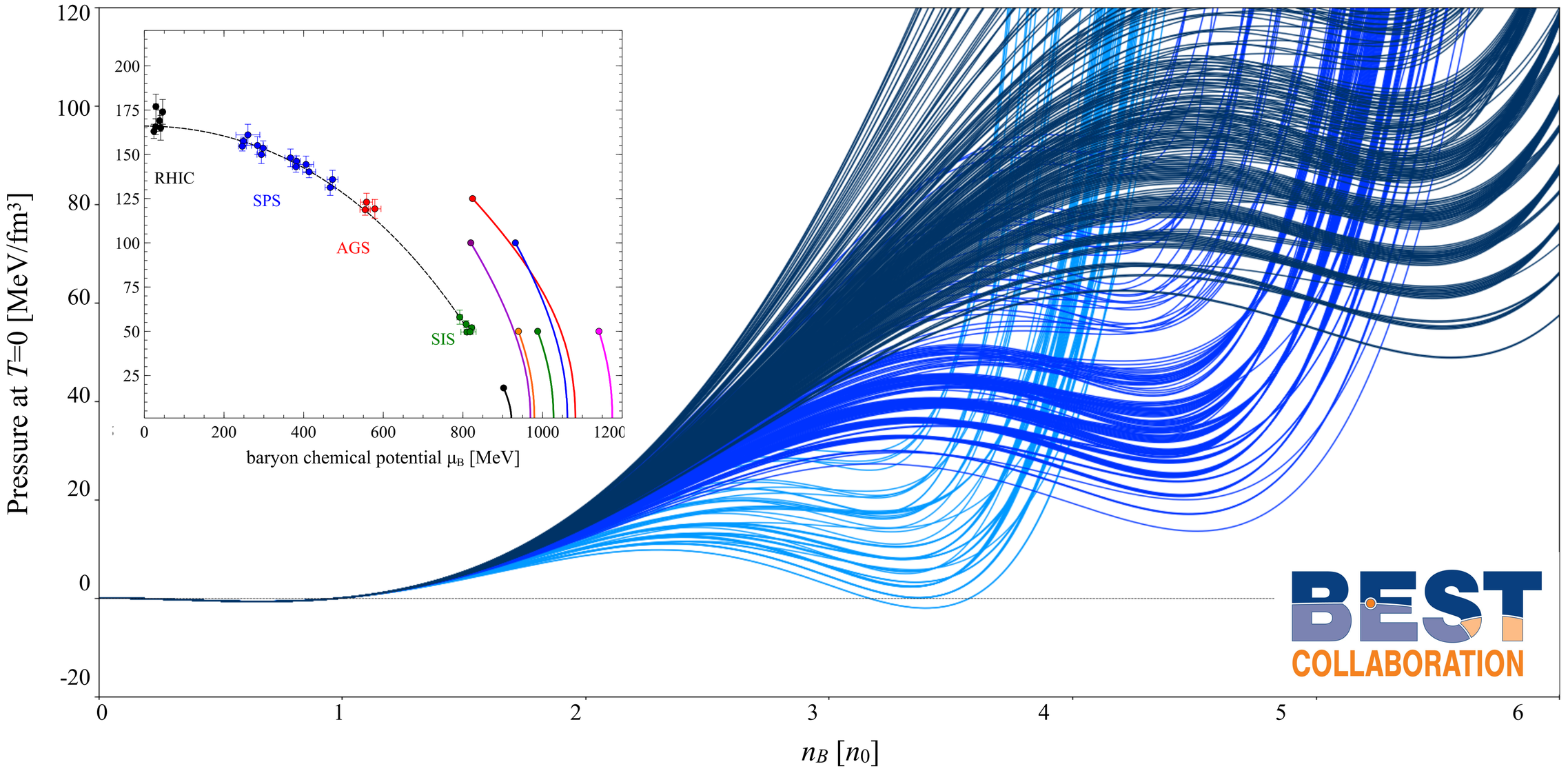

VDF model: relativistic potentials with two 1st order phase transitions

A. Sorensen, V. Koch, Phys. Rev. C **104** (2021) 3, 034904, arXiv:2011.06635

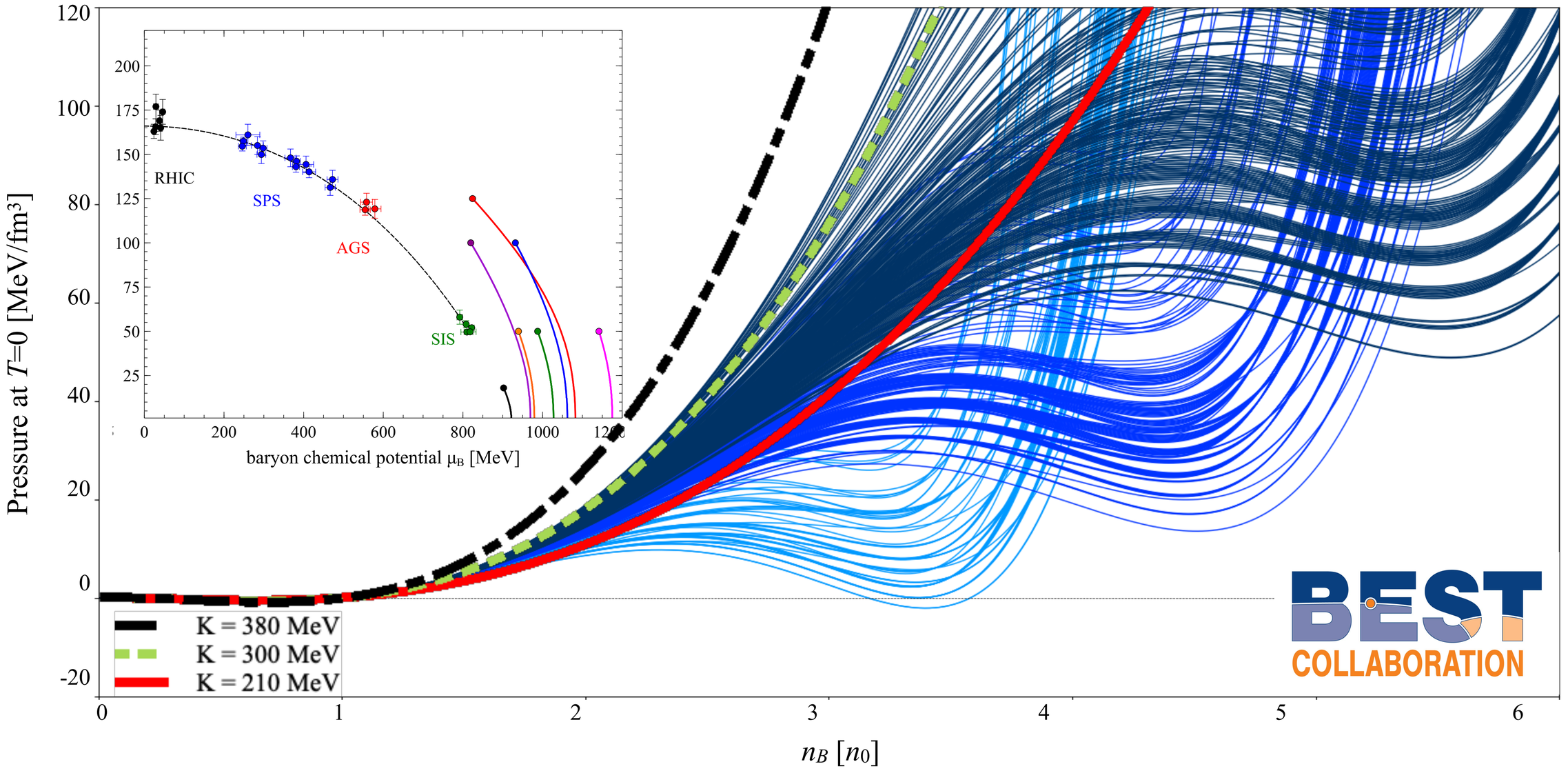

VDF model: relativistic potentials with two 1st order phase transitions

A. Sorensen, V. Koch, Phys. Rev. C **104** (2021) 3, 034904, arXiv:2011.06635

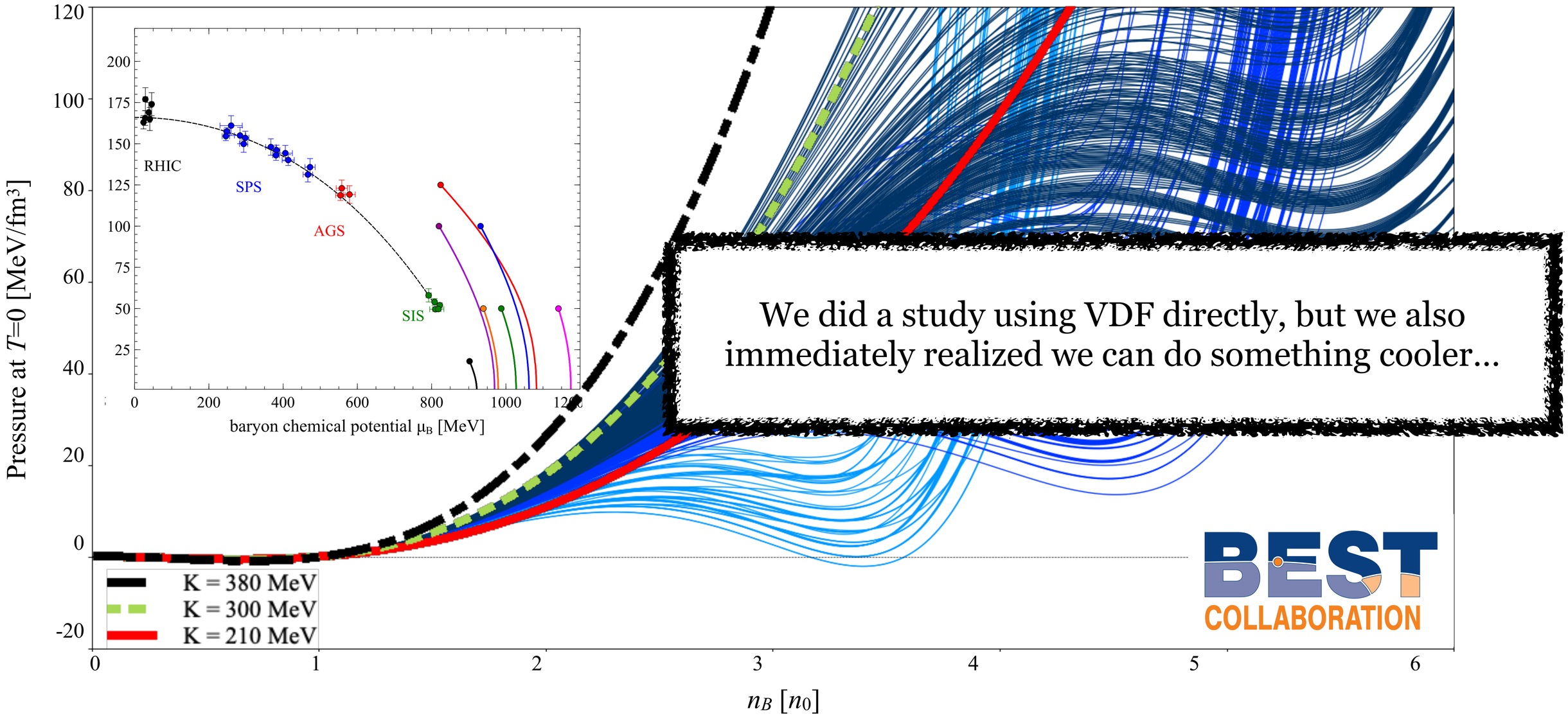

We did a study using VDF directly, but we also immediately realized we can do something cooler...

BEST COLLABORATION

Part 1.5: Recent developments for BES-I energies

Lattice QCD EOS at finite μ_B

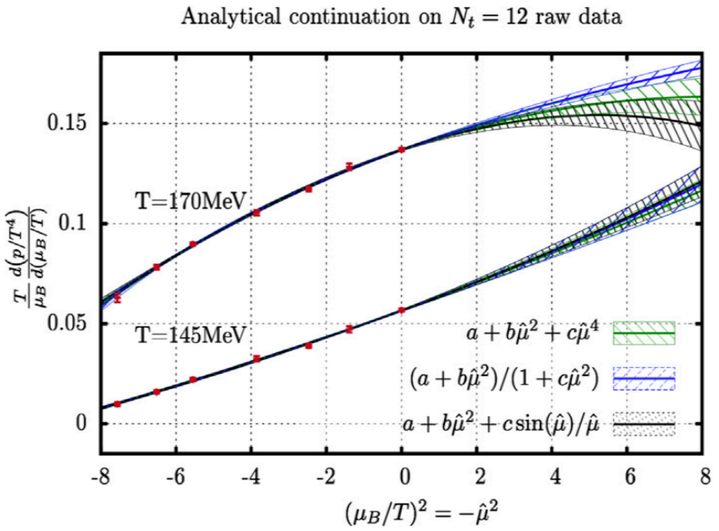

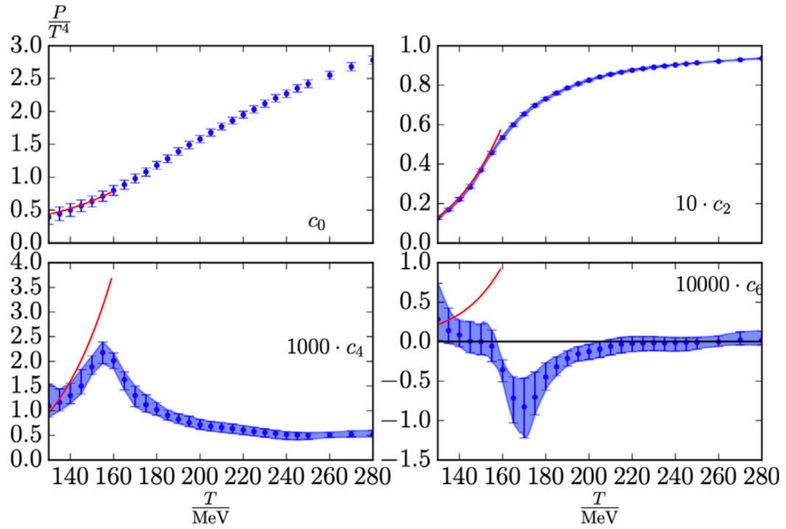

J.N. Guenther *et al.*, Nuclear Phys. A 967 (2017) 720–723 arXiv:1607.02493

Lattice QCD EOS at finite μ_B

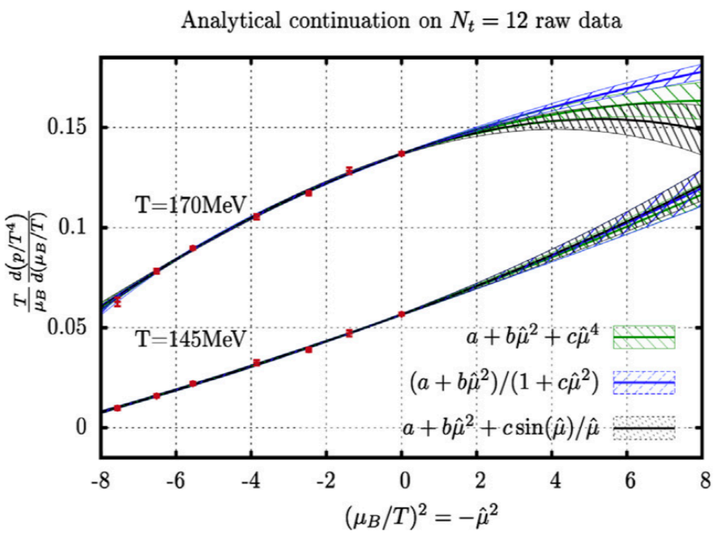

S. Borsányi *et al.*, Phys. Rev. Lett. 126 (23) (2021) 232001, arXiv:2102.06660

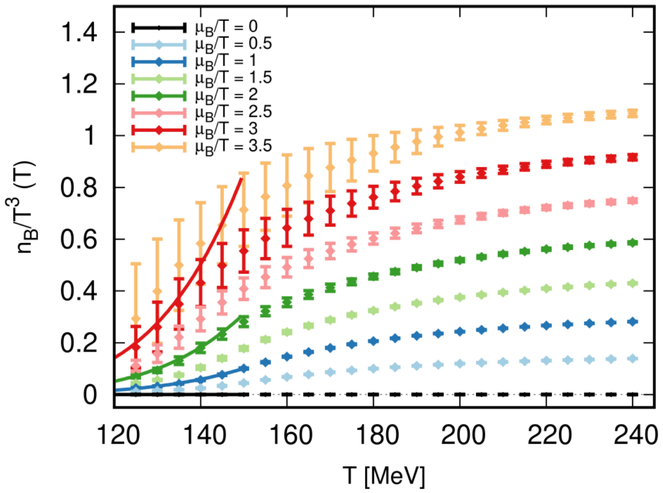

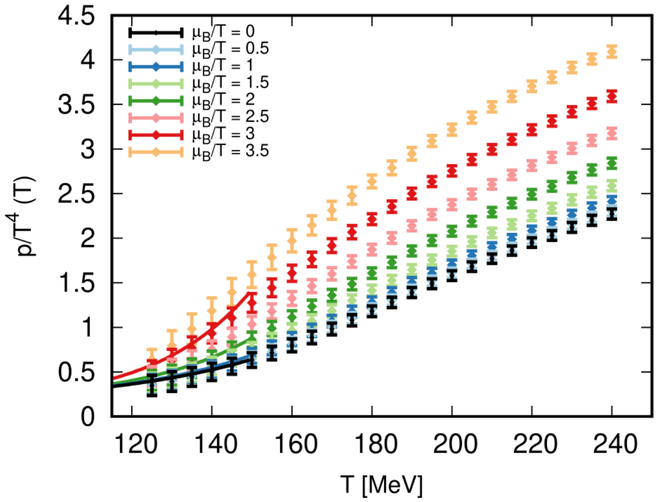

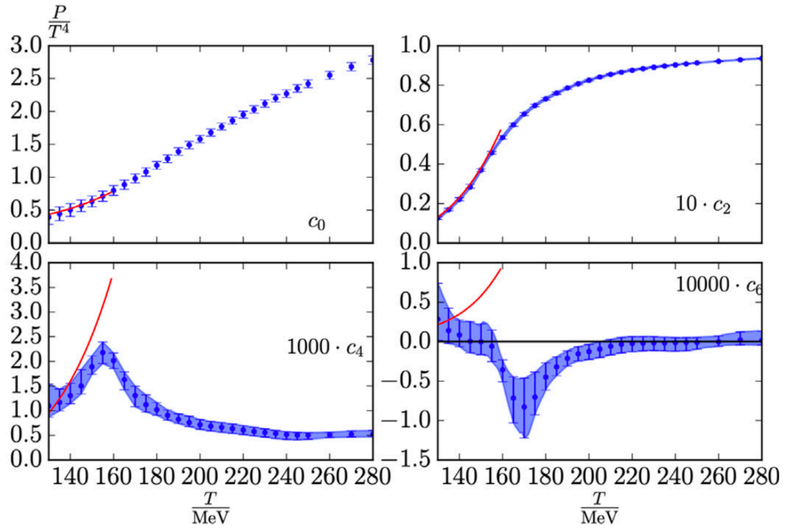

J.N. Guenther *et al.*, Nuclear Phys. A 967 (2017) 720–723 arXiv:1607.02493

Lattice QCD EOS at finite μ_B

S. Borsányi *et al.*, Phys. Rev. Lett. 126 (23) (2021) 232001, arXiv:2102.06660

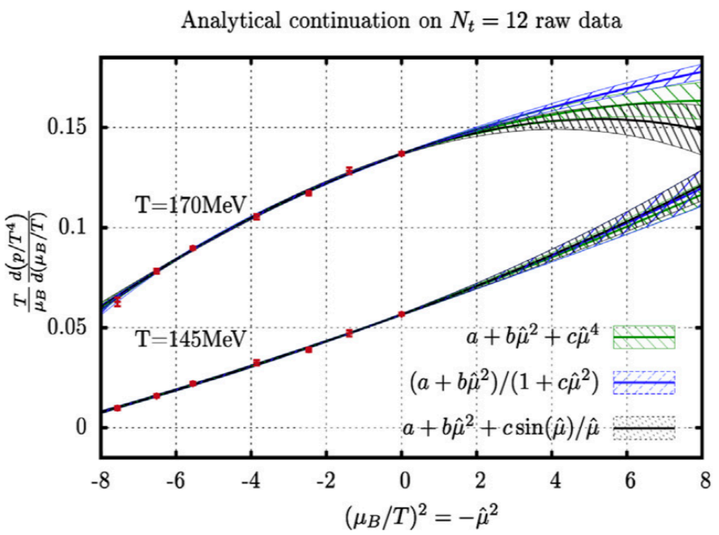

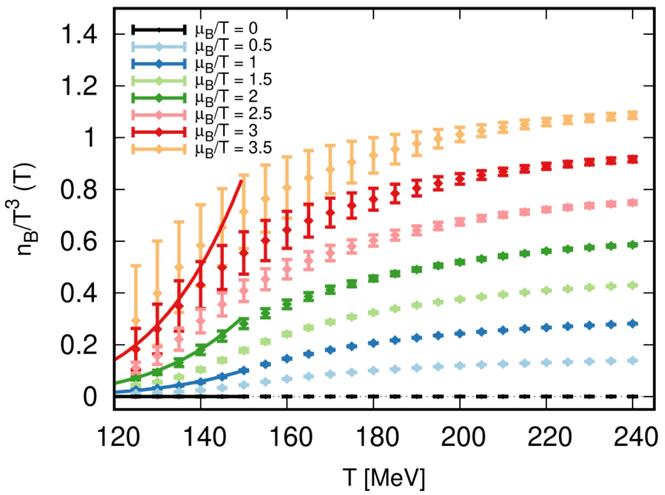

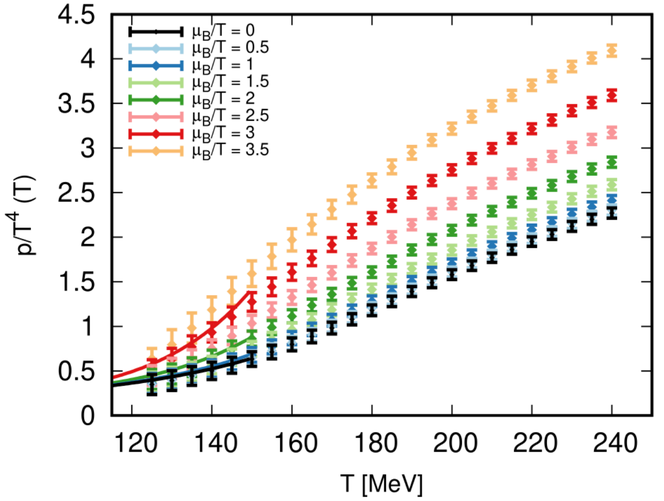

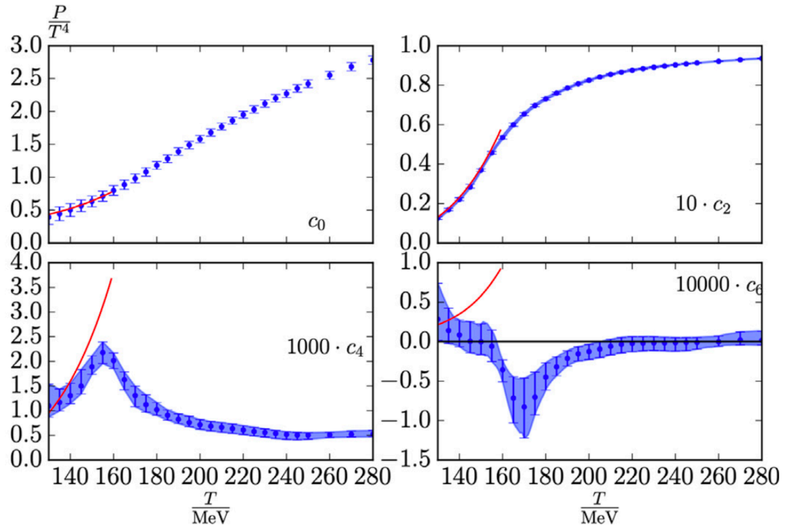

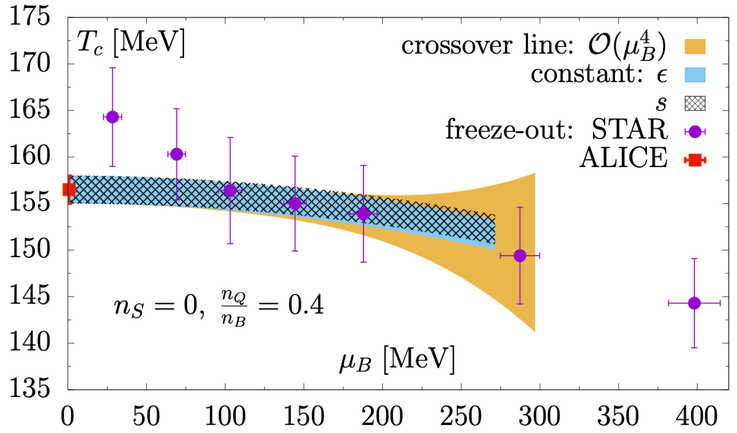

A. Bazavov *et al.* (HotQCD)
Phys. Lett. B **795**, 15 (2019), arXiv:1812.08235

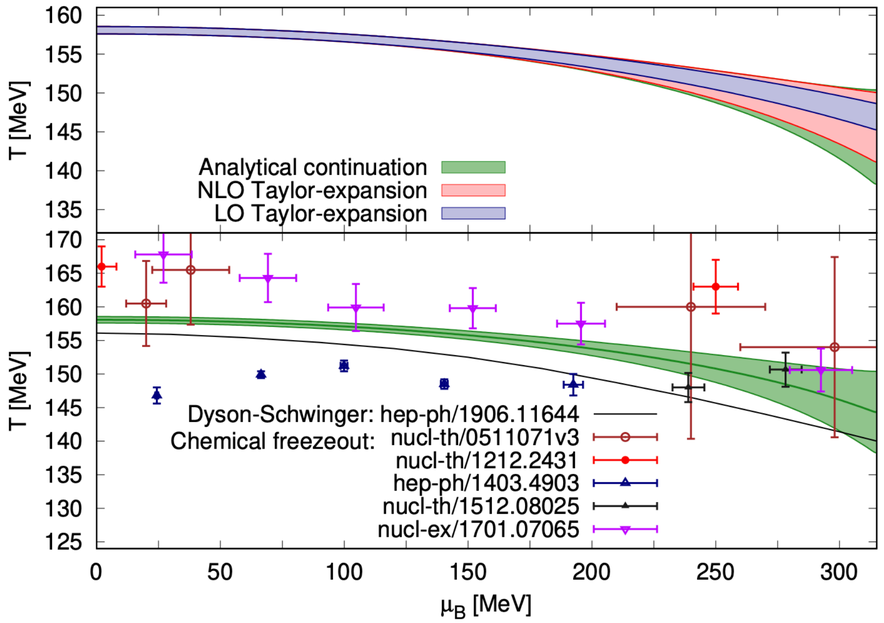

J.N. Guenther *et al.*, Nuclear Phys. A 967 (2017) 720–723 arXiv:1607.02493

S. Borsányi *et al.*, Phys. Rev. Lett. **125**, 052001 (2020), arXiv:2002.02821

Input to hydrodynamics: EOS with 3D-Ising model critical point

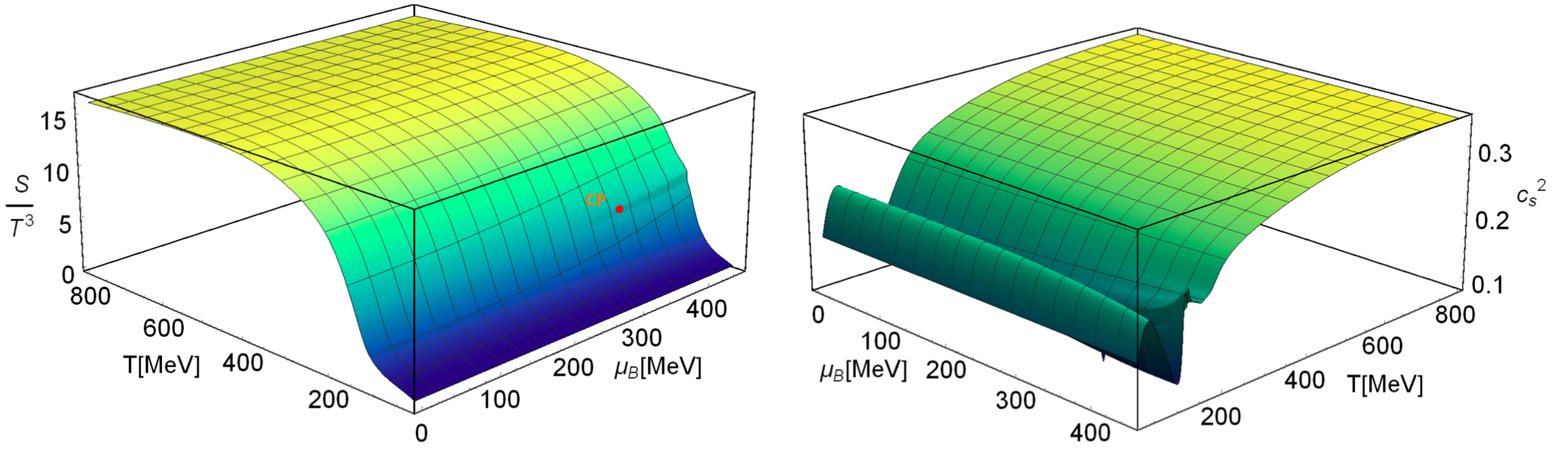

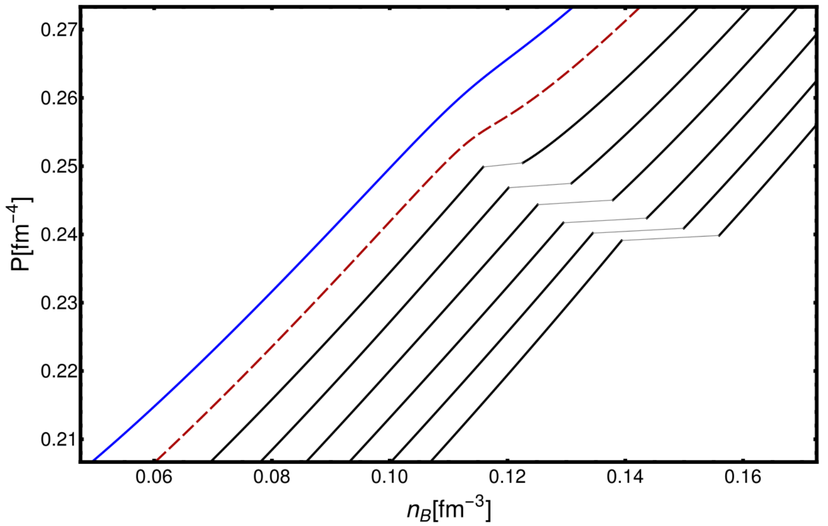

P. Parotto *et al.*, Phys. Rev. C 101, 034901 (2020), arXiv:1805.05249

Input to hydrodynamics: EOS with 3D-Ising model critical point

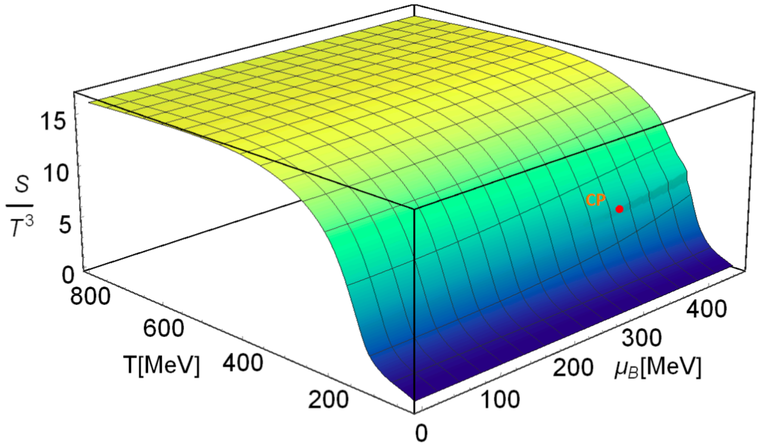

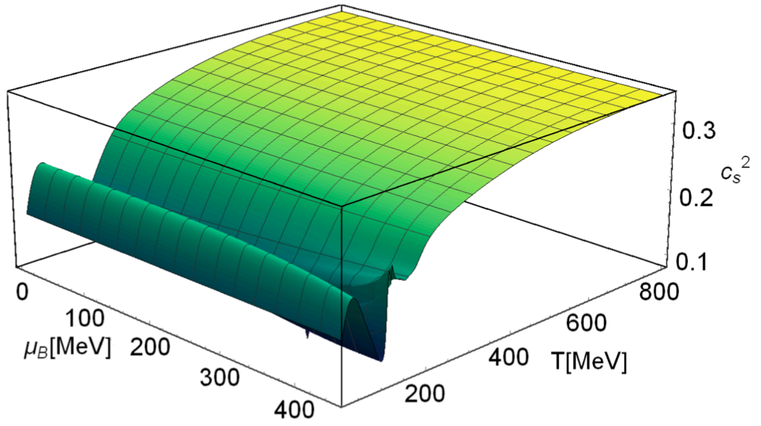

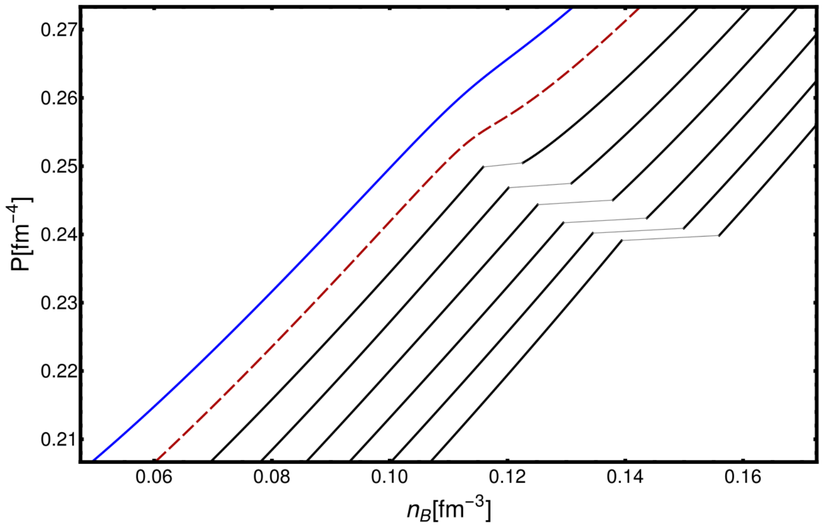

P. Parotto *et al.*, Phys. Rev. C 101, 034901 (2020), arXiv:1805.05249

with strangeness-neutrality:

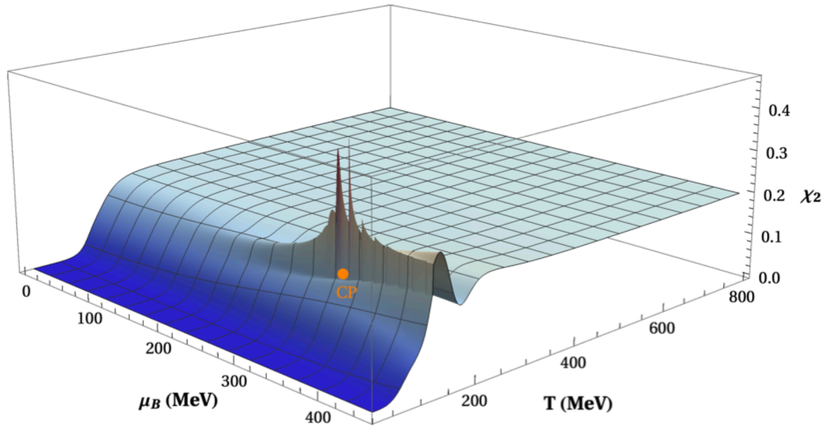

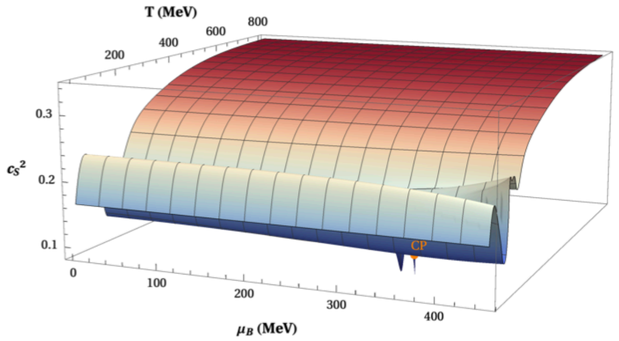

J.M. Karthein *et al.*, Eur. Phys. J. Plus **136** 6, 621 (2021) arXiv:2103.08146

Input to hydrodynamics: EOS with 3D-Ising model critical point

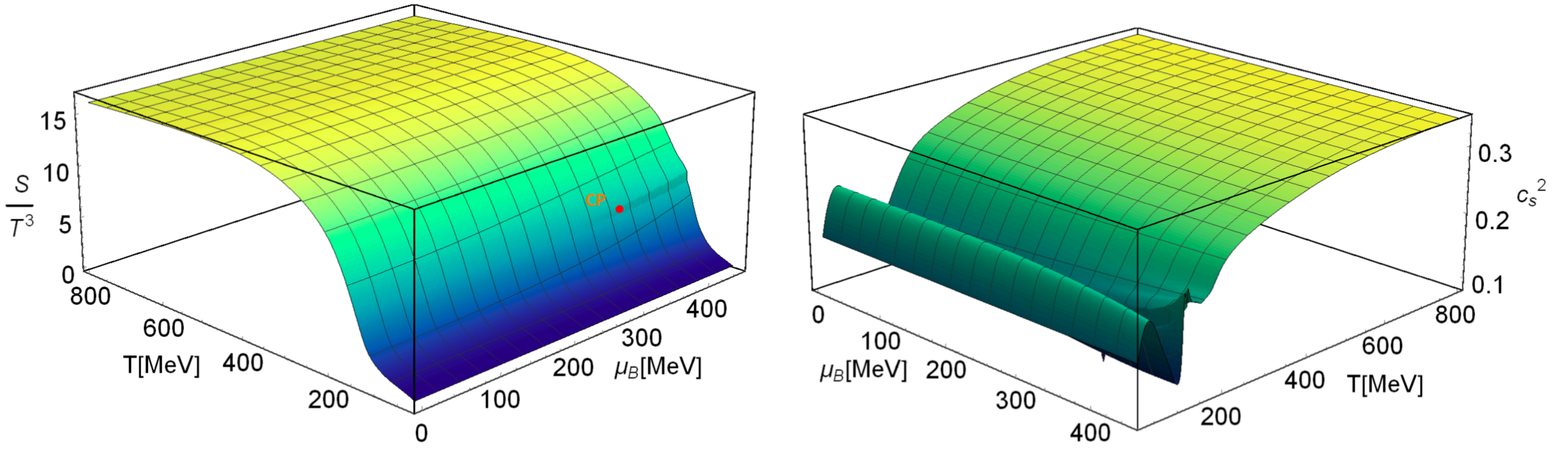

P. Parotto *et al.*, Phys. Rev. C 101, 034901 (2020), arXiv:1805.05249

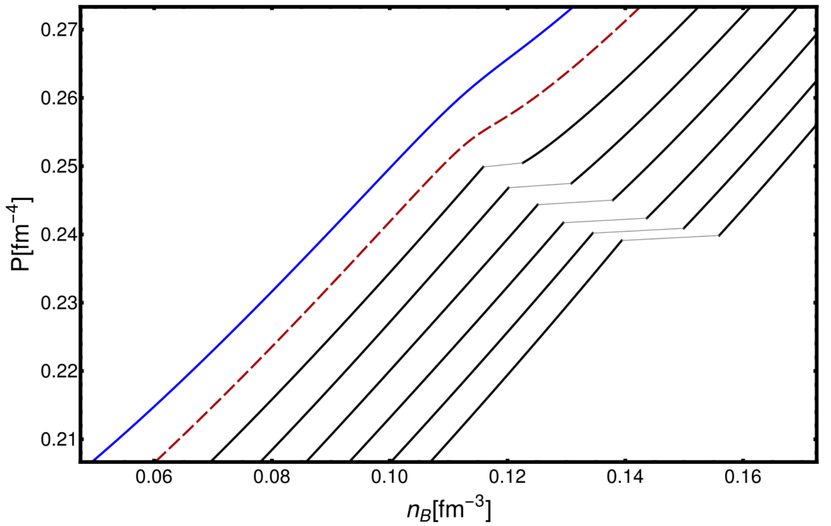

with strangeness-neutrality:

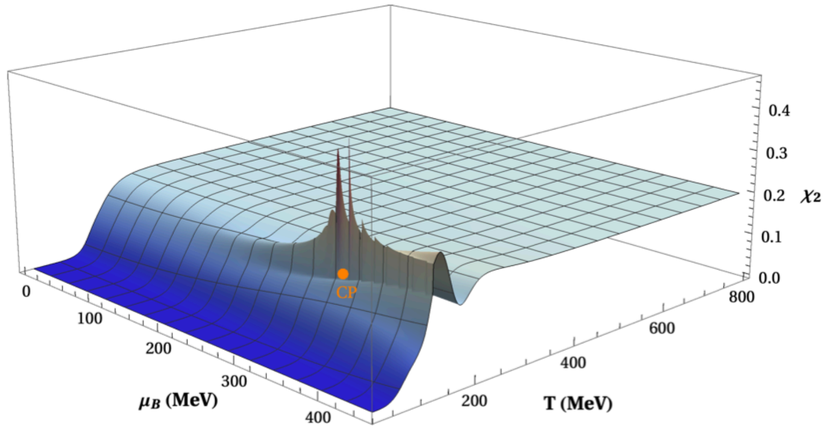

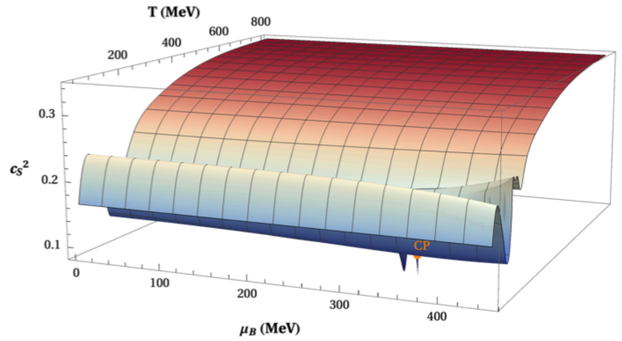

J.M. Karthein *et al.*, Eur. Phys. J. Plus **136** 6, 621 (2021) arXiv:2103.08146

with spinodal regions:

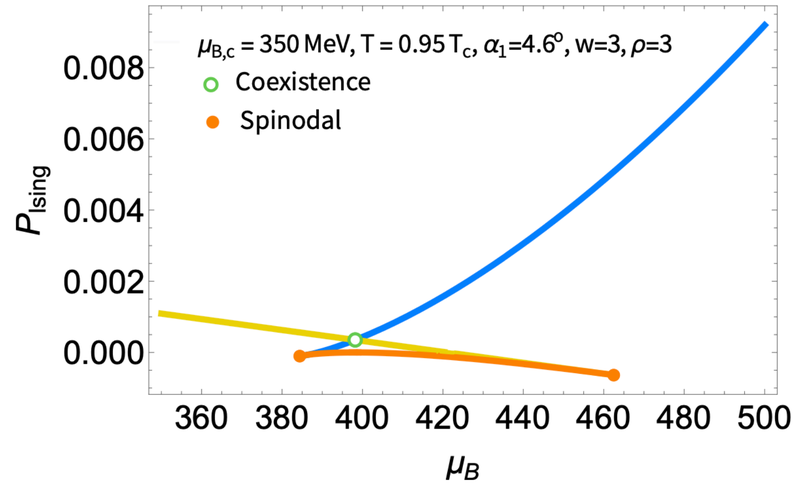

J.M. Karthein, V. Koch, C. Ratti,
Phys. Rev. D **111** 3, 034013 (2025), arXiv:2409.13961

EOS is only one of many aspects of hydrodynamics

low collision energy = prolonged initial stage:

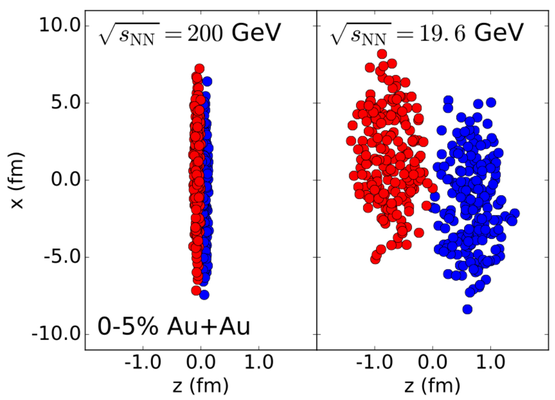

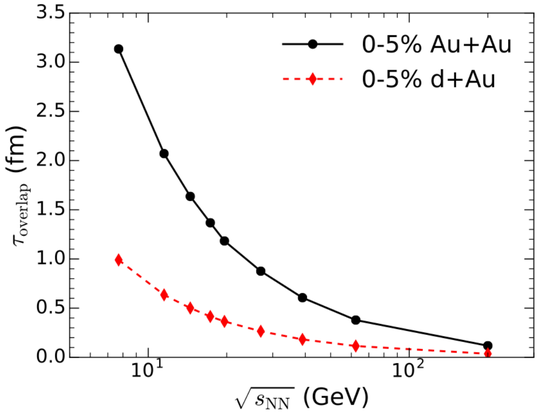

C. Shen, B. Schenke, Phys. Rev. C. **97** (2), 024907 (2018) arXiv:1710.00881

EOS is only one of many aspects of hydrodynamics

low collision energy = prolonged initial stage:

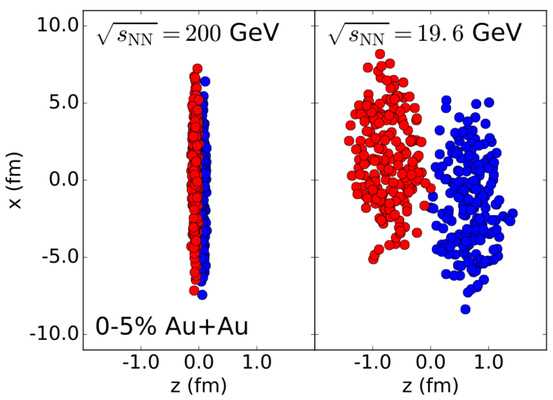

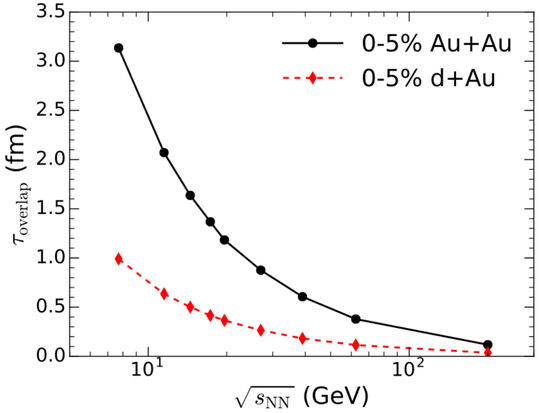

C. Shen, B. Schenke, Phys. Rev. C. **97** (2), 024907 (2018) arXiv:1710.00881

parametric initial distributions for energy and baryon density:

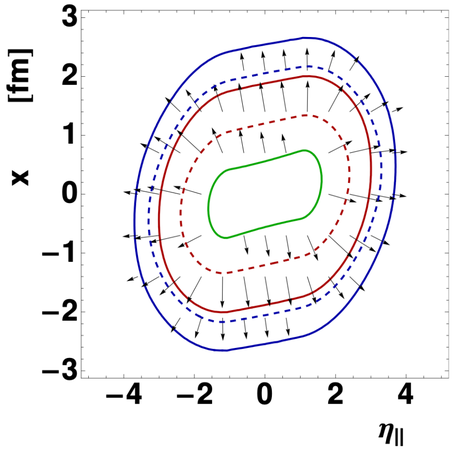

P. Bozek, I. Wyskiel, Phys. Rev. C. 81, 054902 (2010) arXiv:1002.4999

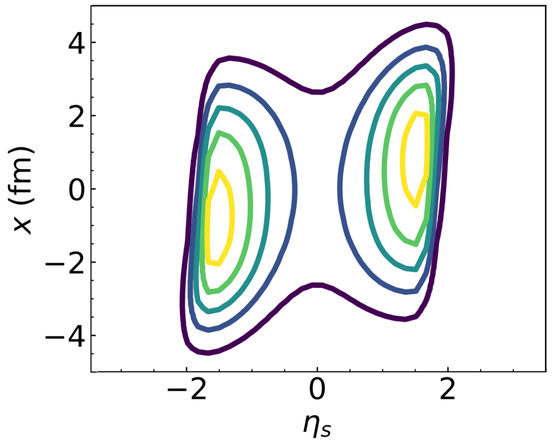

L. Du, C. Shen, S. Jeon, C. Gale, Phys. Rev. C. 108(4), L041901 (2023) arXiv:2211.16408

EOS is only one of many aspects of hydrodynamics

low collision energy = prolonged initial stage:

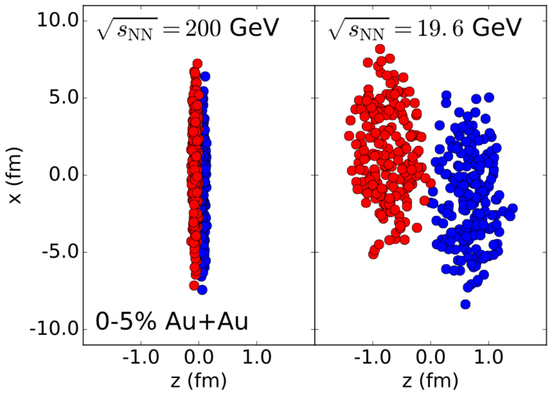

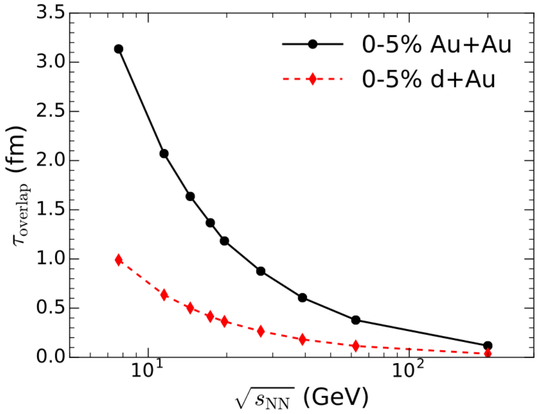

C. Shen, B. Schenke, Phys. Rev. C. **97** (2), 024907 (2018) arXiv:1710.00881

parametric initial distributions for energy and baryon density:

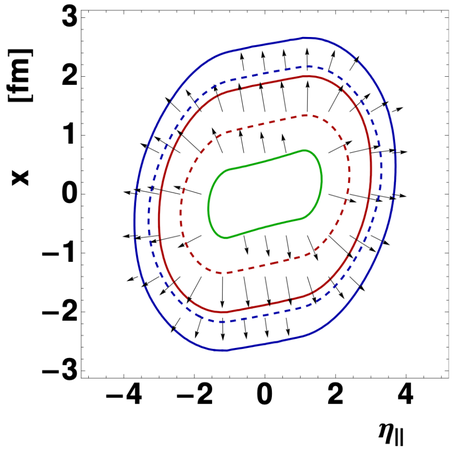

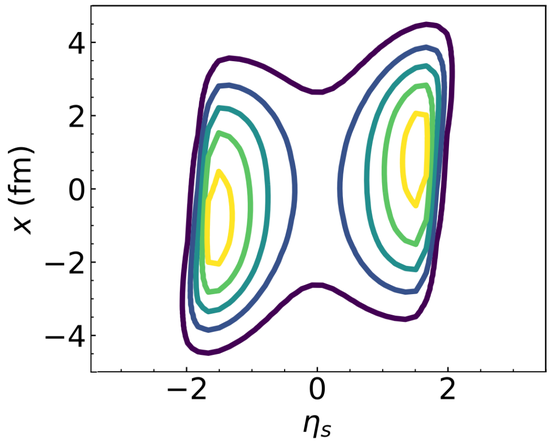

P. Bozek, I. Wyskiel, Phys. Rev. C. 81, 054902 (2010) arXiv:1002.4999

L. Du, C. Shen, S. Jeon, C. Gale, Phys. Rev. C. 108(4), L041901 (2023) arXiv:2211.16408

multiple conserved charges initialized with ICCING (Initial Conserved Charges in Nuclear Geometry)

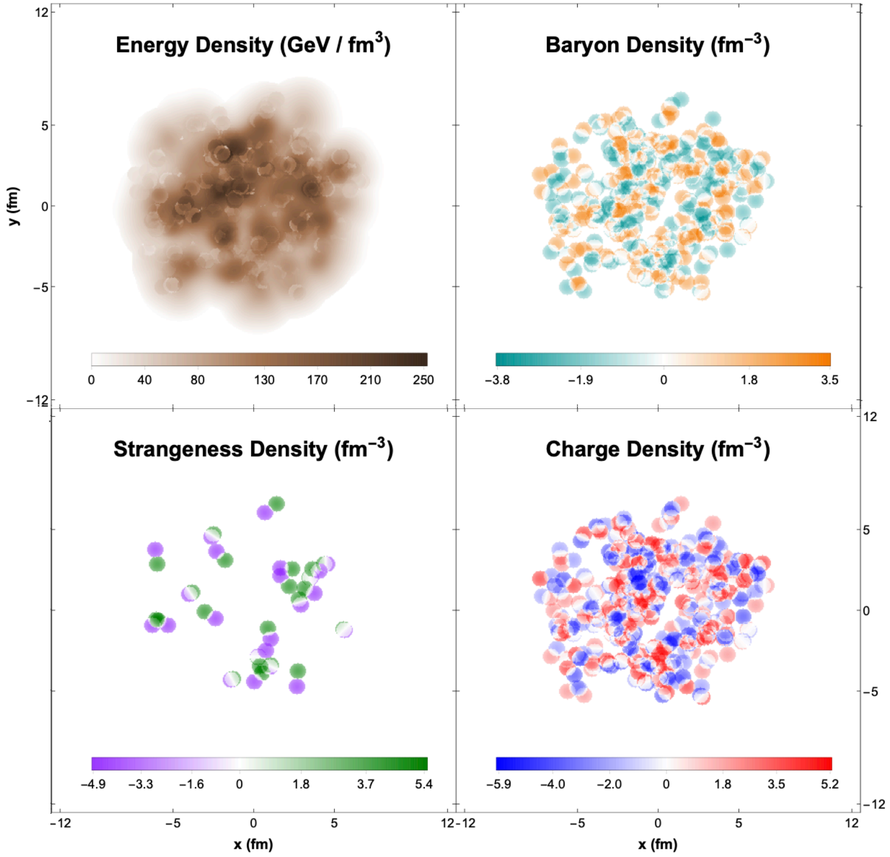

P. Carzon *et al.*, Phys. Rev. C. 105(3), 034908 (2022) arXiv:1911.12454
P. Carzon *et al.*, Phys. Rev. C. 108 (6), 064905 (2023) arXiv:2301.04572

EOS is only one of many aspects of hydrodynamics

low collision energy = prolonged initial stage:

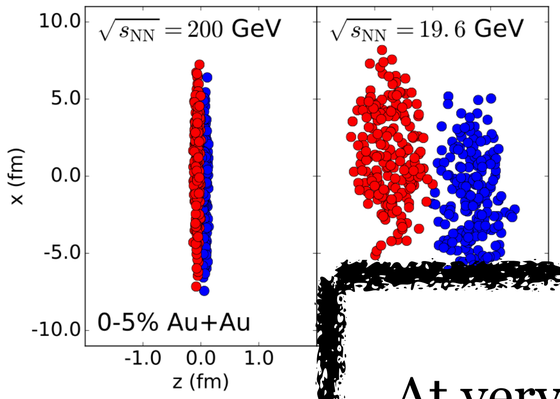

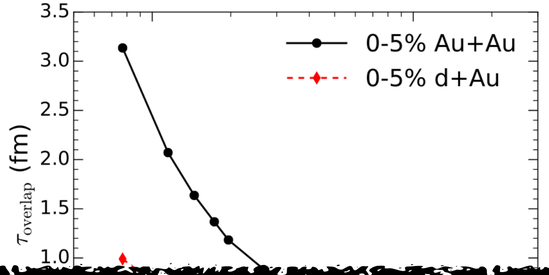

C. Shen, B. Schen

parametric
energy and

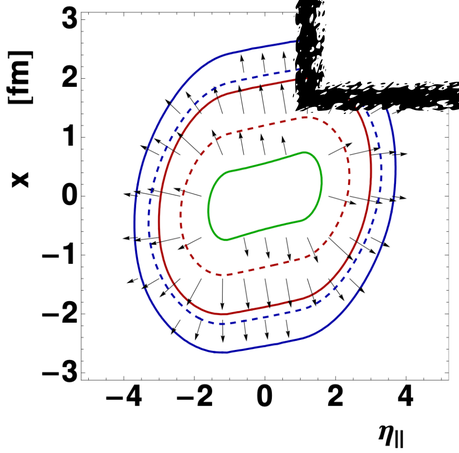

P. Bozek, I. Wyskiel, Phys. Rev. C. 81, 054902 (2010) arXiv:1002.4999

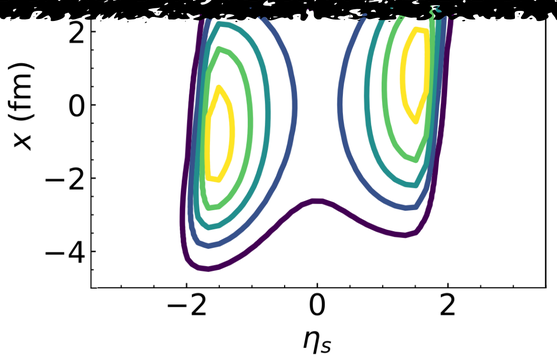

L. Du, C. Shen, S. Jeon, C. Gale, Phys. Rev. C. 108(4), L041901 (2023) arXiv:2211.16408

multiple conserved charges initialized with ICCING
(Initial Conserved Charges in Nuclear Geometry)

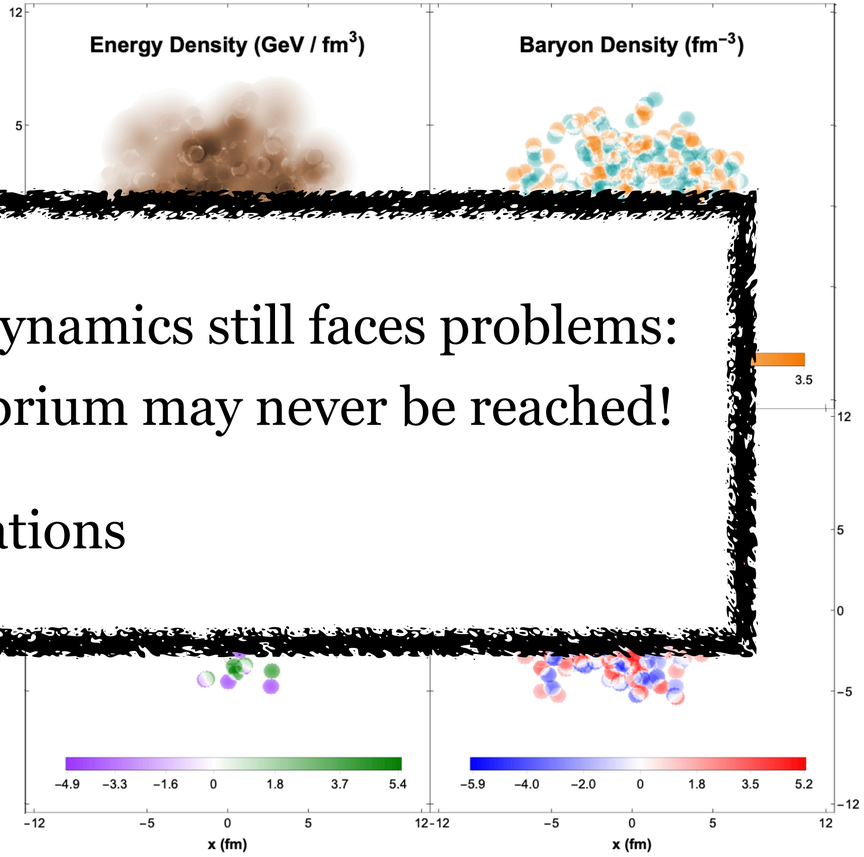

P. Carzon *et al.*, Phys. Rev. C. 105(3), 034908 (2022) arXiv:1911.12454
P. Carzon *et al.*, Phys. Rev. C. 108 (6), 064905 (2023) arXiv:2301.04572

At very low energies ($\sqrt{s_{NN}} \leq 7$ GeV) hydrodynamics still faces problems:
approach to equilibrium is so long that equilibrium may never be reached!

Enter transport simulations

Part 5: Connections to neutron stars

Intriguing results from analyses of astrophysical observations

Recent astrophysical measurements suggest NS EOS may have a nontrivial density-dependence

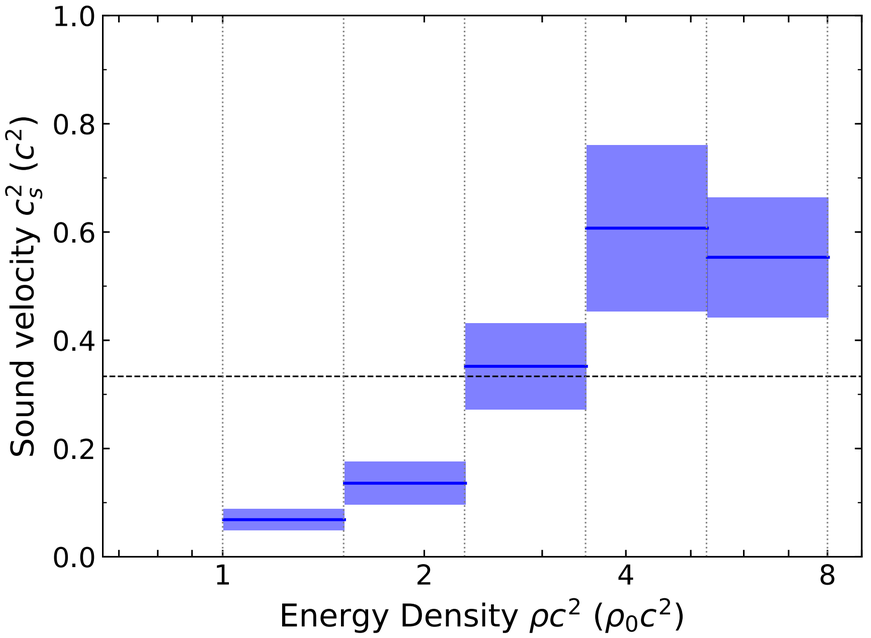

Y. Fujimoto, K. Fukushima, K. Murase,
Phys. Rev. D **101**, 5, 054016 (2020), arXiv:1903.03400

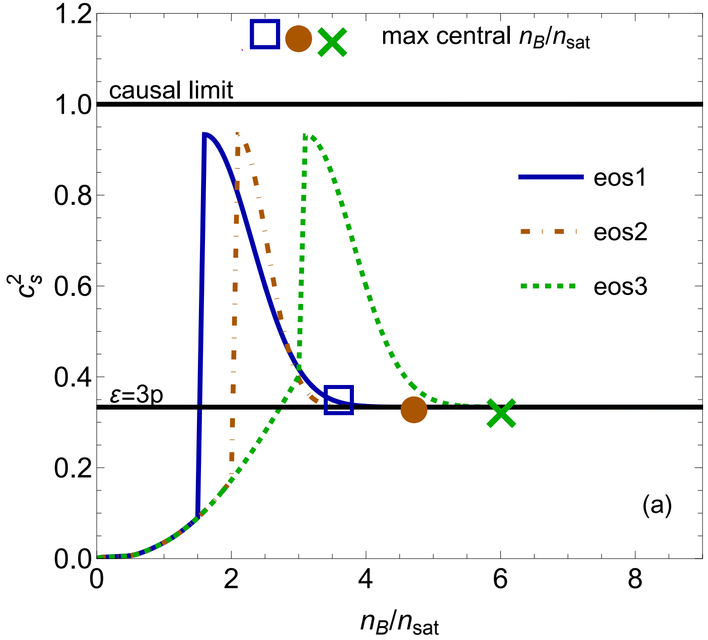

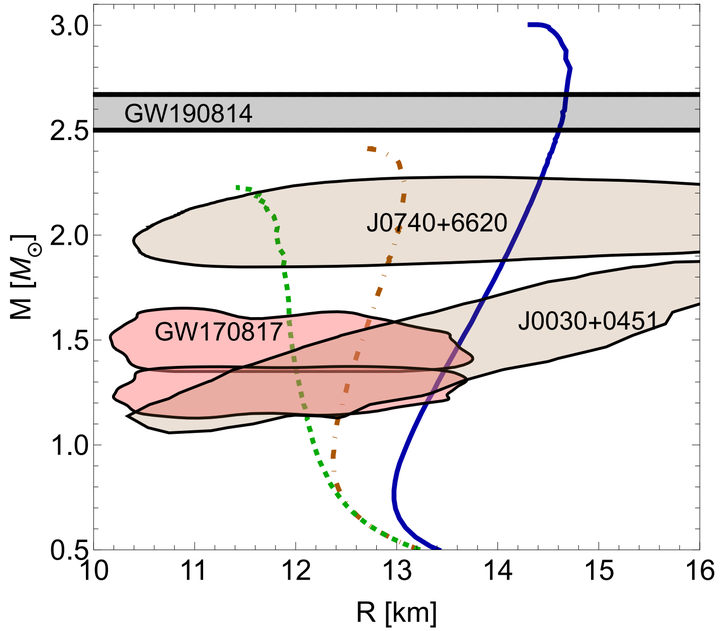

N. Yao, **A. Sorensen,** V. Dexheimer, J. Noronha-Hostler, arXiv:2311.18819
H. Tan, T. Dore, V. Dexheimer, J. Noronha-Hostler, N. Yunes, Phys. Rev. D **105** 2, 023018 (2022)

Intriguing results from analyses of astrophysical observations

Recent astrophysical measurements suggest NS EOS may have a nontrivial density-dependence

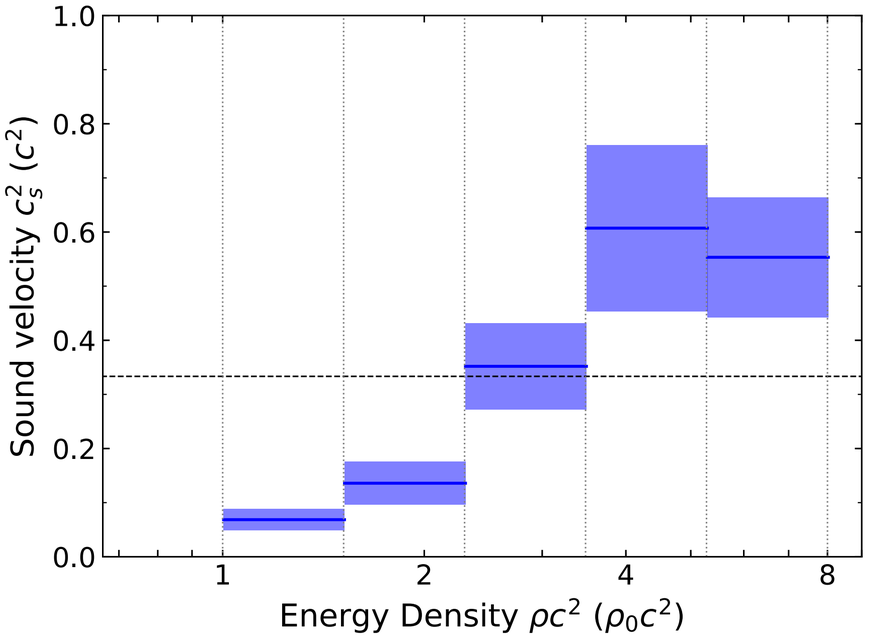

Y. Fujimoto, K. Fukushima, K. Murase,
Phys. Rev. D **101**, 5, 054016 (2020), arXiv:1903.03400

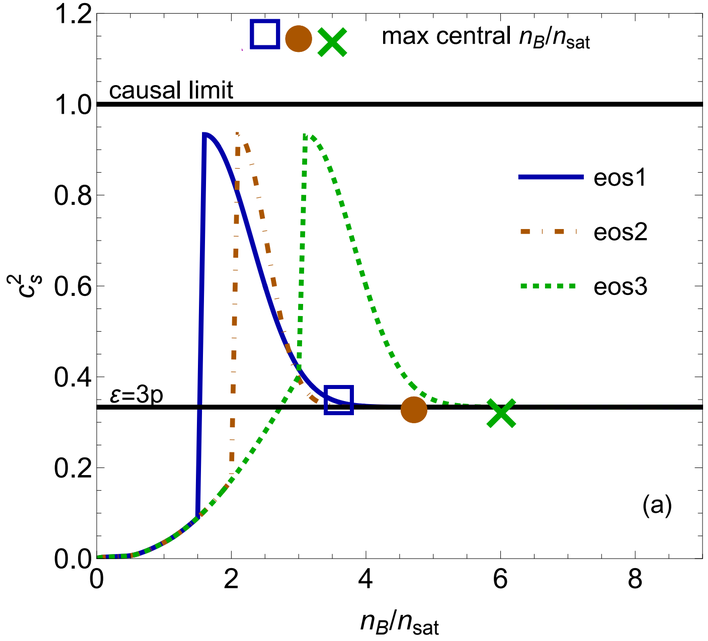

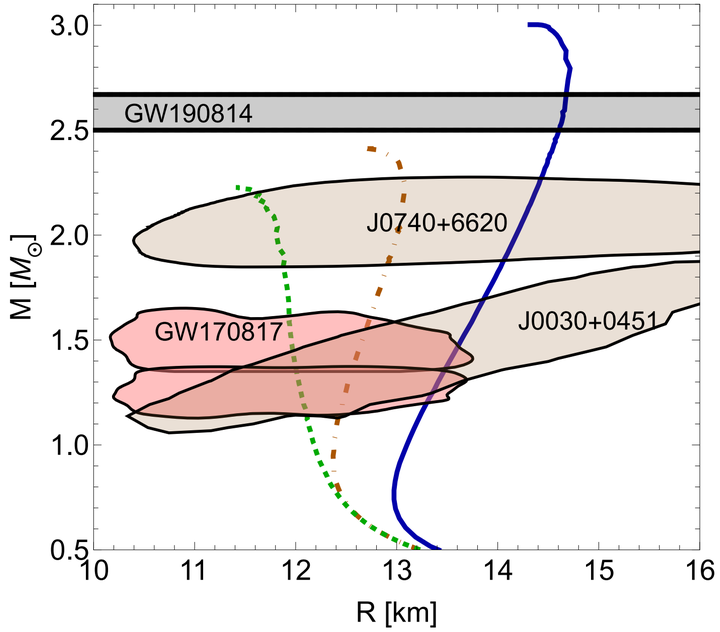

N. Yao, **A. Sorensen,** V. Dexheimer, J. Noronha-Hostler, arXiv:2311.18819
H. Tan, T. Dore, V. Dexheimer, J. Noronha-Hostler, N. Yunes, Phys. Rev. D **105** 2, 023018 (2022)

Which of the allowed NS EOSs are compatible with heavy-ion collision measurements?

EOS from neutron stars to heavy-ion collisions

Use symmetry energy parameters exploring the allowed parameter space:

N. Yao, **A. Sorensen**, V. Dexheimer, J. Noronha-Hostler, arXiv:2311.18819

$$\mathcal{E}_{\rm HIC} = \mathcal{E}_{\rm NS} - n_B \underbrace{\left[E_{\rm sym} + \frac{L_{\rm sym}}{3}\left(\frac{n_B}{n_0}-1\right) + \frac{K_{\rm sym}}{18}\left(\frac{n_B}{n_0}-1\right)^2 + \frac{J_{\rm sym}}{162}\left(\frac{n_B}{n_0}-1\right)^3 \right]}_{\approx \text{ symmetry energy } S(n_B)} \delta^2 \,, \qquad \delta \equiv \frac{n_N - n_P}{n_N + n_P}$$

Coefficient	Range	Step size
$E_{\rm sym,sat}$	27 – 40	1 MeV
$L_{\rm sym,sat}$	30 – 130	10 MeV
$K_{\rm sym,sat}$	-220 – 180	50 MeV
$J_{\rm sym,sat}$	-200 – 800	100 MeV

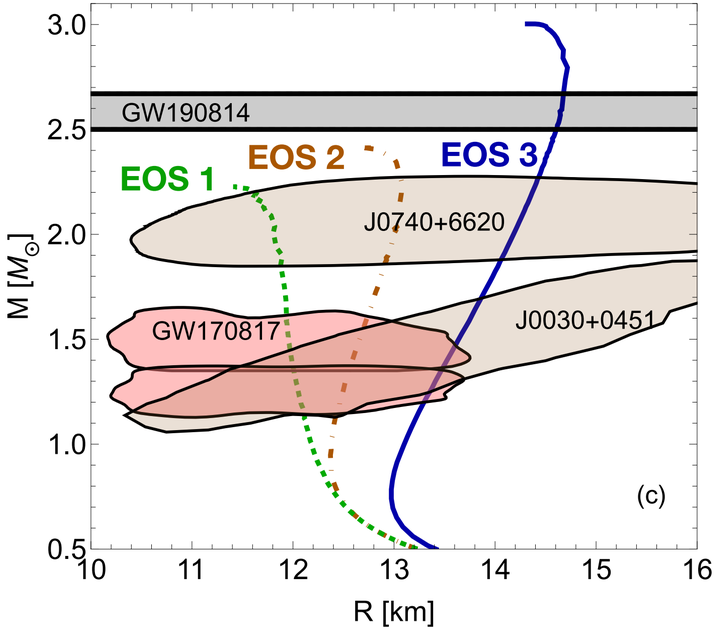

H. Tan, T. Dore, V. Dexheimer, J. Noronha-Hostler, N. Yunes, Phys. Rev. D **105** 2, 023018 (2022)

EOS from neutron stars to heavy-ion collisions

Use symmetry energy parameters exploring the allowed parameter space:

N. Yao, **A. Sorensen**, V. Dexheimer, J. Noronha-Hostler, arXiv:2311.18819

$$\mathcal{E}_{\rm HIC} = \mathcal{E}_{\rm NS} - n_B \underbrace{\left[E_{\rm sym} + \frac{L_{\rm sym}}{3}\left(\frac{n_B}{n_0}-1\right) + \frac{K_{\rm sym}}{18}\left(\frac{n_B}{n_0}-1\right)^2 + \frac{J_{\rm sym}}{162}\left(\frac{n_B}{n_0}-1\right)^3 \right]}_{\approx \text{ symmetry energy } S(n_B)} \delta^2 \,, \qquad \delta \equiv \frac{n_N - n_P}{n_N + n_P}$$

Coefficient	Range	Step size
$E_{\rm sym,sat}$	27 – 40	1 MeV
$L_{\rm sym,sat}$	30 – 130	10 MeV
$K_{\rm sym,sat}$	-220 – 180	50 MeV
$J_{\rm sym,sat}$	-200 – 800	100 MeV

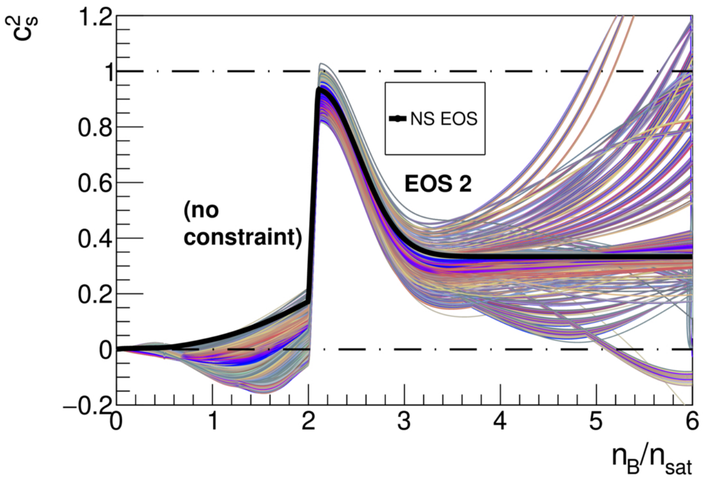

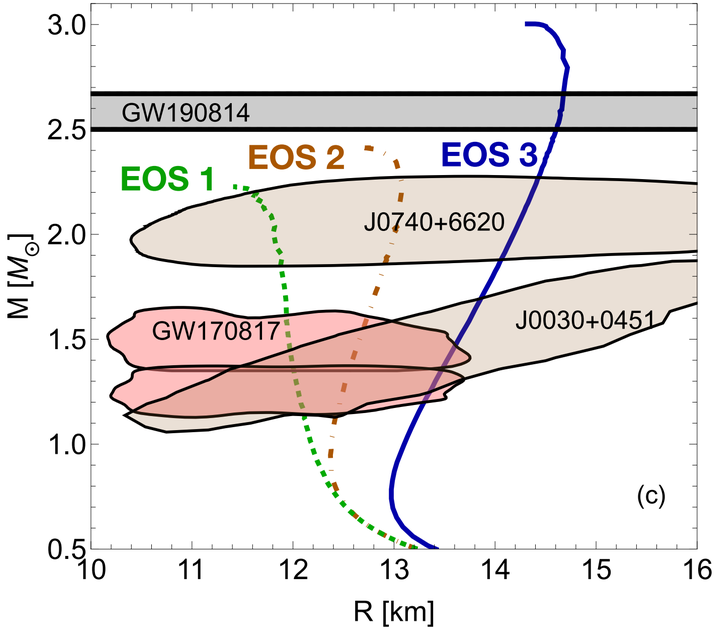

H. Tan, T. Dore, V. Dexheimer, J. Noronha-Hostler, N. Yunes, Phys. Rev. D **105** 2, 023018 (2022)

EOS from neutron stars to heavy-ion collisions

Use symmetry energy parameters exploring the allowed parameter space:

N. Yao, **A. Sorensen**, V. Dexheimer,
J. Noronha-Hostler, arXiv:2311.18819

$$\mathcal{E}_{\rm HIC} = \mathcal{E}_{\rm NS} - n_B \underbrace{\left[E_{\rm sym} + \frac{L_{\rm sym}}{3}\left(\frac{n_B}{n_0}-1\right) + \frac{K_{\rm sym}}{18}\left(\frac{n_B}{n_0}-1\right)^2 + \frac{J_{\rm sym}}{162}\left(\frac{n_B}{n_0}-1\right)^3 \right]}_{\approx \text{ symmetry energy } S(n_} \delta^2 \,, \qquad \delta \equiv \frac{n_N - n_P}{n_N + n_P}$$

Coefficient	Range	Step size
$E_{\rm sym,sat}$	27 – 40	1 MeV
$L_{\rm sym,sat}$	30 – 130	10 MeV
$K_{\rm sym,sat}$	-220 – 180	50 MeV
$J_{\rm sym,sat}$	-200 – 800	100 MeV

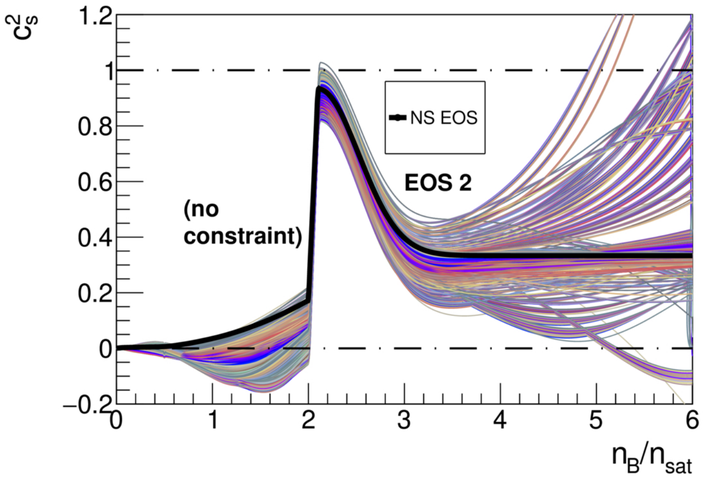

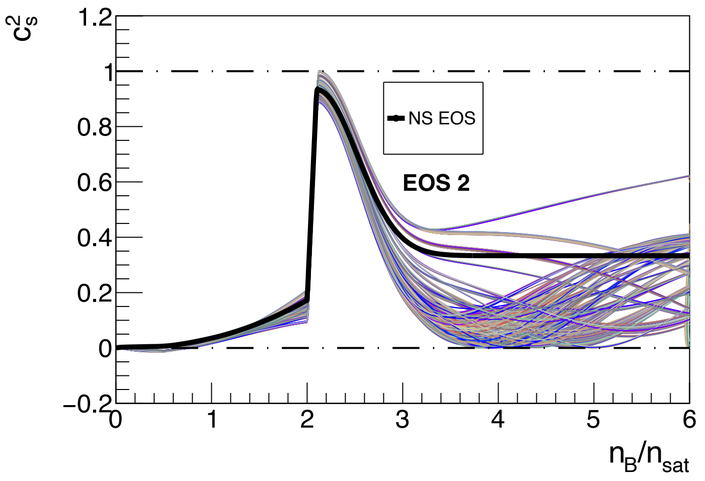

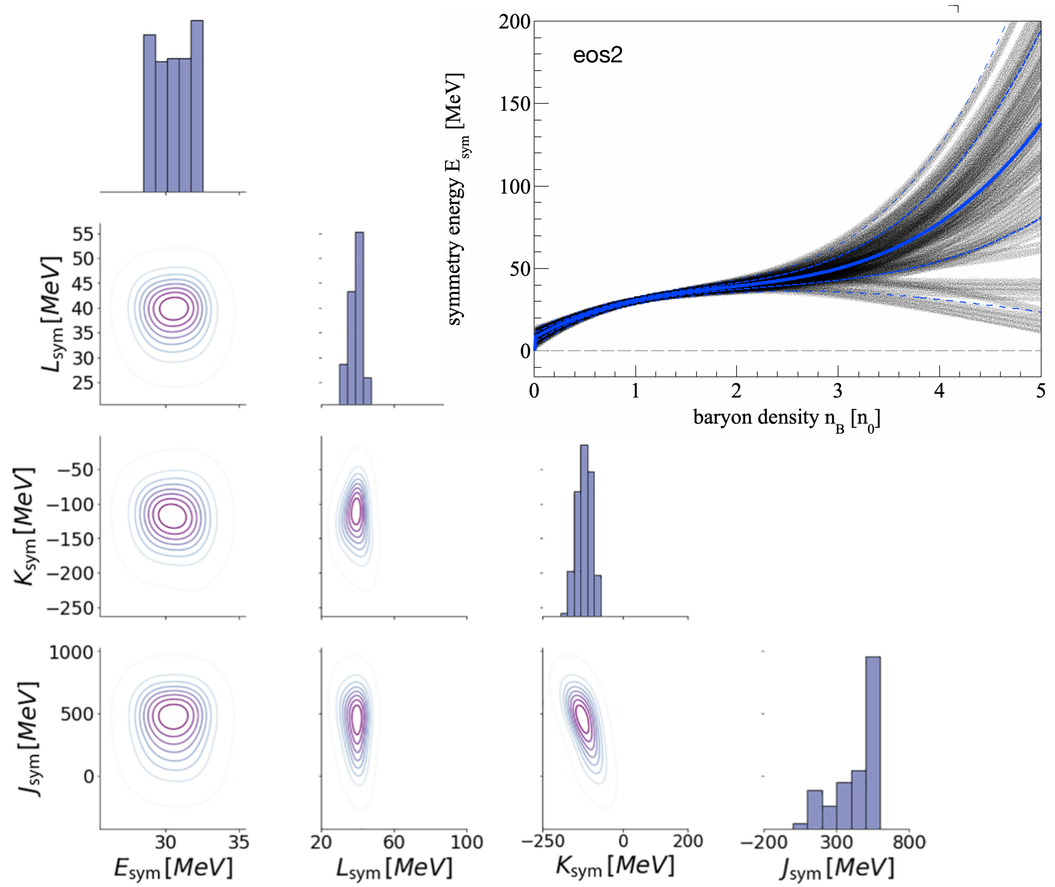

Enforcing nuclear matter properties, causality, and stability above $n_B \approx n_0$ leads to constraints on $E_{\rm sym}$, $L_{\rm sym}$, $K_{\rm sym}$, $J_{\rm sym}$

EOS from neutron stars to heavy-ion collisions

"Minimal" and "maximal" EOSs from each family tested against heavy-ion measurements:

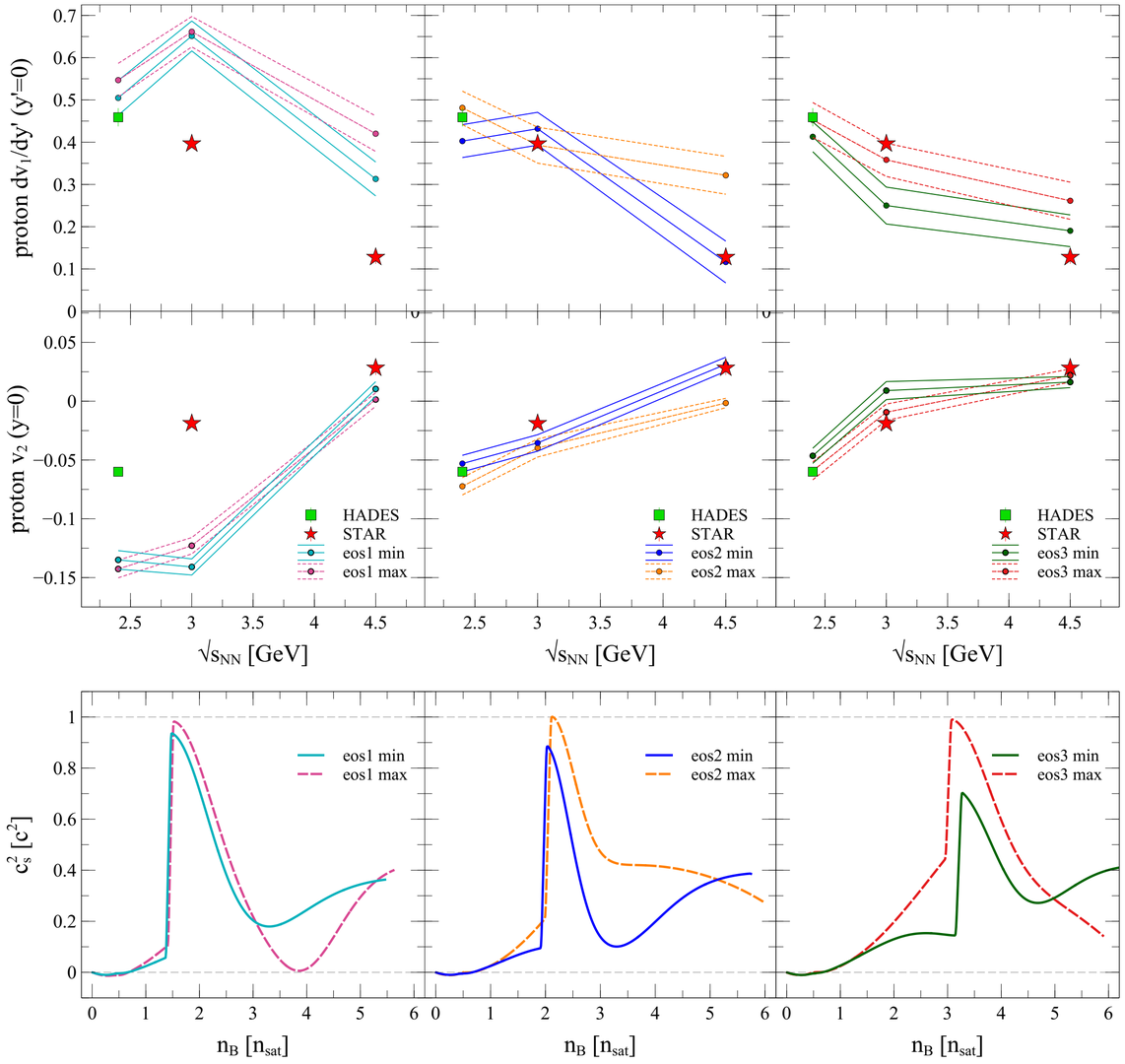

EOS	$n_{\rm sat}$ [fm^{-3}]	B [MeV]	K_0 [MeV]	$c_s^2(n_B = n_{\rm sat})$
eos1 min	0.175	-14.6	200.5	0.024
eos1 max	0.171	-17.8	325.9	0.039
eos2 min	0.167	-14.6	206.7	0.025
eos2 max	0.161	-16.9	214.8	0.026
eos3 min	0.153	-14.8	220.2	0.027
eos3 max	0.162	-16.5	201.7	0.024

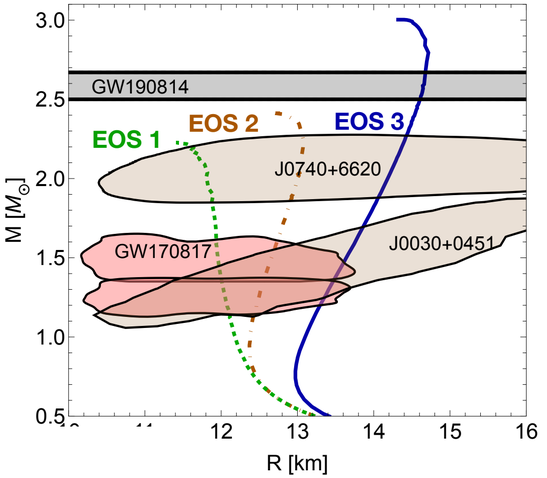

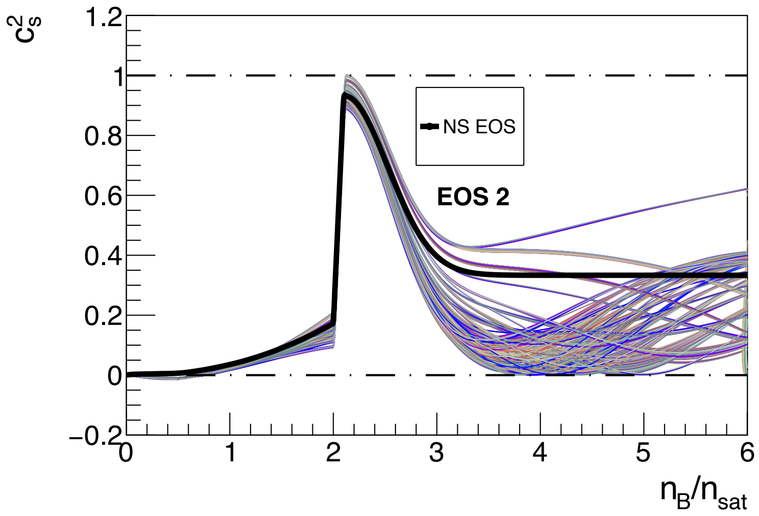

N. Yao, **A. Sorensen**, V. Dexheimer, J. Noronha-Hostler, arXiv:2311.18819

EOS from neutron stars to heavy-ion collisions

"Minimal" and "maximal" EOSs from each family tested against heavy-ion measurements:

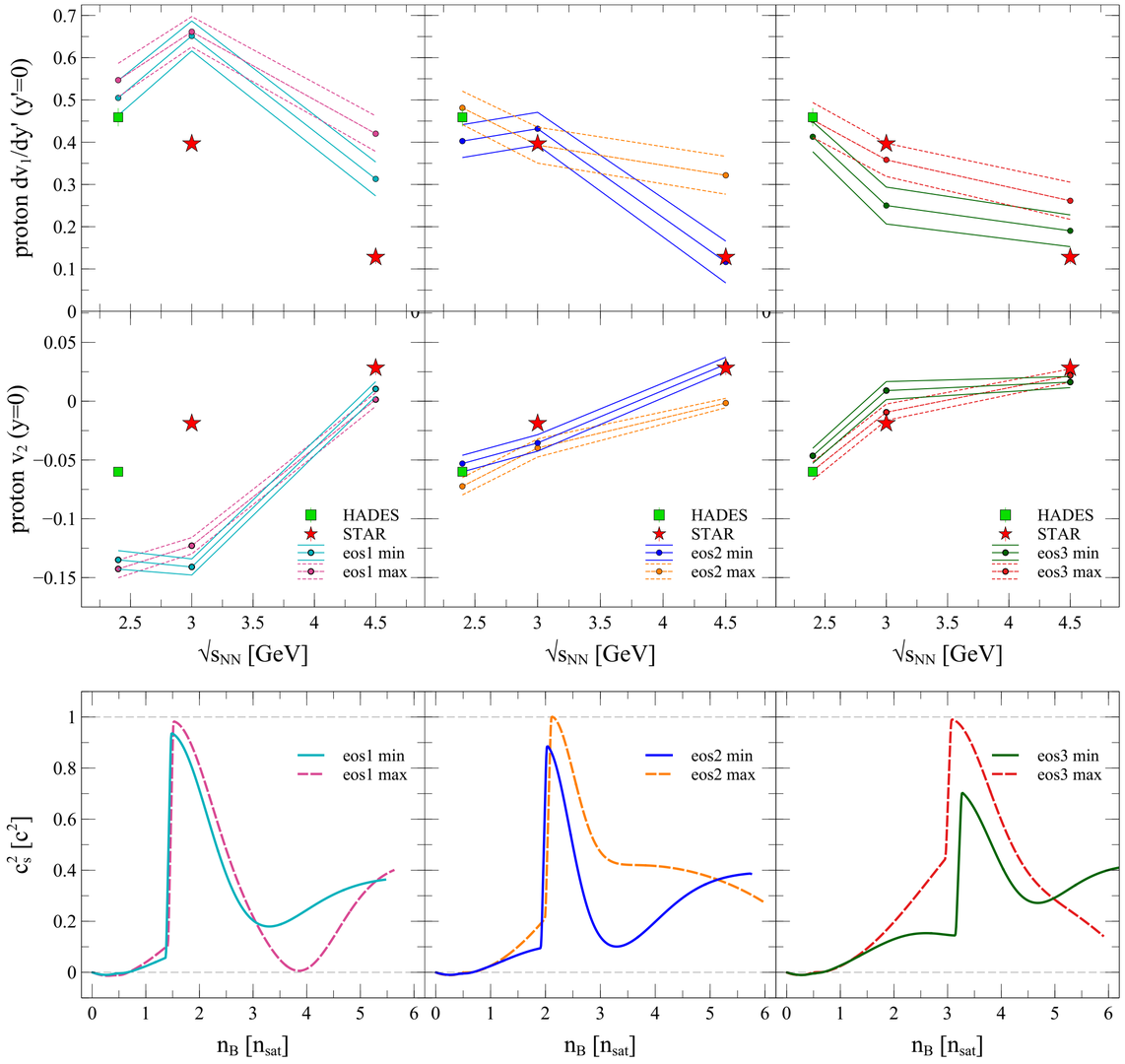

EOS	$n_{\rm sat}$ [fm^{-3}]	B [MeV]	K_0 [MeV]	$c_s^2(n_B = n_{\rm sat})$
eos1 min	0.175	-14.6	200.5	0.024
eos1 max	0.171	-17.8	325.9	0.039
eos2 min	0.167	-14.6	206.7	0.025
eos2 max	0.161	-16.9	214.8	0.026
eos3 min	0.153	-14.8	220.2	0.027
eos3 max	0.162	-16.5	201.7	0.024

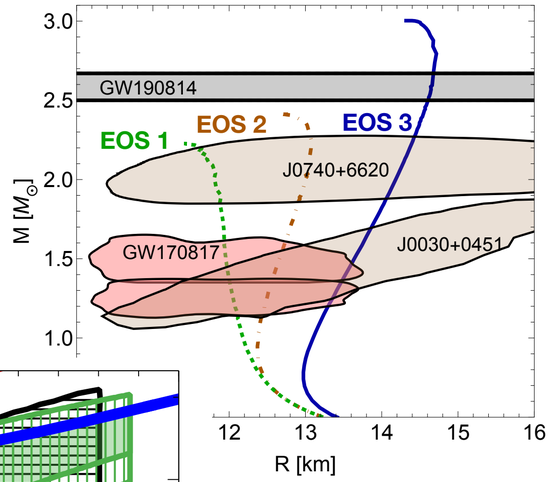

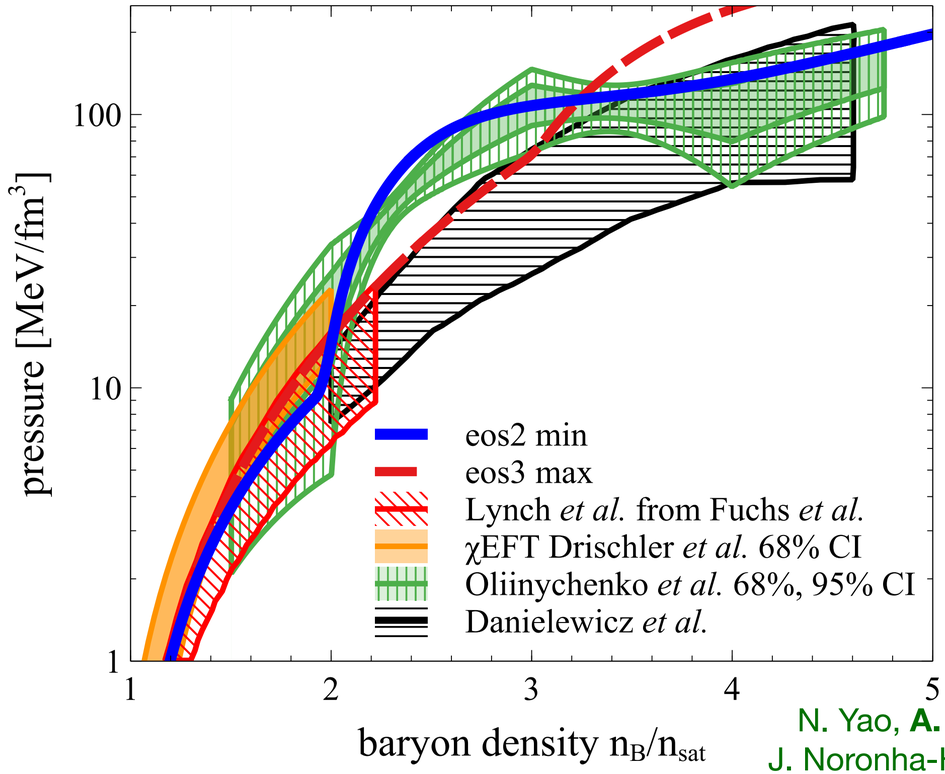

N. Yao, **A. Sorensen**, V. Dexheimer, J. Noronha-Hostler, arXiv:2311.18819

EOS from neutron stars to heavy-ion collisions

"Minimal" and "maximal" EOSs from each family tested against heavy-ion measurements:

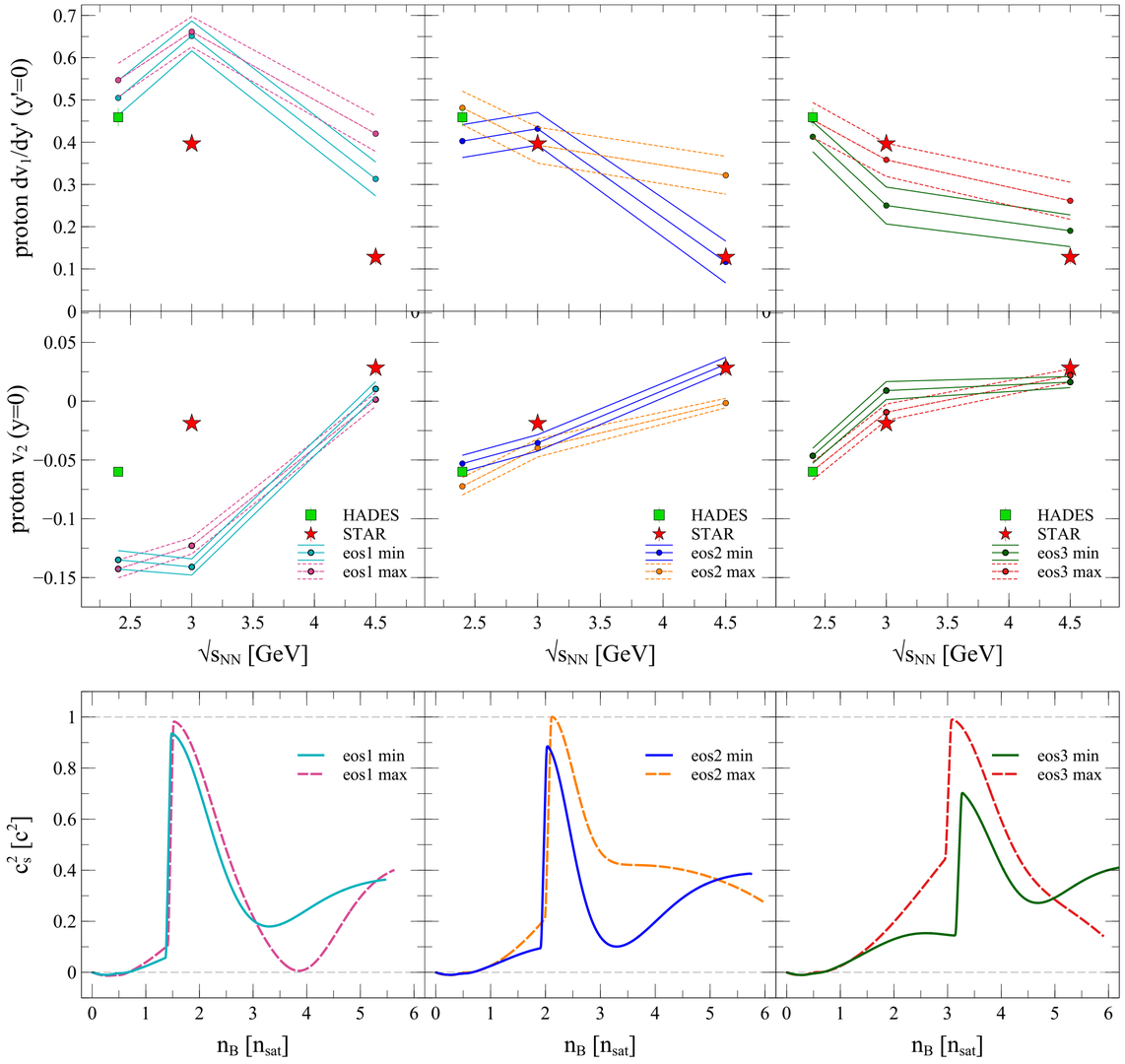

EOS	n_{sat} [fm^{-3}]	B [MeV]	K_0 [MeV]	$c_s^2(n_B = n_{sat})$
eos				
eos				
eos				
eos2				
eos				
eos3 max	0.162	-16.5	201.7	0.024

Massive neutron stars and heavy-ion collision data can be described with one EOS

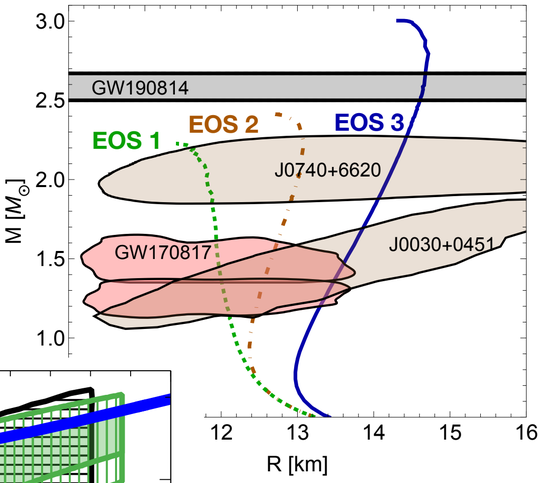

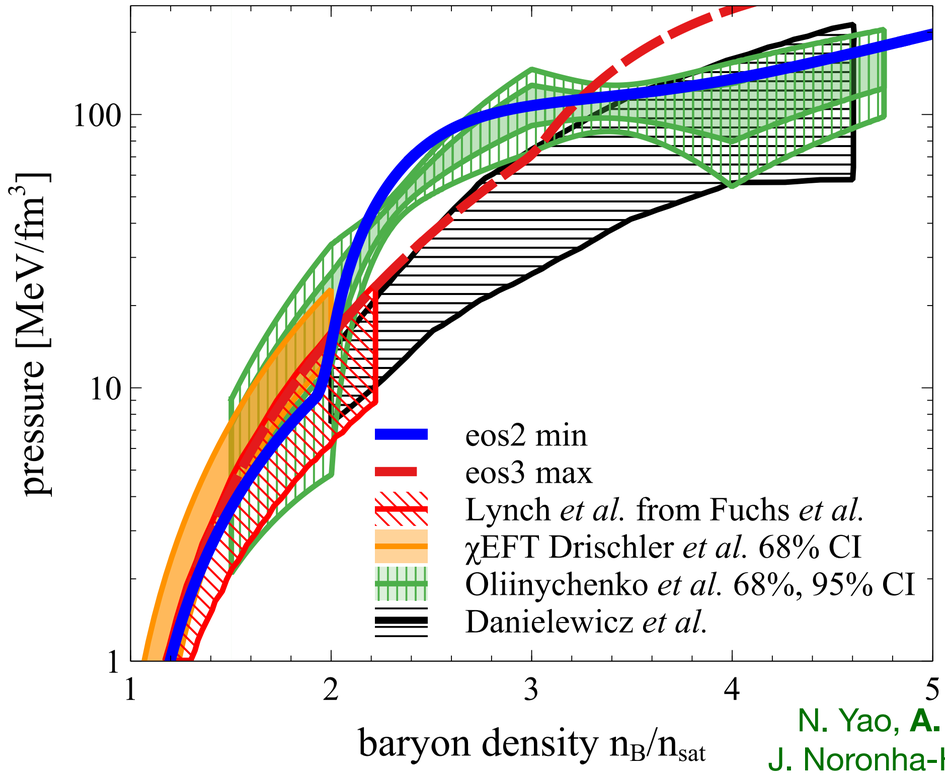

N. Yao, **A. Sorensen**, V. Dexheimer, J. Noronha-Hostler, arXiv:2311.18819

The QCD CP from finite-size scaling: Where can we expect scaling?

- For fluids far from the critical region, a mean-field treatment is good enough.
  The transition between the critical scaling region, intermediate scaling region, and extended scaling region has been studied: for fluids, the extended scaling region essentially covers the entire phase diagram where fluctuation contributions are small but finite.

  M.A. Anisimov, S.B. Kiselev, J.V. Sengers, S.Tang, Crossover approach to global critical phenomena in fluids, Physica A 188, 4 (1992)

- In the region of the phase diagram where the bulk of the evolution is well described by a scale free theory (hydrodynamics), the data follows Taylor's Law: $\sigma^2 = a\lambda^p$ (scale free)

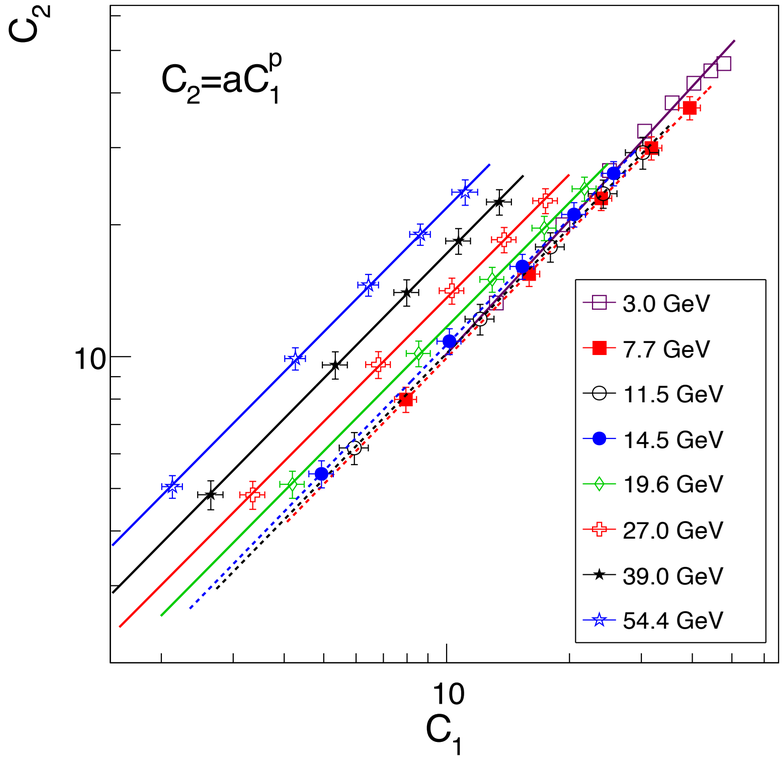

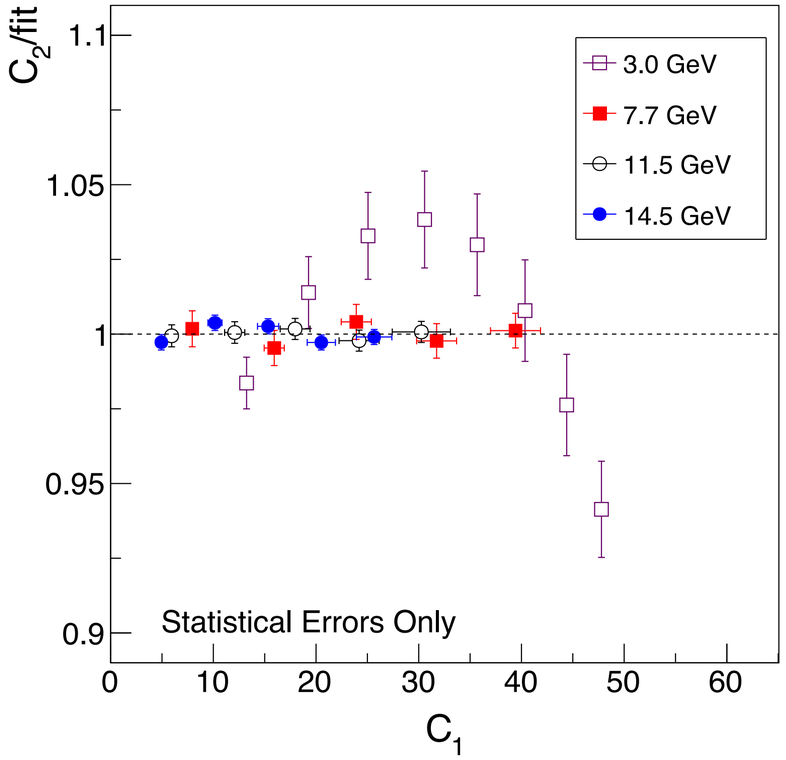

$$C_2 = aW^p$$
$$C_2 = a(xW)^p = ax^pW^p = a'W^p$$
where $C_1 \propto W$ in this energy range

Scale invariance supports the applicability of FSS
(not for collisions at 3 GeV)

Results from UrQMD with (non-relativistic) VDF

J. Steinheimer, A. Motornenko, **A. Sorensen**, Y. Nara, V. Koch, M. Bleicher,
Eur. Phys. J. C **82**, 10, 911 (2022) arXiv:2208.12091

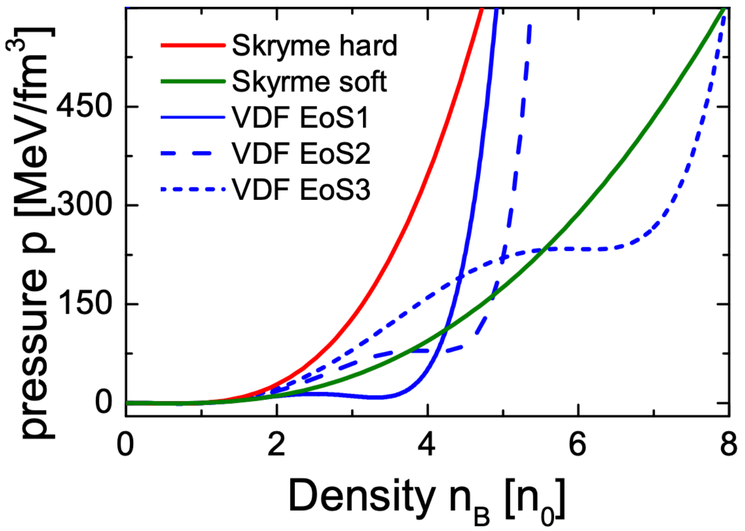

EoS	$T_c^{(N)}$[MeV]	$n_c^{(Q)}[n_0]$	$T_c^{(Q)}$[MeV]	K_0[MeV]
VDF1	18	3.0	100	261
VDF2	18	4.0	50	279
VDF3	22	6.0	50	356

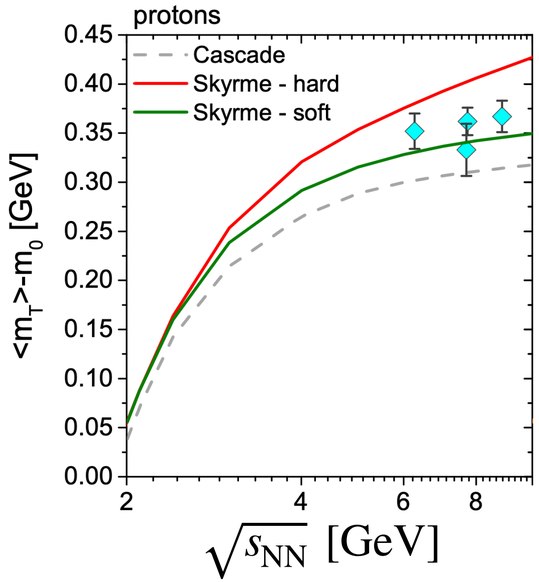

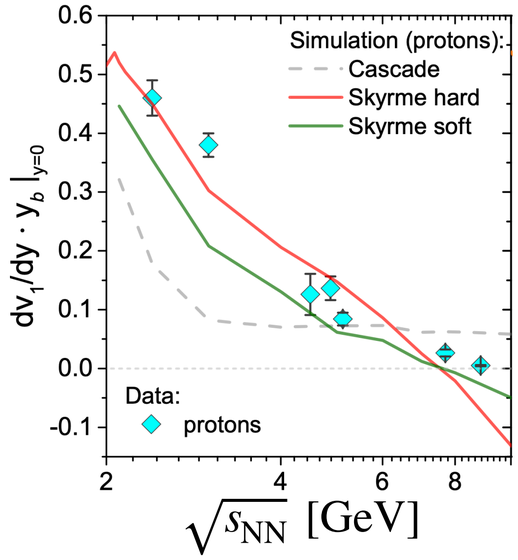

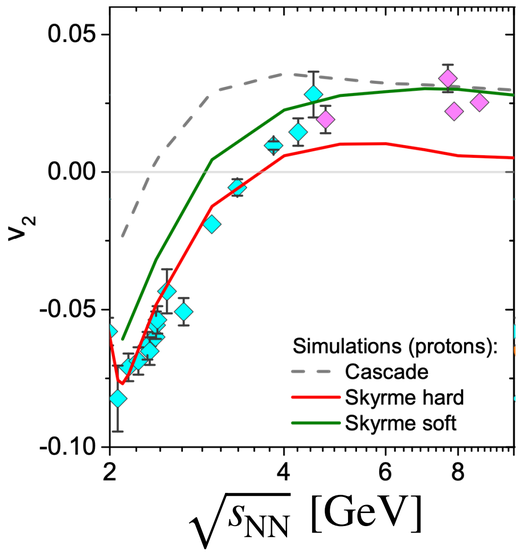

Results from UrQMD with (non-relativistic) VDF

J. Steinheimer, A. Motornenko, **A. Sorensen**, Y. Nara, V. Koch, M. Bleicher,
Eur. Phys. J. C **82**, 10, 911 (2022) arXiv:2208.12091

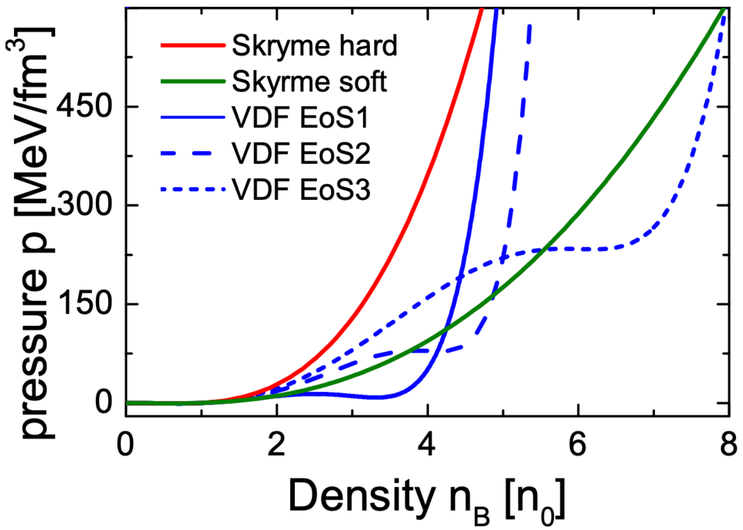

EoS	$T_c^{(N)}$[MeV]	$n_c^{(Q)}[n_0]$	$T_c^{(Q)}$[MeV]	K_0[MeV]
VDF1	18	3.0	100	261
VDF2	18	4.0	50	279
VDF3	22	6.0	50	356

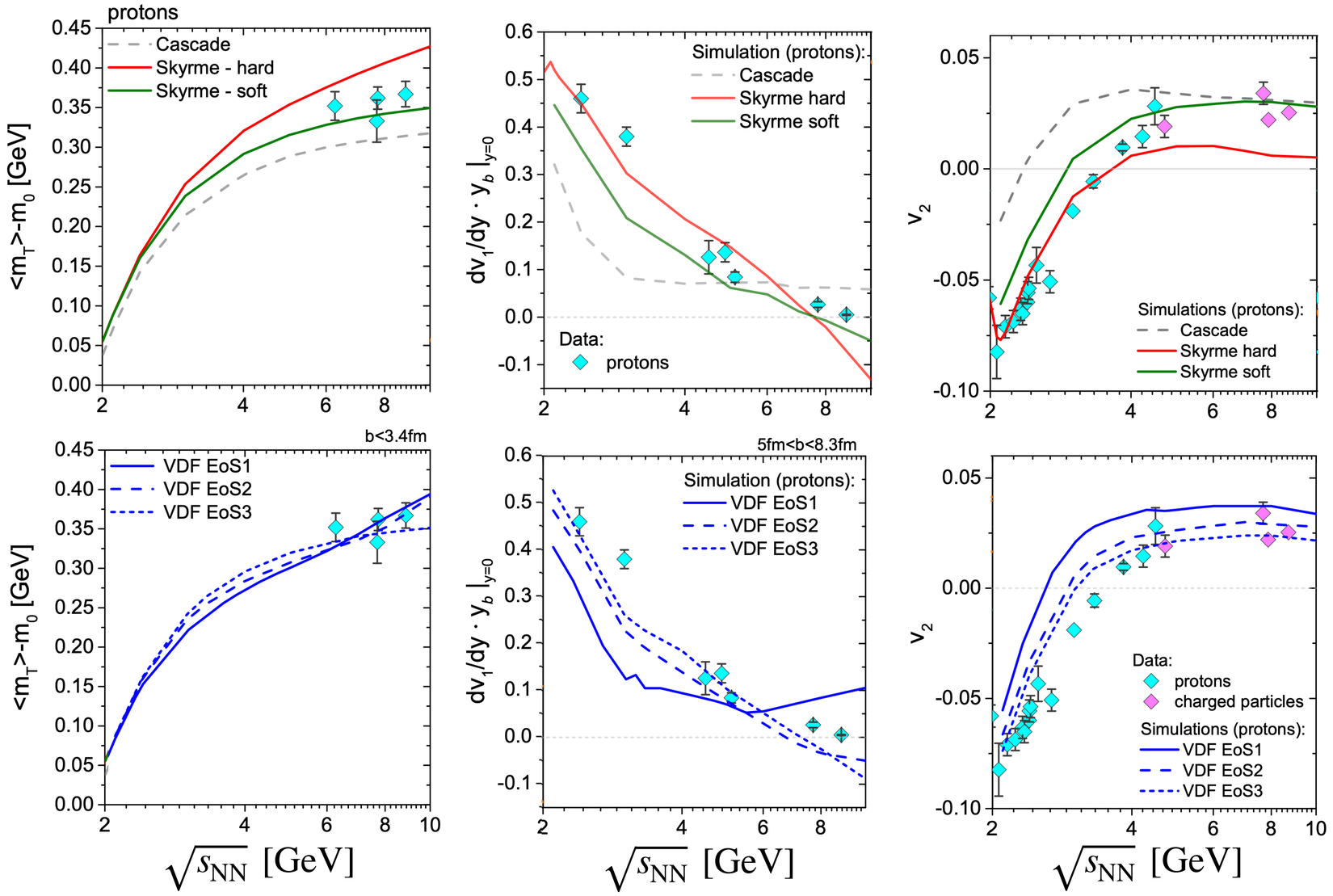

Results from UrQMD with (non-relativistic) VDF

J. Steinheimer, A. Motornenko, **A. Sorensen**, Y. Nara, V. Koch, M. Bleicher,
Eur. Phys. J. C **82**, 10, 911 (2022) arXiv:2208.12091

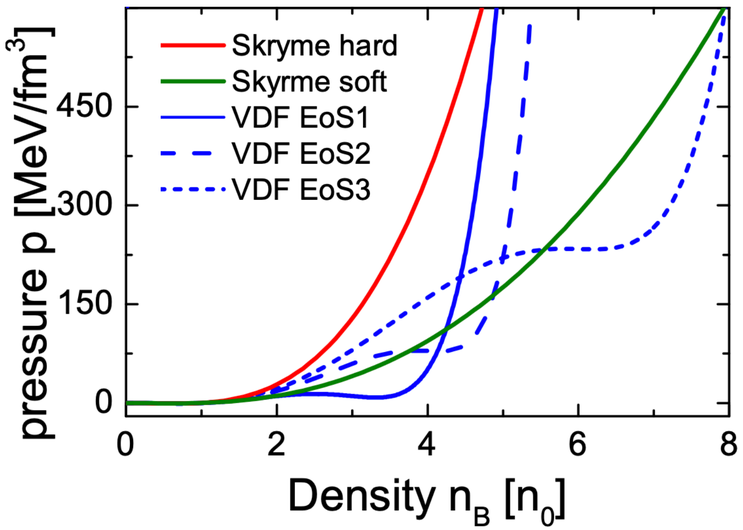

EoS	$T_c^{(N)}$[MeV]	$n_c^{(Q)}[n_0]$	$T_c^{(Q)}$[MeV]	K_0[MeV]
VDF1	18	3.0	100	261
VDF2	18	4.0	50	279
VDF3	22	6.0	50	356

Very soft EOS at $n_B \in (2,3)n_0$
not supported in VDF+UrQMD

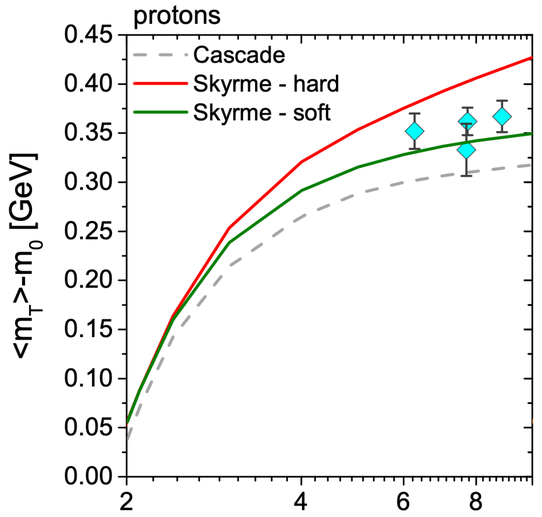

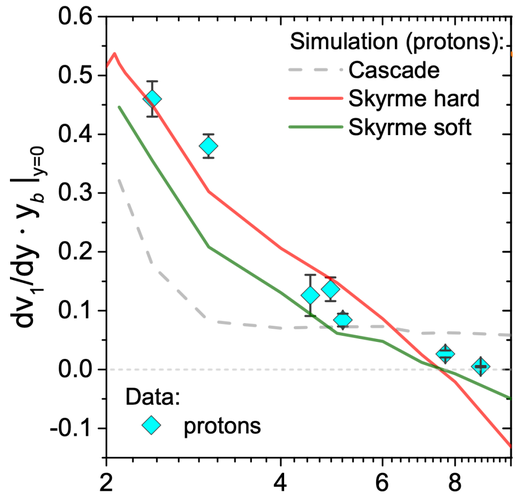

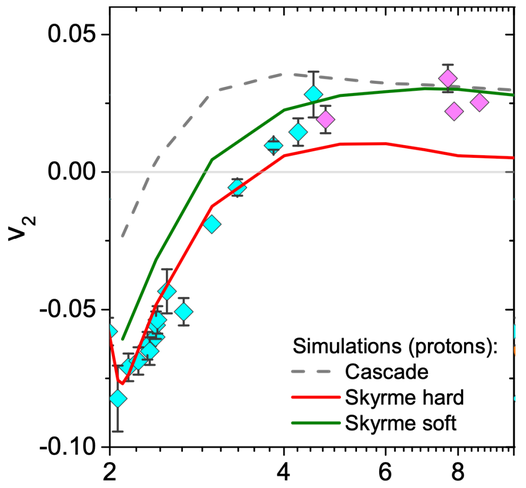

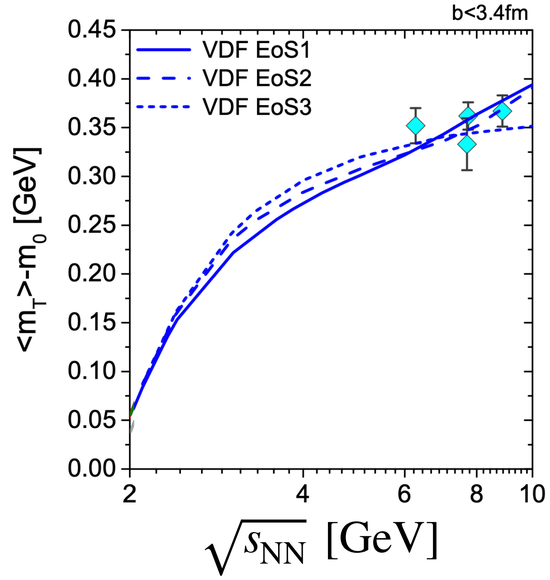

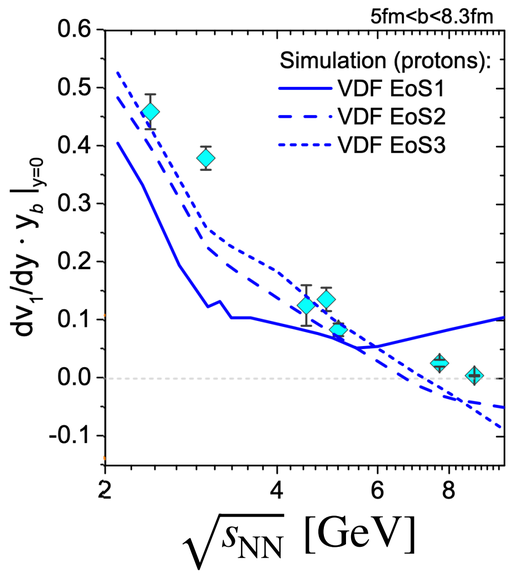

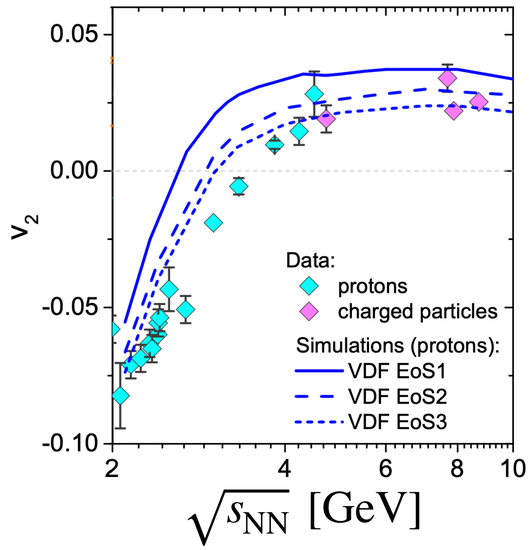

Results from UrQMD with (non-relativistic) VDF

J. Steinheimer, A. Motornenko, **A. Sorensen**, Y. Nara, V. Koch, M. Bleicher,
Eur. Phys. J. C **82**, 10, 911 (2022) arXiv:2208.12091

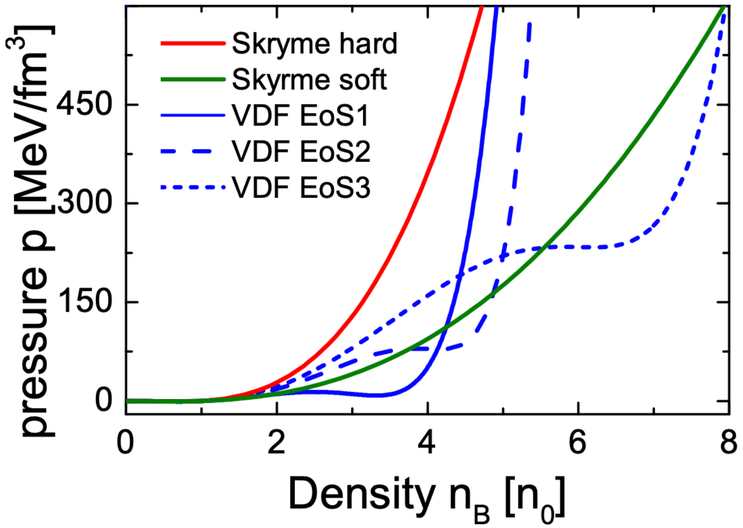

EoS	$T_c^{(N)}$[MeV]	$n_c^{(Q)}[n_0]$	$T_c^{(Q)}$[MeV]	K_0[MeV]
VDF1	18	3.0	100	261
VDF2	18	4.0	50	279
VDF3	22	6.0	50	356

Very soft EOS at $n_B \in (2,3)n_0$
not supported in VDF+UrQMD

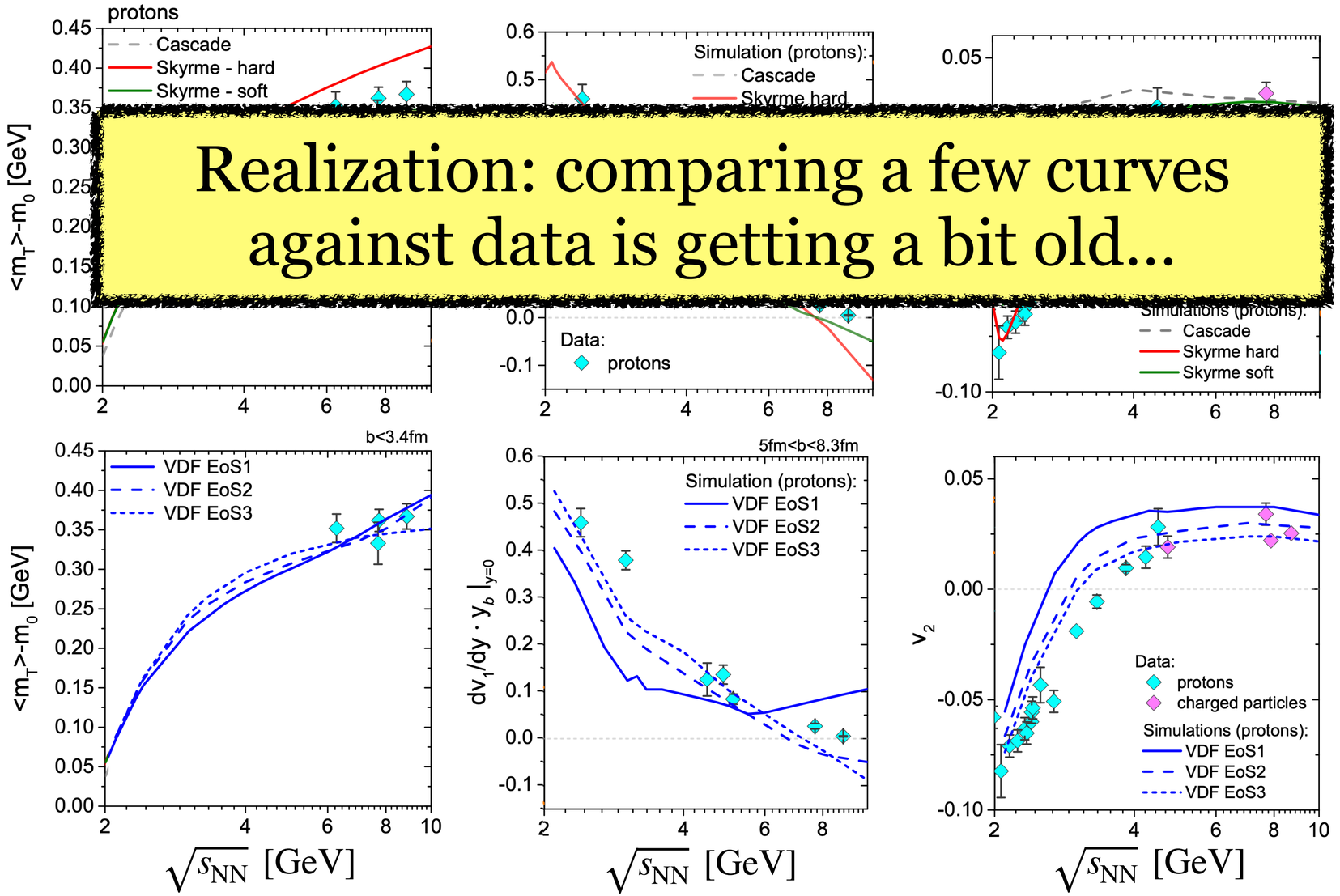

Realization: comparing a few curves against data is getting a bit old...

Sensitivity of HIC observables to the EOS at different beam energies

Mean-field piecewise-parametrized by values of c_s^2 for $n_i < n_B < n_j$:

D. Oliinychenko, **A. Sorensen**, V. Koch, L. McLerran, Phys. Rev. C **108**, 3, 034908 (2023), arXiv:2208.11996

Simulation results:

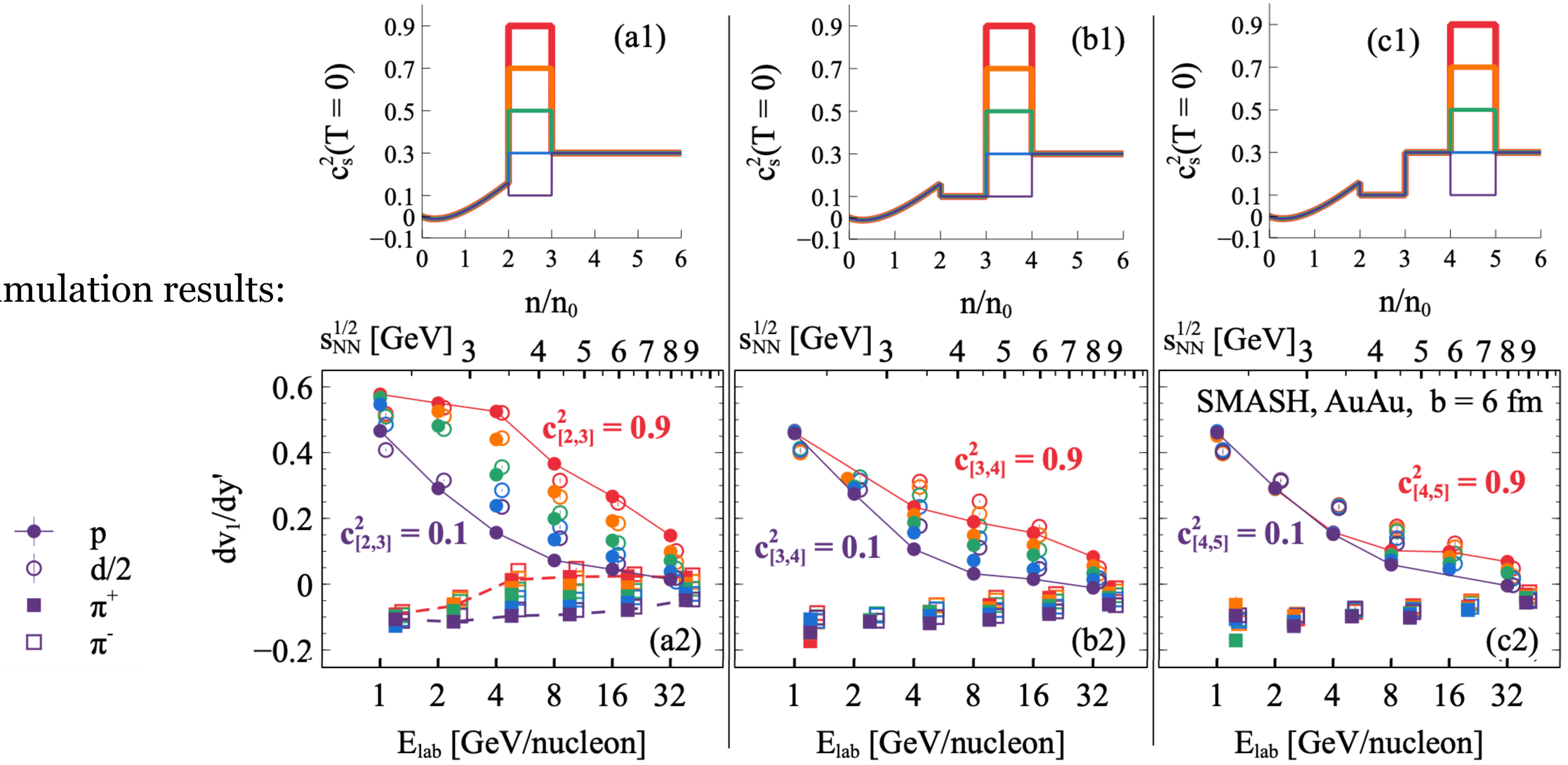

Sensitivity of HIC observables to the EOS at different beam energies

Mean-field piecewise-parametrized by values of c_s^2 for $n_i < n_B < n_j$:

D. Oliinychenko, **A. Sorensen**, V. Koch, L. McLerran, Phys. Rev. C **108**, 3, 034908 (2023), arXiv:2208.11996

Simulation results:

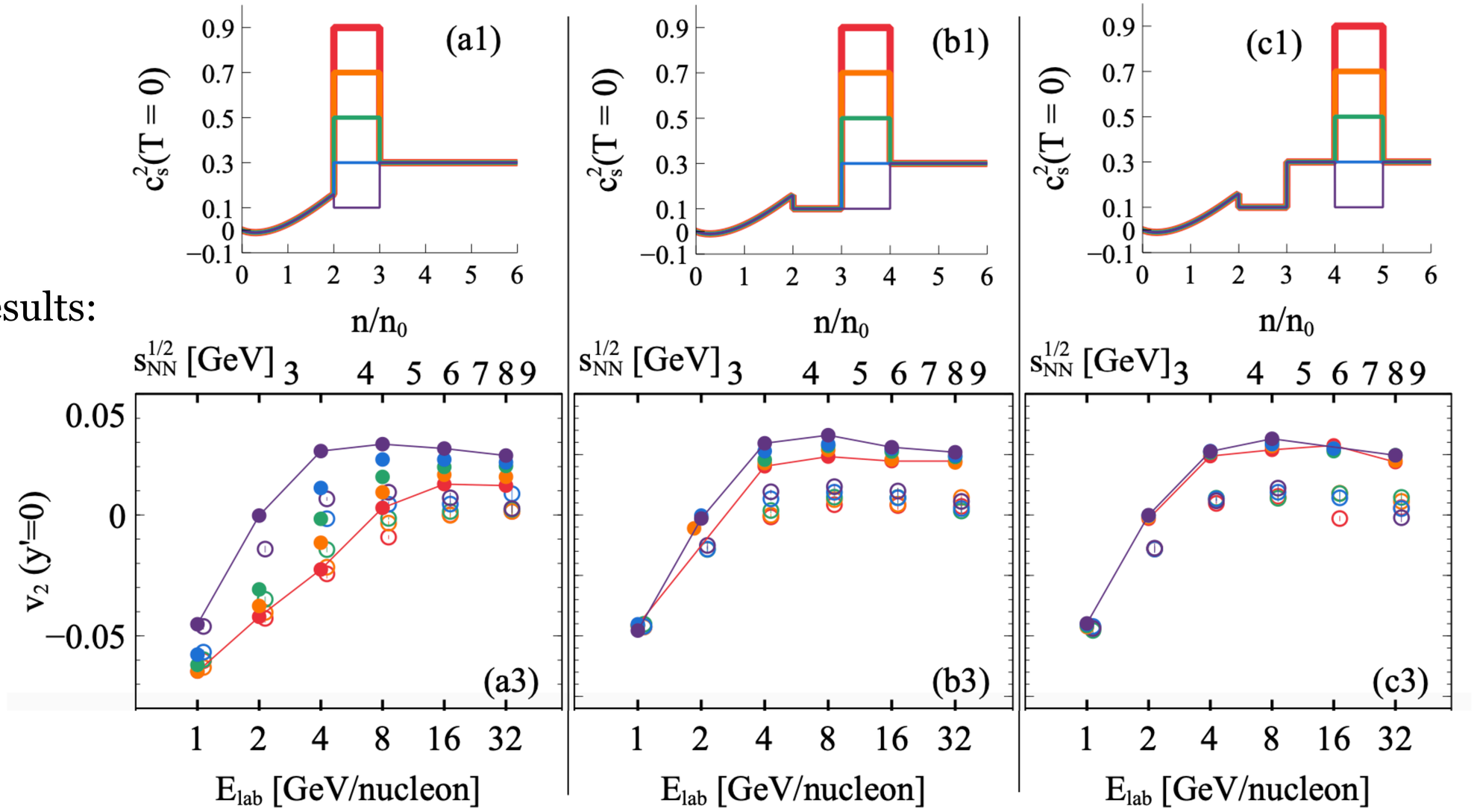

Sketch of a heavy-ion collision evolution and development of flow

** the sketch is informative but not highly realistic*

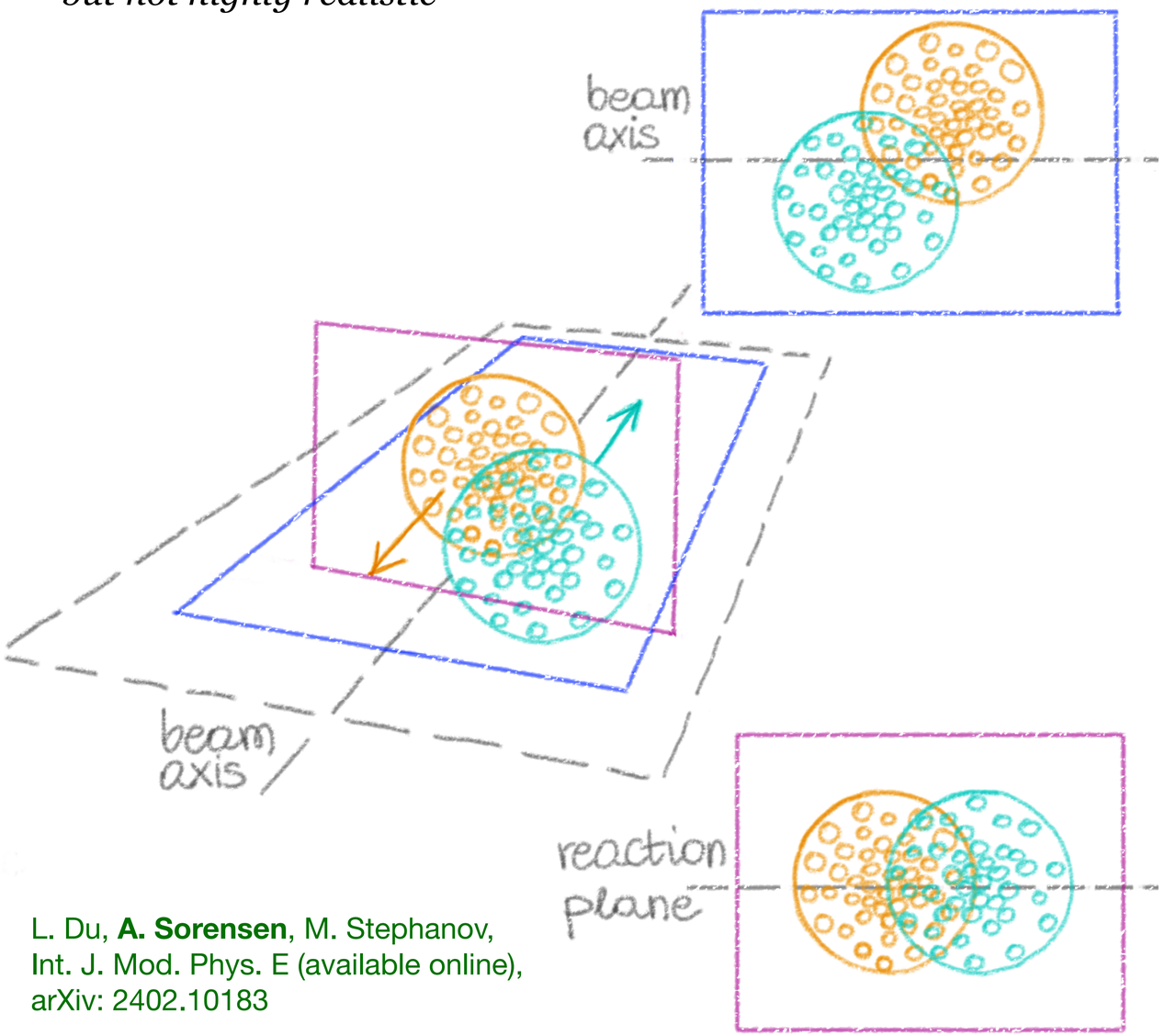

L. Du, **A. Sorensen**, M. Stephanov, Int. J. Mod. Phys. E (available online), arXiv: 2402.10183

Sketch of a heavy-ion collision evolution and development of flow

** the sketch is informative but not highly realistic*

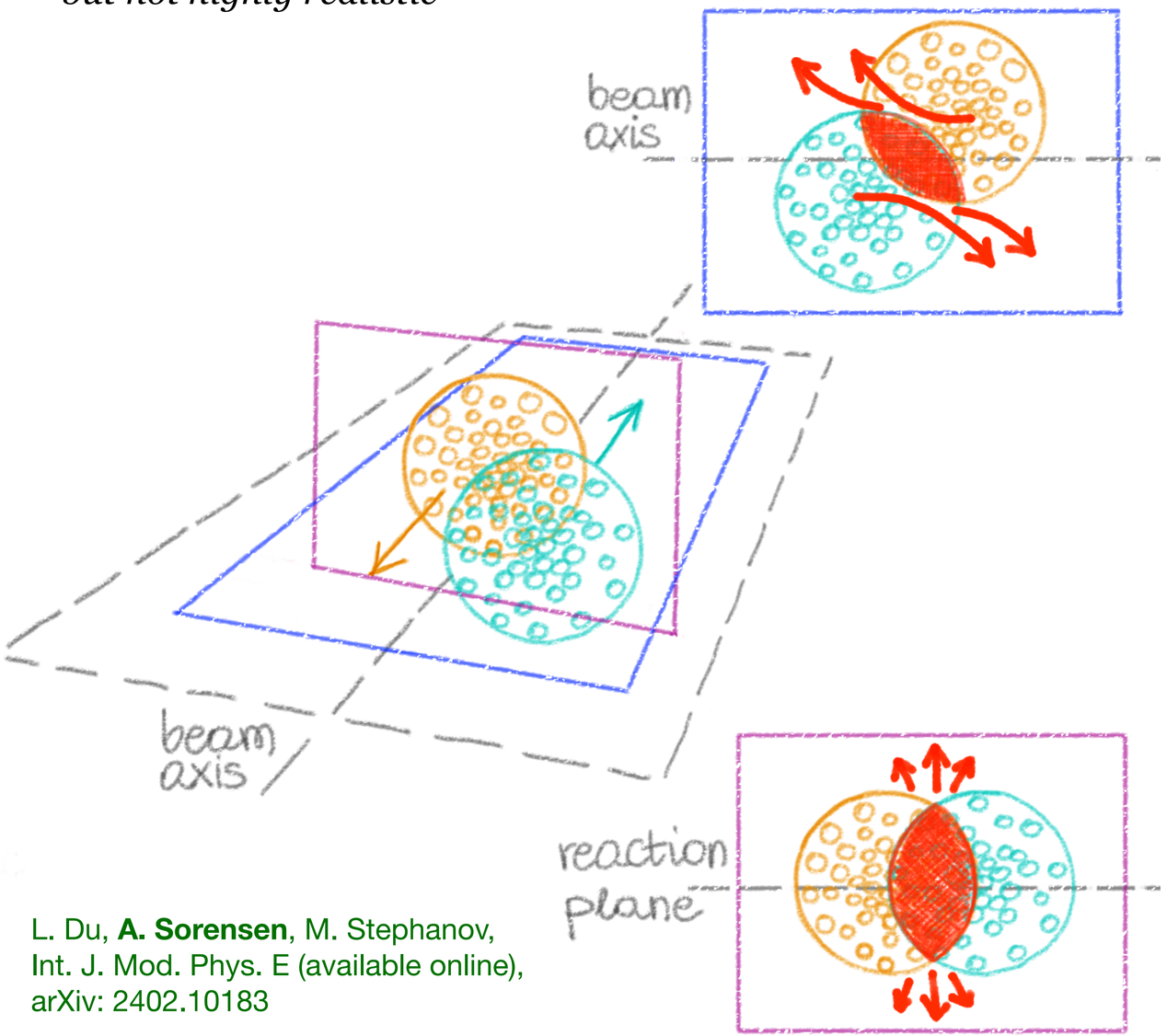

L. Du, **A. Sorensen**, M. Stephanov, Int. J. Mod. Phys. E (available online), arXiv: 2402.10183

Sketch of a heavy-ion collision evolution and development of flow

** the sketch is informative but not highly realistic*

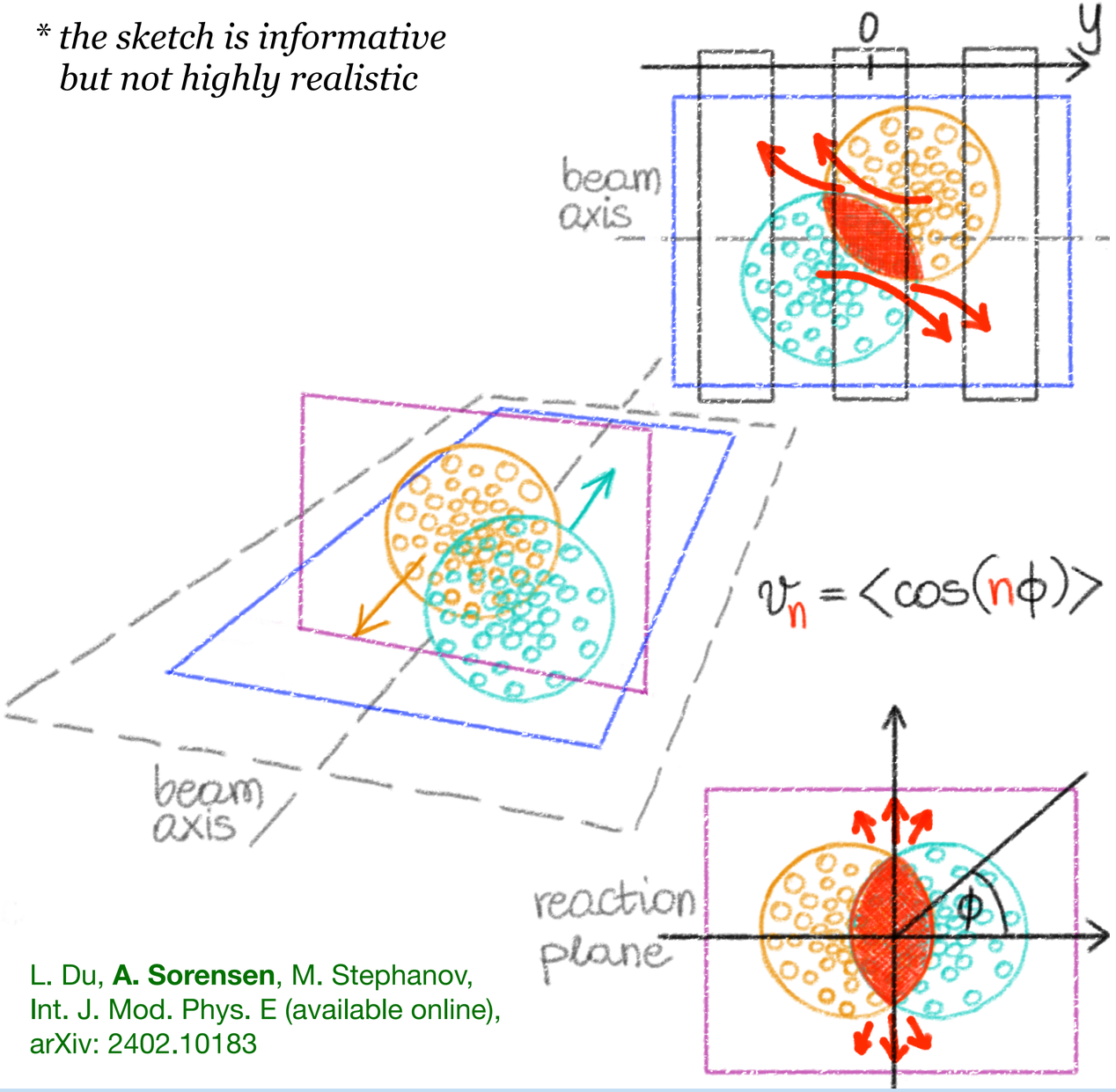

L. Du, **A. Sorensen**, M. Stephanov, Int. J. Mod. Phys. E (available online), arXiv: 2402.10183

Sketch of a heavy-ion collision evolution and development of flow

** the sketch is informative but not highly realistic*

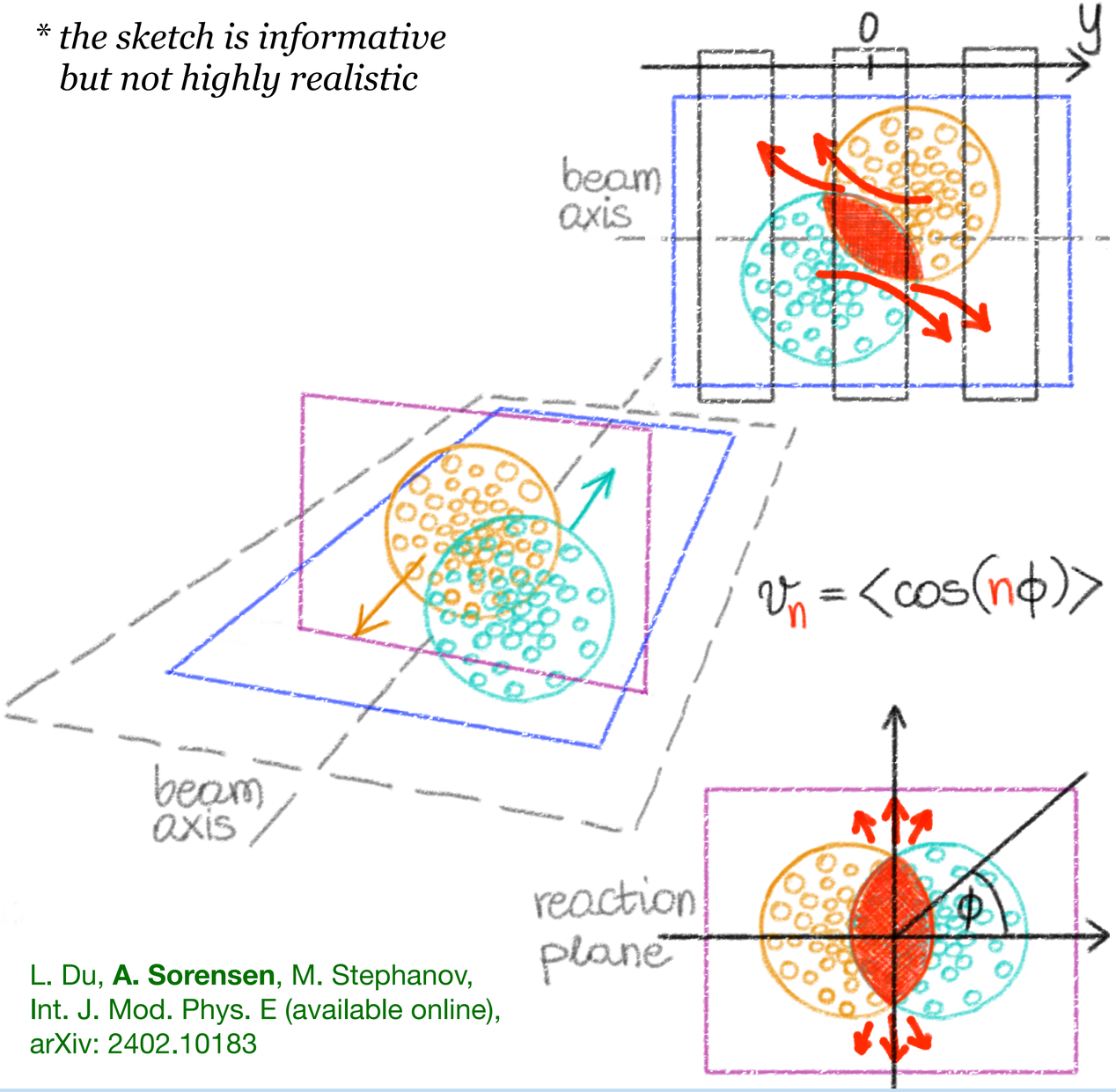

v_1 = directed flow

stiffer EOS
=
more pushing

v_2 = elliptic flow

L. Du, **A. Sorensen**, M. Stephanov, Int. J. Mod. Phys. E (available online), arXiv: 2402.10183

Sketch of a heavy-ion collision evolution and development of flow

** the sketch is informative but not highly realistic*

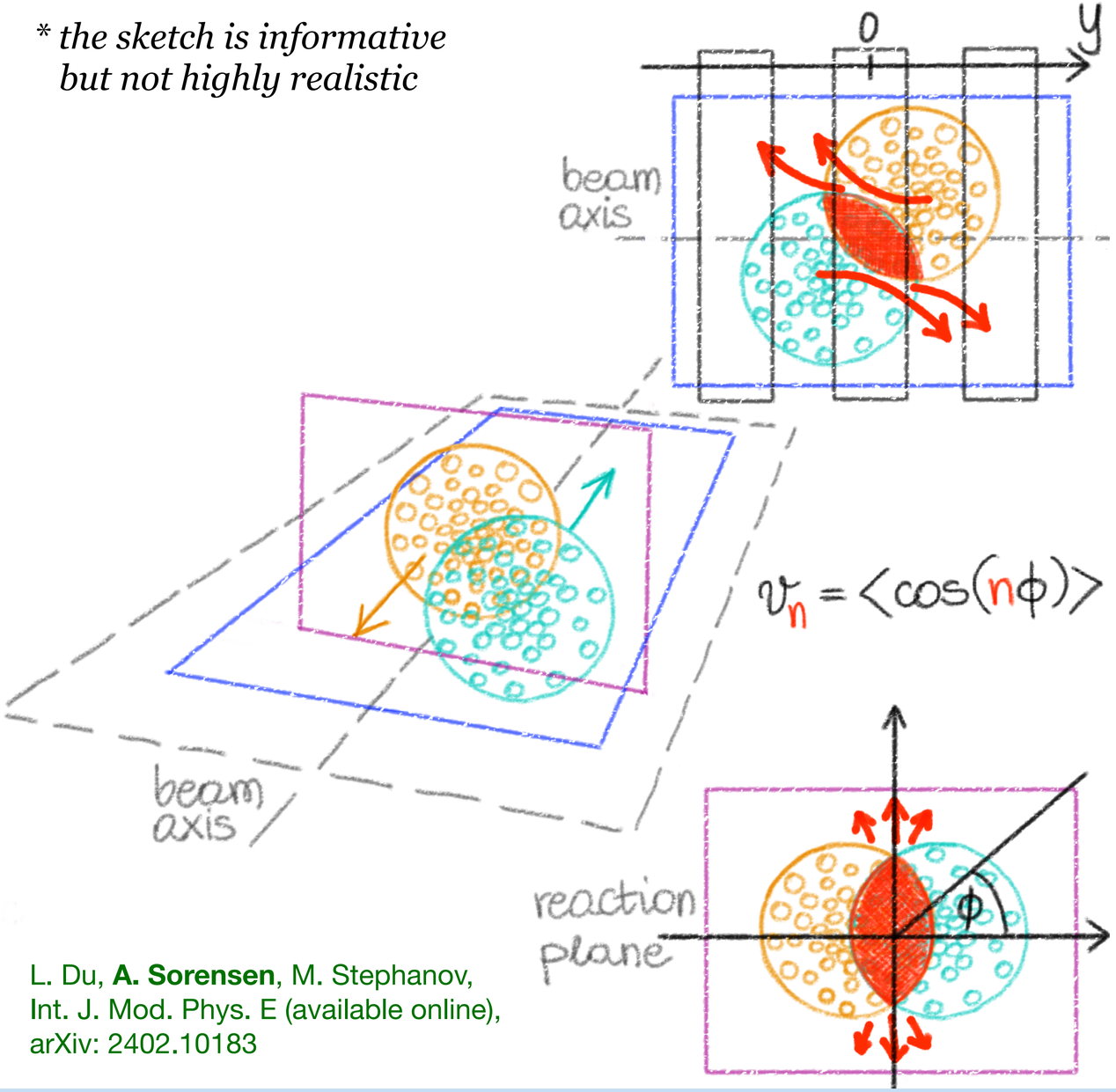

L. Du, **A. Sorensen**, M. Stephanov, Int. J. Mod. Phys. E (available online), arXiv: 2402.10183

J. Adamczewski-Musch *et al.* (HADES), Eur.Phys.J.A 59 (2023) 4, 80, arXiv:2208.02740

v_1 = directed flow

stiffer EOS
=
more pushing

v_2 = elliptic flow

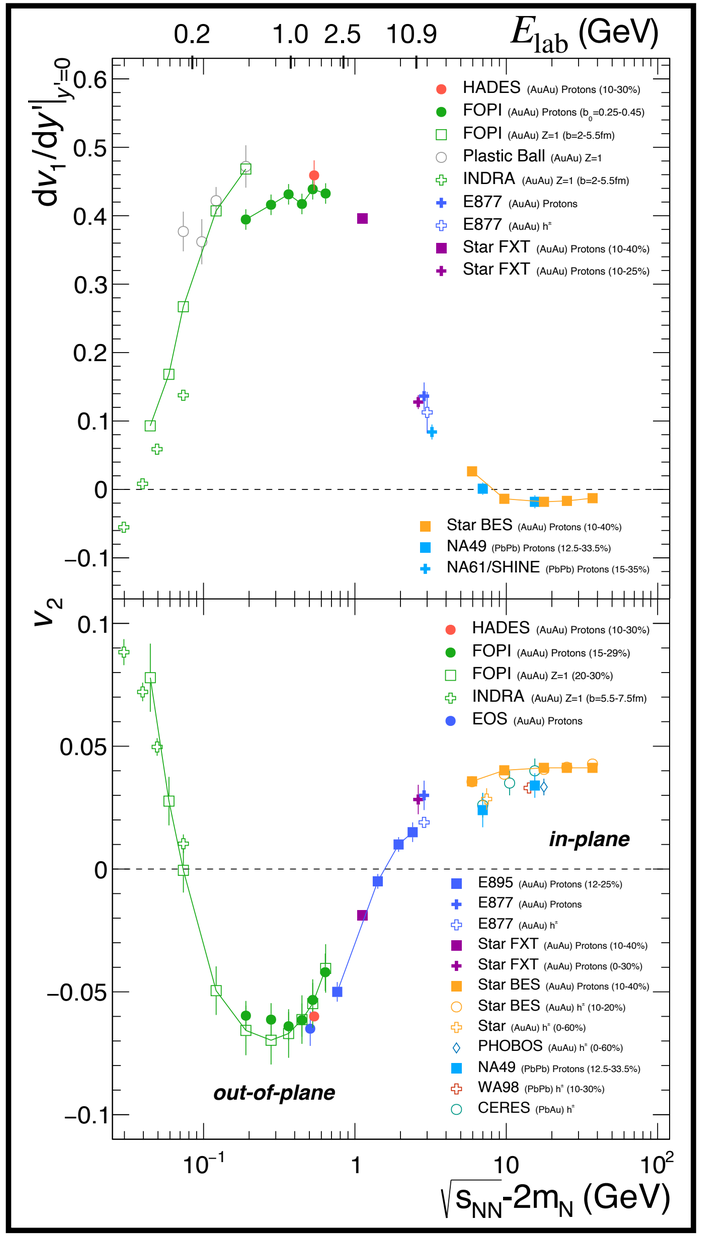

Sketch of a heavy-ion collision evolution and development of flow

** the sketch is informative but not highly realistic*

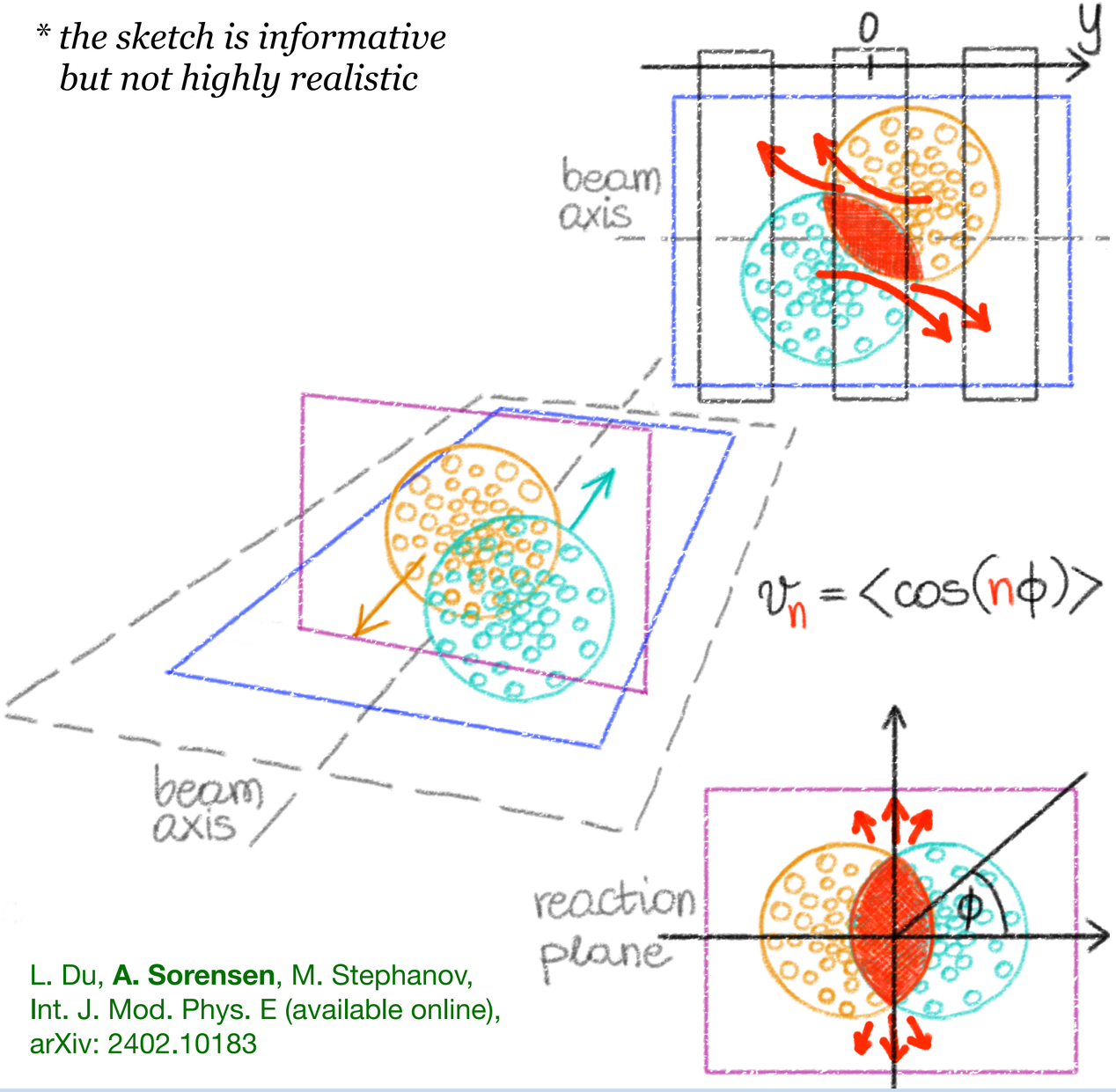

L. Du, **A. Sorensen**, M. Stephanov, Int. J. Mod. Phys. E (available online), arXiv: 2402.10183

J. Adamczewski-Musch *et al.* (HADES), Eur.Phys.J.A 59 (2023) 4, 80, arXiv:2208.02740

v_1 = directed flow

Experiments:
FRIB & FRIB400,
BES FXT,
HADES, CBM, ...

v_2 = elliptic flow

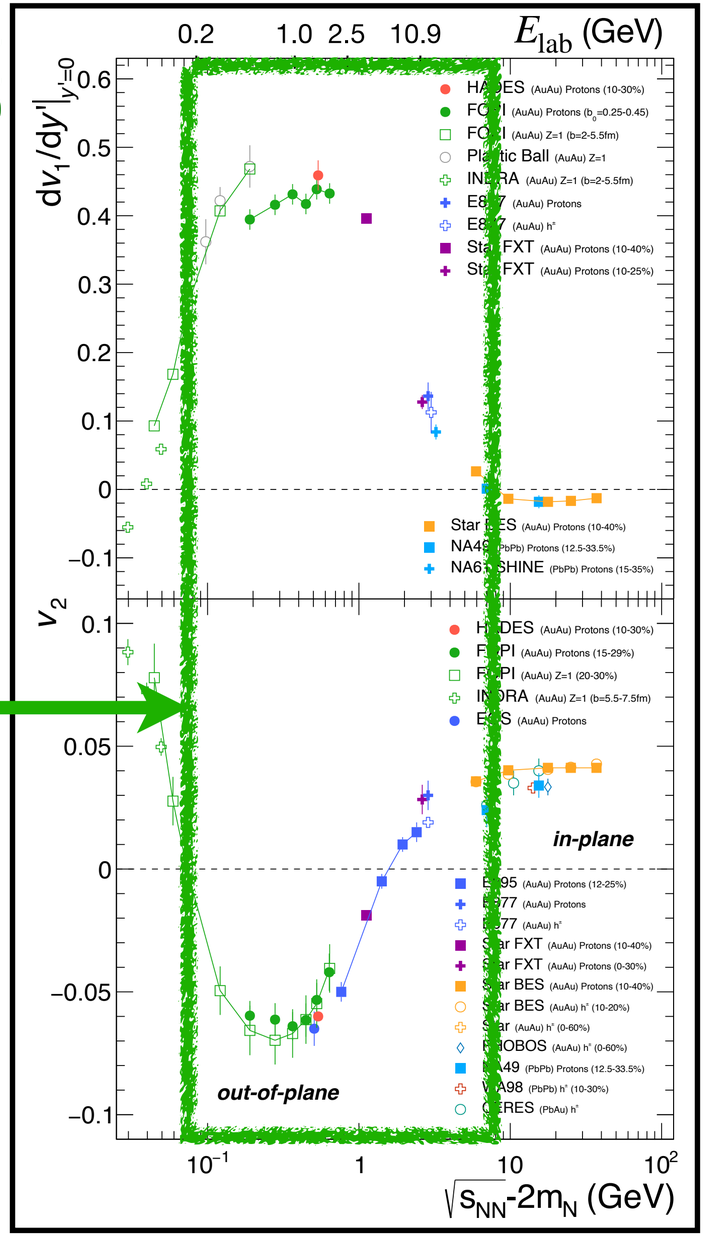

STAR and E895 data cannot be simultaneously described

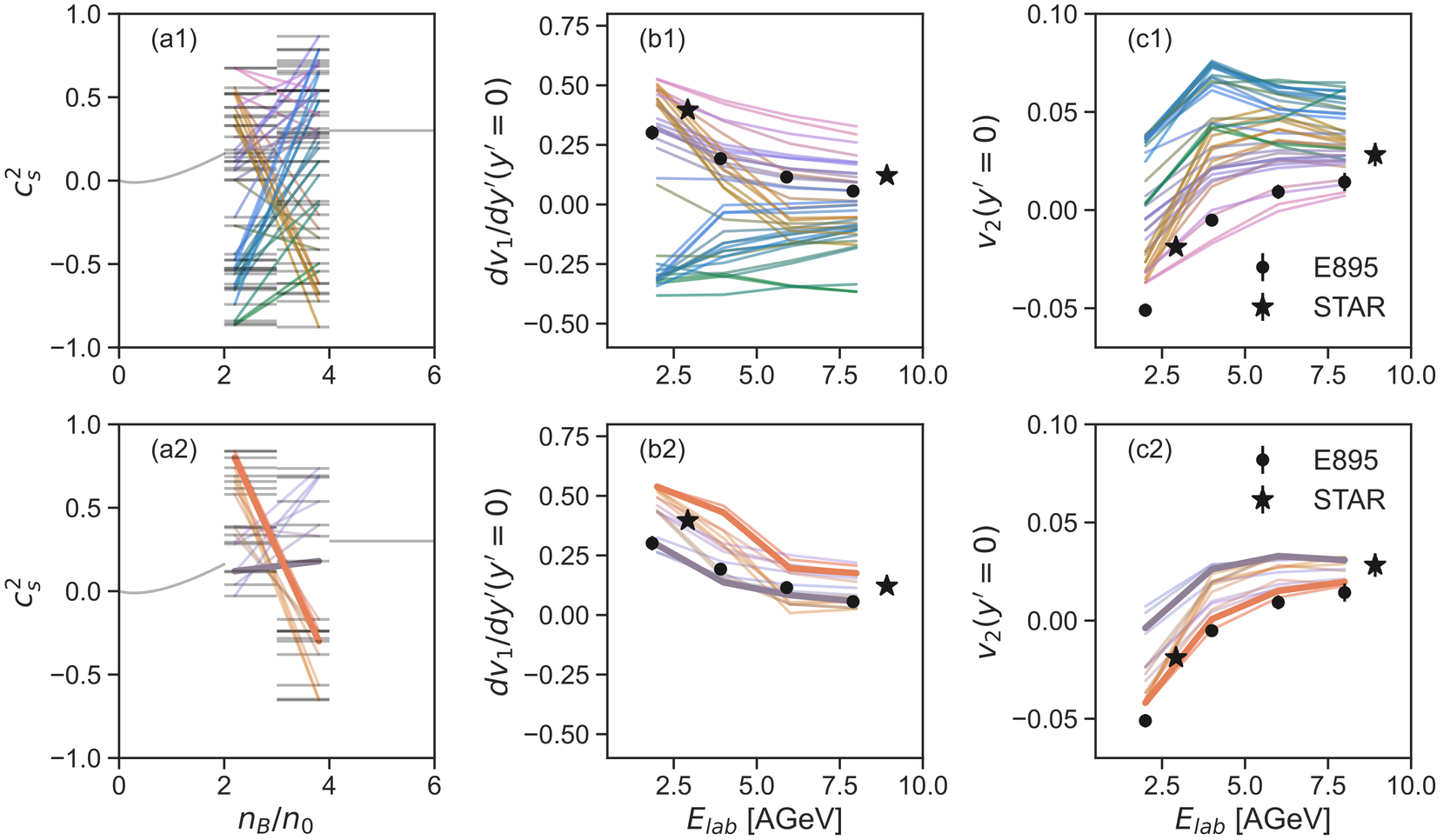

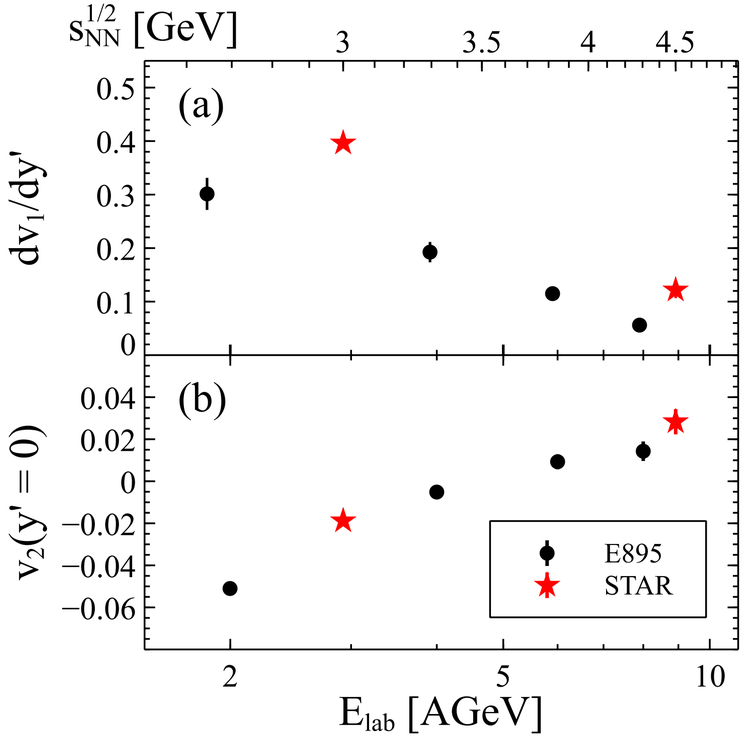

tension between the data sets

D. Oliinychenko, **A. Sorensen**, V. Koch, L. McLerran,
Phys. Rev. C **108**, 3, 034908 (2023), arXiv:2208.11996

STAR and E895 data cannot be simultaneously described

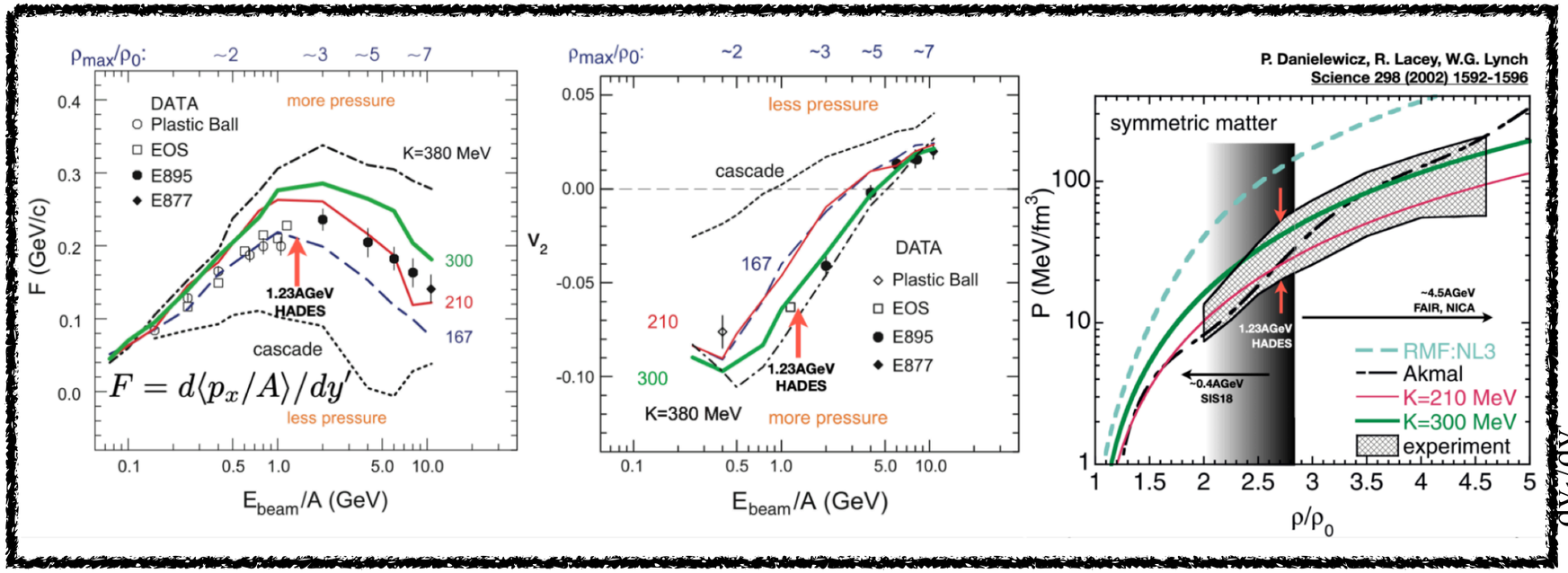

Same problem as
in the DLL constraint!

Danielewicz, Lacey, Lynch,
Science **298**,1592–1596 (2002)

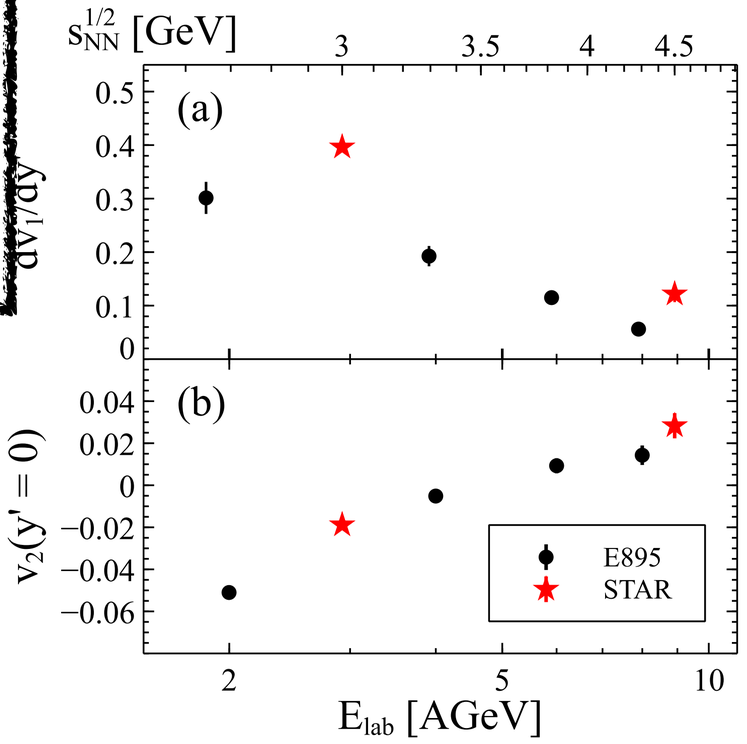

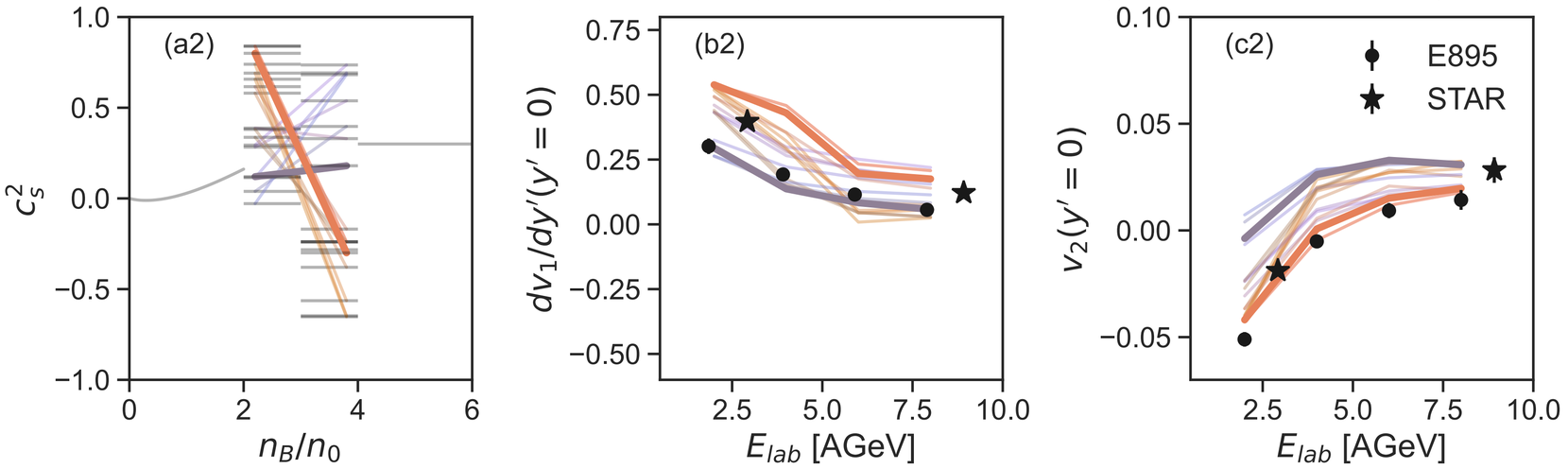

tension between the data sets

D. Oliinychenko, **A. Sorensen**, V. Koch, L. McLerran,
Phys. Rev. C **108**, 3, 034908 (2023), arXiv:2208.11996

Bayesian analysis of STAR flow data with varying K_0, $c^2_{[2,3]n_0}$, $c^2_{[3,4]n_0}$

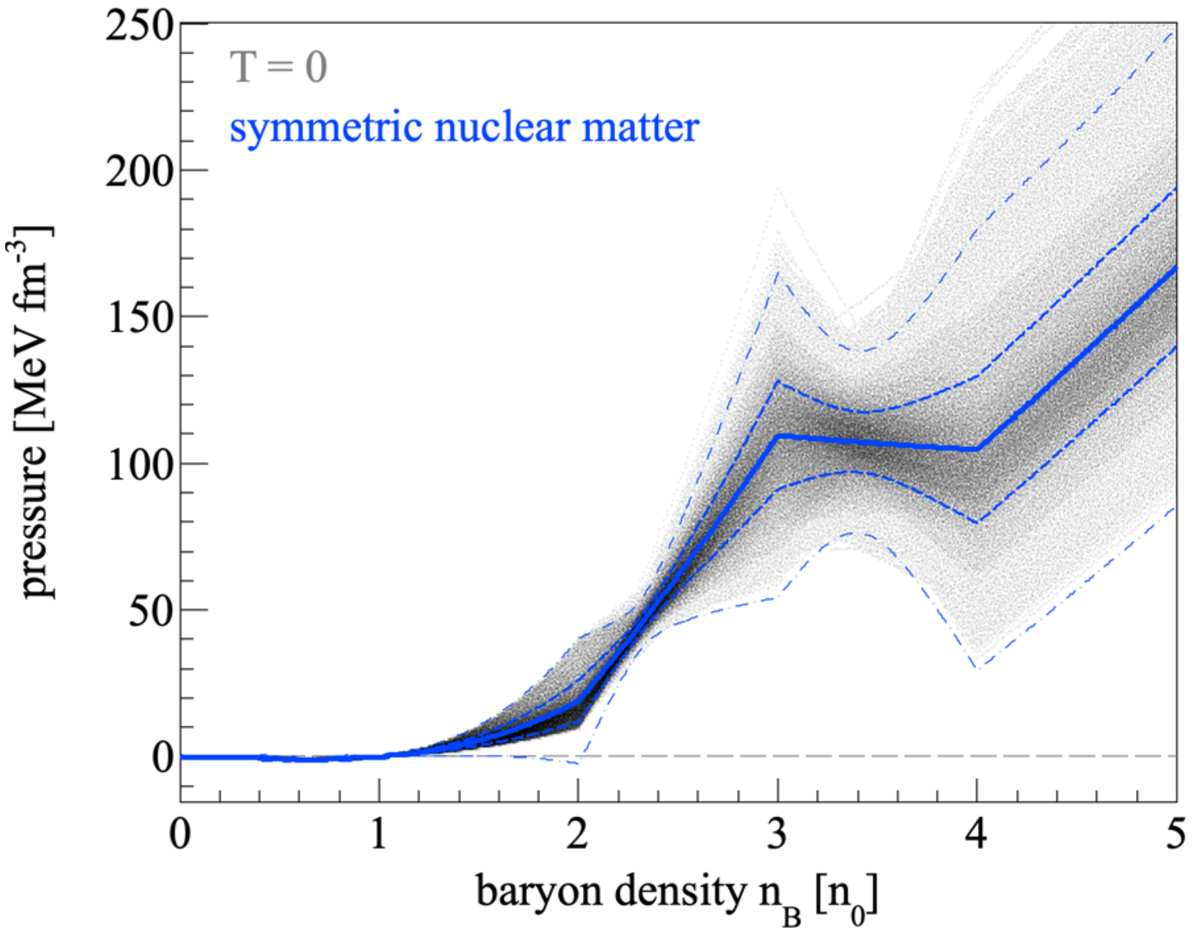

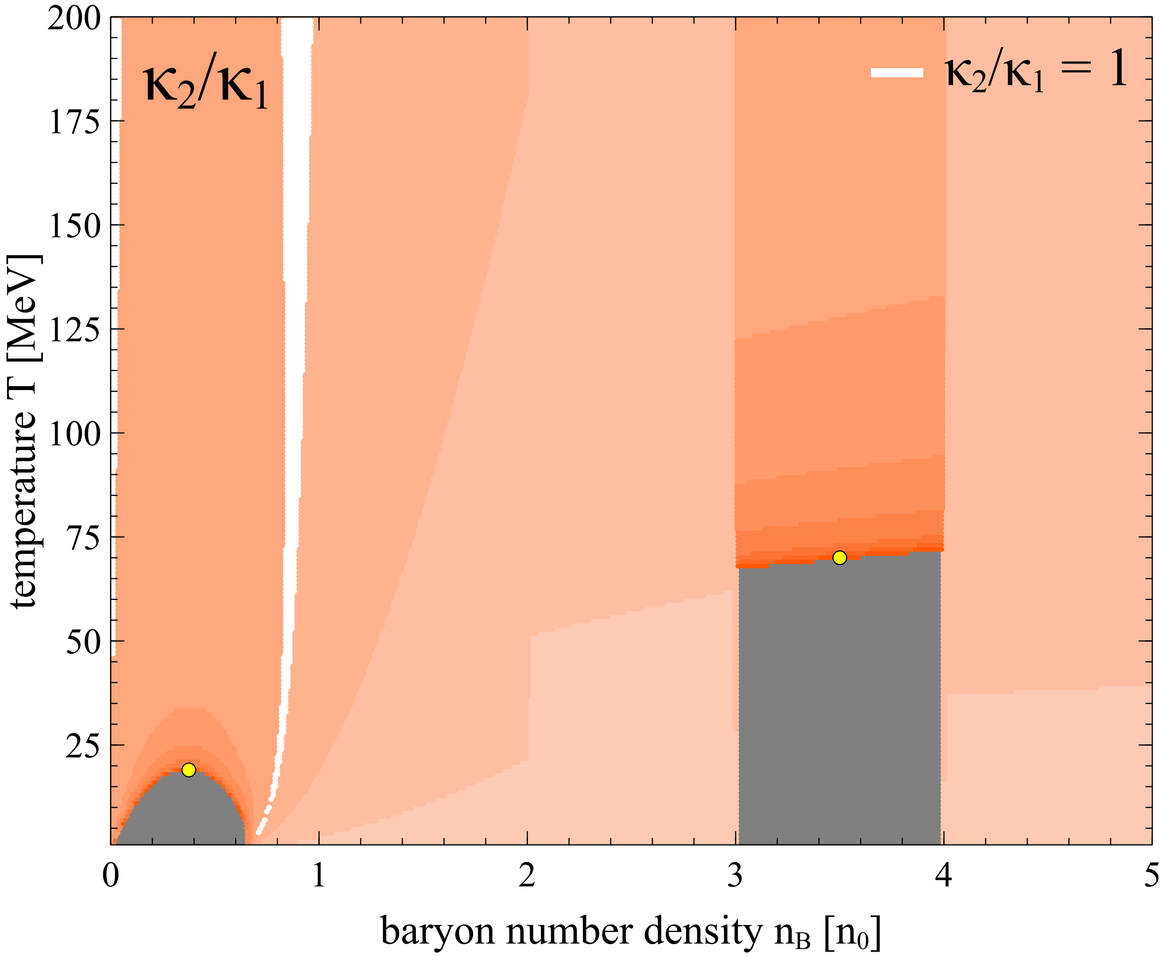

The maximum a posteriori probability (MAP) parameters are

$K_0 = 300 \pm 60\text{MeV}, \quad c^2_{[2,3]n_0} = 0.47 \pm 0.12, \quad c^2_{[3,4]n_0} = -0.08 \pm 0.14$

D. Oliinychenko, **A. Sorensen**, V. Koch, L. McLerran, Phys. Rev. C **108**, 3, 034908 (2023), arXiv:2208.11996

Describing proton flow is not enough

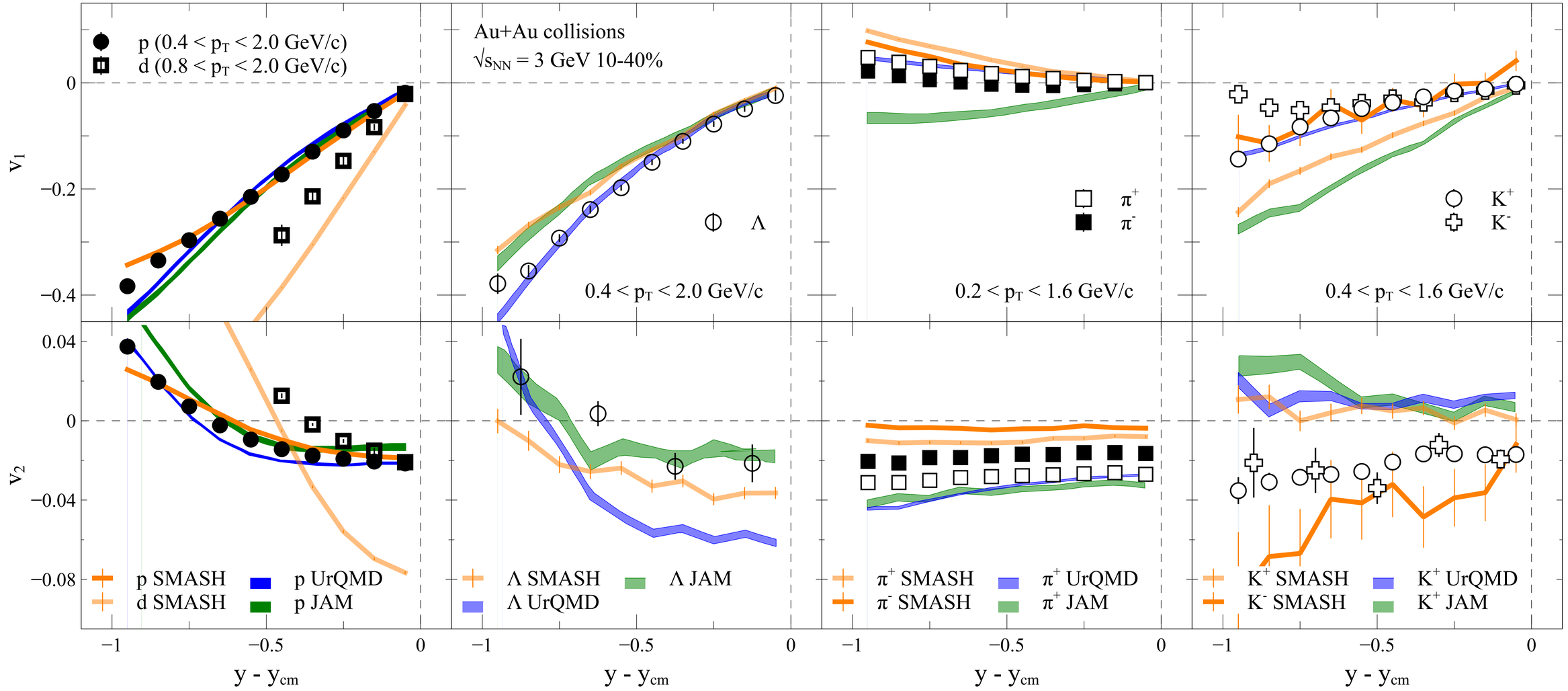

STAR, Phys. Lett. B **827**, 137003 (2022) arXiv:2108.00908

D. Oliinychenko, **A. Sorensen**, V. Koch, L. McLerran, Phys. Rev. C **108**, 3, 034908 (2023), arXiv:2208.11996

A. Sorensen *et al.*, arXiv:2301.13253, to appear in JPPNP

Describing proton flow is not enough

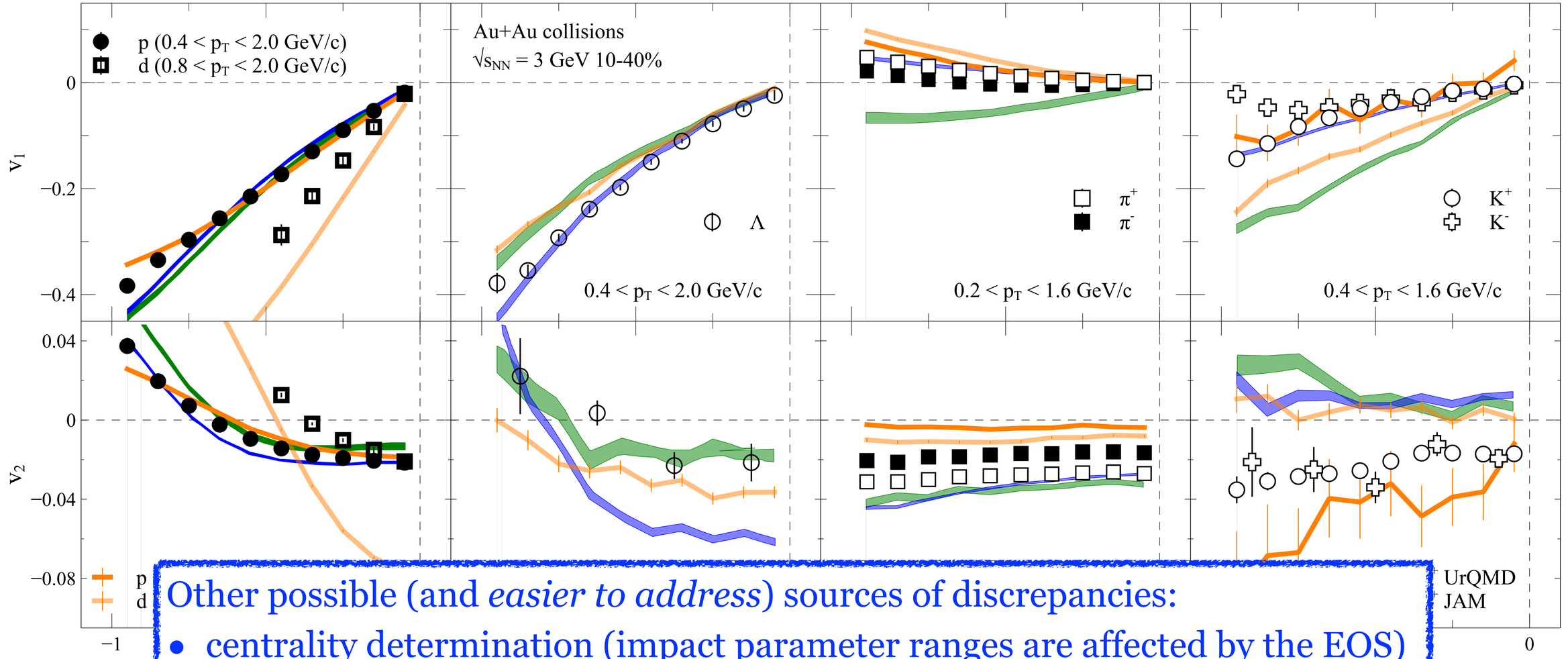

Other possible (and *easier to address*) sources of discrepancies:

- centrality determination (impact parameter ranges are affected by the EOS)
  Note: simulations are numerically costly & this will increase that cost
- method of calculating flow (event plane vs. two-particle correlations)
  (are experiment-experiment and experiment-theory comparisons reliable?)

STAR, Phys. Lett. B 8
D. Oliinychenko, **A. S**
A. Sorensen *et al.*, a